ICES Journal of Marine Science

ICES International Council for the Exploration of the Sea
CIEM Conseil International pour l'Exploration de la Mer

ICES Journal of Marine Science (2014), 71(4), 907–908. doi:10.1093/icesjms/fst219

Contribution to the Themed Section: 'Larval Fish Conference'

Introduction

The early life history of fish—there is still a lot of work to do!

Howard I. Browman* and Anne Berit Skiftesvik

Institute of Marine Research, Austevoll Research Station, 5392 Storebø, Norway

**Corresponding author: tel: +47 9886 0778; e-mail: howard.browman@imr.no*

Browman, H. I., and Skiftesvik, A. B. 2014. The early life history of fish—there is still a lot of work to do! – ICES Journal of Marine Science, 71: 907–908.

Received 6 November 2013; accepted 16 November 2013; advance access publication 9 January 2014.

The themed set of articles that follows this introduction contains a selection of the papers that were presented at the 36th Annual Larval Fish Conference (ALFC), convened in Osøyro, Norway, 2–6 July 2012. The conference was organized around four theme sessions, three of which are represented with articles in this collection: "*Assessing the relative contribution of different sources of mortality in the early life stages of fishes*"; "*The contribution of mechanistic, behavioural, and physiological studies on fish larvae to ecosystem models*"; "*Effects of oil and natural gas surveys, extraction activity and spills on fish early life stages*". Looking back at the main themes of earlier conferences about the early life history of fish reveals that they were not very different from those of ALFC2012. Clearly, we still have a lot of work to do on these and other topics related to the biology and ecology of fish early life stages.

Keywords: Growth, ichthyoplankton, oil pollution impacts, mortality, physiology, predator–prey interactions, recruitment, simulation modelling, survival.

The Annual Larval Fish Conferences (ALFCs) evolved from a series of informal, freshwater-oriented symposia that began with the "*First Symposium on Freshwater Larval Fish*", convened in Charlotte, North Carolina, 24–25 February 1977 (a list of all the ALFCs can be found at: www2.ncsu.edu/elhs/elhspubs.html). A long tradition of themed article collections on the early life history of fishes (ELHF) began with this first ALFC (Olmstead, 1978). In addition, there is a series of three seminal article collections on the ELHF that emanated from ICES Symposia (Blaxter, 1974; Lasker and Sherman, 1981; Blaxter *et al.*, 1989). The themed set (TS) of articles that follows this introduction contains a selection of the papers that were presented at the 36th ALFC, convened in Osøyro, Norway, 2–6 July 2012. The conference attracted 142 delegates from 33 countries. The program was diverse, with 110 oral and 40 poster presentations. The conference was organized around four theme sessions, three of which are represented with articles in this collection.

"*Assessing the relative contribution of different sources of mortality in the early life stages of fishes*" was a theme session organized by Richard Nash, Audrey Geffen and Guðrún Marteinsdóttir. Rates and drivers of mortality have been a central theme of many ALFCs, and was a prominent part of the three ICES Symposia mentioned above. Clearly, a detailed knowledge and understanding of the sources and stage-specific rates of mortality, and of the relative roles of density-independent versus density-dependent processes, remains elusive. Reduction in abundance during the ELHF, from eggs through to settlement by juveniles on nursery grounds, results from a range of causes. Losses can occur from physical transport mechanisms, whereby eggs and larvae are advected to unsuitable habitats (articles in this TS that touch upon this are Lechner *et al.*, 2014; Myksvoll *et al.*, 2014a, b), and through predation, feeding-growth (or lack thereof), environmental factors, or other even more difficult-to-determine causes such as disease. Articles in this TS that touch upon these latter themes are Anderson and Scharf (2014), Kinoshita *et al.* (2014), Ohata *et al.* (2014), Paulsen *et al.* (2014), Polte *et al.* (2014) and Robert *et al.* (2014).

"*The contribution of mechanistic, behavioural, and physiological studies on fish larvae to ecosystem models*" was a theme session organized by Frode Vikebø and Geir Huse. Ecosystem and process modelling is a central component of the ecosystem-based approach to managing marine resources. Recent studies have emphasized the incorporation of flexible individual behaviour motivated through individual states and environmental cues, resulting in emergent rather than determined responses. However, an important limitation of these models is the scarcity of empirical observations to parameterize them. This session represented an attempt to bridge that gap. Articles in this TS that contribute to this are Jørgensen *et al.* (2014), Myksvoll *et al.* (2014a, b) and Staaterman and Paris (2014).

"*Effects of oil and natural gas surveys, extraction activity and spills on fish early life stages*" was a theme session organized by Sonnich Meier, Bjørn Einar Grøsvik and Erik Olsen. Fish embryos and larvae are sensitive to low concentrations of dissolved oil compounds that result not from major spills but from everyday leakage or operational discharges of water from offshore platform activity. There is a need for more research on how oil and oil dispersants at low concentration affect the ELHF, and that was the focus of this theme session. The article in this TS by Vikebø *et al.* (2014) is a contribution to this topic.

Looking back at the main themes of the third ICES Symposium on the ELHF, held in Bergen, Norway, 3–5 October 1988, reveals that they were not very different from those of ALFC2012: (i) spawning studies; (ii) field investigations of distribution and transport, growth and feeding, late larvae and juveniles; (iii) recruitment; (iv) experimental studies on feeding, growth and metabolism, predation and locomotion; and (v) pollution studies. Clearly, we still have a lot of work to do on these and other topics related to the biology and ecology of fish early life stages.

Acknowledgements

For their assistance with the conference program, we thank the theme session organizers—Lee Fuiman, Audrey Geffen, Bjørn Einar Grøsvik, Geir Huse, Guðrún Marteinsdóttir, Sonnich Meier, Richard Nash, Erik Olsen, Amos Tandler and Frode Vikebø. The following friends and colleagues helped with various aspects of organizing, preparations for and running of the conference: Reidun Bjelland, Caroline Durif, Yuichi Fukunishi, Ingegjerd Opstad and Steve Shema. Finally, we wish to thank the 142 delegates, whose participation in the conference was the main reason for its success.

Funding

ALFC2012 was supported by a grant from the Research Council of Norway (Project #196184/S40). The Institute of Marine Research, Norway (IMR), provided significant financial support in the form of operating funds made available by the Institute's Administrative Director, Tore Nepstad. IMR's Research Programs Økosystem og bestandsdynamikk, Ojle-Fisk and Akvakultur provided funds to support the participation of keynote speakers. Additional sponsors were The Bergen Marine Cluster, The University of Bergen, the Taylor and Francis Group, Oxford University Press, Cambridge University Press, Springer, Wiley-Blackwell, Ecocean, The Global Aquaculture Alliance, Skretting, Clean Algae, Bathybiologica A/S, SimboliQ, Harald Kryvi and Espen Rekdal Photography. HB's and ABS's editorial contribution to this article TS was supported by the IMR.

References

Anderson, D. A., and Scharf, F. S. 2014. The effect of variable winter severity on size-dependent overwinter mortality caused by acute thermal stress in juvenile red drum (*Sciaenops ocellatus*). ICES Journal of Marine Science, 71: 1010–1021.

Blaxter, J. H. S. (Ed.) 1974. The Early Life History of Fish; The Proceedings of an International Symposium Held at the Dunstaffnage Marine Research Laboratory, Scottish Marine Biological Association at Oban, Scotland, from May 17–23, 1973. Springer-Verlag. 765 pp.

Blaxter, J. H. S., Gamble, J. C., and von Westernhagen, H. (Eds) 1989. The Early Life History of Fish. The Third ICES Symposium, Bergen, 3–5 October 1988. Rapports et Procès-Verbaux des Réunions de Conseil International pour l'Exploration de la Mer, 191.

Jørgensen, C., Frugård Opdal, A., and Fiksen, Ø. 2014. Can behavioural ecology unite hypotheses for fish recruitment? ICES Journal of Marine Science, 71: 909–917.

Kinoshita, H., Kamimura, Y., Mizuno, K-I., and Shoji, J. 2014. Night-time predation on post-settlement Japanese black rockfish *Sebastes cheni* in a macroalgal bed: effect of body length on the predation rate. ICES Journal of Marine Science, 71: 1022–1029.

Lasker, R., and Sherman, K. (Eds) 1981. The early life history of fish: recent studies. Rapports et Procès-Verbaux des Réunions de Conseil International pour l'Exploration de la Mer, 178, 607 pp.

Lechner, A., Keckeis, H., Schludermann, E., Loisl, F., Humphries, P., Glas, M., Tritthart, M., *et al.* 2014. Shoreline configurations affect dispersal patterns of fish larvae in a large river. ICES Journal of Marine Science, 71: 930–942.

Myksvoll, M. S., Jung, K-M., Albretsen, J., and Sundby, S. 2014a. Modelling dispersal of eggs and quantifying connectivity among Norwegian coastal cod subpopulations. ICES Journal of Marine Science, 71: 957–969.

Myksvoll, M. S., Sandvik, A. D., Asplin, L., and Sundby, S. 2014b. Effects of river regulations on fjord dynamics and retention of coastal cod eggs. ICES Journal of Marine Science, 71: 943–956.

Ohata, R., Masuda, R., Takahashi, K., and Yamashita, Y. 2014. Moderate turbidity enhances schooling behaviour in fish larvae in coastal waters. ICES Journal of Marine Science, 71: 925–929.

Olmstead, L. L. (Ed.) 1978. Proceedings of the First Symposium on Freshwater Larval Fish. Duke Power Company, Cornelius, North Carolina, USA.

Paulsen, M., Hammer, C., Malzahn, A. M., Polte, P., von Dorrien, C., and Clemmesen, C. 2014. Nutritional situation for larval Atlantic herring (*Clupea harengus* L.) in two nursery areas in the western Baltic Sea. ICES Journal of Marine Science, 71: 991–1000.

Polte, P., Kotterba, P., Hammer, C., and Gröhsler, T. 2014. Survival bottlenecks in the early ontogenesis of Atlantic herring (*Clupea harengus*, L.) in coastal lagoon spawning areas of the western Baltic Sea. ICES Journal of Marine Science, 71: 982–990.

Robert, D., Pepin, P., Dower, J. F., and Fortier, L. 2014. Individual growth history of larval Atlantic mackerel is reflected in daily condition indices. ICES Journal of Marine Science, 71: 1001–1009.

Staaterman, E., and Paris, C. B. 2014. Modelling larval fish navigation: the way forward. ICES Journal of Marine Science, 71: 918–924.

Vikebø, F. B., Rønningen, P., Lien, V. S., Meier, S., Reed, M., Ådlandsvik, B., and Kristiansen, T. 2014. Spatio-temporal overlap of oil spills and early life stages of fish. ICES Journal of Marine Science, 71: 970–981.

ICES Journal of Marine Science

ICES Journal of Marine Science (2014), 71(4), 909–917. doi:10.1093/icesjms/fst083

Contribution to the Themed Section: 'Larval Fish Conference'

Food for Thought

Can behavioural ecology unite hypotheses for fish recruitment?

Christian Jørgensen[1]*, Anders Frugård Opdal[1], and Øyvind Fiksen[1,2]

[1]*Uni Research, PO Box 7810, N-5020 Bergen, Norway*
[2]*Department of Biology, University of Bergen, PO Box 7803, N-5020 Bergen, Norway*

**Corresponding Author: tel: (+47) 55584618; fax: (+47) 55584450; Email: Christian.Jorgensen@uni.no*

Jørgensen, C., Opdal, A. F., and Fiksen, Ø. 2014. Can behavioural ecology unite hypotheses for fish recruitment? – ICES Journal of Marine Science, 71: 909–917.

Received 2 November 2012; accepted 9 May 2013; advance access publication 19 July 2013.

Since the classical works by Hjort linked the survival of early life stages of fish to year-class strength and recruitment, fisheries science has struggled to understand the fate of fish eggs and larvae. Here we discuss how food availability will influence growth and survival of larvae when foraging behaviour is flexible and involves predation risk. We use theory to show that small larval fish with a high risk of predation should nevertheless forage intensely and maintain high growth rates. The implication of this is that food availability is more important to recruitment success than is often assumed from studies of growth rate, since the main effect of low food availability appears as increased predation rates. As larvae develop and grow bigger, they are expected to tailor their behaviour to balance food intake and predation risk, which makes it more probable that environmental fluctuations will cause growth differences. A theoretical framework including larval behaviour thus illustrates how several existing hypotheses, i.e. "bigger is better", "stage duration", and "growth-selective predation", emphasize different aspects of larval success but can be understood more generally and coherently when interpreted in the light of behavioural trade-offs. This may lead to more consistent consideration of larval behaviour in biophysical models of fish recruitment.

Keywords: adaptations, larval fish behaviour, life history theory, recruitment success, trade-offs.

Introduction

Many pelagic fish larvae hatch as vulnerable and almost immobile particles, but can quickly develop locomotory capabilities (Clark *et al.*, 2005) and may eventually adopt schooling behaviours (Leis, 2007). The extraordinary high mortality experienced during their earliest life stages (McGurk, 1986) exerts strong selective pressures to fine-tune their behavioural strategies through Darwinian evolution. *A priori*, one would therefore expect them to have adapted behaviours such as activity level, depth positioning, and aggregation tendency to maximize survival, and that these strategies would be flexible with regards to their size, internal condition (e.g. hunger), and the anticipated risk of predation in their current environment (based on e.g. light levels or direct cues). Behavioural capacities are known to have profound effects on the interplay between environment, growth and survival (Lima and Dill, 1990); in this paper we assess the value of a behavioural perspective for understanding recruitment processes in fish larvae.

In Hjort's time, data was scarce, which had the side-effect of leaving ample room for speculation. A common contemporary belief was that all herring belonged to one inexhaustible population in the Arctic and that variable migratory routes explained why local fishing grounds were fluctuating (Sinclair and Solemdal, 1988). Using age reading from fish scales, Hjort and his co-workers were able to show how some strong year-classes swept through the population like a wave and could dominate for almost a decade (Hjort, 1914). At the same time, these strong year-classes could not be linked to a large parental population, so their formation seemed almost random or caused by some undetermined environmental factor. Attempting to provide a mechanistic link to the observed fluctuations, Hjort (1914) formulated the "critical period" hypothesis, stating that newly hatched larvae that "did not succeed in finding the very special food they wanted would die from hunger" (Hjort, 1926). This hypothesis was later explored in detail for Norwegian spring spawning herring (Dragesund, 1970), and refined to become

the more general match–mismatch hypothesis by Cushing (1973; 1990). The match–mismatch hypothesis proposed that larvae hatching near the peak abundance of their zooplankton prey would survive and recruit better, thus forming strong year-classes.

Hjort's (1914; 1926) concept of a "critical period" still dominates fisheries recruitment science a century later, although it has been complemented by more specific hypotheses that attempt to explain how food can be mechanistically and causally linked to recruitment success. The "bigger is better" hypothesis (Houde, 1987; Litvak and Leggett, 1992) is based on the observation that predation rates are high but decline rapidly with size in marine organisms in general (Peterson and Wroblewski, 1984) and for fish larvae in particular (McGurk, 1986; Houde, 1987). An implicit consequence is the closely related "stage duration" hypothesis. Rather than explicitly addressing size, it focuses on the time spent in the smaller and vulnerable size-classes; if growth increases, this period is shortened and survival is therefore higher (Shine, 1978; Houde, 1997). A third perspective is the "growth-selective predation" hypothesis, based on observations that slow-growing larvae were more likely to be eaten, presumably because too little food reduced performance and anti-predator behaviours (Takasuka *et al.*, 2003).

The common assumption made by the three hypotheses is that favourable food conditions will increase growth rate, which in turn has a positive effect on survival. In this paper we suggest that behavioural responses play a central role in this chain of causal mechanisms, based on developments made within behavioural ecology and life-history theory over recent decades. A core mechanism is that food abundance will increase survival through changes in behaviour, whereas there can be little or no concurrent change in growth (McNamara and Houston, 1987; Fiksen and Jørgensen, 2011). Our manuscript is structured as follows.

We first point to mechanisms and selection pressures that link growth rate to predation risk in larval fish. Our focus is on species from high latitudes with a pelagic larval phase, but many of the mechanisms and relationships are general and would apply to tropical regions as well. With reference to a detailed state-variable dynamic optimization model for growth and survival in fish larvae, we argue that a main role for adaptive larval behaviour is to maintain high growth rates across a wide range of food concentrations, but that survival can be compromised (Fiksen and Jørgensen, 2011). We highlight some key predictions from this model and use them to demonstrate links between behaviour, growth, and survival.

Whereas Hjort's (1926) starting point was that larval fish suffering mismatch "would die from hunger", the theory we present indicates that less food may alter foraging behaviour and cause larvae to take more risks, making predation rather than starvation the main cause of death. The distinction between these two views is discussed.

The above points indicate that evolved strategies and environmental variation are two sources of differences between individuals. These are compared and contrasted. We then illustrate how a focus on larval fish behaviour may help bring together the perspectives of the "bigger is better", "stage duration", and "growth-selective predation" hypotheses. Finally, we end the paper with a brief discussion of implications for biophysical models that explicitly consider the larval phase.

Trade-offs between growth and survival

What does theory have to say about how animal behaviour can modify growth and survival? Think of an animal with some foraging behaviour, for instance activity level or boldness during foraging. Pivotal to understanding the selection pressures on such behaviours is to identify the involved trade-offs, i.e. how an individual may need to sacrifice ingestion to achieve survival, or the other way around. If predation rate is plotted as a function of growth rate, Gilliam's rule (Werner and Gilliam, 1984) can be applied to find the evolutionarily optimal growth rate. Graphically, this is done by drawing the tangent through the origin, and it will intersect the curve at the point where the ratio between mortality and growth is minimized, i.e. where growth is optimal (denoted with *) because a larger size is achieved with the lowest probability of predation (Figure 1).

The exact relationship between growth rate and predation rate is variable and depends on the type of predator, the type of prey, the environment, the individual's behaviour, and strategic life history trade-offs (Huse and Fiksen, 2010). The relationship is furthermore expected to change with development as larvae aquire increased capabilities of locomotion, sensing, escape, and defence. In herring larvae, it is for example observed that responsiveness to a predation cue increases with age, presumably due to development, but also with size (Skajaa *et al.*, 2004) in line with the expectation of more cautious behavioural strategies as size-dependent mortality declines. At the broad scale, growth rate is a trait that has evolved to an optimal level to maximize expected offspring production during a lifetime (Arendt, 1997). Many processes contribute to growth, some of which affect acquisition or foraging rates, and some that determine how growth is prioritized over other processes that compete for resources (Enberg *et al.*, 2012). A good starting point when thinking about all these processes can be to ask the two following questions about the benefits and costs.

What can be achieved by increasing foraging activity?

Generally, growth will increase with increasing foraging activity, although there will typically be diminishing returns. Behaviour can cause this due to: (i) a functional response with handling time limitation, causing ingestion rate to approach a ceiling even though further foraging increases the encounter rate with prey (Holling, 1965), which is particularly relevant for species such as planktivorous fish that ingest single food particles that are small relative to body size; (ii) inclusion of less-preferred items in the diet, which may reduce the energy efficiency of foraging (Emlen, 1966); or (iii) first utilizing the hours of the day that are most efficient for foraging, typically at dusk and dawn, (Clark and Levy, 1988), then extending foraging to

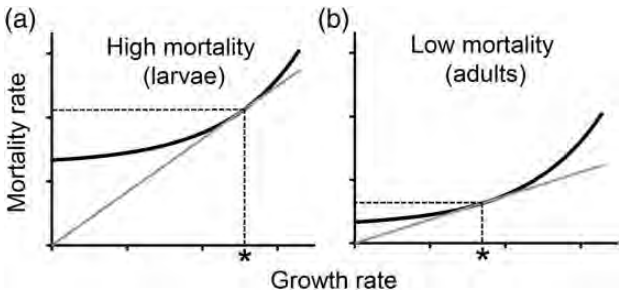

Figure 1. A graphical illustration of optimal growth rates (*) under different mortality levels, given a behavioural trade-off between growth rate and survival. By drawing the tangent to the mortality curve through the origin, the point is found where the ratio between mortality and growth is minimized, analogous to Gilliam's rule (Werner and Gilliam, 1984). The optimal growth rate (*) is higher when mortality is high (**a**), compared with a situation where mortality is lower (**b**). Note that the figure shows growth rate on the *x*-axis and each panel assumes a constant size; the generally declining mortality rate with increasing size is visible in the contrast between panels (a) and (b).

times with less favourable conditions. One can also think of other mechanisms, as well as constraints e.g. from the processing capacity of the gut, but in general we expect growth to increase, but to approach an asymptote, with increasing foraging activity.

What are the costs of increasing foraging activity?

Increased foraging may require a larger gut or better swimming muscles, which have energetic costs that will reduce the energetic efficiency of foraging or may incur elevated maintenance costs when running idle. Still, survival costs are probably most important, especially for small fish larvae that may encounter many potential predators while having limited abilities to escape. An overall finding is that an individual who follows a strategy of faster growth will suffer increased mortality risk because it takes more chances during foraging. More swimming generally makes the individual more easily detected by predators (Kiørboe, 2011). Some modes of predation have been modelled mechanistically. For example, if the foraging activity of a larval fish is swimming speed, and the main predators are ambush predators, then the rate of predation will be proportional to foraging activity (Visser and Kiørboe, 2006). An individual can also increase its ingestion rate by visiting more well-lit layers, but with a concomitant increase in predation rate (Iwasa, 1982). In an elegant series of experiments, it was shown that rapid digestion leaves less aerobic scope for escaping predation attempts (Billerbeck *et al.*, 2001; Lankford *et al.*, 2001; Arnott *et al.*, 2006). Fast growth may furthermore consume resources that become unavailable for other processes that may reduce mortality, such as cellular maintenance and repair, immune defence, or armoury (reviewed in Arendt, 1997; Enberg *et al.*, 2012).

Together, the benefits and costs of foraging typically scale in such a way that predation risk is an accelerating function of growth rate (Figure 1), and that the optimal growth rate is faster when the mortality rate is higher (Figure 1a vs. 1b).

This insight is particularly relevant for fish larvae because they suffer very high predation rates, particularly early in their ontogeny (McGurk, 1986). An important role for behaviour may then be to keep growth at high levels, by making sure that the digestive system has sufficient food to process at all times. Should the environment become worse, ingestion can be kept high by accepting more risk (Fiksen *et al.*, 2007). As development progresses, growth rates can be expected to fall as more cautious foraging behaviours become adaptive due to the general reduction of size-dependent predation mortality.

Starvation or predation?

From an individual perspective, death by starvation is a dramatic and irreversible situation that individuals will go to great lengths to avoid. Theoretical studies have highlighted that one cannot infer from the frequency of starvation whether food is important, because individuals will increase their risk-taking long before starvation happens (McNamara and Houston, 1987; Krebs and Kacelnik, 1991). While Hjort (1914, 1926) was right when he linked food abundance to recruitment success, he may have jumped to conclusions when he reasoned that larvae who suffered mismatch "would die from hunger". It is more likely that they died from predation because hunger made their behaviour more risk-prone. There is also growing awareness of the distinction between prey abundance and prey availability, i.e. the former is only the numbers or biomass of prey, whereas the latter also includes other factors that make that potential prey more or less easy to capture and consume—such as light, turbulence, prey-size spectra (Sheldon *et al.*, 1972; Pope *et al.*, 1994), and ontogenetic development of the larva's sensory and locomotory capabilities.

Using a detailed state-variable optimization model for the foraging of and predation on larval fish, Fiksen and Jørgensen (2011) found optimal behavioural responses (vertical habitat selection and foraging activity) in a range of environmental settings (Figure 2). Optimality was defined as the behaviour that maximized the probability of survival to a given size (metamorphosis). The key assumptions linking behaviour to growth and predation risk were: (i) that more swimming activity led to higher encounters with both prey and ambush predators; and (ii) that more light increased both the detection of prey and the chance of being detected by a predatory fish. Behavioural strategies of activity and light-exposure therefore had consequences for both growth and survival, and the optimal strategy was found by state-dependent optimization (Clark and Mangel, 2000). When food levels were varied from very low to very high, there was a gradual increase in survival, but the optimal behavioural strategies maintained growth close to the maximum possible, except for in the very worst environments where starvation occurred (Figure 2). In the model, the high mortality that fish larvae experience makes it optimal for them to keep their physiological machinery running at maximum rates (even if this has survival costs), and behaviour is modified adaptively to ensure sufficient food is supplied. At higher food levels survival improves, as less risky behaviours are needed to maintain high growth rates. This model's predictions are consistent with several observations. A review of growth studies in Atlantic cod concluded that cod larvae grew at their temperature-dependent maximum rates under field conditions, whereas sub-maximal growth was often observed in laboratory studies, presumably because larvae cannot express their behaviour fully (Folkvord, 2005). Similarly, a large field study of Japanese anchovy larvae found no effect of prey density on growth rates (Takasuka and Aoki, 2006).

It should be noted that situations exist where food limitation appears to actually constrain growth rate (e.g. Huwer *et al.*, 2011). As individuals grow bigger, their feeding strategies are expected to become more cautious. In those situations, a perceived presence of predators can induce less foraging and more time spent in safety. This is often referred to as a non-consumptive effect of predation and is contrasted to the consumptive effect by which the prey is eaten by the predator (Peacor *et al.*, 2013). A trait change commonly has both consumptive and non-consumptive consequences.

Two sources of individual variation

In a given population there may not be a single optimum or a single dominating strategy, but there is often between-individual variation in how much risk individuals accept (Biro *et al.*, 2006). Commonly, a strategy is only optimal under a narrow range of environmental conditions, and if the future environment is uncertain, patchy or variable, it can be adaptive for parents to hedge their bets by producing a clutch of offspring that follow strategies that differ from one another (Crean and Marshall, 2009). If these behavioural and growth traits are heritable, then the larvae with higher survival will be more likely to produce the descendants for the next generation, and in this way natural selection may fine-tune larval strategies for behaviour and growth. It may also be that heritable lines coexist in the same population because differences from year to year or area to area select for a range of strategies.

Another source of individual variation is short-term environmental variability that may influence individual state. Because two individuals who follow the same strategy may differ in the history of their environmental exposure, this can lead to differences first

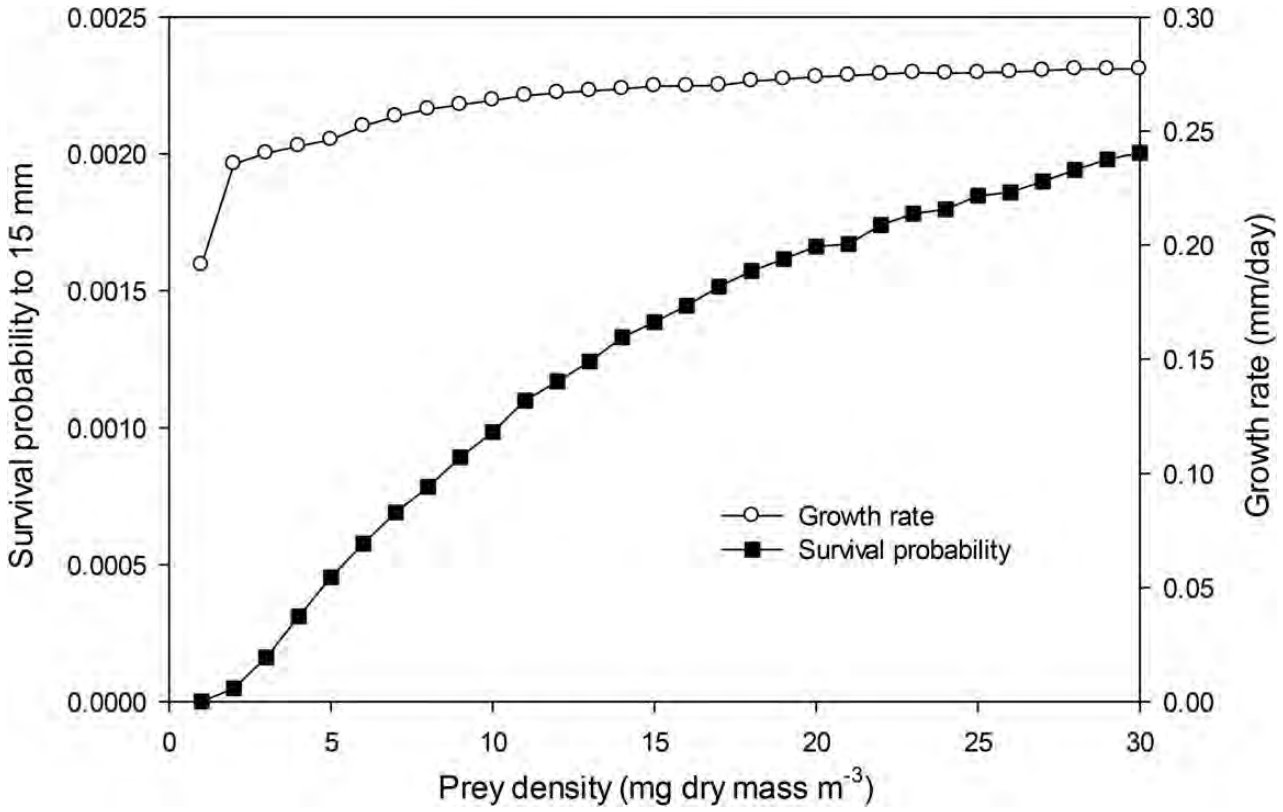

Figure 2. Predictions of optimal growth and resulting survival over a range of prey densities according to a detailed simulation model for state-dependent larval behaviour (Fiksen and Jørgensen, 2011). The model includes mechanistic behavioural trade-offs between growth and predation, and follows a larva hour by hour over day and night while it adjusts its behaviour adaptively to the prey availability. Larval survival was quantified as the probability of survival from 5 mm to a length of 15 mm, and the figure shows the corresponding average growth rate (open circles) and survival (solid squares) as a function of prey density in the water column.

in how much food their guts contain or how full their energy stores are, then over time this can cause growth differences and variation in size. Behavioural ecology has a rich tradition for studying how differences in state may affect behavioural decisions (Houston and McNamara, 1999; Clark and Mangel, 2000). Food is more valuable for a hungry larva than for one who is satiated, and in one experiment well-fed cod larvae spent more time in the safety of a group whereas hungry larvae foraged more solitarily (Skajaa *et al.*, 2003). Initial size and condition during egg and early life stages can also influence survival. Jørgensen *et al.* (2011) show in a theoretical model how optimal offspring size in fish may depend on both environmental and parental conditions. Such state-dependent strategies illustrate how individual larvae, but also their parents, may influence larval risk-taking depending on their current state, which reflects recent history.

The combination of strategic and environmental effects on rates of growth and predation are shown in Figure 3. Because fish larvae suffer high mortality rates (Peterson and Wroblewski, 1984; McGurk, 1986), low food availability leads to minor reductions in growth but major increases in predation as individuals compensate behaviourally by taking more risk (Figure 3b and top-right end of Figure 3c). Thus, when behaviour can be fully expressed, fish larvae grow near their maximum rates, and the price of a bad environment becomes reduced survival.

As fish larvae develop, better sensory apparatus and improved locomotory capabilities make surviving a predator attack more likely, and mortality generally becomes lower. Larvae also form a larger visual image as they grow bigger, and therefore become more vulnerable to visual predators such as fish (Aksnes and Utne, 1997; Vikebø *et al.*, 2007). Experiments have revealed that younger larvae do not respond to predators while older ones do (Fuiman, 1989; Skajaa *et al.*, 2003). For instance, herring larvae develop bullae and a gas-filled lateral organ capable of hearing at ~ 26 mm of length, and this implies a quantum leap in their ability to avoid predation attempts (Fuiman, 1989). In sum, reduced overall mortality, increased visibility to predators, and increased sensory and locomotory capabilities make it profitable, in evolutionary terms, for fish larvae to gradually become more risk-sensitive with age and ontogenetic development (exemplified in Figure 3a), and this will likely continue until adulthood (gradually moving towards the lower-left corner of Figure 3c).

Recruitment hypotheses in fisheries science

If behaviour can modify growth and survival, what is the relevance for fisheries science and recruitment success? In Figure 4 we assume that mortality decreases with size, as observed and reflected in the "bigger is better" hypothesis, and contrast different views of how growth and mortality may vary over the early life stages of fish. A common assumption, derived from laboratory experiments, is that periods of reduced food availability will translate to periods of reduced growth (Figure 4a). Slower growth implies a longer larval phase. Because total mortality can be visualized as the area under the curve of mortality rate plotted over time, slower growth causes longer "stage duration" and a higher cumulative mortality.

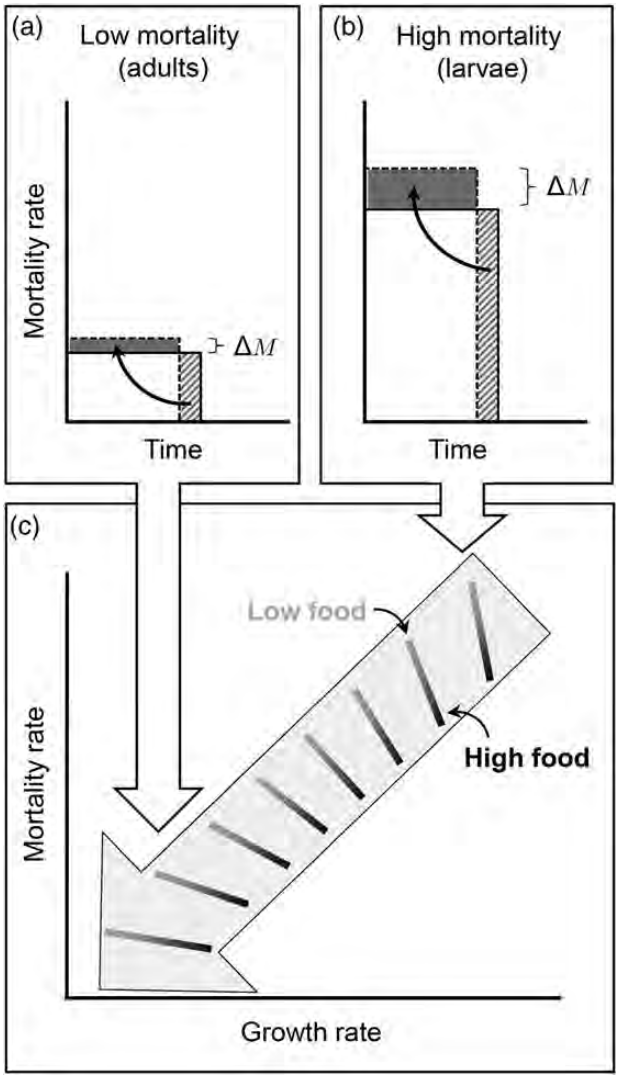

Figure 3. Schematic illustration of how adaptive growth and environmental effects of food variability influence growth and mortality through ontogeny. (**a**) In older individuals, the mortality rate is comparatively low, and due to trade-offs strategies that grow faster may shorten the duration of a given mortality rate (removing the mortality in the hatched area) but incur a higher mortality rate (ΔM), which together influence the overall survival (faster growth increases fitness if the grey area is smaller than the hatched area). (**b**) For larval fish, the mortality rate is usually higher, and reducing the time one is exposed to that mortality has a large effect on survival. To attain that effect, fish larvae may evolve rapid growth strategies that accept higher instantaneous mortality, again being selected for as long as the grey area is smaller than the hatched area. (**c**) The difference in this trade-off between larval fish and older individuals suggests two broad patterns. First, larval fish will likely grow faster and take higher risks, this being at the upper-right corner of the graph. As they develop and the mortality rate declines, it becomes optimal to reduce risk level and grow slower, and through ontogeny one would therefore expect that they move towards the lower-left corner of the figure (indicated with wide grey arrow). At each ontogenetic stage, food variability can induce changes in growth and risk-taking. If food is abundant, mortality will be lower (the black end of each little line), but in larval fish it is expected that food variation will translate mostly to changes in survival (lines are almost vertical), whereas for older fish the extra risk may not be worth taking and food variation will have stronger effects on growth (lines are more horizontal).

This would be the case also if mortality was assumed to be independent of size. Under food-limited growth, a slowing down at early ages will have more pronounced effects because it prolongs development at a size where the mortality rate is higher.

An alternative mechanism, explained above, is that growth is a trait subject to trade-offs, and that behaviour plays the role of jointly determining risk exposure and growth rate. For example, herring larvae reduce their foraging behaviour in experimental tanks where they can see a potential predator (Skajaa *et al.*, 2003) but maintain their escape response (Skajaa and Browman, 2007), thus suggesting that behaviour can be environmentally conditioned. Given such trade-offs, reducing growth rate entails a more cautious behavioural strategy that will incur lower mortality rates but also lengthen the exposure to mortality because growth to a given size takes a longer time (Figure 4b). Note that here a longer "stage duration" is not necessarily linked to higher mortality; if growth is faster than optimal then slower growth and longer duration would decrease the overall mortality.

The two perspectives from panels 4a and 4b are combined in panel 4c, where it is assumed that behaviour is plastic and can change rapidly and according to local environmental variables. When food availability varies over time, these fish larvae may change their behaviour to accept more risk when food is scarce, thus maintaining rates of ingestion, digestion, and growth, albeit at costs in terms of survival (Fiksen and Jørgensen, 2011). This also describes a role for individual states, as lower food availability is likely to first reduce gut levels, then energy stores, and if behavioural changes are insufficient to bring ingestion back up, then finally growth.

From this behavioural perspective it is easier to see how the three recruitment hypotheses are related:

The "bigger is better" hypothesis cannot be used to infer that larvae should hatch bigger because evolution of egg size is determined by selection pressures on maternal investment (Smith and Fretwell, 1974; Jørgensen *et al.*, 2011), but it can guide our understanding of the role of behaviour. This hypothesis recognizes the overall pattern that mortality rate declines rapidly with size for fish eggs and larvae, which has a sound empirical (McGurk, 1986) and theoretical basis (Peterson and Wroblewski, 1984; Andersen and Beyer, 2006) related to development of e.g. locomotory capabilities, sensory systems, adaptive colouration, scales, and immune defence. The pattern of declining mortality with size leads to the prediction that behaviour should be more risk-taking for small larvae, and gradually become more cautious as the larvae grow bigger. The "bigger is better" hypothesis also emphasizes the importance of body size for larval ecology, for example how the growing larval body forms a larger visual image that behaviour can counteract by seeking darker surroundings, or by conferring advantages in terms of intraspecific competition (Reznick *et al.*, 2006) or surf-riding of size-spectra (Pope *et al.*, 1994).

Whether "stage duration" has a positive or negative effect on survival depends on the behavioural strategy. This hypothesis focuses on the time spent in vulnerable size-classes where longer stage duration is assumed to increase mortality, but taking behavioural trade-offs into account suggests that prolonged stage duration may be caused by a more cautious behavioural strategy, with slower growth and lower mortality rate. Whether the overall effect on survival is positive or negative depends on the area under the curve of mortality rate plotted over time, until a given size is reached. Thus, stage duration has no simple effect on survival or recruitment; it depends on the environment and behaviour.

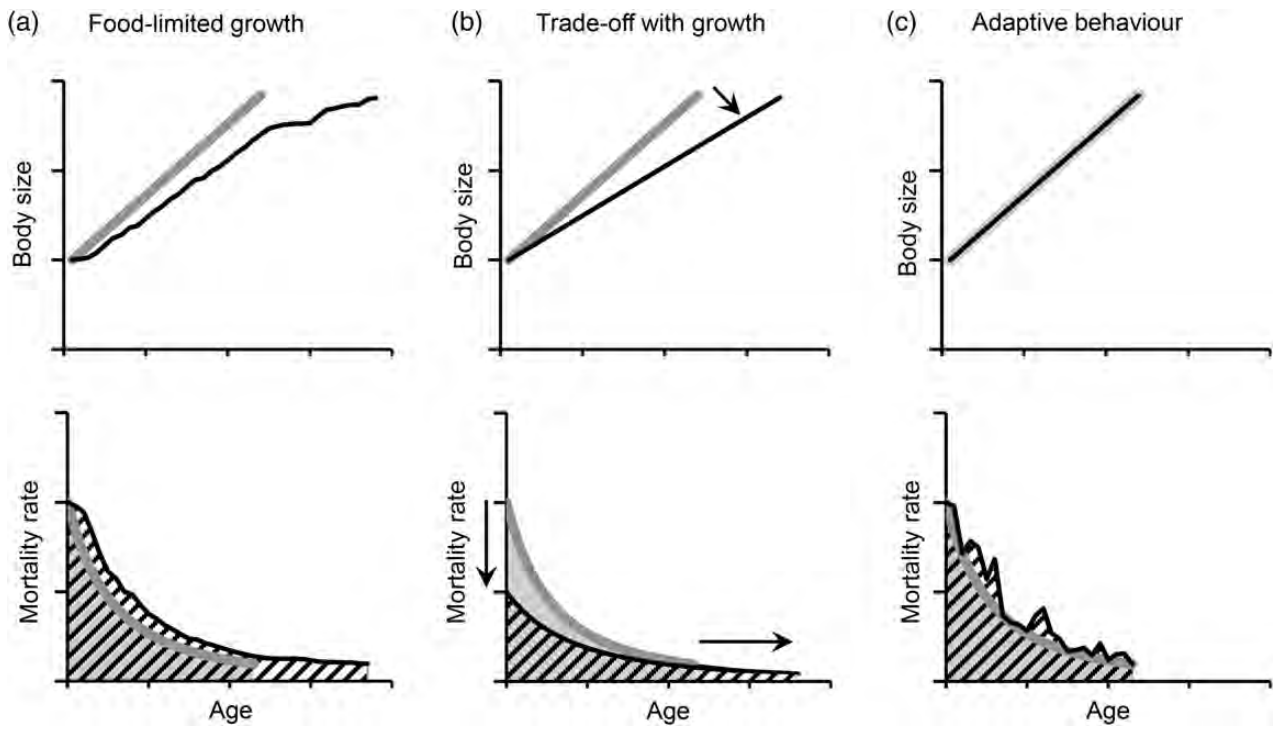

Figure 4. Schematic illustration comparing mechanisms that link growth and survival in larval fish. (**a**) Under food-dependent growth, periods of low food availability (black lines) will reduce growth below the physiological maximum (grey line in all panels) and thus prolong the developmental phase. Assuming mortality is size-dependent, it will be higher at any given age and last longer because development to metamorphosis takes more time. (**b**) Behavioural ecology focuses on trade-offs with growth, and how risk acceptance and growth rate are related. Growth rate could be reduced by following a more cautious strategy (black line), which would incur a lower mortality rate at any given size (indicated by vertical arrow next to the mortality axis) but a longer duration (horizontal arrow). The trajectory of age-dependent mortality with lowest area under the curve has the highest survival and will likely be favoured by natural selection. (**c**) Behaviour can change rapidly, and optimization models suggest that fish larvae increase their risk-taking during periods of low food availability to maintain high growth rates (Fiksen and Jørgensen, 2011). Environmental variation in food levels (black lines) would then not be visible in growth rates, but would reduce survival because mortality is elevated when food is low).

Behavioural trade-offs may also cause patterns of "growth-selective predation". Although Figure 2 emphasizes how the main effect of variation in food is to affect survival, it also shows a correlation between growth rate and survival rate. If the environment is sufficiently severe, larvae may grow more slowly and take higher levels of risk, thus reducing their survival, which could be observed as "growth-selective predation".

To some degree, it might therefore seem that the various hypotheses appearing in the oceanography literature have remained as catchy phrases that identify isolated parts of a larger puzzle. A more coherent perspective can be gained by adopting evolutionary thinking and concepts from behavioural ecology. As an example, consider how adaptive behaviour may explain the abovementioned observed relationships between food and survival: Beaugrand *et al.* (2003) showed that recruitment of North Sea cod over 42 years was correlated to a broadly composed plankton index, which seemingly contrasts the observation that cod larvae in the sea apparently grow close to their temperature-dependent capacity, independent of food density (Folkvord, 2005). To reconcile these observations, the key is to de-emphasize the link between food and growth: through adaptive behaviour, variation in food and match–mismatch can cause large variations in risk-taking, survival, and recruitment, but may not involve variation in growth. The optimality model referred to above (Fiksen and Jørgensen, 2011) suggests a role for food availability in influencing survival that extends far beyond the level where it becomes limiting for growth (Figure 2), which in fact strengthens the importance of prey availability for recruitment success. It should be borne in mind that all these factors may explain how efficient a given spawning stock biomass is at producing recruits; it does not challenge the very real effect of the size of the spawning stock on recruitment to fish stocks. Still, in a modelling study of developing fish larvae in a water column of observed environmental parameters, vertical migration increased survival from 6 to 18 mm by several thousand times compared to random behaviour (Kristiansen *et al.*, 2009), suggesting that adequate larval behaviour can improve fitness by a magnitude that can rarely be achieved e.g. through increased maternal production of gonads.

We are also aware that not all species fit within this framework. In some species, larvae depend on benign environments to find ephemeral patches of food (Winemiller and Rose, 1993) or to drift into profitable nursery habitats (Siegel *et al.*, 2008); for these species, variable strategies and bet-hedging may be more important for recruitment success than the growth-survival trade-offs on which we have focused. In other species, the bottleneck is not at the larval stage but later, and in those species detailing the early life stages will have little bearing on predictions of recruitment.

Implications for biophysical models of fish larvae

To assess larval survival and recruitment success, modern fisheries science relies heavily on large-scale physically-coupled ecosystem models. In linking recruitment success to environmental conditions, the emphasis has been on how differences in temperature

and food availability lead to fluctuations in growth, survival and recruitment success. While mortality is usually parameterized as constant or size-dependent, the focus has been on how food variation may induce differences in growth, with consequences for survival (e.g. Peck and Hufnagl, 2012). This is natural, since these processes can be studied in the laboratory and used as input to biophysical models. Several experiments have quantified how well-fed larvae grow at different temperatures (Otterlei *et al.*, 1999; Houde, 1989), and how much larvae feed and grow when administered different food rations (Letcher and Bengtson, 1993). The loss due to mortality in the field is much more difficult to observe and quantify due to obvious logistic reasons.

The above arguments suggest that improved predictions for recruitment may require a focus on how adaptive behaviour can have strong effects on survival. A first and easy modification is to replace the current assumption that reduced food reduces growth with implications for survival, with the perspective suggested in this paper, whereby reduced food leads to reduced survival through adaptive behaviour, but with few implications for growth. A more explicit way to do it is to implement the trade-offs directly into the model, for instance by a suite of behavioural options (such as swimming speed and depth selection) which influence growth and mortality. The assumption that individuals instantly minimize the ratio between mortality and growth (Gilliam's Rule, see Figure 1) is a good approximation to fitness, and this will incorporate the direct survival-effect from increased food availability (see Vikebø *et al.*, 2007; Kristiansen *et al.*, 2009 for examples). These types of model mechanistically connect environmental conditions to larval survival (Vikebø *et al.*, 2007; Opdal *et al.*, 2008), allow incorporation of behavioural strategies that are responsive to individual state (Kristiansen *et al.*, 2009), and may link larval traits to parental reproductive strategies (Opdal *et al.*, 2011).

If prey is size-structured, then models need to specify which prey should be included in the diet, and a similar approach could be taken by use of optimal foraging theory, for which an algorithm has been developed for larval fish (Letcher *et al.*, 1996). A similar behavioural approach to diet breadth may also be useful in ecosystem models (Visser and Fiksen, 2013). The inclusion of flexible or adaptive behaviours in mass-balanced ecosystem models is currently a central theme in ecology, and marine ecosystem models with behaviourally responsive agents are emerging (Castellani *et al.*, 2013).

Finally, biophysical models would benefit from incorporating predation more mechanistically (Huse and Fiksen, 2010). This would require careful and detailed consideration of larval behaviour, predator–prey mechanics, and the proximate aspects of sensory systems, decision-making, and behaviour. This is definitely not an easy task and presupposes basic research in a range of disciplines, but may offer a route to more reliable models and better understanding of the role of ocean productivity in the formation of strong year-classes.

Acknowledgements

We thank Howard Browman, Kenneth Rose and an anonymous reviewer for constructive comments.

Funding

We thank the Reseach Council of Norway for funding.

References

Aksnes, D. L., and Utne, A. C. W. 1997. A revised model of visual range in fish. Sarsia, 82: 137–147.

Andersen, K. H., and Beyer, J. E. 2006. Asymptotic size determines species abundance in the marine size spectrum. American Naturalist, 168: 54–61.

Arendt, J. D. 1997. Adaptive intrinsic growth rates: an integration across taxa. Quarterly Review of Biology, 72: 149–177.

Arnott, S. A., Chiba, S., and Conover, D. O. 2006. Evolution of intrinsic growth rate: metabolic costs drive trade-offs between growth and swimming performance in *Menidia menidia*. Evolution, 60: 1269–1278.

Beaugrand, G., Brander, K. M., Lindley, J. A., Souissi, S., and Reid, P. C. 2003. Plankton effect on cod recruitment in the North Sea. Nature, 426: 661–664.

Billerbeck, J. M., Lankford, T. E., and Conover, D. O. 2001. Evolution of intrinsic growth and energy acquisition rates. I. Trade-offs with swimming performance in *Menidia menidia*. Evolution, 55: 1863–1872.

Biro, P. A., Abrahams, M. V., Post, J. R., and Parkinson, E. A. 2006. Behavioural trade-offs between growth and mortality explain evolution of submaximal growth rates. Journal of Animal Ecology, 75: 1165–1171.

Castellani, M., Rosland, R., Urtizberea, A., and Fiksen, Ø. 2013. A mass-balanced pelagic ecosystem model with size-structured behaviourally adaptive zooplankton and fish. Ecological Modelling, 251: 54–63.

Clark, C. W., and Levy, D. A. 1988. Diel vertical migrations by juvenile sockeye salmon and the antipredation window. American Naturalist, 131: 271–290.

Clark, C. W., and Mangel, M. 2000. Dynamic State Variable Models in Ecology. Oxford University Press, New York.

Clark, D. L., Leis, J. M., Hay, A. C., and Trnski, T. 2005. Swimming ontogeny of larvae of four temperate marine fishes. Marine Ecology Progress Series, 292: 287–300.

Crean, A. J., and Marshall, D. J. 2009. Coping with environmental uncertainty: dynamic bet hedging as a maternal effect. Philosophical Transactions of the Royal Society of London. Series B, Biological Sciences, 364: 1087–1096.

Cushing, D. H. 1973. Dependence of recruitment on parent stock. Journal of the Fisheries Research Board of Canada, 30: 1965–1976.

Cushing, D. H. 1990. Plankton production and year-class strength in fish populations: an update of the match mismatch hypothesis. Advances in Marine Biology, 26: 249–293.

Dragesund, O. 1970. Factors influencing year-class strength of Norwegian spring spawning herring. Fiskeridirektoratets skrifter serie havundersøkelser, 15: 381–450.

Emlen, J. M. 1966. The role of time and energy in food preference. American Naturalist, 100: 611–617.

Enberg, K., Jørgensen, C., Dunlop, E. S., Varpe, Ø., Boukal, D. S., Baulier, L., Eliassen, S., *et al.* 2012. Fishing-induced evolution of growth: concepts, mechanisms, and the empirical evidence. Marine Ecology, 33: 1–25.

Fiksen, Ø., and Jørgensen, C. 2011. Model of optimal behaviour in fish larvae predicts that food availability determines survival, but not growth. Marine Ecology Progress Series, 432: 207–219.

Fiksen, Ø., Jørgensen, C., Kristiansen, T., Vikebø, F., and Huse, G. 2007. Linking behavioural ecology and oceanography: larval behaviour determines growth, mortality and dispersal. Marine Ecology Progress Series, 347: 195–205.

Folkvord, A. 2005. Comparison of size-at-age of larval Atlantic cod (*Gadus morhua*) from different populations based on size- and temperature-dependent growth models. Canadian Journal of Fisheries and Aquatic Sciences, 62: 1037–1052.

Fuiman, L. A. 1989. Vulnerability of Atlantic herring larvae to predation by yearling herring. Marine Ecology Progress Series, 51: 291–299.

Hjort, J. 1914. Fluctuations in the great fisheries of Northern Europe viewed in the light of biological research. Rapports et Procès-verbaux des Réunions du Conseil International pour l'Exploration de la Mer, 20: 1–228.

Hjort, J. 1926. Fluctuations in the year classes of important food fishes. ICES Journal of Marine Science, 1: 5–38.

Holling, C. S. 1965. The functional response of predators to prey density and its role in mimicry and population regulation. Memoirs of the Entomological Society of Canada, 45: 3–60.

Houde, E. D. 1987. Fish early life dynamics and recruitment variability. American Fisheries Society Symposium, 2: 17–29.

Houde, E. D. 1989. Comparative growth, mortality, and energetics of marine fish larvae: temperature and implied latitudinal effects. Fishery Bulletin, 87: 471–495.

Houde, E. D. 1997. Patterns and consequences of selective processes in teleost early life histories. *In* Early Life History and Recruitment in Fish Populations, pp. 173–196. Ed. by R. C. Chambers, and E. A. Trippel. Chapmann & Hall, London.

Houston, A. I., and McNamara, J. M. 1999. Models of Adaptive Behaviour. An Approach Based on State. Cambridge University Press, Cambridge.

Huse, G., and Fiksen, Ø. 2010. Modelling encounter rates and distribution of mobile predators and prey. Progress in Oceanography, 84: 93–104.

Huwer, B., Clemmesen, C., Grønkjær, P., and Köster, F. W. 2011. Vertical distribution and growth performance of Baltic cod larvae – Field evidence for starvation-induced recruitment regulation during the larval stage? Progress in Oceanography, 91: 382–396.

Iwasa, Y. 1982. Vertical migration of zooplankton: a game between predator and prey. American Naturalist, 120: 171–180.

Jørgensen, C., Auer, S. K., and Reznick, D. N. 2011. A model for optimal offspring size in fish, including livebearing and parental effects. American Naturalist, 177: E119–E135.

Kiørboe, T. 2011. How zooplankton feed: mechanisms, traits and trade-offs. Biological Reviews, 86: 311–339.

Krebs, J. R., and Kacelnik, A. 1991. Decision making. *In* Behavioural Ecology: An Evolutionary Approach, pp. 105–137. Ed. by J. R. Krebs, and N. B. Davies. Blackwell Scientific Publishers, Oxford.

Kristiansen, T., Jørgensen, C., Lough, R. G., Vikebø, F., and Fiksen, Ø. 2009. Modeling rule-based behavior: habitat selection and the growth-survival trade-off in larval cod. Behavioral Ecology, 20: 490–500.

Lankford, T. E., Billerbeck, J. M., and Conover, D. O. 2001. Evolution of intrinsic growth and energy acquisition rates. II. Trade-offs with vulnerability to predation in *Menidia menidia*. Evolution, 55: 1873–1881.

Leis, J. 2007. Behaviour of fish larvae as an essential input for modelling larval dispersal: behaviour, biogeography, hydrodynamics, ontogeny, physiology and phylogeny meet hydrography. Marine Ecology Progress Series, 347: 185–193.

Letcher, B. H., and Bengtson, D. A. 1993. Effects of food density on growth and on patterns of prey depletion by larval silverside fish, *Menidia-beryllina* (cope) – a laboratory investigation with image-analysis. Journal of Experimental Marine Biology and Ecology, 167: 197–213.

Letcher, B. H., Rice, J. A., Crowder, L. B., and Rose, K. A. 1996. Variability in survival of larval fish: disentangling components with a generalized individual-based model. Canadian Journal of Fisheries and Aquatic Sciences, 53: 787–801.

Lima, S. L., and Dill, L. M. 1990. Behavioral decisions made under the risk of predation: a review and prospectus. Canadian Journal of Zoology-Revue Canadienne De Zoologie, 68: 619–640.

Litvak, M. K., and Leggett, W. C. 1992. Age and size-selective predation on larval fishes: the bigger-is-better hypothesis revisited. Marine Ecology Progress Series, 81: 13–24.

McGurk, M. D. 1986. Natural mortality of marine pelagic fish eggs and larvae: role of spatial patchiness. Marine Ecology Progress Series, 34: 227–242.

McNamara, J. M., and Houston, A. I. 1987. Starvation and predation as factors limiting population-size. Ecology, 68: 1515–1519.

Opdal, A. F., Vikebø, F., and Fiksen, Ø. 2008. Relationships between spawning ground identity, latitude and early life thermal exposure in Northeast Arctic cod. Journal of Northwest Atlantic Fishery Science, 41: 13–22.

Opdal, A. F., Vikebø, F. B., and Fiksen, Ø. 2011. Parental migration, climate and thermal exposure of larvae: spawning in southern regions gives Northeast Arctic cod a warm start. Marine Ecology Progress Series, 439: 255–262.

Otterlei, E., Nyhammer, G., Folkvord, A., and Stefansson, S. O. 1999. Temperature- and size-dependent growth of larval and early juvenile Atlantic cod (*Gadus morhua*): a comparative study of Norwegian coastal cod and northeast Arctic cod. Canadian Journal of Fisheries and Aquatic Sciences, 56: 2099–2111.

Peacor, S. D., Peckarsky, B. L., Trussell, G. C., and Vonesh, J. R. 2013. Costs of predator-induced phenotypic plasticity: a graphical model for predicting the contribution of nonconsumptive and consumptive effects of predators on prey. Oecologia, 171: 1–10.

Peck, M. A., and Hufnagl, M. 2012. Can IBMs tell us why most larvae die in the sea? Model sensitivities and scenarios reveal research needs. Journal of Marine Systems, 93: 77–93.

Peterson, I., and Wroblewski, J. S. 1984. Mortality rate of fishes in the pelagic ecosystem. Canadian Journal of Fisheries and Aquatic Sciences, 41: 1117–1120.

Pope, J. G., Shepherd, J. G., and Webb, J. 1994. Successful surf-riding on size spectra: the secret of survival in the sea. Philosophical Transactions of the Royal Society of London Series B, Biological Sciences, 343: 41–49.

Reznick, D. N., Schultz, E., Morey, S., and Roff, D. 2006. On the virtue of being the first born: the influence of date of birth on fitness in the mosquitofish, *Gambusia affinis*. Oikos, 114: 135–147.

Sheldon, R. W., Prakash, A., and Sutcliffe, W. H., Jr. 1972. The size distribution of particles in the ocean. Limnology and Oceanography, 17: 327–340.

Shine, R. 1978. Propagule size and parental care: the "safe harbor" hypothesis. Journal of Theoretical Biology, 75: 417–424.

Siegel, D. A., Mitarai, S., Costello, C. J., Gaines, S. D., Kendall, B. E., Warner, R. R., and Winters, K. B. 2008. The stochastic nature of larval connectivity among nearshore marine populations. Proceedings of the National Academy of Sciences U S A 105: 8974–8979.

Sinclair, M., and Solemdal, P. 1988. The development of 'population thinking' in fisheries biology between 1878 and 1930. Aquatic Living Resources, 1: 189–213.

Skajaa, K., and Browman, H. I. 2007. The escape response of food-deprived cod larvae (*Gadus morhua* L.). Journal of Experimental Marine Biology and Ecology 353: 135–144.

Skajaa, K., Fernö, A., and Folkvord, A. 2003. Swimming, feeding and predator avoidance in cod larvae (*Gadus morhua L.*): trade-offs between hunger and predation risk. *In* The Big Fish Bang: Proceedings of the 26th Annual Larval Fish Conference, pp. 105–121. Ed. by H. I. Browman, and A. B. Skiftesvik.

Skajaa, K., Fernö, A., and Folkvord, A. 2004. Ontogenetic- and condition-related effects of starvation on responsiveness in herring larvae (*Clupea harengus* L.) during repeated attacks by a model predator. Journal of Experimental Marine Biology and Ecology 312: 253–269.

Smith, C. C., and Fretwell, S. D. 1974. The optimal balance between size and number of offspring. The American Naturalist, 108: 499–506.

Takasuka, A., and Aoki, I. 2006. Environmental determinants of growth rates for larval Japanese anchovy *Engraulis japonicus* in different waters. Fisheries Oceanography, 15: 139–149.

Takasuka, A., Aoki, I., and Mitani, I. 2003. Evidence of growth-selective predation on larval Japanese anchovy *Engraulis japonicus* in Sagami Bay. Marine Ecology Progress Series, 252: 223–238.

Vikebø, F. B., Jørgensen, C., Kristiansen, T., and Fiksen, Ø. 2007. Drift, growth and survival of larval Northeast Arctic cod with simple rules of behaviour. Marine Ecology Progress series, 347: 207–219.

Visser, A. W., and Fiksen, Ø. 2013. Optimal foraging in marine ecosystem models: selectivity, profitability and switching. Marine Ecology Progress Series, 473: 91–101.

Visser, A. W., and Kiørboe, T. 2006. Plankton motility patterns and encounter rates. Oecologia, 148: 538–546.

Werner, E. E., and Gilliam, J. F. 1984. The ontogenetic niche and species interactions in size-structured populations. Annual Review of Ecological Systems, 15: 393–425.

Winemiller, K. O., and Rose, K. A. 1993. Why do most fish produce so many tiny offspring? American Naturalist, 142: 585–603.

Handling editor: Howard Browman

ICES Journal of Marine Science

ICES Journal of Marine Science (2014), 71(4), 918–924. doi:10.1093/icesjms/fst103

Contribution to the Themed Section: 'Larval Fish Conference'

Quo Vadimus

Modelling larval fish navigation: the way forward

Erica Staaterman and Claire B. Paris*

Applied Marine Physics and Marine Biology and Fisheries, Rosenstiel School of Marine and Atmospheric Science, University of Miami, 4600 Rickenbacker Causeway, Miami, FL 33149, USA

**Corresponding author: tel: +1 305 421 4219; fax: +1 305 421 4701; e-mail: cparis@rsmas.miami.edu*

Staaterman, E., and Paris, C. B. 2014. Modelling larval fish navigation: the way forward. – ICES Journal of Marine Science, 71: 918–924.

Received 2 November 2012; accepted 30 May 2013; advance access publication 24 August 2013.

Recent advances in high-resolution ocean circulation models, coupled with a greater understanding of larval behaviour, have increased the sophistication of individual-based, biophysical models used to study the dispersal of larvae in the sea. Fish larvae, in particular, have the ability to swim directionally and increasingly fast during ontogeny, indicating that they may not only disperse, but also migrate using environmental signals. How and when larvae use local and large-scale cues remains a mystery. Including three-dimensional swimming schemes into biophysical models is becoming essential to address these questions. Here, we highlight state-of-the-art modelling of vertical and horizontal migrations of fish larvae, as well as current challenges in moving towards more realistic larval movements in response to cues. Improved understanding of causes for orientation will provide insight into the evolutionary drivers of dispersal strategies for fish and marine organisms in general.

Keywords: behaviour, biophysical model, dispersal, fish larvae, migration, orientation.

Introduction

Within the past decades, the realism of high-resolution ocean circulation models that represent a range of oceanographic features (Kingsford, 1990; Gawarkiewicz *et al.*, 2007) at a variety of spatial scales (Monismith, 2007) has provided the basis for effective Lagrangian tools to quantify larval dispersal and reveal the critical role of the pelagic larval stage in structuring marine populations (Werner *et al.*, 2007). The rapid development of many-task parallel computing techniques allows the coupling of operational (i.e. validated) ocean circulation models with individual-based model (IBM) applications, thus simulating the movement of million of particles with individual behaviours and biological traits. These coupled applications are typically referred to as "biophysical" models and are indispensable tools for addressing the complex physical–biological interactions that occur during the pelagic phase of marine organisms.

As more information emerges about the sensory and locomotor abilities of marine larvae (reviewed in Montgomery *et al.*, 2001; Kingsford *et al.*, 2002; Leis, 2006), it is becoming essential to incorporate into biophysical models not only larval traits, but also larval swimming in response to environmental signals (Armsworth, 2000; Paris *et al.*, 2007; Willis, 2011). In addition, the empirical study of larval navigation and sensitivity to cues is a growing field of exciting research, particularly for coral reef fish (e.g. Leis and Carson-Ewart, 1998; Atema *et al.*, 2002; Simpson *et al.*, 2005; Leis, 2006; Mann *et al.*, 2007; Paris *et al.*, 2008; Radford *et al.*, 2012). Including orientation to various types of proximal reef cues has thus become a central issue in modelling the pelagic phase of coral reef fish (Leis, 2007; Leis *et al.*, 2011). How and when during ontogeny large-scale cues play a role in the transport of fish larvae is still a mystery. Here, we will focus on the current state-of-the-art modelling of vertical and horizontal "migrations" of fish larvae and further suggest a series of improvements towards modelling more realistic three-dimensional movements.

Physical vs. biological stochasticity

Stochasticity in IBMs can result from two different processes: physical processes unresolved by the hydrodynamic model and parameterized as turbulent diffusivity representing subgrid scale turbulence or biological processes representing intrinsic variability that result in individual capabilities, choices, and movements. The differences between these two types of stochasticity are often unclear, but should be stated explicitly, because they originate from different sources.

Particles are advected by space and time-interpolated currents in circulation models and have an additional stochastic component to represent the effects of turbulence. Turbulent diffusion can be introduced in various ways. Simple solutions vary the particles' initial boundary conditions over space while interpolating the velocity field from adjacent grids (Mitarai *et al.*, 2008). These solutions can be augmented with Lagrangian stochastic particle models (LSPMs; Griffa, 1996). Random walk models can take various forms such as purely random displacement models (Brickman and Smith, 2002) and correlated random walks (CRWs), where previous steps are remembered, have been adopted (Paris *et al.*, 2007; Willis, 2011). These LSPMs can be implemented in the horizontal or in the vertical and are typically scaled by a turbulent diffusivity parameter that represents the subgrid scale turbulent motion (Okubo, 1971; Paris *et al.*, 2002). If the only stochasticity that exists in the model is from turbulence, it is important to emphasize that although each individual follows a unique trajectory, the randomness observed is a result of physics, not a result of animal behaviour. However, using different techniques, it is possible to explicitly include stochasticity that results from animal behaviour as well (explained in the swimming section below). Again, the distinction between biological and physical stochasticity is often overlooked or confused; yet, it is critical to explicitly state these two different sources of individual variability in the models.

Swimming behaviour

More than a decade ago, vertical migrations were identified as a critical component influencing transport outcomes (Werner *et al.*, 1993; Paris and Cowen, 2004; Parada *et al.*, 2008; Irisson *et al.*, 2010). Although ontogenetic vertical migrations typically represent a retention mechanism and increase settlement near the natal habitat (Werner *et al.*, 1993; Paris and Cowen, 2004), shorter term vertical migrations related to diel light cycles (Parada *et al.*, 2008; Ospina-Alvarez *et al.*, 2012), salinity and chlorophyll gradients (Cowen *et al.*, 2003), and/or tidal cycles (Cox *et al.*, 2006; Sentchev and Korotenko, 2007) can also affect settlement location and settlement success. The effect of vertical movement on reducing dispersal kernels was the initial focus (Paris and Cowen, 2004; Paris *et al.*, 2007), but further questions in causal effects of vertical migration have emerged. For example, Bonhommeau *et al.* (2009) conducted a sensitivity analysis on the extent of vertical migration in European eels to determine whether these larvae could possibly cross the Atlantic in 6 months, as otolith data suggested, without any horizontal swimming. Other recent studies have used more complex rule-based behaviours to move larvae vertically in search of food or to avoid predators and have examined the ecological trade-offs of these individual behavioural choices (Fiksen *et al.*, 2007; Vikebø *et al.*, 2007; Kristiansen *et al.*, 2009). Thus, vertical migration models have become more sophisticated and investigators can now ask questions related to behavioural strategies, population connectivity, and evolutionary processes (Lett *et al.*, 2010; Foster *et al.*, 2012).

The addition of horizontal swimming to biophysical models has been more recent, but is equally important, as many larval fish are fast swimmers (Fisher, 2005). Several studies have included simple horizontal swimming, where animals swim into the current (Healey *et al.*, 2000; Mork *et al.*, 2012), or directly towards their targets (Wolanski *et al.*, 1997; Porch, 1998; James *et al.*, 2002), which significantly affects settlement success. Yet, these models failed to include biologically driven stochasticity, which is essential to represent variability in individual traits (Thorrold *et al.*, 1997; Llopiz and Cowen, 2009) and behavioural choices. Individual traits can be introduced simply by changing the boundary conditions of the particles in both time and space (Berkley *et al.*, 2010), or more realistically by varying the attributes of particles, following an observed range and distribution of traits. Randomness in larval orientation behaviour is included intrinsically when using a biased CRW (BCRW), which chooses the direction of animal movement in each time-step from a distribution of possible angles (Codling *et al.*, 2004). Here, the model keeps track of the animal's previous direction, similar to the CRW, but also gives it a preferred direction, such as the location of settlement habitat (Codling *et al.*, 2004). For fish larvae, BCRWs have been explored predominantly in the theoretical realm, using unidirectional currents or single patch habitats (Armsworth, 2000; Armsworth *et al.*, 2001; Codling *et al.*, 2004). Recently, Staaterman *et al.* (2012) merged a BCRW with a biophysical model that utilized real-time-varying flowfields, realistic settlement habitats, and variable particle traits. In this study, the transport of fish larvae was driven by currents and larval swimming vectors, and swimming speed increased throughout ontogeny following Fisher (2005). The cues to which the larvae were able to orient were radially propagating cues, similar to acoustic signals (Kalmijn, 1988), and orientation behaviour only took place when larvae were within a given detection distance from the reef. A unique aspect of the study by Staaterman *et al.* (2012) was the combination of both ontogenetic vertical migration inferred from field-based observations (Paris and Cowen, 2004) and horizontal orientation behaviour. Because marine organisms inhabit a three-dimensional medium and constantly encode three-dimensional information (Holbrook and Burt de Perera, 2009), models that only address horizontal or vertical components of movement will be inherently limited.

In general, it is most appropriate to include three-dimensional movements of animals throughout their pelagic life. Given limited food resources and depleting energy reserves during swimming, fish larvae may experience a trade-off in local habitat selection (Vikebø *et al.*, 2007). Vertical and horizontal movement strategies can allow individuals to seek food, avoid advection, and minimize predation, with varying levels of risks and rewards. These trade-offs should be investigated through biophysical models that track individual fitness (see the "The internal state of the organism" section). In general, a better understanding of the individual motivations of vertical and horizontal movements will enhance the sophistication of biophysical models and the questions that researchers can ask (Irisson *et al.*, 2010; Leis *et al.*, 2011).

Swimming speeds and behaviours are known to differ between species, ontogenetic stages, and water temperatures (Leis *et al.*, 2013). In a rare study of larval fish behaviour at night, Fisher and Bellwood (2003) noted that the proportion of time larvae spent swimming at night tends to increase throughout ontogeny, while certain species also experience an increase in swimming speed. When modelling orientation behaviours, these species-specific day–night and ontogenetic changes should be taken into account. Furthermore, species that occur in temperate waters tend to have slower larvae (5–10 body length s^{-1}; Leis, 2010), while most tropical taxa have fast-swimming larvae (15–20 body length s^{-1}; Leis, 2010; also reviewed in Leis *et al.*, 2013). One possible explanation is that the transition from a viscous to an inertial hydrodynamic regime occurs at smaller sizes in tropical larvae than temperate larvae (Leis, 2010). Therefore, tropical larvae spend a large proportion of their pelagic life as effective swimmers (Fisher, 2005). However, these trends have exceptions in some cold water species

that swim slower with increased temperatures (Guan *et al.*, 2008). Modellers should use known swimming speeds, but when empirical data are lacking, it becomes critical to use values that are reasonable for the region of interest (e.g. temperate, tropical). A recent review by Leis *et al.* (2013) indicates that there are quantifiable differences in the swimming behaviour of fish larvae between low and high latitudes.

Orientation in response to multiple navigational cues

Recent work examined orientation behaviour in response to relatively small-scale, radially propagating cues, such as the soundscape of a coral reef (Staaterman *et al.*, 2012). It is more likely, however, that larvae utilize a suite of cues throughout ontogeny and at different distances from the reef (e.g. Kingsford *et al.*, 2002; Leis, 2010; Leis *et al.*, 2011). Furthermore, individual larvae from any given cohort will have different orientation abilities (Leis, 2007), which can be included by varying the detection distance of cues. An ideal model would shift cue usage and sensitivity throughout space and time, as described below (Figure 1).

It is also reasonable to expect that the early pelagic stages of fish may use guidance from magnetic and celestial cues, similar to adult fish species that undertake homing migrations (Jorge *et al.*, 2012; Putman *et al.*, 2013). The simplest mechanism for orientation behaviour would be to use a simple vector-navigation strategy to swim in a particular cardinal direction. This can be done with sensitivity to location-independent signals such as magnetic and solar compasses (Flamarique and Browman, 2000; Kingsford *et al.*, 2002; Leis *et al.*, 2011). A more complex mechanism for true navigation would be the use of both a compass and a map. For example, larvae could detect map-like cues originating at the sea surface and compensate for displacement, while using a sun compass to swim directionally (Paris *et al.*, in review). These types of behaviours using large-scale cues would be relevant early in the pelagic phase or while fish are still far from the settlement habitat, unable to detect proximal cues (e.g. Figure 1, region A).

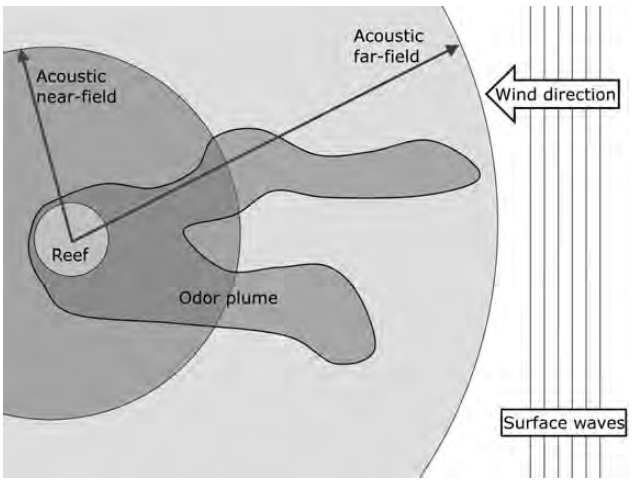

Figure 1. A theoretical framework shows the various cues available to larvae as they move throughout space. Region A: Far from the reef, orientation is limited to use of magnetic cues, polarized light, or sun compass; larvae simply swim towards a particular cardinal direction or maintain an angle relative to the mean direction of surface capillary waves. Region B: Inside the acoustic far field, organisms with the ability to detect acoustic pressure can use it as a navigational signal; larvae swim towards the origin of this radially propagating cue. Region C: Inside of an odour plume, chemical signals may provide information about the source of the odour; larvae that encounter an odour plume may swim upstream (taxis) or swim at a different speed (kinesis). Regions D and E: Within the acoustic nearfield, fish can detect the direction of the sound source; larvae swim towards the origin of this radially propagating cue. In areas such as D and C, where multiple cues are available, larvae should orient using a rule-based hierarchy based on empirical data. The actual size of regions B – E depends on the intensity and frequency components of the soundscape, the concentration of chemicals on the reef, the magnitude of turbulence, the mean current speed and direction near the reef, as well as detection abilities of the study species.

Chemical signals emanating from nursery areas are typically transported several kilometres offshore before dissipating and could be sensed by fish larvae (Atema, 2012). Odours may be used as a signal to switch to directional cues, as an orientation beacon, or through spatial mapping (Rossier and Schenk, 2003; Arvedlund and Kavanagh, 2009; Jacobs, 2012). However, chemical signatures may be somewhat less predictable in space due to their dependence on physical properties such as tidal currents and eddy fields or in time due to the stochastic nature of storms (Atema *et al.*, 2002; Leis *et al.*, 2011). To properly model the presence of a chemical signal, a dye-release Eulerian module should be used to create an "odour plume". Then, various types of rule-based behaviours could be assigned to the larvae when they encounter the plume (e.g. Figure 1, region C). For example, when the concentration of the odour exceeds a given threshold, larvae could begin orienting towards its source using an infotaxis search strategy (Vergassola *et al.*, 2007).

For radially propagating signals such as acoustic cues, the size of the maximum detection distance can be changed for individuals or throughout ontogeny (Leis, 2007). For example, instead of assigning a cohort of individuals the same maximum detection distance, their detection distances can be chosen from a distribution, reflecting maternal effects (Green and Chambers, 2007). In addition, the size of the detection distance can increase throughout ontogeny as sensory abilities increase (Blaxter, 1986; Leis, 2007). These changes could apply to the entire cohort or could change based on an animal's feeding history (see section on rule-based behaviours below).

There should also be an attempt to distinguish between the near-field region, where acoustic particle motion dominates, and the far-field region, where acoustic pressure dominates (Kalmijn, 1988; Mann *et al.*, 2007), as marine organisms have different sensitivities to these components of the acoustic field (Popper and Fay, 2011). Furthermore, the actual distance of detection will depend on not only the hearing abilities of the species of interest, but also the dominant frequency of the reef spectrum. Lower-frequency sounds have longer wavelengths and thus a larger acoustic nearfield, whereas higher-frequency sounds, such as those emitted by snapping shrimp, have a smaller acoustic nearfield (Kalmijn, 1988). Although most marine fish can detect acoustic particle motion via direct stimulation of the otoliths, far fewer species can detect acoustic pressure (Popper and Fay, 2011). Thus, the decision of whether to include orientation behaviour in the far-field (Figure 1, region B) and not just the nearfield (Figure 1, regions D and E) will depend on the species of interest.

The internal state of the organism

The internal state of the organism at any point during its pelagic journey will influence its motivation to move, its movement capabilities, and its navigational abilities (Nathan *et al.*, 2008), which

in turn will influence the degree to which orientation behaviour shapes its path. Furthermore, the feeding history and total distance travelled by the larva will affect its state upon arrival at the reef and its ability to survive post-settlement processes (Searcy and Sponaugle, 2001; Grorud-Colvert and Sponaugle, 2006). Therefore, it is important to keep track of the internal state of the larva within each time-step and to assess its state at the end of the pelagic larval phase (Irisson *et al.*, 2004).

New algorithms have been developed to test behavioural strategies for larvae as they migrate vertically (Fiksen *et al.*, 2007; Kristiansen *et al.*, 2009). These models allow larvae to move based on a strategy that is informed by both their external state (e.g. their present depth layer and the trade-off between the presence of food and predators), as well as their internal state (e.g. gut fullness; Kristiansen *et al.*, 2009). These strategies can change with ontogenetic stage (Vikebø *et al.*, 2007) or environmental conditions (Kristiansen *et al.*, 2011). Finally, the fitness of the organism at the end of its pelagic phase can be evaluated based on its history and the location where it settled (Vikebø *et al.*, 2007). These types of rule-based models are extremely useful for determining an optimal strategy for the survival and settlement of larvae, but one critical piece is missing: the role of orientation behaviour.

Future work with orientation behaviour should be used in conjunction with such rule-based vertical migration behaviours as outlined above. Although Staaterman *et al.* (2012) did include ontogenetic vertical migration, all larvae of each cohort were moved with a time-varying probability matrix where individuals moved at random between adjacent depth bins, following Paris *et al.* (2007). Also, all larvae moved with the same swimming speed, which changed throughout ontogeny. A more sophisticated approach would incorporate rules and keep track of feeding behaviour for each individual in each time-step. The feeding history would inform the growth rate and size, and thus the magnitude of vertical and horizontal swimming that each larva can. At the end of the simulation, the total swimming distance travelled and the energetic state of individual larvae should be incorporated into fitness calculations, because the condition upon arrival to suitable nursery grounds can affect survival during post-settlement or post-metamorphosis processes, as well as future reproductive success (Searcy and Sponaugle, 2001).

Variability in settlement habitats

In the BCRW, the parameter representing the strength of a cue emanating from a habitat is k (Codling *et al.*, 2004) and was represented as a single value assigned to all habitat polygons in Staaterman *et al.* (2012). To reflect spatial variability in habitat quality, different values of k should be assigned to each polygon based on data from various habitat indices (e.g. CREMP; Palandro *et al.*, 2008; Ruzicka *et al.*, 2009). One useful avenue for this type of research is to determine the best location for Marine Protected Areas (MPAs), which has been examined previously, but not with active orientation behaviour (Jones *et al.*, 2007; Botsford *et al.*, 2009).

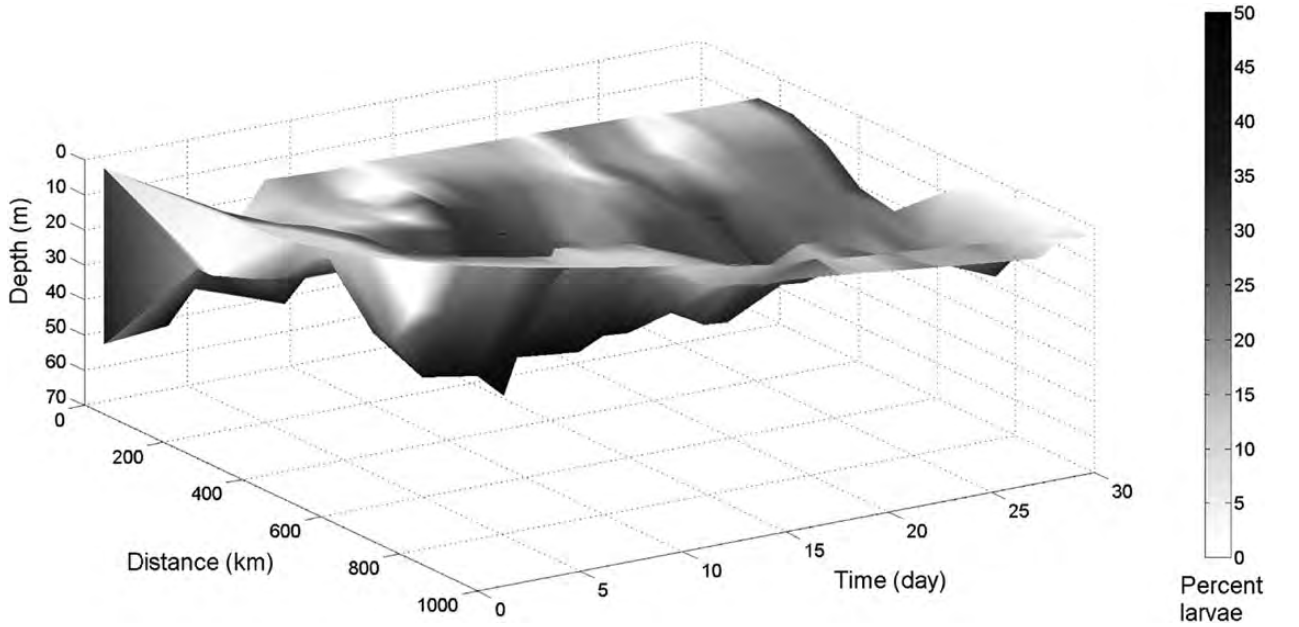

Figure 2. Behavioural seascape—larval two-dimensional (horizontal and vertical) dispersal kernels through time due to behaviour alone, without accounting for displacement due to currents. Here, we show the theoretical behavioural transport of fish larvae expending their vertical migration (Irisson *et al.*, 2010) and swimming faster (Fisher *et al.*, 2005) through ontogeny. We used larval traits (i.e. vertical migration and PLD) of the mutton snapper, *Lutjanus analis* (Lindeman *et al.*, 2005; D'Alessandro *et al.*, 2010) showing species-specific peaks and valleys in the behavioural seascape. In this simulation, 1000 particles (larvae) were spawned the origin location (i.e. zero represents the birth place). The particles were moved stochastically in the vertical following a (depth × time) matrix of field-based larval probability density distribution through ontogeny (Paris *et al.*, 2007) and swam horizontally with variable speed that increased with age (i.e. using model 1 from Fisher *et al.*, 2005; length-at-hatch = 0.2 cm, velocity-at-hatch = 1.9 cm s^{-1}) and hypothetically increasing with depth (i.e. velocity-at-settlement = 0.55 cm s^{-1} m^{-1}). At all times, larvae were keeping a one-dimensional bearing along the distance axis. Colour-code indicates the proportion of larvae in space and time, where the *x*-axis is the pelagic larval duration (PLD), the *y*-axis is the cumulative distance travelled, and the *z*-axis is the depth. This representation indicates that in theory, ~25% of *L. analis* larvae that swim with a constant bearing could transport themselves up to ca. 150 km in 30 d. This simple model further suggests that some larvae could overcome similar ranges of drift and potentially come back home, assuming that they can feed to replenish the energy utilized for swimming, and ignoring pelagic mortality.

While the size and spacing of MPAs is important for ensuring appropriate levels of connectivity (Jones *et al.*, 2007), enhanced larval attraction to protected areas may play a role as well. To test this hypothesis, reef polygons inside existing or suggested MPAs could be assigned large *k*-values, and the resulting recruitment success could be examined.

Finally, it would be informative to change the *k*-value for different individuals to examine the effects of individual preferences. For example, a group of reefs close to an individual's natal reef could be assigned a larger *k*-value to examine the potential impacts of homing behaviour. Or the magnitude of *k* could change throughout ontogeny, since larvae may be more attracted to nearby reefs as they become desperate to settle towards the end of their pelagic phase (Knight-Jones, 1953). Orientation during the "critical period" appears to have remarkable demographic consequences (Staaterman *et al.*, 2012); larvae would need to begin orientation behaviour soon after hatching to increase their chance of finding any reef or to come back to their home reef. This notion of "larval homing behaviour" is a new concept, but it makes sense when compared with other essential larval developmental traits, such as first-feeding and swimming. If early fish larvae can sense their way home, biophysical models have been missing an important component that would have the potential to improve predictions of marine population connectivity. Using numerical modelling, we can add "behaviour" as a key factor in Hjorts' hypothesis that contributes to the survivorship of the larvae. Such models have been used to discover that successful reef-fish replenishment is linked to signals perceived by the pelagic larvae; if the signals disappear or weaken, larvae can get lost (Codling *et al.*, 2004; Staaterman *et al.*, 2012). Therefore, the health of the nursery habitat and its cues are not only critical to adult benthic species, but it is also essential to the survivorship of their pelagic larvae.

How to move forward?

The above suggestions have the potential to improve existing modelling techniques by including orientation behaviour for fish larvae. However, the best models will only be as good as their parameters. Although much information is now available for vertical migration (e.g. Paris and Cowen, 2004; Irisson *et al.*, 2010), swimming speeds (e.g. Leis and Carson-Ewart, 1997; Fisher *et al.*, 2005), and orientation behaviour (e.g, Leis *et al.*, 2011) of settlement-stage larval fish, very little information is available on the development of sensory abilities throughout ontogeny (Blaxter, 1986; Leis, 2010). Furthermore, the distance at which cues become available to larvae as they progress from the pelagic to the coastal environment is not well understood, and empirical research revealing these critical pieces is needed. Meanwhile, developing biophysical models that include both navigational capabilities and environmental signals are essential to generate hypotheses and to ask "what if" questions related to demographic consequences of individual movements in response to environmental cues.

In conclusion, because larval fish are capable of significant vertical and horizontal migrations and can travel significant distances regardless of the transport by currents (Figure 2), realistic three-dimensional swimming should be included routinely into biophysical models in order for this field to move forward. With the modelling framework for oriented swimming outlined above, and existing models for vertical migration, scientists can already ask questions about the relative role of different animal behaviours in the dispersal and migration of fish larvae. Improved understanding of proximal causes for orientation can also provide insight into the evolutionary drivers of dispersal strategies for fish and marine organisms in general.

References

Armsworth, P. R. 2000. Modelling the swimming response of late stage larval reef fish to different stimuli. Marine Ecology Progress Series, 195: 231–247.

Armsworth, P. R., James, M. K., and Bode, L. 2001. When to press on or turn back: dispersal strategies for reef fish larvae. The American Naturalist, 157: 434–450.

Arvedlund, M., and Kavanagh, K. 2009. The senses and environmental cues used by marine larvae of fish and decapod crustaceans to find tropical coastal ecosystems. *In* Ecological Connectivity among Tropical Coastal Ecosystems, pp. 135–184. Ed. by I. Nagelkerken. Springer Science + Business Media, Frederiksberg, Denmark.

Atema, J. 2012. Aquatic odor dispersal fields: opportunities and limits of detection, communication and navigation. *In* Chemical Ecology in Aquatic Systems, pp. 1–18. Ed. by C. Bronmark, and L-A. Hansson. Oxford University Press.

Atema, J., Kingsford, M., and Gerlach, G. 2002. Larval reef fish could use odour for detection, retention and orientation to reefs. Marine Ecology Progress Series, 241: 151–160.

Berkley, H. A., Kendall, B. E., Mitarai, S., and Siegel, D. A. 2010. Turbulent dispersal promotes species coexistence. Ecological Letters, 13: 360–371.

Blaxter, J. H. S. 1986. Development of sense organs and behaviour of teleost larvae with special reference to feeding and predator avoidance. Transactions of the American Fisheries Society, 115: 98–114.

Bonhommeau, S., Blanke, B., Tréguier, A-M., Grima, N., Rivot, E., Vermard, Y., Greiner, E., *et al.* 2009. How fast can the European eel (*Anguilla anguilla*) larvae cross the Atlantic Ocean? Fisheries Oceanography, 18: 371–385.

Botsford, L. W., White, J. W., Coffroth, M. A., Paris, C. B., Planes, S., Shearer, T. L., Thorrold, S. R., *et al.* 2009. Connectivity and resilience of coral reef metapopulations in marine protected areas: matching empirical efforts to predictive needs. Coral Reefs, 28: 327–337.

Brickman, D., and Smith, P. C. 2002. Lagrangian stochastic modelling in coastal oceanography. Journal of Atmospheric and Oceanic Technology, 19: 83–99.

Codling, E., Hill, N., Pitchford, J., and Simpson, S. 2004. Random walk models for the movement and recruitment of reef fish larvae. Marine Ecology Progress Series, 279: 215–224.

Cowen, R. K., Paris, C. B., Olson, D. B., and Fortuna, J. L. 2003. The role of long distance dispersal versus local retention in replenishing marine populations. Journal of Physical Oceanography, 14: 129–137.

Cox, C. J., Mccloghrie, P., Young, E. F., and Nash, R. D. M. 2006. The importance of individual behaviour for successful settlement of juvenile plaice (*Pleuronectes platessa* L.): a modeling and field study in the eastern Irish Sea. Fisheries Oceanography, 15: 301–313.

D'Alessandro, E. K., Sponaugle, S., and Serafy, J. E. (2010) Larval ecology of a suite of snappers (Family: Lutjanidae) in the Straits of Florida, western Atlantic Ocean, Marine Ecology Progress Series 140: 159–175.

Fiksen, Ø., Jorgensen, C., Kristiansen, T., Vikebø, F., and Huse, G. 2007. Linking behavioural ecology and oceanography: larval behaviour determines growth, mortality, and dispersal. Marine Ecology Progress Series, 347: 195–205.

Fisher, R. 2005. Swimming speeds of larval coral reef fishes: impacts on self-recruitment and dispersal. Marine Ecology Progress Series, 285: 223–232.

Fisher, R., and Bellwood, D. R. 2003. Undisturbed swimming behaviour and nocturnal activity of coral reef fish larvae. Marine Ecology Progress Series, 263: 177–188.

Fisher, R., Leis, J. M., Clark, D. L., and Wilson, S. K. 2005. Critical swimming speeds of late-stage coral reef fish larvae: variation within

species, among species and between locations. Marine Biology, 147: 1201–1212.

Flamarique, I. N., and Browman, H. I. 2000. Wavelength-dependent polarization orientation in Daphnia. Journal of Comparative Physiology A, 186: 1073–1087.

Foster, N., Paris, C. B., Kool, J., Baums, I. B., Stevens, J., Sanchez, J., Bastidas, C., *et al.* 2012. Connectivity of Caribbean coral populations: complementary insights from empirical and modelled gene flow. Molecular Ecology, 21: 1143–1157.

Gawarkiewicz, G. G., Monismith, S. G., and Largier, J. 2007. Observing larval transport processes affecting population connectivity. Oceanography, 20: 40–53.

Green, B., and Chambers, R. 2007. Maternal effects vary between source populations in the Atlantic tomcod *Microgadus tomcod*. Marine Ecology Progress Series, 344: 185–195.

Griffa, A. 1996. Applications of stochastic particle models to oceanographic problems. *In* Stochastic Modelling in Physical Oceanography, pp. 114–140. Ed. by R. J. Adler, P. Muller, and B. L. Rozovskii. Birkhaüser, Boston, MA.

Grorud-Colvert, K., and Sponaugle, S. 2006. Influence of condition on behavior and survival potential of a newly settled coral reef fish, the bluehead wrasse *Thalassoma bifasciatum*. Marine Ecology Progress Series, 327: 279–288.

Guan, L., Snelgrove, P. V. R., and Gamperl, A. K. 2008. Ontogenetic changes in the critical swimming speed of *Gadus morhua* (Atlantic cod) and *Myoxocephalus scorpius* (shorthorn sculpin) larvae and the role of temperature. Journal of Experimental Marine Biology and Ecology, 360: 31–38.

Healey, M. C., Thomson, K. A., Leblond, P. H., Huato, L., Hinch, S. G., and Walters, C. J. 2000. Computer simulations of the effects of the Sitka eddy on the migration of sockeye salmon returning to British Columbia. Fisheries Oceanography, 9: 271–281.

Holbrook, R. I., and Burt de Perera, T. 2009. Separate encoding of vertical and horizontal components of space during orientation in fish. Animal Behaviour, 78: 241–245.

Irisson, J-O., LeVan, A., De Lara, M., and Planes, S. 2004. Strategies and trajectories of coral reef fish larvae optimizing self-recruitment. Journal of Theoretical Biology, 227: 205–218.

Irisson, J. O., Paris, C. B., Guigand, C., and Planes, S. 2010. Vertical distribution and ontogenetic "migration" in coral reef fish larvae. Limnology and Oceanography, 55: 909–919.

Jacobs, L. F. 2012. From chemotaxis to the cognitive map: the function of olfaction. Proceedings of the National Academy of Sciences of the USA, 109: 10693–10700.

James, M. K., Armsworth, P. R., Mason, L. B., and Bode, L. 2002. The structure of reef fish metapopulations: modelling larval dispersal and retention patterns. The Royal Society Proceedings: Biological Sciences, 269: 2079–2086.

Jones, G. P., Srinivasan, M., and Almany, G. R. 2007. Population connectivity and conservation of marine biodiversity. Oceanography, 20: 100–111.

Jorge, P. E., Almada, F., Goncalves, A. R., Duarte-Coelho, P., and Almada, V. C. 2012. Homing in rocky intertidal fish. Are *Lipophrys pholis* L. able to perform true navigation? Animal Cognition, 15: 1173–1181.

Kalmijn, A. J. 1988. Hydrodynamic and acoustic field detection. *In* Sensory Biology of Aquatic Animals, pp. 83–130. Ed. by J. Atema, R. R. Fay, A. N. Popper, and W. N. Tavolga. Springer-Verlag, New York.

Kingsford, M. J. 1990. Linear oceanographic features: a focus for research on recruitment processes. Australian Journal of Ecology, 15: 391–401.

Kingsford, M. J., Leis, J. M., Shanks, A., Lindeman, K. C., Morgan, S. G., and Pineda, J. 2002. Sensory environments, larval abilities and local self-recruitment. Bulletin of Marine Science, 70: 309–340.

Knight-Jones, E. 1953. Decreased discrimination during settling after prolonged planktonic life in larvae of *Spirorbis borealis* (Serpulidae). Journal of the Marine Biological Association of the UK, 32: 337–345.

Kristiansen, T., Drinkwater, K. F., Lough, R. G., and Sundby, S. 2011. Recruitment variability in North Atlantic cod and match-mismatch dynamics. PLoS One, 6: 1–11.

Kristiansen, T., Jørgensen, C., Lough, R. G., Vikebø, F., and Fiksen, Ø. 2009. Modeling rule-based behavior: habitat selection and the growth-survival trade-off in larval cod. Behavioral Ecology, 20: 1–11.

Leis, J. M. 2006. Are larvae of demersal fishes plankton or nekton? Advances in Marine Biology, 51: 58–141.

Leis, J. M. 2007. Behaviour as input for modelling dispersal of fish larvae: behaviour, biogeography, hydrodynamics, ontogeny, physiology, and phylogeny meet hydrography. Marine Ecology Progress Series, 347: 185–193.

Leis, J. M. 2010. Ontogeny of behaviour in larvae of marine demersal fishes. Ichthyological Research, 57: 325–342.

Leis, J. M., and Carson-Ewart, B. M. 1997. *In situ* swimming speeds of the late pelagic larvae of some Indo-Pacific coral-reef fishes. Marine Ecology Progress Series, 159: 165–174.

Leis, J. M., and Carson-Ewart, B. M. 1998. Complex behaviour by coral-reef fish larvae in open-water and near-reef pelagic environments. Environmental Biology of Fishes, 53: 259–266.

Leis, J. M., Caselle, J. E., Bradbury, R. I., Kristiansen, T., Llopiz, J. K., Miller, M. J., O'Connor, M. I., Paris, C. B., Shanks, A. L., Sogard, S. M., Swearer, S. E., Treml, E. A., Vetter, R. D., and Warner, R. R. (2013) Does fish larval dispersal differ between high and low latitudes? Proceedings of the Royal Society B. rspb20130327–1/3/13–18:33.

Leis, J. M., Siebeck, U., and Dixson, D. L. 2011. How Nemo finds home: the neuroecology of dispersal and of population connectivity in larvae of marine fishes. Integrative and Comparative Biology, 51: 826–843.

Lett, C., Ayata, S-D., Huret, M., and Irisson, J-O. 2010. Biophysical modelling to investigate the effects of climate change on marine population dispersal and connectivity. Progress in Oceanography, 87: 106–113.

Lindeman, K. C., Richards, W. J., Lyczkowski-Shultz, J., Drass, D. M., Paris, C. B., Leis, J. M., Lara, M., and Comyns, B. H. (2005) Lutjanidae: Snappers. *In* Early Stages of Atlantic Fishes, Chapter 137, pp. 1549–1586. Ed. by W. J. Richards. CRC Press, Boca Raton.

Llopiz, J. K., and Cowen, R. K. 2009. Variability in the trophic role of coral reef fish larvae in the oceanic plankton. Marine Ecology Progress Series, 381: 259–272.

Mann, D. A., Casper, B. M., Boyle, K. S., and Tricas, T. C. 2007. On the attraction of larval fishes to reef sounds. Marine Ecology Progress Series, 338: 307–310.

Mitarai, S., Siegel, D. A., and Winters, K. B. 2008. A numerical study of stochastic larval settlement in the California Current system. Journal of Marine Systems, 69: 295–305.

Monismith, S. G. 2007. Hydrodynamics of coral reefs. Annual Review of Fluid Mechanics, 39: 37–55.

Montgomery, J. C., Tolimieri, N., and Haine, O. S. 2001. Active habitat selection by pre-settlement reef fishes. Fish and Fisheries, 2: 261–277.

Mork, K. A., Gilbey, J., Hansen, L. P., Jensen, A. J., Jacobsen, J. A., Holm, M., Holst, J. C., *et al.* 2012. Modelling the migration of post-smolt Atlantic salmon (*Salmo salar*) in the Northeast Atlantic. ICES Journal of Marine Science, 69: 1616–1624.

Nathan, R., Getz, W. M., Revilla, E., Holyoak, M., Kadmon, R., Saltz, D., and Smouse, P. E. 2008. A movement ecology paradigm for unifying organismal movement research. Proceedings of the National Academy of Sciences of the USA, 105: 19052–19059.

Okubo, A. 1971. Oceanic diffusion diagrams. Deep Sea Research and Oceanographic Abstracts, 18: 789–802.

Ospina-Alvarez, A., Parada, C., and Palomera, I. 2012. Vertical migration effects on the dispersion and recruitment of European

anchovy larvae: from spawning to nursery areas. Ecological Modelling, 231: 65–79.

Palandro, D. A., Andréfouët, S., Hu, C., Hallock, P., Müller-Karger, F. E., Dustan, P., Callahan, M. K., *et al.* 2008. Remote Sensing of Environment Quantification of two decades of shallow-water coral reef habitat decline in the Florida Keys National Marine Sanctuary using Landsat data (1984–2002). Remote Sensing of Environment, 112: 3388–3399.

Parada, C., Mullon, C., Roy, C., Freon, P., Hutchings, L., and Van der Lingen, C. 2008. Does vertical migratory behaviour retain fish larvae onshore in upwelling ecosystems? A modelling study of anchovy in the southern Benguela. African Journal of Marine Science, 30: 437–452.

Paris, C. B., Chérubin, L. M., and Cowen, R. K. 2007. Surfing, spinning, or diving from reef to reef: effects on population connectivity. Marine Ecology Progress Series, 347: 285–300.

Paris, C. B., and Cowen, R. K. 2004. Direct evidence of a biophysical retention mechanism for coral reef fish larvae. Limnology and Oceanography, 49: 1964–1979.

Paris, C. B., Cowen, R. K., Lwiza, K., Wang, D., and Olson, D. 2002. Objective analysis of three-dimensional circulation in the vicinity of Barbados, West Indies: implication for larval transport. Deep Sea Research, 49: 1363–1386.

Paris, C. B., Guigand, C. M., Irisson, J-O., Fisher, R., and D'Alessandro, E. 2008. Orientation with no frame of reference (OWNFOR): a novel system to observe and quantify orientation in reef fish larvae. *In* Caribbean Connectivity: Implications for Marine Protection Area Management, pp. 54–64. Ed. by R. Grober-Dunsmore, and B. D. Keller. Belize City, Belize.

Paris, C. B., Irisson, J. O., Leis, J. M., Bogucki, D., Piskozub, J., Siebeck, U., and Guigand, C. M. Sun compass orientation for reef fish larvae. Ethology, in review.

Popper, A. N., and Fay, R. R. 2011. Rethinking sound detection by fishes. Hearing Research, 273: 25–36.

Porch, C. E. 1998. A numerical study of larval fish retention along the southeast Florida coast. Ecological Modeling, 109: 35–59.

Putman, N. F., Lohmann, K. J., Putman, E. M., Quinn, T. P., Klimley, A. P., and Noakes, D. L. G. 2013. Evidence for geomagnetic imprinting as a homing mechanism in Pacific salmon. Current Biology, 23: 312–316.

Radford, C. A., Sim-Smith, C. J., and Jeffs, A. G. 2012. Can larval snapper, *Pagrus auratus*, smell their new home? Marine and Freshwater Research, 63: 898–904.

Rossier, J., and Schenk, F. 2003. Olfactory and/or visual cues for spatial navigation through ontogeny: olfactory cues enable the use of visual cues. Behavioral Neuroscience, 117: 412–425.

Ruzicka, R., Semon, K., Colella, M., Brinkhuis, V., Kidney, J., Morrison, J., Macaulay, K., *et al.* 2009. Coral Reef Evaluation & Monitoring Project, Final Report. Saint Petersburg, FL.

Searcy, S., and Sponaugle, S. 2001. Selective mortality during the larval-juvenile transition in two coral feef Fishes. Ecology, 82: 2452–2470.

Sentchev, A., and Korotenko, K. 2007. Modelling distribution of flounder larvae in the eastern English Channel: sensitivity to physical forcing and biological behaviour. Marine Ecology Progress Series, 347: 233–245.

Simpson, S. D., Meekan, M., Montgomery, J., McCauley, R., and Jeffs, A. 2005. Homeward sound. Science, 308: 221.

Staaterman, E. R., Paris, C. B., and Helgers, J. 2012. Orientation behavior in fish larvae: a missing piece to Hjort's critical period hypothesis. Journal of Theoretical Biology, 304: 188–196.

Thorrold, S. R., Jones, C. M., and Camapana, S. E. 1997. Response of otolith microchemistry to environmental variations experienced by larval and juvenile Atlantic croaker (*Micropogonias undulatus*), Limn. Oceanography, 42: 102–111.

Vergassola, M., Villermaux, E., and Shraiman, B. I. 2007. "Infotaxis" as a strategy for searching without gradients. Nature, 445: 406–409.

Vikebø, F., Jørgensen, C., Kristiansen, T., and Fiksen, Ø. 2007. Drift, growth, and survival of larval northeast Arctic cod with simple rules of behaviour. Marine Ecology Progress Series, 347: 207–219.

Werner, F. E., Cowen, R. K., and Paris, C. B. 2007. Coupled biological and physical models. Oceanography, 20: 54–69.

Werner, F. E., Page, F. H., Lynch, D. R., Loder, J. W., Lough, R. G., Perry, R. I., Greenberg, D. A., *et al.* 1993. Influences of mean advection and simple behavior on the distribution of cod and haddock early life stages on Georges Bank. Fisheries Oceanography, 2: 43–64.

Willis, J. 2011. Modelling swimming aquatic animals in hydrodynamic models. Ecological Modelling, 222: 3869–3887.

Wolanski, E., Doherty, P., and Carleton, J. 1997. Directional swimming of fish larvae determines connectivity of fish populations on the great barrier reef. Naturwissenschaften, 84: 262–268.

Handling editor: Howard Browman

ICES Journal of Marine Science

ICES International Council for the Exploration of the Sea
CIEM Conseil International pour l'Exploration de la Mer

ICES Journal of Marine Science (2014), 71(4), 925–929. doi:10.1093/icesjms/fss194

Contribution to the Themed Section: 'Larval Fish Conference'

Original Articles

Moderate turbidity enhances schooling behaviour in fish larvae in coastal waters

Ryosuke Ohata*, Reiji Masuda, Kohji Takahashi, and Yoh Yamashita

Maizuru Fisheries Research Station, Field Science Education and Research Center, Kyoto University, Nagahama, Maizuru, Kyoto 625-0086, Japan

**Corresponding author: tel: +81 773 62 5512; fax: +81 773 62 5513; e-mail: ohata@kais.kyoto-u.ac.jp*

Ohata, R., Masuda R., Takahashi K., and Yamashita, Y. 2014. Moderate turbidity enhances schooling behaviour in fish larvae in coastal waters. – ICES Journal of Marine Science, 71: 925–929.

Received 27 September 2012; accepted 3 December 2012; advance access publication 8 January 2013.

We evaluated the effects of turbidity on school formation in ayu (*Plecoglossus altivelis*) [24.5 ± 2.2 mm standard length (L_s)], Japanese anchovy (*Engraulis japonicus*) (29.1 ± 3.1 mm L_s) larvae, which often live in turbid coastal waters, and yellowtail (*Seriola quinqueradiata*) juveniles (37.1 ± 2.5 mm L_s), which live in clear offshore waters. Fish were introduced into experimental tanks at one of five turbidity levels obtained by dissolving 0, 5, 20, 50, or 300 mg l^{-1} of kaolin in seawater. Their behaviour was video recorded, and the nearest neighbour distance (D_{NN}) and separation angle (A_S) were compared among turbidity levels. Mean D_{NN} of ayu was significantly smaller at 20 and 50 mg l^{-1} than any other level of turbidity, as was A_S at 20 mg l^{-1} compared with 0 mg l^{-1}. Mean A_S of anchovy was smaller at 50 mg l^{-1} of turbidity than any others. In contrast, mean D_{NN} of yellowtail was larger at 300 mg l^{-1} than any others. These results suggest that moderate turbidities enhance schooling behaviour in ayu and Japanese anchovy larvae, whereas turbidity has an inhibitive effect on schooling of yellowtail juveniles, corresponding well to the habitat characteristics of each species.

Keywords: anti-predatory strategy, ayu, Japanese anchovy, schooling behaviour, turbidity, yellowtail.

Introduction

Larvae of some fish species are often highly concentrated in turbid coastal waters, as are typically observed in ayu (*Plecoglossus altivelis altivelis*) (Tago, 2002) and Japanese anchovy (Uotani *et al.*, 2000). Ayu is an amphidromous species spending only the larval stage in the ocean (Senta and Kinoshita, 1985; Otake and Uchida, 1998), whereas Japanese anchovy is an oceanic species. The major morphological similarity of these is that both species have the larval stage of *shirasu*, i.e. transparent and elongate body form. Therefore *shirasu* larvae are likely to be adapted to turbid waters.

Most piscivorous fish rely on vision for feeding (Guthrie and Muntz, 1993) and so their feeding efficiencies decline with increased turbidity (Utne-Palm, 2002). Turbidity dramatically improved the survival rate in larvae of red sea bream (*Pagrus major*) [6 mm standard length (L_s)], ayu (6 and 23 mm L_s) and Japanese anchovy (6–25 mm L_s) when they were exposed to jack mackerel (*Trachurus japonicus*) juveniles as predators (Ohata *et al.*, 2011a, b). These results suggest that turbid waters function as refuges for fish larvae from visual predators. In contrast, turbidity had no major positive effect on survival when these larvae were exposed to moon jellyfish, except the case of ayu (see below).

Schooling behaviour can provide fish an advantage of detecting predators faster, confusing predators and thus increasing the chance of escape from predators (reviewed by Pitcher and Parrish, 1993). In our previous study, the survival rate of ayu post-larvae was slightly higher in turbid conditions than in the non-turbid treatment when moon jellyfish were used as predators (Ohata *et al.*, 2011a). In addition, we observed that ayu larvae formed a school more frequently at 50 mg l^{-1} than 0 and 300 mg l^{-1} of kaolin during the predation experiments (Ohata, unpublished). Therefore, turbidity might have enhanced school formation in ayu post-larvae with which they detected moon jellyfish and escaped from them more efficiently.

Schools of fish are mainly maintained by visual stimuli with, in some cases, additional information transmitted by mechanosensory

or chemosensory systems (reviewed by Partridge and Pitcher, 1980). Fish fail to school at low light intensities, presumably due to visual limitation, as is reported in gulf menhaden (*Brevoortia patronus*), walleye pollock (*Theragra chalcogramma*), and striped jack (*Pseudocaranx dentex*) (Higgs and Fuiman, 1996; Ryer and Olla, 1998; Miyazaki *et al.*, 2000). Although turbidity may well have effects on the formation of fish schools, this has not yet been verified. Therefore in the present study, the effect of turbidity on school formation was tested in the larvae of Japanese anchovy and ayu, which use turbid water for refuge from visual predators, and compared with juveniles of yellowtail (*Seriola quinqueradiata*). Unlike the former two species, yellowtail remains in offshore waters with low turbidity for most of their early life stage (Sakakura and Tsukamoto, 1997).

Material and methods

Rearing and husbandry of fish

Ayu post-larvae were obtained from the Fisheries Cooperative Association of Hidakagawa in Wakayama Prefecture on 24 January 2009. They were third-generation individuals from local origin broodstock. Commercial pellets (N250 Kyowa Hakko Bio Co., Ltd; www.kyowahakko-bio.co.jp) were provided three times a day. After the experiment, all the fish were measured for L_s after MS222 anaesthesia. The mean $\pm$ *SD* L_s of ayu was 24.5 $\pm$ 2.2 mm ($n = 125$).

Japanese anchovy larvae were raised from fertilized eggs spawned from broodstock that were obtained with a commercial set-net in Tai, Maizuru, Kyoto, Japan (35°56′N, 135°45′E). The broodstock were collected and transferred to the Maizuru Fisheries Research Station (MFRS) of Kyoto University on 19 March and 9 April 2009, and were stocked in two black round tanks (4 m in diameter, 30 m^3 in volume) filled with filtered seawater. They were fed defrosted krill *Euphausia* sp. twice a day. Larvae were provided with rotifers (*Brachionus plicatilis*), *Artemia* sp. nauplii and formulated food (Kyowa N250 and N400, Kyowa Hakko Bio Co., Ltd; www.kyowahakko-bio.co.jp), depending on their developmental stage. Rotifers and *Artemia* were enriched with commercial highly unsaturated fatty acid oil (Marine Gloss, Nisshin Marinetech, Ltd; www.nisshin-marinetech.com). After the experiment, all the fish were measured for L_s after MS222 anaesthesia. The mean $\pm$ *SD* L_s of Japanese anchovy was 29.1 $\pm$ 3.1 mm ($n = 125$).

Yellowtail juveniles were obtained from the A-marine Kindai Co., Ltd. (www.a-marine.co.jp) in Wakayama Prefecture on 23 June 2011. Juveniles were transferred to the MFRS and were reared in 500-l transparent circular polycarbonate tanks. Commercial pellets (Otohime C1 and S2, Marubeni Nisshin Feed Co., Ltd; www.mn-feed.com) were provided twice a day. After the experiment, all the fish were measured for L_s after MS222 anaesthesia. The mean $\pm$ *SD* L_s of yellowtail was 37.1 $\pm$ 2.5 mm ($n = 150$).

Experimental procedure

A 30 × 40 cm acrylic square tank was used for the trials of ayu larvae. The same tank was first used in Japanese anchovy and yellowtail, yet abnormal behaviours caused by stress were often observed such as biting the bottom of the tank or being attracted to the tank wall. Therefore a 30-l transparent circular polycarbonate tank was used for the latter two species. Five levels of turbidity were obtained by dissolving 0, 5, 20, 50, or 300 mg l^{-1} of kaolin (Wako Pure Chemical Industries, Ltd; www.wako-chem.co.jp). Five individuals were transferred to an experimental tank filled with a depth of 5 cm water. This shallow water depth was set to minimize the difference of light intensity among turbidity levels. After adaption for 10 min, video recording of fish behaviour was conducted from above on five different turbidity levels for 5 min. Fish were not reused and new individuals at each turbidity level were used. The seawater was changed in every trial, and the kaolin was newly prepared before that. We confirmed that levels of turbidity were maintained for more than 15 min. Two fluorescent lights (18 W) were provided from under the experimental tank so that even *shirasu* larvae would be recognized in high-turbidity conditions. The light intensity was 250 and 1100 lux above and under the tank, respectively. Water temperature was 14.9 $\pm$ 0.4°C ($n = 25$), 21.5 $\pm$ 0.2°C ($n = 25$), and 23.9 $\pm$ 0.3°C ($n = 30$) during the experiment of ayu, Japanese anchovy, and yellowtail, respectively. These water temperatures reflected ambient temperature in the habitat of each species. Five replicates in Japanese anchovy and ayu trials, and six replicates in yellowtail were conducted in each turbidity.

Although Uotani *et al.* (2000) reported that turbidity of 5 mg l^{-1} was chosen by Japanese anchovy larvae in their experiment, turbidity of 50 mg l^{-1} is the preferred level in European anchovy (*Engraulis encrasicolus*) larvae in the wild (Drake *et al.*, 2007), and has been observed in Suruga Bay where a major fishery of Japanese anchovy larvae occurs (Uotani *et al.*, 2000). Turbidity of 300 mg l^{-1} is typical in Ariake Bay, Japan (Suzuki *et al.*, 2009).

Schooling behaviour was analysed using the nearest neighbour distance (D_{NN}) and separation angle (A_S) following Masuda *et al.* (2003). D_{NN} was defined as the snout-to-snout distance between nearest neighbouring two individuals divided by fish L_s to be standardized. A_S was defined as the angle between these two individuals; A_S is expected to be close to 90° when fish are randomly located, and to decrease when a parallel orientation develops. Sixteen frames were sampled in a 20 s interval for 5 min, and D_{NN} and A_S were measured on each of the five individuals; the average of 80 measurements were taken to represent D_{NN} or A_S in each trial.

Statistical analyses

The D_{NN} and A_S were compared among different turbidities using ANOVA followed by Tukey's honestly significant difference (HSD) test. The D_{NN} data were Log_{10} transformed to improve the homogeneity of variance, whereas A_S data had homoscedasticity (Shapiro–Wilk test). A_S was also compared with 90° by one sample *t*-test.

Ethical notes

All fish larvae used as prey animals were hatchery reared and so negative impacts on the natural population should be minimum. All the experiments were performed according to the guidelines of Regulation on Animal Experimentation at Kyoto University.

Results

Mean D_{NN} of ayu larvae was significantly smaller at 20 and 50 mg l^{-1} compared with other turbidity levels ($p < 0.05$, Tukey's HSD test; Figure 1a), and so was their mean A_S at 20 mg l^{-1} than 0 or 50 mg l^{-1} ($p < 0.05$, Tukey's HSD test; Figure 2a). Their mean A_S was significantly smaller than 90° at 5, 20, and 300 mg l^{-1} of turbidity ($p < 0.05$, one sample *t*-test).

Although mean D_{NN} of Japanese anchovy larvae was not significantly different among turbidity levels ($p > 0.05$, ANOVA;

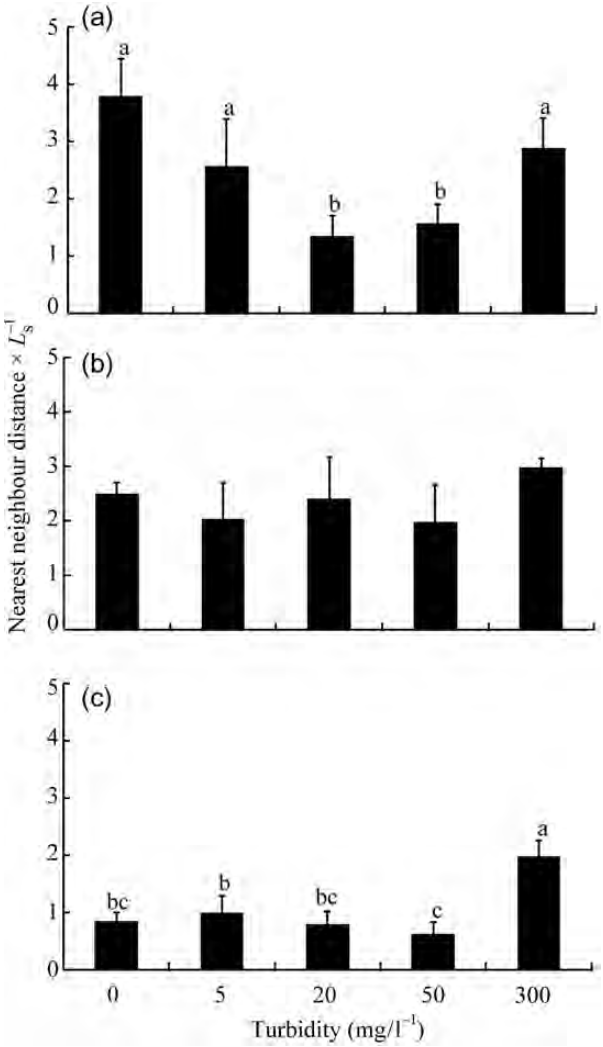

Figure 1. Nearest neighbour distance (D_{NN}) of (a) ayu, (b) Japanese anchovy, and (c) yellowtail at the turbidities of 0, 5, 20, 50, and 300 mg l^{-1} of kaolin levels. Different letters indicate significant differences in D_{NN} among turbidity conditions (Tukey's HSD test, $p < 0.05$). Vertical bars indicate standard deviations (a and b, $n = 5$; c, $n = 6$).

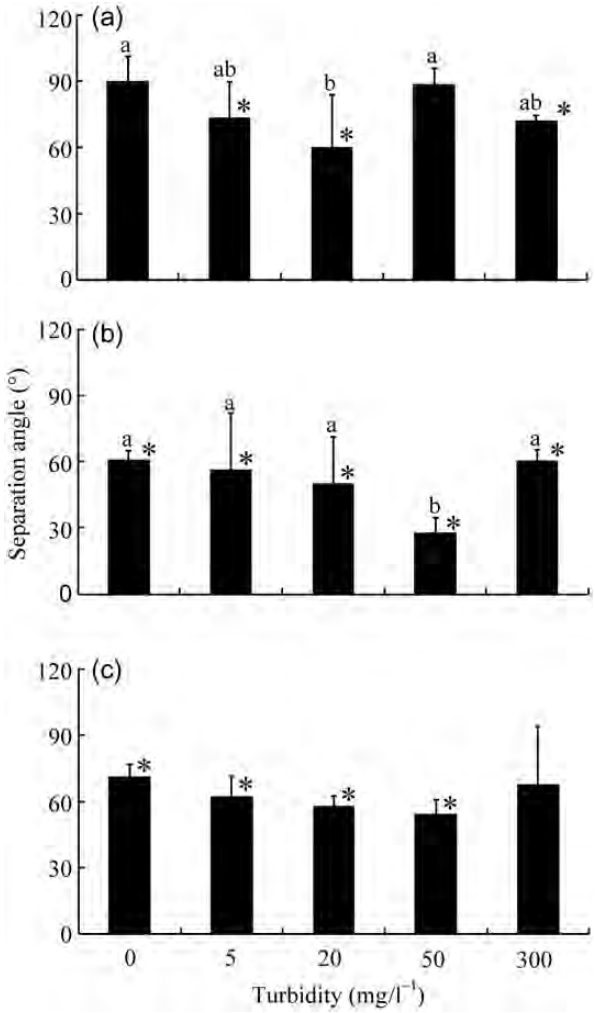

Figure 2. Separation angle (A_S) of (a) ayu, (b) Japanese anchovy, and (c) yellowtail at the different turbidity levels. Different letters indicate significant differences in A_S among turbidity levels (Tukey's HSD test, $p < 0.05$). Asterisks indicate significantly smaller A_S than 90° (one sample *t*-test, $p < 0.05$). Vertical bars indicate standard deviations (a and b, $n = 5$; c, $n = 6$).

Figure 1b), mean A_S was significantly smaller at 50 mg l^{-1} compared with others ($p < 0.05$, Tukey's HSD test; Figure 2b). Their mean A_S was significantly smaller than 90° at all the turbidity levels ($p < 0.05$, one sample *t*-test).

Mean D_{NN} of yellowtail juvenile was significantly larger at 300 mg l^{-1} compared with other turbidity levels ($p < 0.05$, Tukey's HSD test; Figure 1c), whereas there was no difference in A_S among turbidity levels ($p > 0.05$, ANOVA; Figure 2c). Their mean A_S was significantly smaller than 90° at 0, 5, 20, and 50 mg l^{-1} turbidity ($p < 0.05$, one sample *t*-test).

Discussion

Moderate turbidities (20 and 50 mg l^{-1}) induced schooling behaviour of ayu and Japanese anchovy larvae, whereas in high turbidity (300 mg l^{-1}) yellowtail juveniles reduced their schooling behaviour. These results corresponded well with the habitat characteristics of each species; ayu and Japanese anchovy larvae occur in coastal and estuarine regions with highly turbid waters whereas yellowtail live in clear offshore waters during the larval and juvenile stages.

Vision, olfactory organs, and the lateral line system are important factors to understand physiological mechanism in adapting to turbid waters. Uyan *et al.* (2006a) reported that anchovy larvae [12–30.8 mm total length (L_t)] had well-developed eyes with duplex retina, grouped rods and dense retinal tapetum, making them sensitive to low light levels and enabling them to inhabit and feed in deeper waters within the photic zone. Therefore, these larvae are likely to have an efficient eye structure for utilizing low light intensities, and thus should have an advantage in school formation in turbid waters. Furthermore, Uyan *et al.* (2006a) suggested that olfaction may help larvae maintain the school when the light intensity is low in Japanese anchovy larvae. The lateral line system may also help the Japanese anchovy maintain the school in turbid waters. In general, adult clupeoid fish that form a large

school such as herring, gulf menhaden, and gizzard shad (*Dorosoma cepedianum*) have cephalic lateral line canals with many small branches (Gunter and Demoran, 1961; Blaxter *et al.*, 1983; Stephens, 1985). Uyan *et al.* (2006b) reported that this was also the case in adult Japanese anchovy (9–13 cm L_t), and suggested that the dense branching of the cephalic lateral line canals ensures the sensitivity to the movement of water and might be a characteristic of schooling pelagic fish. In larval ayu, free neuromasts are located surrounding eyes and noses, the structure of which can be adapted to receive stimulus from all direction (Mukai *et al.*, 1992). Therefore, sensory organs of Japanese anchovy and ayu provide substantial advantage for school formation in turbid waters. Furthermore, the lateral line systems may also work for the transference of predator's information in a school. These may explain the relatively high survival rate of ayu larvae exposed to moon jellyfish at turbid conditions compared with the transparent condition in our previous study (Ohata *et al.*, 2011a).

High-turbidity condition had a negative effect on school formation in yellowtail. This may be because visual contact among individuals was difficult in a highly turbid environment for them. High turbidity may also be stressful; indeed some individuals stopped swimming and stayed on the bottom. Turbidity is reported to cause some changes in the behaviour of fish. Engström-Öst and Mattila (2008) reported that in the presence of competitors and the stimuli of a visual predator, turbidity reduced swimming activity in northern pike (*Esox lucius*) larvae. Contrarily, activity of walleye (*Sander vitreus*) and herring increased in turbid environment (Rieger and Summerfelt, 1997; Utne-Palm, 2004). Furthermore, Meager and Batty (2007) reported that swimming activity in Atlantic cod (*Gadus morhua*) juveniles was non-linearly affected by turbidity. Because turbidity can either increase or decrease the activity of fish, the effect of turbidity on fish activity should be confirmed on a species-to-species basis.

The cohesiveness of fish school is different depending on developmental stages; for example both D_{NN} and A_S reach consistently low values when Japanese anchovy attain 35 mm L_s (Masuda, 2011). Therefore the effects of turbidity on school formation may change ontogenetically from the larval to the juvenile stage. Future study should include such an ontogenetic aspect.

Acknowledgments

Ayu larvae were provided by Mr Y. Ikenaga at the Fisheries Cooperative Association of Hidakagawa. Rotifers required for rearing Japanese anchovy larvae were kindly provided by Notojima Station, National Center for Stock Enhancement. This research was funded by the STOPJELLY PROJECT from the Agriculture, Forestry and Fisheries Research Council, and the Sasakawa Scientific Research Grant from The Japan Science Society. Comments from two anonymous reviewers substantially improved the quality of the manuscript. All the experiments were performed according to the guidelines of Regulation on Animal Experimentation at Kyoto University.

References

Blaxter, J. H. S., Gray, J. A. B., and Best, A. C. G. 1983. Structure and development of the free neuromasts and lateral line system of the herring. Journal of the Marine Biological Association of the United Kingdom, 63: 247–260.

Drake, P., Borlán, A., González-Ortegón, E., Baldó, F., Vilas, C., and Fernández-Delgado, C. 2007. Spatio-temporal distribution of early life stages of the European anchovy *Engraulis encrasicolus* L. within a European temperate estuary with regulated freshwater inflow: effects of environmental variables. Journal of Fish Biology, 70: 1689–1709.

Engström-Öst, J., and Mattila, J. 2008. Foraging, growth and habitat choice in turbid water: an experimental study with fish larvae in the Baltic Sea. Marine Ecology Progress Series, 359: 275–281.

Gunter, G., and Demoran, W. J. 1961. Lateral lines and an undescribed sensory area on the head of the gulf menhaden, *Brevoortia patronus*. Copeia, 1: 39–42.

Guthrie, D. M., and Muntz, W. R. A. 1993. Role of vision in fish behavior. *In* Behaviour of Teleost Fishes, 2nd edn, pp. 89–121. Ed. by T. J. Pitcher. Chapman and Hall, London. 715 pp.

Higgs, D. M., and Fuiman, L. A. 1996. Light intensity and schooling behavior in larval gulf menhaden. Journal of Fish Biology, 48: 979–991.

Masuda, R. 2011. Ontogeny of swimming speed, schooling behaviour and jellyfish avoidance by Japanese anchovy *Engraulis japonicus*. Journal of Fish Biology, 78: 1323–1335.

Masuda, R., Shoji, J., Nakayama, S., and Tanaka, M. 2003. Development of schooling behavior in Spanish mackerel *Scomberomorus niphonius* during early ontogeny. Fisheries Science, 69: 772–776.

Meager, J. J., and Batty, R. S. 2007. Effects of turbidity on the spontaneous and prey-searching activity of juvenile Atlantic cod (*Gadus morhua*). Philosophical Transactions of the Royal Society B: Biological Science, 362: 2123–2130.

Miyazaki, T., Shiozawa, S., Kogane, T., Masuda, R., Maruyama, K., and Tsukamoto, K. 2000. Developmental changes of the light intensity threshold for school formation in the striped jack *Pseudocaranx dentex*. Marine Ecology Progress Series, 192: 267–275.

Mukai, Y., Kobayashi, H., and Yoshikawa, H. 1992. Development of free and canal neuromasts and their directions of maximum sensitivity in the larvae of ayu, *Plecoglossus altivelis*. Japanese Journal of Ichthyology, 38: 411–417 (in Japanese with English abstract).

Ohata, R., Masuda, R., Ueno, M., Fukunishi, Y., and Yamashita, Y. 2011a. Effects of turbidity on survival of larval ayu and red sea bream exposed to predation by jack mackerel and moon jellyfish. Fisheries Science, 77: 207–215.

Ohata, R., Masuda, R., and Yamashita, Y. 2011b. Ontogeny of antipredator performance in hatchery-reared Japanese anchovy *Engraulis japonicus* larvae exposed to visual or tactile predators in relation to turbidity. Journal of Fish Biology, 79: 2007–2018.

Otake, T., and Uchida, K. 1998. Application of otolith microchemistry for distinguishing between amphidromous and non-amphidromous stocked ayu, *Plecoglossus altivelis*. Fisheries Science, 64: 517–521.

Partridge, B. L., and Pitcher, T. J. 1980. The sensory basis of fish schools: relative roles of lateral line and vision. Journal of Comparative Physiology A, 135: 315–325.

Pitcher, T. J., and Parrish, J. K. 1993. Functions of shoaling behavior in teleosts. *In* Behaviour of Teleost Fishes, 2nd edn, pp. 363–439. Ed. by T. J. Pitcher. Chapman and Hall, London. 715 pp.

Rieger, P. W., and Summerfelt, R. C. 1997. The influence of turbidity on larval walleye, *Stizostedion vitreum*, behavior and development in tank culture. Aquaculture, 159: 19–32.

Ryer, C. H., and Olla, B. L. 1998. Effect of light on juvenile walleye pollock shoaling and their interaction with predators. Marine Ecology Progress Series, 167: 215–226.

Sakakura, Y., and Tsukamoto, K. 1997. Age composition in the schools of juvenile yellowtail *Seriola quinqueradiata* associated with drifting seaweeds in the East China Sea. Fisheries Science, 63: 37–41.

Senta, T., and Kinoshita, I. 1985. Larval and juvenile fishes occurring in surf zones of western Japan. Transactions of the American Fisheries Society, 114: 609–618.

Suzuki, K. W., Nakayama, K., and Tanaka, M. 2009. Horizontal distribution and population dynamics of the dominant mysid

Hyperacanthomysis longirostris along a temperate macrotidal estuary (Chikugo River estuary, Japan). Estuarine, Coastal and Shelf Science, 83: 516–528.

Stephens, R. R. 1985. The lateral line system of the gizzard shad, *Dorosoma cepedianum* Lesueur (Pisces: Clupeidae). Copeia, 3: 540–556.

Tago, Y. 2002. Larval distribution of ayu *Plecoglossus altivelis* in the surface layer of estuary regions in Toyama Bay. Nippon Suisan Gakkaishi, 68: 61–71 (in Japanese with English abstract).

Uotani, I., Fukui, A., Kobayashi, H., Saito, H., and Kawaguchi, K. 2000. The intensity of scattered light in turbid seawater is a major factor in the turbiditaxis of Japanese anchovy larvae. Fisheries Science, 66: 294–298.

Utne-Palm, A. C. 2002. Visual feeding of fish in a turbid environment: physical and behavioural aspects. Marine and Freshwater Behaviour and Physiology, 35: 111–128.

Utne-Palm, A. C. 2004. Effects of larvae ontogeny, turbidity, and turbulence on prey attack rate and swimming activity of Atlantic herring larvae. Journal of Experimental Marine Biology and Ecology, 310: 147–161.

Uyan, S., Kawamura, G., and Archdale, M. V. 2006a. Morphology of the sense organs in larval anchovy *Engraulis japonicus* caught by midwater trawl. Aquaculture Science, 54: 275–282.

Uyan, S., Kawamura, G., and Archdale, M. V. 2006b. Morphology of the sense organs of anchovy *Engraulis japonicus*. Fisheries Science, 72: 540–545.

Handling editor: Howard Browman

ICES Journal of Marine Science

ICES Journal of Marine Science (2014), 71(4), 930–942. doi:10.1093/icesjms/fst139

Contribution to the Themed Section: 'Larval Fish Conference'

Original Article

Shoreline configurations affect dispersal patterns of fish larvae in a large river

Aaron Lechner[1]*, Hubert Keckeis[1], Elisabeth Schludermann[1], Franz Loisl[1], Paul Humphries[2], Martin Glas[3], Michael Tritthart[3], and Helmut Habersack[3]

[1]*Department of Limnology, Faculty of Life Sciences, University of Vienna, Althanstrasse 14, Vienna 1090, Austria*
[2]*School of Environmental Sciences, Charles Sturt University, PO Box 789, Albury, NSW 2640, Australia*
[3]*Christian Doppler Laboratory for Advanced Methods in River Monitoring, Modelling and Engineering, Department of Water, Atmosphere and Environment, Institute of Water Management, Hydrology and Hydraulic Engineering, BOKU—University of Natural Resources and Life Sciences Vienna, Muthgasse 107, Vienna 1190, Austria*

**Corresponding author: tel: +43 66911011653; e-mail: aaron.lechner@univie.ac.at*

Lechner, A., Keckeis, H., Schludermann, E., Loisl, F., Humphries, P., Glas, M., Tritthart, M., and Habersack, H. 2014. Shoreline configurations affect dispersal patterns of fish larvae in a large river. – ICES Journal of Marine Science, 71: 930–942.

Received 4 February 2013; accepted 30 July 2013; advance access publication 7 September 2013.

The dispersal patterns of marked larvae of the nase carp (*Chondrostoma nasus* L.) were observed alongside dissimilar shoreline configurations in the main channel of the free-flowing Austrian Danube and compared with those of floating particles to investigate the mode of dispersal (active–passive). Individuals of different larval stages and floats at similar densities were released at an artificial rip-rap with groynes and a rehabilitated gravel bar. In both habitats, marked individuals were recaptured during the sampling period of 4 d after release. Relevant shoreline attributes for larval dispersal, such as the accessibility of nursery habitats, connectivity between adjacent habitats, and retention potential, were more pronounced at the gravel bar than at the rip-rap. At the gravel bar, larvae moved upstream and downstream within the connected bankside nurseries and displayed longer residence times. Larvae settled in groyne fields along the rip-rap as well; however, longitudinal dispersal was disrupted by groynes, forcing larvae to enter the main channel. Rather than settling in subsequent groyne fields, we assume that these larvae are displaced downstream and potentially lost from the local population.

Keywords: Danube, gravel bar, groyne fields, hydraulic conditions, larval drift, settlement.

Introduction

Dispersal is a key component of species' life-history strategies (Stevens *et al.*, 2012) and a valuable adaptation in spatially and temporally fluctuating environments (Tauber *et al.*, 1986). Dispersal is an active or passive transport process between two sites and includes distinct phases (departure–transport–settlement; Bennetts *et al.*, 2001). Investigations of fish dispersal in both marine and freshwater habitats have traditionally focused on the dispersal of young developmental stages (i.e. eggs, larvae, juveniles) between spawning sites and nurseries (Hjort, 1926; Pavlov, 1994). Spawning areas often do not match larval requirements (Humphries, 2005). Therefore, a rapid transport to, and settlement in, food-rich, safe nurseries is crucial (Pavlov *et al.*, 1978; Urho, 1999) and impacts future year-class strength via survival (Hinrichsen *et al.*, 2001; Houde, 2002; Dickey-Collas *et al.*, 2009). Furthermore, the spatial scale and degree of connectivity between these habitats is essential for genetic diversification, the design of marine protected areas as well as river and fisheries management (Huret *et al.*, 2007; Savina *et al.*, 2010; Basterretxea *et al.*, 2012). Identifying the triggers and mechanisms of dispersal is a prerequisite to draw well-founded conclusions about the rate of larval exchange between spawning sites and nurseries. In both marine and freshwater habitats, the transport of larvae and eggs combines passive elements related to abiotic factors as currents (Hogan and Mora, 2005; Rochette *et al.*, 2012), discharge (Harvey 1987), windforcing (Dalley *et al.*, 2002) or temperature (Peck *et al.*, 2009), and a suite of active behavioural reactions (i.e. olfaction, vision, vertical and horizontal movements: reviewed in Leis, 2007; phototaxis: Reichard *et al.*, 2002a; habitat choice: Robinson et al., 1998; orientation: Staaterman *et al.*, 2012).

Although many marine studies have included individual-based models and particle tracing approaches to model the dispersal of young fish (see review in Peck and Hufnagl, 2012), the corresponding efforts in the world's large rivers are rare (Korman *et al.*, 2004; Wolter and Sukhodolov, 2008; Schludermann *et al.*, 2012).

By observing movement patterns of introduced nase carp (*Chondrostoma nasus* L.) larvae in the Austrian Danube, the present study is designed to improve our understanding of dispersal and retention processes of early stages in fluvial ecosystems. The nase is a characteristic rheophilic cyprinid species inhabiting the hyporithral and epipotamal zones of large European rivers. It is a good model organism in applied river restoration, inter alia as physiological and morphological features of larval nase are well analysed (Kamler *et al.*, 1998; Keckeis *et al.*, 2001; Schludermann *et al.*, 2009) and their habitat requirements are representative for the early stages of many fluvial fish species (Schiemer *et al.*, 2002). The larvae hatch at fast-flowing spawning sites (aeration of demersal eggs is essential) necessitating subsequent movements in suitable nurseries, characterized as highly productive, shallow ($\leq$0.4 m), low-current ($<$0.1 m s^{-1}) areas along the shoreline which provide a variety of microhabitats (Keckeis *et al.*, 1997). Due to the comparatively weak swimming performance of free-embryos and larvae, as well as the highly dynamic environment of the spawning sites, dispersal of ichthyoplankton in large rivers is often referred to as passive drift: individuals are transported from site to site by the flow (Pavlov, 1994). Recent studies have revealed that larval fish use hydraulic gradients for orientation (Stoll and Beeck, 2012; Lechner *et al.*, 2013), even while drifting and are capable of actively piloting towards the shoreline (Schludermann *et al.*, 2012). Nonetheless, nurseries should be easily available (accessibility), connected with spawning sites and adjacent nurseries (connectivity) and offer long residence times (retention). High accessibility and longitudinal connectivity will reduce drift duration and thereby mortality (Brown and Armstrong, 1985; Harvey, 1987; Keckeis *et al.*, 1997). A high inshore retention will enhance community persistence and minimize washout effects once young fish are settled (Schiemer *et al.*, 2001).

The littoral zones of large rivers have undergone major alterations in the course of channelization and development (Dynesius and Nilsson, 1994). Few natural riverbanks remain intact, and the artificial shorelines have long been considered inappropriate and un-colonizable for young fish (Schiemer *et al.*, 1991). At the same time, several studies have revealed that frequently used structural components of river engineering, such as rip-raps and groynes, enhance physical diversity and habitat complexity on small scales and may be valuable habitats for young fish (White *et al.*, 2010). Nevertheless, alterations to the shoreline clearly change the hydrological and hydraulic characteristics of bankside zones (Shields *et al.*, 1995; Tritthart *et al.*, 2009), what may affect dispersal relevant attributes and thereby drift and settlement patterns of young fish. Therefore, a disruption of the natural dispersal process during early development due to improper river management and the increased fragmentation of key habitats could lead to a decrease or loss of characteristic fluvial species (Keckeis *et al.*, 1996).

In this study dispersal of nase larvae was investigated alongside a revitalized, near natural (gravel bar) and an artificial (rip-rap) shoreline. We hypothesized that the gravel bar performs better regarding accessibility, connectivity, and retention potential. This should be manifested in (a) higher entry rates of drifting larvae into suitable inshore habitats, (b) larval exchange processes between adjacent nurseries, and (c) longer residence times of young fish in these areas compared with the rip-rap. The simultaneous observation of early and later larval stages and passive particles addresses the character of dispersal (active–passive) at both shores.

Material and Methods

Study area

The study was conducted in the main channel of the Austrian Danube, within the "Danube Alluvial Zone National Park", east of Vienna (Figure 1). The stretch between river kilometres 1890 and 1893.8 provides shoreline situations with distinctly different hydrogeomorphological characteristics. On the right shore, straightened artificial embankments with basaltic blocks (rip-rap) and groynes arranged perpendicularly to the main channel axis deflect flow to improve the navigability at low water and simultaneously stabilize and protect banks against erosion. Alternating groynes and groyne fields, create characteristic embayments along the regulated riverbank. Groyne fields are temporally stochastic habitats and their availability for the riverine fauna depends on the discharge. At low flows (discharges smaller than mean flow in the study area), groyne fields are deposition zones with typical hydraulic patterns and prolonged water retentivity (Sukhodolov *et al.*, 2002). They may serve as important nurseries and refuges for young fish (Bischoff and Wolter, 2001) as well as incubator areas for planktonic algae (Engelhardt *et al.*, 2004). On the left shore, the riparian zone was adjusted to a near-natural state (gravel bar) in the course of an ecologically oriented river engineering project in the years 2007–2009. The rip-rap was removed and the groyne shapes structurally altered (cutting at the groyne roots to re-establish bankside flow) to improve habitat quality by enhancing longitudinal and lateral connectivity and self-dynamic processes.

Study design

Acquisition and rearing of larvae

Ripe adults of *C. nasus* from a natural spawning population were caught in a tributary of the Danube (Schwechat River) by electrofishing. In all, 10 females (2093 g eggs in total) and 14 males (201 g milt in total) were hand-stripped. Promiscuous fertilization of the spawn was applied (one clutch was mixed up with sperm of several males) using the dry method. Thereafter, fish were returned to the river.

The fertilized eggs were divided into two identical, well-oxygenated through-flow rearing flumes with attached temperature control units. The duration of incubation, growth rate, and differentiation of tissue are positively correlated with water temperature (Keckeis *et al.*, 2001). Therefore, running different temperature regimes in both flumes provided an opportunity to accelerate and decelerate fish development. Embryos in the cooler flume (mean water temperature $\pm$ s.d. = 11.7 $\pm$ 0.7°C) hatched on day 22 post-fertilization and were in the second larval stage (mean standard length $\pm$ s.d. = 11.7 $\pm$ 1.9 mm) at release (12 d post-hatching). Embryos in the warmer flume (14.8 $\pm$ 3.3°C) hatched 8 d earlier and were already in the fourth larval stage at release (12.7 $\pm$ 1.8 mm).

According to Penaz (2001), the second larval stage (L2) constitutes the transition to an exclusively exogenous feeding (yolk sac fully depleted). Individuals are characterized by a finfold instead of ventral and anal fins and a diphycerkal caudal fin. At this stage, *C. nasus* larvae show a positive phototaxis and fill the posterior chamber of their swimbladder. In the fourth larval stage (L4), fish already possess a two-chambered swimbladder, rays in the slightly incised caudal fin, anlagen of ventral fins, and shaped mesenchymal lobes at the position of the dorsal and anal fins. Swimming ability is

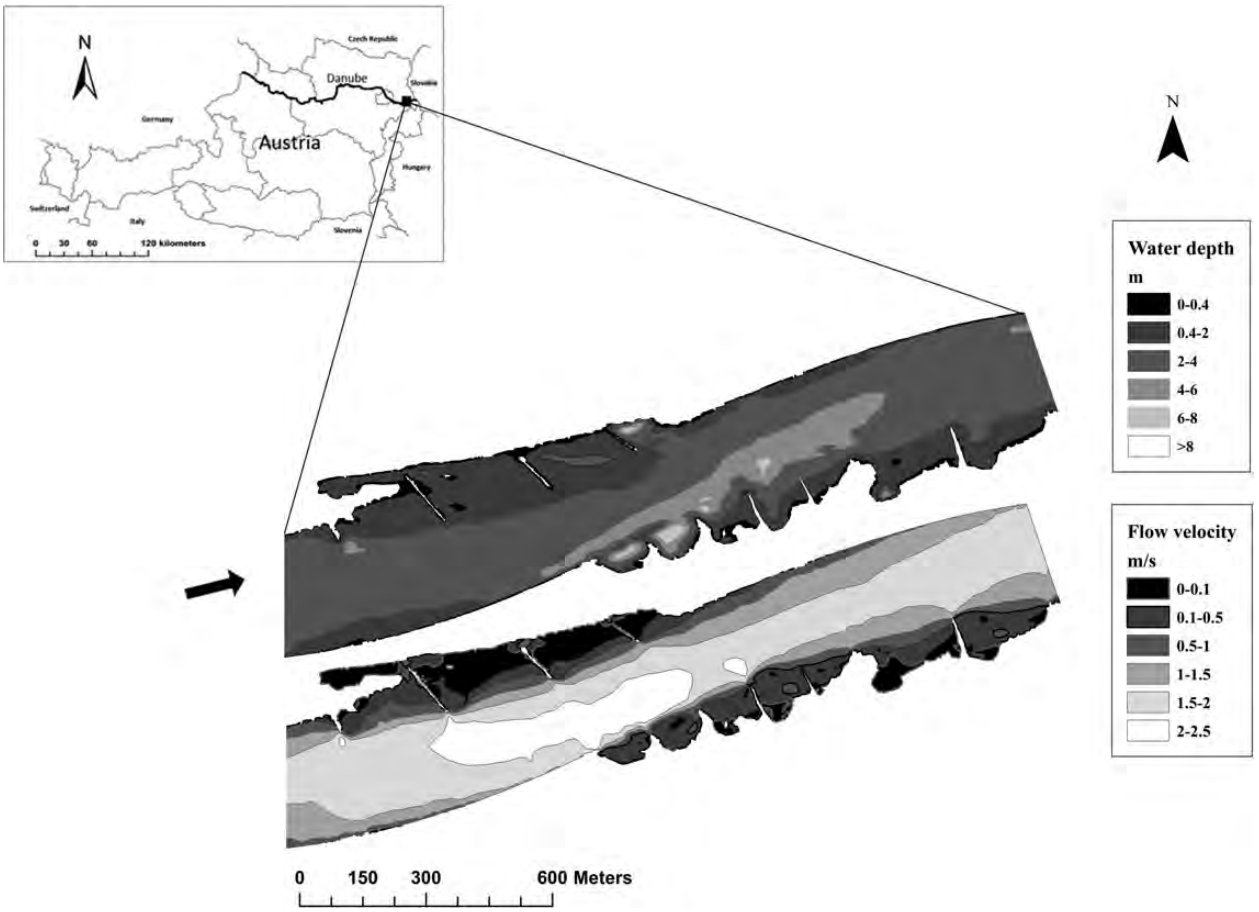

Figure 1. Overview of the study area with flow velocity and depth profiles for a discharge of 1143 $m^3 s^{-1}$. Flow direction is indicated by the arrow.

known to increase with body length (Flore and Keckeis, 1998) and differentiation of fins (Leavy and Bonner, 2009).

Marking larvae

The otoliths of larvae were labelled with a fluorochrome dye (Alizarin Red S, ARS; Sigma Aldrich®) to help identify recaptured individuals and determine their origin and initial developmental stage at release. Short-term mass-marking was applied according to Beckman and Schulz (1996). In brief, larvae were immersed for 3 min in a buffered (pH 8) ARS-solution (1%). NaCl (5%) was added to facilitate the incorporation of the chemical (osmotic shock). A dichotomous labelling key was developed for the release attributes "Shore" (left, right), "Developmental Stage" (L2, L4), and "Point" (Inshore, Offshore), whereas a mark encodes one of both features (Table 1). Therefore, multiple staining events were carried out, with individuals receiving up to four rings in their otoliths. First staining was applied 14 (warm flume) and 6 d (cold flume) after hatching, respectively. The last staining took place on the day before release (on days 23 and 15 post-hatching). Two-day intervals between successive markings were maintained to minimize mortality rates. The total numbers of marked individuals and the conversion of the ring sequence are shown in Table 1.

Release and field sampling

All marked larvae were acclimatized to the prevailing water temperatures in the Danube and subsequently released in the river. At both shorelines, fish larvae were introduced in habitats with distinctly different hydraulic conditions. At the rip-rap, these were the shallow deposition zone of a groyne field (inshore release, IR) and the head of the adjacent groyne (offshore release, OR). At the gravel bar, the riparian zone of the gravel shore (IR) and a point 10 m away in the fast flow (OR) served as release points. To match the natural circadian rhythm of drift activity (Reichard *et al.*, 2002b), larvae were released at dusk (19:30–20:30 h). Both shorelines were sampled alternately.

Table 1. Total numbers of released nase larvae differentiated for shorelines, developmental stages (L2–L4), and release points (inshore, IR; offshore, OR).

Shore	Stage	Release	Code	Number
Gravel bar	L2	IR	1-0-0	11 585
		OR	1-1-0	14 202
	L4	IR	1-0-0-1	12 558
		OR	1-1-0-1	10 116
Rip-rap	L2	IR	1-0-1	14 428
		OR	1-1-1	12 428
	L4	IR	1-0-1-1	7 062
		OR	1-1-1-1	14 812
			$\sum$	97 191

Mark sequences in the otoliths are shown as binary code, where numbers indicate days with staining (1) and no-staining (0) and (−) indicate two-dimensional intervals.

At each release point, larvae were introduced together with equal numbers of floats (spherical resin pellets, 4 mm diameter, density: 0.93–0.95 g cm^{-3}, white-coloured for OR and black for IR) representing passive elements of dispersal. Diverging drift and settlement patterns between these floats and released larvae may therefore indicate active mechanisms and reveal shore-specific differences of dispersal mechanisms.

Field sampling started on both shorelines contemporaneously with release (day 1) and was repeated 1 (day 2) and 4 (day 5) days post-release on each shore. A combination of stationary driftnets and point abundance sampling (PAS) was applied to survey larval drift and settlement patterns (Figure 2). Drift sampling aimed to capture larvae that were washed downstream or entered the current. Triplets of conically shaped driftnets (0.5 m diameter, 1.5 m long, 500 μm mesh) were exposed in the flow at three (rip-rap) to four (gravel bar) sampling sites encompassing a stretch of 2–870 m (rip-rap), respectively, 20–520 m (gravel bar) downstream of the release points. Simultaneous exposure of the net triplets at all sampling sites started at dusk and was carried out for 30 min in hourly intervals for a total of 5 h. A flowmeter

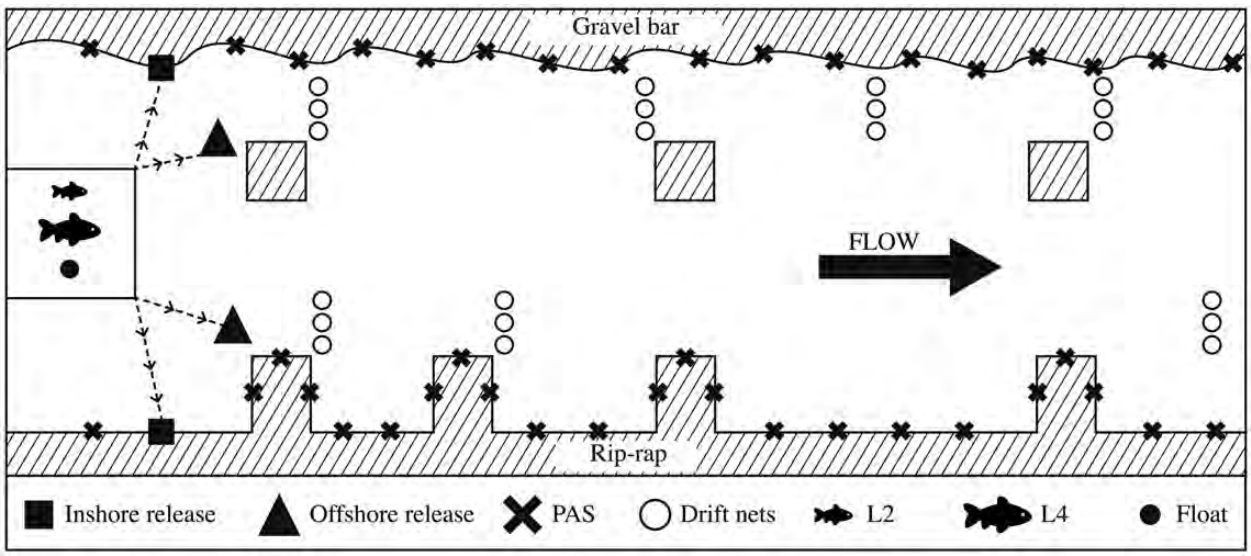

Figure 2. Sampling design. Shaded squares along the gravel bar represent remains of former groynes.

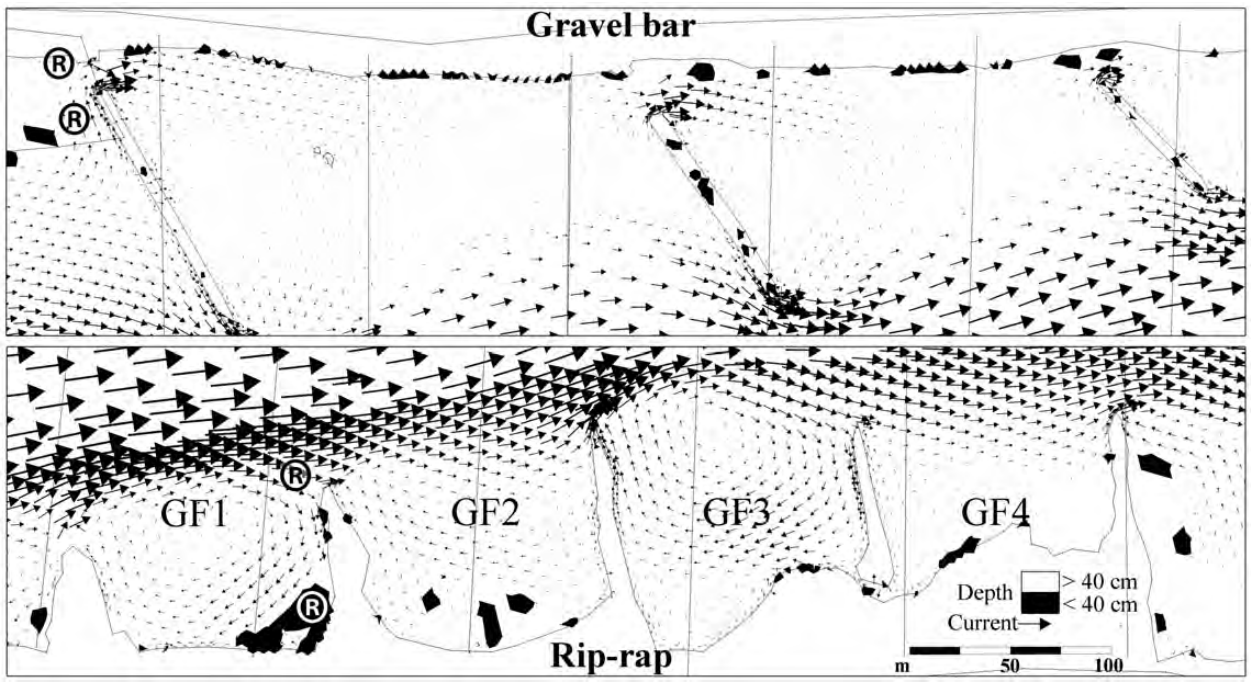

Figure 3. Flow patterns on both shores are illustrated by arrows. Arrow size is proportional to current speed and directly comparable between shores. Shallow areas, preferred by fish larvae, are shown as black areas. Consecutive groyne fields along the rip-rap are labelled (GF1–GF4).

(2030R, General Oceanics®, Miami) was attached to the lower third of each net entrance to measure the volume of filtered water.

The PAS intended to collect individuals that left the current and settled in inshore areas or maintained their position therein. This approach addresses the microhabitats and is quite robust against temporal and spatial heterogeneity of distribution (Persat and Copp, 1990). Using a dipnet (0.4 m diameter, 400 μm mesh size), a figure-8 sweep pattern was carried out, covering an area of ~0.75 m^2 (Schludermann *et al.*, 2012) every 10–30 m along the shoreline. The PAS sampling stretch was adjusted to the shoreline accessibility and ranged from 220 m (gravel bar) and 50 m (rip-rap) upstream of the release points to 540 m (gravel bar), respectively, 880 m (rip-rap) downstream of these points.

Exact positions of PAS and drift sampling points were mapped with a dGPS device (GS 20, Leica®, St Gallen). All captured fish were overdosed with Tricaine (MS-222, Sigma-Aldrich®, St Louis), preserved in 96% ethanol and taken to the laboratory for further analyses.

Sample processing

In a first step, fish were separated from other (mostly organic) material and separated into different families (i.e. Cottidae, Cyprinidae, Gobiidae, Percidae, and others). As no reliable key is available for species determination of early larval stages, potential recaptures were separated from autochthonous cyprinids based on the criteria of developmental stage and body length (mean body length at release ± 5 mm; growth rates in Keckeis *et al.*, 2001). From the potentially recaptured individuals, subsamples were taken (50% of the sample or 30 individuals if sample size was >60 individuals) and checked for ARS-marks. For this purpose, otoliths (lapilli) were dissected, embedded in synthetic resin (Crystalbond™, Aremco®, New York) polished with abrasive paper and screened under wavelengths of 515–565 nm with an epifluorescence-light microscope (Zeiss® Axio Imager M1 with Axio Vision 4.8.2 software for image analysis).

Data analysis

Recapture rates (RRs) were calculated (N_{rec}/N_{rel}; N, number of individuals; rec, recaptured; rel, released) for the particular groups (gravel bar and rip-rap; IR; OR, L2 and L4, and floats). The numbers of released larvae and floats were corrected for the number of removed individuals over time. To make single drift samples comparable, RRs were standardized by the volume of filtered water. The measured RR_Vol refers to the number of individuals per 1000 m^3. For PAS, RR_Vol is given in individuals per 0.75 m^2. In the following, the terms "drift rate" (DR) and "settlement rate" (SR) are used instead of RR_Vol-drift/settlement. Shore-specific differences in accessibility, retention potential, and connectivity were analysed performing systematic pairwise comparisons of DRs and SRs (Bonferroni adjusted Mann–Whitney *U*-tests and Wilcoxon tests in SPSS 20.0®) and illustrations of spatio-temporal dispersal patterns (in Arc Gis 10.0® and SigmaPlot 12.0®).

The hydraulic conditions alongside both shores were analysed using the fully three-dimensional model RSim-3D (Tritthart, 2005). This model approximates fluid motion (as governed by the Reynolds-averaged Navier–Stokes equations), numerically based on a polyhedral computation mesh. Flow and pressure fields were linked iteratively to each other using the SIMPLE method (Patankar and Spalding, 1972). A standard k-ε model (Launder and Spalding, 1974) was applied to achieve turbulence closure. Water surface elevations were derived from computed pressure fields. The model RSim-3D has been validated on several flume experiments and river engineering applications, as detailed in Tritthart (2005) and Tritthart and Gutknecht (2007). Within the study area, bathymetric measurements (single- and multibeam measurements) in combination with airborne laser scannings were conducted by the Austrian waterways authority (via donau) between February 2010 and October 2011. These served as a basis for a digital terrain model. Readings of a water level gauge at the downstream boundary of the study area (May 2011) were taken at several discharges. Thereafter, a rating curve was created based on these data and the catalogue of officially published characteristic water levels of the Danube River (which correspond to characteristic run-off values). This rating curve served as a boundary condition for the hydrodynamic model. Water surface elevations were measured within the study area at various discharges between May 2011 and December 2012. Additionally, several flow velocity measurements were conducted in two cross sections (river kilometres 1892.3 and 1893.4) using Acoustic Doppler Current Profiler (ADCP) and Acoustic Doppler Velocimetry (ADV) devices. The hydrodynamic model for the study reach was successfully calibrated and validated for five characteristic discharges where measured and officially published water levels as well as flow velocity measurements were available. The equivalent bed roughness had a value of 0.03 m; the equivalent bank roughness was estimated at 0.30 m, and

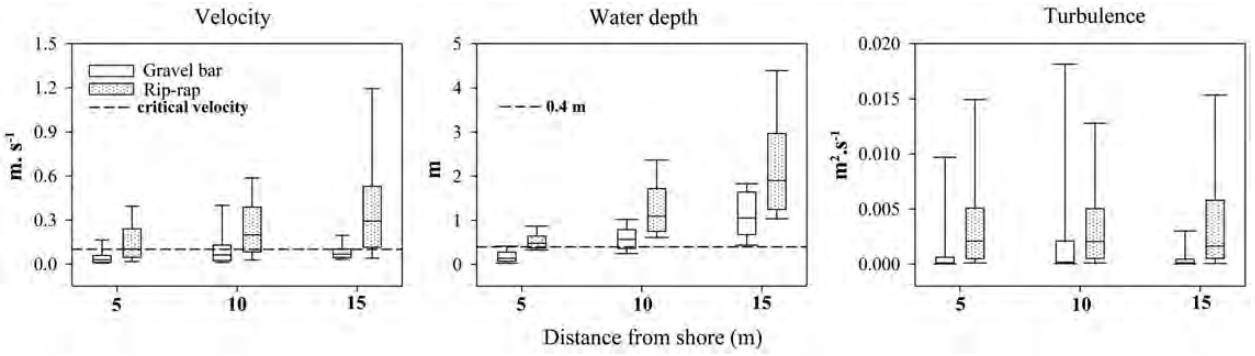

Figure 4. Lateral gradients of flow velocity, water depth, and turbulence at both shorelines. Values were derived from the hydrodynamic model (RSim-3D) by calculating the variables every 2 m on modelled lines (0.5, 5, and 15 m offshore) extending from the release point to the downstream end of the sampling site. Horizontal lines represent observed thresholds of suitability in 0+ nase habitats (Keckeis *et al.*, 1997).

groynes and rip raps were characterized by an equivalent roughness of 0.80 m.

Results

Shoreline characteristics

The gravel bar was characterized by large low-flow areas between adjacent groynes, ranging from the immediate bank line up to 150 m offshore (Figure 3). Smaller areas with stronger currents close to the bank were situated at the former groyne roots. Shallow reaches (water depth $\leq$0.4 m) preferred by young fish were evenly distributed along the whole sampling site. No pronounced lateral gradient of current velocity was observed, and the median value was below 0.1 m s^{-1} even 15 m offshore (Figure 4). The riverbed morphology comprised a shallow slope with median values of water depth increasing from 0.14 m (0.5 m offshore) to 1.05 m (15 m offshore). The turbulent kinetic energy 5 m offshore was higher than both closer and farther away from the bank. At a prevailing discharge of 1143 m^3 s^{-1}, the investigated gravel bar provided $\sim$671 m^2 of suitable larval habitats (according to Keckeis *et al.*, 1997) per 100 m shoreline length (and a total of 3627 m^2 at the whole sampling site, Table 2). The rip-rap was characterized by a steep velocity gradient between the groyne fields and the main channel (Figure 3). The recirculating flow patterns varied between adjacent groyne fields (GF1–GF4) relative to current strength, current direction, and vortices profile (Figure 3). Shallow areas were scattered at inshore deposition zones. The current velocity and water depth increased with distance from shore and were at the threshold of suitability even in proximate inshore areas (Figure 4). The turbulent flows along the rip-rap were stronger than at the gravel bar and apparently independent of the distance to the shoreline. The rip-rap offered $\sim$153 m^2 of suitable nursery areas per 100 m shoreline length (and a total of 2785 m^2, Table 2).

Larval dispersal

A total of 97,191 marked nase larvae were released and 3054 individuals were recaptured during the first week of observation, yielding an overall RR of 3.14%. Most larvae were caught in the stationary driftnets (2462) and fewer individuals (592) were counted in the PAS samples (Table 3). Altogether, 93% of recaptured drifting larvae (2293) were caught along the gravel bar whereas 74.1% of all settling individuals (439) were derived from the rip-rap.

Mean DRs of all groups (L2, L4, F; IR, OR) tended to be greater at the gravel bar (Figure 5). Here, DRs of all larvae combined were significantly higher than at the rip-rap (Figure 6). Furthermore, overall larval DRs at the gravel bar explicitly outran those of floats at the same shore (Figure 6). No distinct differences between overall DRs of larvae and floats were observed within the rip-rap

Table 2. Total length of investigated shoreline, total area of suitable nurseries, and nursery area per 100 m shoreline length are given for both shores.

	Gravel bar	Rip-rap
Shoreline length (m)	540	1 816
Total nursery area (m^2)	3 627	2 785
Nursery area/100 m shoreline (m^2)	671	153
Settlers /100 m shoreline (mean)		
Day 1	16.4	7.0
Day 2	5.1	1.8
Day 5	2.1	0.1

Additionally, mean numbers of settling individuals in nurseries along 100 m shoreline- stretches on each sampling day are given.

Table 3. Total numbers of recaptured larvae and mean RRs (RR Vol) at both shorelines (GB, gravel bar; RR, rip-rap) for both developmental stages (L2, L4) in driftnets (D) and PASs.

					Numbers				Mean RR Vol ± s.d.			
					IR		OR		IR		OR		
Shore	Day	Method	Samples	Individuals	L2	L4	L2	L4	L2	L4	L2	L4	Total larvae
Gravel bar	1	D	33	2 152	187	107	713	1 145	0.6400 ± 1.2346	0.3615 ± 0.7320	1.9618 ± 6.1172	4.5177 ± 16.8591	1.7668 ± 5.4495
		PAS	8	72	28	9	10	25	0.0297 ± 0.0703	0.0089 ± 0.0122	0.0087 ± 0.0166	0.0305 ± 0.0572	0.0183 ± 0.0336
	2	D	59	89	20	43	8	18	0.0233 ± 0.0785	0.0464 ± 0.1267	0.0067 ± 0.0239	0.0279 ± 0.0699	0.0256 ± 0.0477
		PAS	25	65	21	24	11	9	0.0072 ± 0.0123	0.0077 ± 0.0193	0.0031 ± 0.0076	0.0037 ± 0.0095	0.0056 ± 0.0089
	5	D	57	52	22	8	14	8	0.0469 ± 0.1543	0.0148 ± 0.0544	0.0254 ± 0.0687	0.0223 ± 0.0829	0.0273 ± 0.0604
		PAS	14	16	2	10	2	2	0.0011 ± 0.0042	0.0057 ± 0.0213	0.0009 ± 0.0034	0.0013 ± 0.0048	0.0024 ± 0.0064
Rip-rap	1	D	54	152	35	5	58	54	0.1460 ± 0.5345	0.1038 ± 0.6884	0.3670 ± 1.4228	0.1377 ± 0.4134	0.1937 ± 0.6039
		PAS	19	317	6	13	164	134	0.0022 ± 0.0051	0.0097 ± 0.0327	0.0696 ± 0.2622	0.0477 ± 0.1560	0.0344 ± 0.1136
	2	D	58	15	2	5	3	5	0.0027 ± 0.0150	0.0301 ± 0.1427	0.0089 ± 0.0491	0.0089 ± 0.0359	0.0101 ± 0.0286
		PAS	27	117	8	5	55	49	0.0021 ± 0.0094	0.0027 ± 0.0117	0.0163 ± 0.0845	0.0123 ± 0.0599	0.0089 ± 0.0415
	5	D	49	2	2	0	0	0	0.0031 ± 0.0163	0.0000 ± 0.0000	0.0000 ± 0.0000	0.0000 ± 0.0000	0.0009 ± 0.0048
		PAS	23	5	0	0	3	2	0.0000 ± 0.0000	0.0000 ± 0.0000	0.0010 ± 0.0037	0.0006 ± 0.0030	0.0005 ± 0.0013
Total	GB	D	149	2 293	229	158	735	1 171	0.1690 ± 0.6362	0.1041 ± 0.3774	0.4469 ± 2.9581	1.0201 ± 8.0599	0.4119 ± 2.6361
		PAS	47	153	51	43	23	36	0.0092 ± 0.0305	0.0073 ± 0.0186	0.0034 ± 0.0091	0.0076 ± 0.0258	0.0068 ± 0.0160
	RR	D	161	169	77	56	80	80	0.0509 ± 0.3153	0.0457 ± 0.4075	0.1263 ± 0.8372	0.0494 ± 0.2471	0.0689 ± 0.3592
		PAS	69	439	29	47	177	145	0.0014 ± 0.0064	0.0037 ± 0.0187	0.0259 ± 0.1473	0.0182 ± 0.0904	0.0131 ± 0.0653

Results refer to day of release (1) and subsequent samplings 1 (2) and 4 d (5) later.

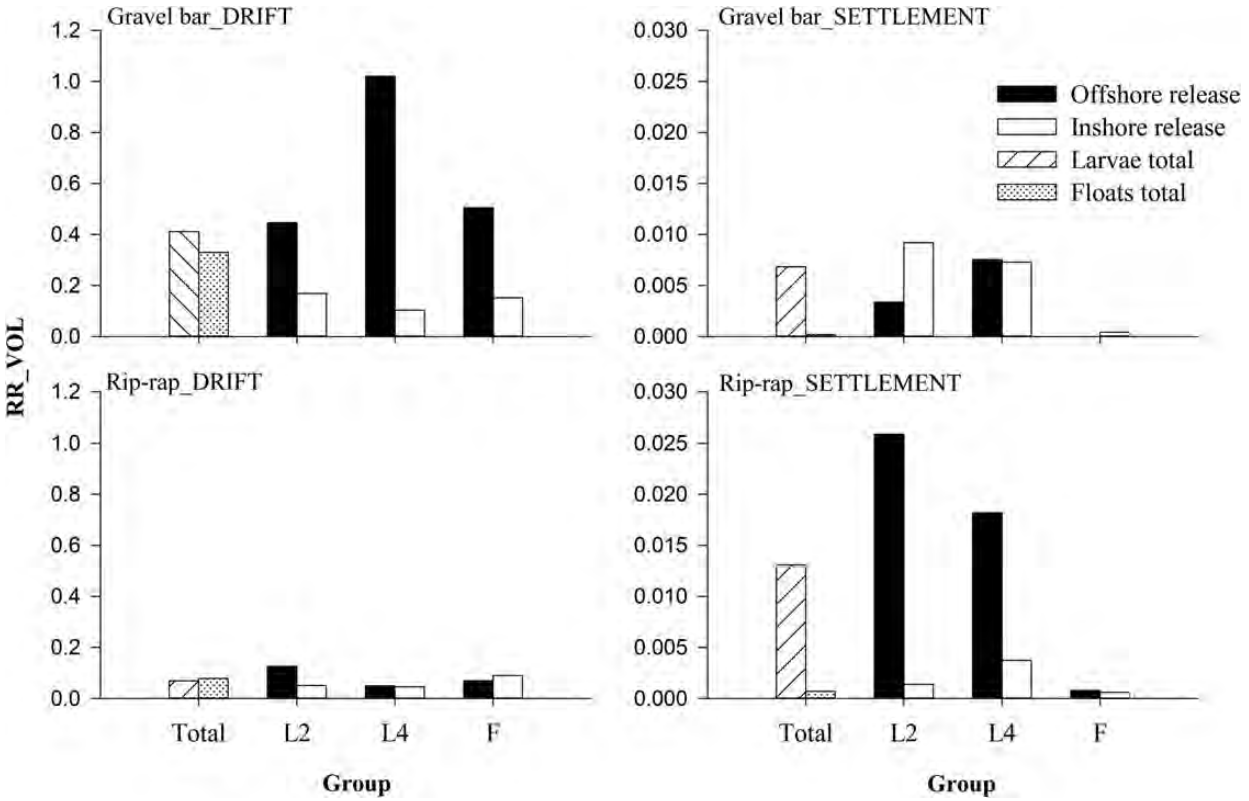

Figure 5. Mean recapture rates (RR_vol) of drifting and settling larvae for both shorelines relating to the total amount of recaptured larvae and floats (F) and single groups (L2, L4) and release points (inshore, offshore).

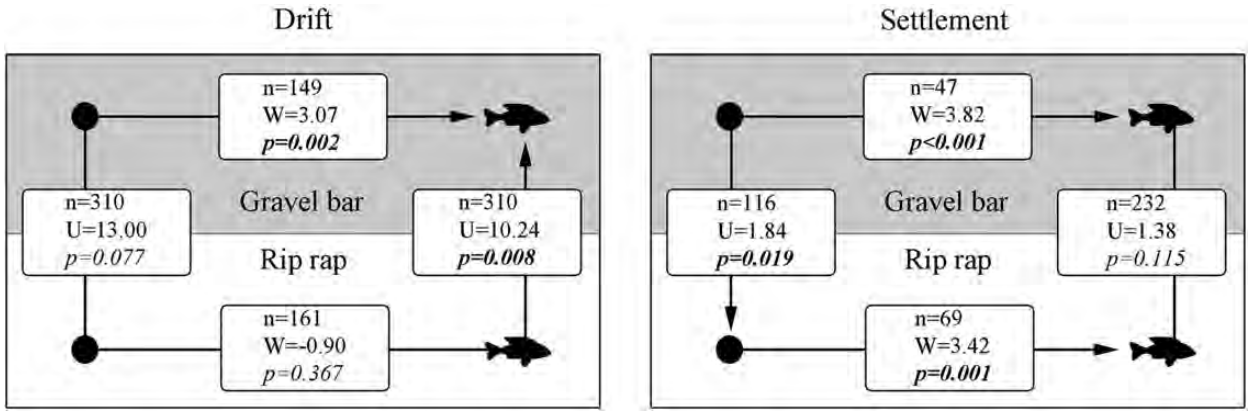

Figure 6. Differences between DRs and SRs of larvae ( ) and floats (filled circles) within (Wilcoxon test) and between (*U*-test) the shorelines. The arrows point towards superior mean values. Significant results in bold letters. Significance level was (Bonferroni) adjusted to 0.025.

(Figure 6). Pronounced differences in DRs of larvae and floats between both release points were found only at the gravel bar, where DRs of OR fish and floats were increased (Figure 5). No clear distinctions between DRs of all groups, originating from the same release points, were detected within each shore (Figure 5).

No inter-shore differences in overall larval SRs could be detected (Figure 6), and only SRs of IR-L2-nase proved to be higher at the gravel bar (Table 4). However, overall larval SRs significantly exceeded float retention at both shores (Figure 6). A detailed analysis of these dissimilarities with regard to shore, point of release, and larval stage is given in Table 5: the mean SRs of IR and OR larvae (L2 and L4) at both shores revealed higher values than float retention but not all combinations proved to be statistically significant. Considerable differences of SRs concerning the point of release were observed at the rip-rap for both larval stages, where OR larvae dominated the catch and clearly exceeded SRs of IR larvae (L2 and L4) at both shores (Figure 5). At the gravel bar, no differences of larval SRs with respect to the point of release were observed. However, a generally higher portion of IR larvae was found compared with the rip-rap (Figure 5). Overall more floats ($p = 0.019$) were retained at the rip-rap (Figure 6).

Analysing the temporal dispersal patterns of larvae at both shorelines revealed peaks in DRs on the first day of sampling at which 94% of all drifters at the gravel bar and 90% at the rip-rap,

Table 4. Pairwise comparisons (Mann–Whitney *U*-test) of larval SRs (L2 and L4) and floats (F) retention between shorelines and for each release point separately.

IR					OR				
		Gravel bar			Gravel bar				
		L2	L4	F	F	L4	L2		
Rip-rap	L2	$n = 116$ $U = 1.27$ $\mathbf{p = 0.002}$					$n = 116$ $U = 1.61$ $p = 0.967$	L2	Rip-rap
	L4		$n = 116$ $U = 1.39$ $p = 0.031$			$n = 116$ $U = 1.55$ $p = 0.568$		L4	
	F			$n = 116$ $U = 1.748$ $p = 0.105$	$n = 116$ $U = 1.78$ $p = 0.025$			F	

Significance level was (Bonferroni) adjusted to 0.01. Significant results in bold letters.

Table 5. Pairwise comparisons (Wilcoxon signed-rank test) of larval (L2 and L4) SRs and floats (F) retention for each release point and each shoreline separately.

	IR		OR	
	Gravel bar Floats	Rip-rap Floats	Gravel bar Floats	Rip-rap Floats
L2	$n = 47$ $W = 3.19$ $\mathbf{p = 0.001}$	$n = 69$ $W = 0.71$ $p = 0.474$	$n = 47$ $W = 2.36$ $p = 0.018$	$n = 69$ $W = 2.84$ $\mathbf{p = 0.004}$
L4	$n = 47$ $W = 2.81$ $\mathbf{p = 0.005}$	$n = 69$ $W = 1.07$ $p = 0.283$	$n = 47$ $W = 2.52$ $p = 0.012$	$n = 138$ $W = 2.47$ $\mathbf{p = 0.01}$

Significance level was (Bonferroni) adjusted to 0.01. Significant results in bold letters.

respectively, were caught within 5 h after release (Figure 7). Subsequently, the mean DR at the rip-rap was characterized by a steep, continuous decrease over time, whereas the mean DR stabilized at a low level from day 2 on at the gravel bar. Overall trends for drifting floats were similar to larvae, although at lower orders of magnitude at the gravel bar. Temporal characteristics of larval settlement also revealed a decreasing trend, with higher SRs on days 1 and 2 at the rip-rap, and conversely on day 5 with higher SRs at the gravel bar (Figure 7). At the gravel bar, floats were recaptured only on day 1, though they were found in PAS samples taken at the rip-rap during the first 2 d of observation.

Spatio-temporal dynamics

Gravel bar. Day 1: the combined spatial and temporal aspects of larval drift and settlement displayed a pronounced drift peak at sampling station 1 (SS1), comprising both stages, but mainly including OR individuals (Figures 8a and 9a). The DRs drastically decreased at successive sampling stations downstream (SS2–SS4) where primarily OR-L2-nase and L4-nase from both release points entered the nets. Settled larvae were detected up to 300 m downstream of the release points (IR-L2).

Day 2: predominately IR-L2-nase drifted along the whole gravel bar (Figure 8b), lower DRs of L4-nase (IR and OR) were detected at all four sampling stations (Figure 9b). Settling individuals from both stages and release points were regularly distributed between 35 m upstream to 425 m downstream of the release points.

Day 5: the DRs of both larval stages at the gravel bar were slightly higher than on day 2 (Figures 8c and 9c), and IR-L2-nase dominated the drift. Settlement of nase larvae ranged from 150 m upstream to 85 m downstream of the release points. The catch comprised IR- and OR-L2-nase (only downstream) as well as IR-L4-nase (only upstream).

Rip-rap. Day 1: the DRs of both stages on day 1 were distinctly lower at the rip-rap compared withy the gravel bar. Instead of peaking at SS1, closest to the points of release, DRs of both stages were highest at SS2. The SRs at the rip-rap were remarkably high but restricted to the first (GF1) and second (GF2) groyne field (max 170 m downstream of release). Settled IR larvae were primarily recaptured in GF1, and OR larvae were dominant in GF2 (Figures 8a and 9a).

Day 2: overall, highest DRs on day 2 were recorded for L4-nase at the rip-rap, whereas IR larvae dominated at SS1 and SS3 and OR larvae at SS2 (Figure 9b). Drift activity of L2-nase was restricted to SS1 and SS2 (with large numbers of OR individuals; Figure 8b). Except one individual (IR-L2) captured along the shoreline 450 m downstream of release, all other observations of larval settlement were made in GF1 and GF2 (Figures 8b and 9b).

Day 5: low DRs of IR-L2-nase were observed only at SS1 (Figures 8c and 9c). Apart from that, no further recaptures in drift were detected. Settling larvae were still found in GF1 (L2-OR) and one single individual was recaptured 700 m further downstream (L4-OR).

Discussion

This study compares two typical shoreline configurations of a free-flowing stretch of a large river with regard to their suitability for, and influence on, larval fish dispersal. Drift and settlement patterns of two introduced larval stages (L2, L4) of the nase carp and passive floats were recorded alongside a revitalized gravel bar and a modified rip-rap with groynes.

Shoreline accessibility

Shoreline accessibility refers to the hydro-geomorphological shore characteristics that enhance the arrival of larvae from offshore spawning habitats in littoral areas by ending the drifting phase and facilitating settlement in suitable nurseries. In this study, SRs of OR larvae and floats served as a basis to discuss accessibility of inshore nursery habitats. Higher SRs of OR larvae at both

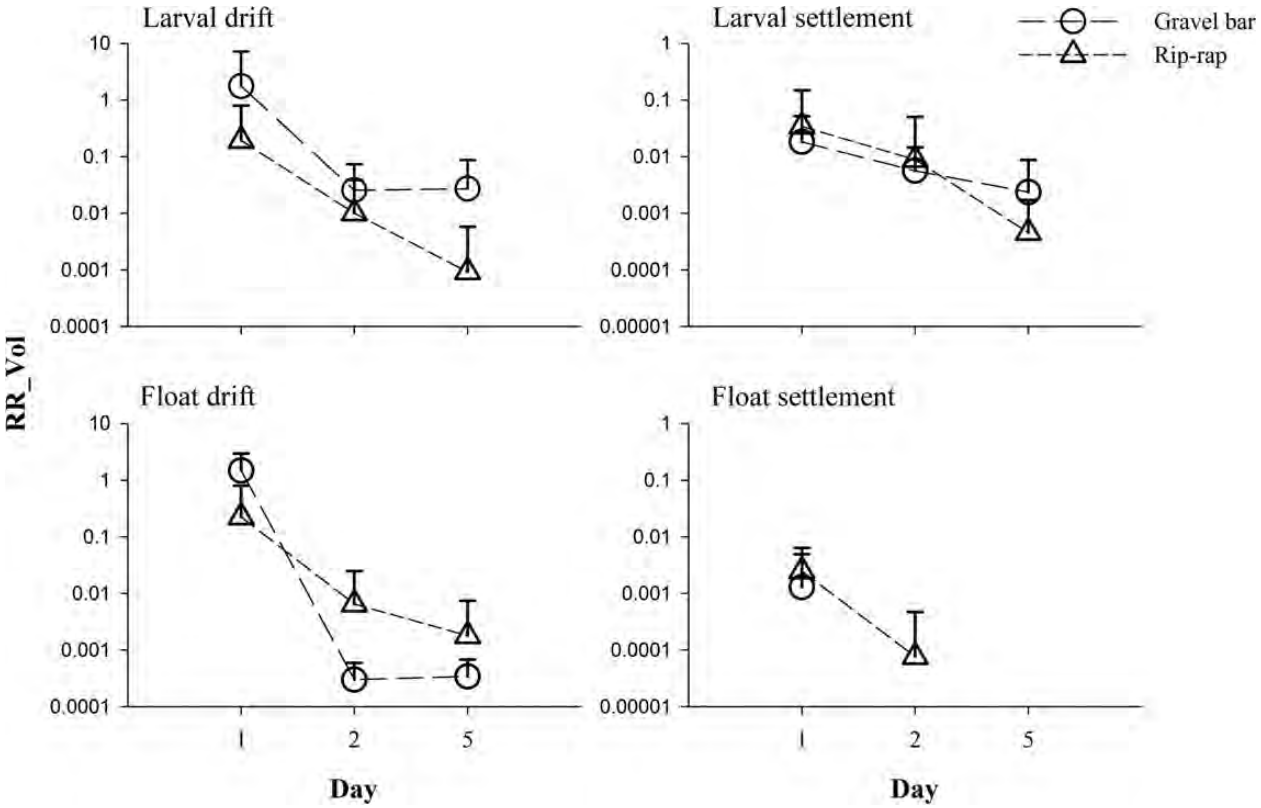

Figure 7. Temporal characteristics of drift and SRs at both shorelines. Values are plotted on a logarithmic scale.

investigated shorelines compared with passive float retention reflected larval swimming ability and behaviour. Mean SRs of OR larvae were even higher at the artificial rip-rap. In contrast to the gravel bar, settlement at the artificial rip-rap shoreline was restricted to nurseries located short distances from the release points. We ascribe the high accessibility of these particular areas partly to passive introduction facilitated by small-scale flow patterns. This was denoted by simultaneous recaptures of OR floats exclusively in GF1 and GF2 and a general higher passive retention rate of passive floats at the rip-rap compared with the gravel bar. Groyne fields along rip-raps are characterized by a large-scale vortex with a clockwise current, interfaced to the main channel by a mixing layer (Sukhodolov *et al.*, 2002). Large turbulent structures in this narrow strip of the mixing field play an important role for the exchange of momentum and matter—and presumably fish larvae—between the river and its groyne fields (Uijttewaal *et al.*, 2001; Schwartz and Kozerski, 2003) and could therefore have enhanced passive larval introduction. The exchange rates between single groyne fields vary, depending on the flow patterns within the fields (Figure 3), the groyne shape, the position of a groyne field in a sequence, the aspect ratio (between groyne length and length of the groyne field), as well as the discharge and flow velocity of the main channel (Uijttewaal *et al.*, 2001; Tritthart *et al.*, 2009). According to the marginal larval SRs downstream of GF2 (of both, OR larvae and IR larvae that entered the flow), we propose the average accessibility of the artificial shoreline to be comparatively low. In general, the active or the passive entrance of drifting larvae into conventional groyne fields along the rip-rap seems to be selective and losses to the main channel may outnumber larval input into these artificial structures by far.

Distinct initial drift peaks caused by OR larvae were recorded at the gravel bar at SS1 (Figures 8 and 9a). Trajectories of those larvae were short and led from the swift flowing areas at the OR points into driftnets placed in a short distance (45 m) downstream. Larval transport over such a short distance in high, overcritical currents may predominantly be a passive process (Pavlov, 1994). However, there is evidence that these washouts do not account for higher population losses: DRs displayed a strong longitudinal decrease (SS1–SS4) on day 1 and OR larvae were still drifting and settling along the gravel bar until day 5. The prolonged drift pattern suggests that OR larvae were able to delay or prohibit dislodgement or they settled before and re-entered the drift. We propose the large areas between adjacent modified groynes at the gravel bar to act as catch basins for drifting larvae, as they feature low current and turbulence regimes (Figures1 and 4) and are "decoupled" from the main channel. These conditions should foster orientated and energy-saving swimming towards the shallow littoral nursery habitats (Flore and Keckeis, 1998, Webb and Cotel, 2011).

Connectivity

Shoreline connectivity refers to the longitudinal and lateral connection of adjacent larval habitats in the sense that young fish can move between these areas. The analysis of connectivity based on spatial-temporal distribution patterns of larvae and floats in driftnets set and in point abundance samples. Longitudinal connectivity at the gravel bar was indicated by the even distribution of settling larvae along the shoreline and the observed upstream migrations of larvae on days 2 and 5. The longitudinal connectivity at the rip-rap, within the investigated shore-length, was distinctly lower than at the gravel bar. To explore and colonize new nursery habitats,

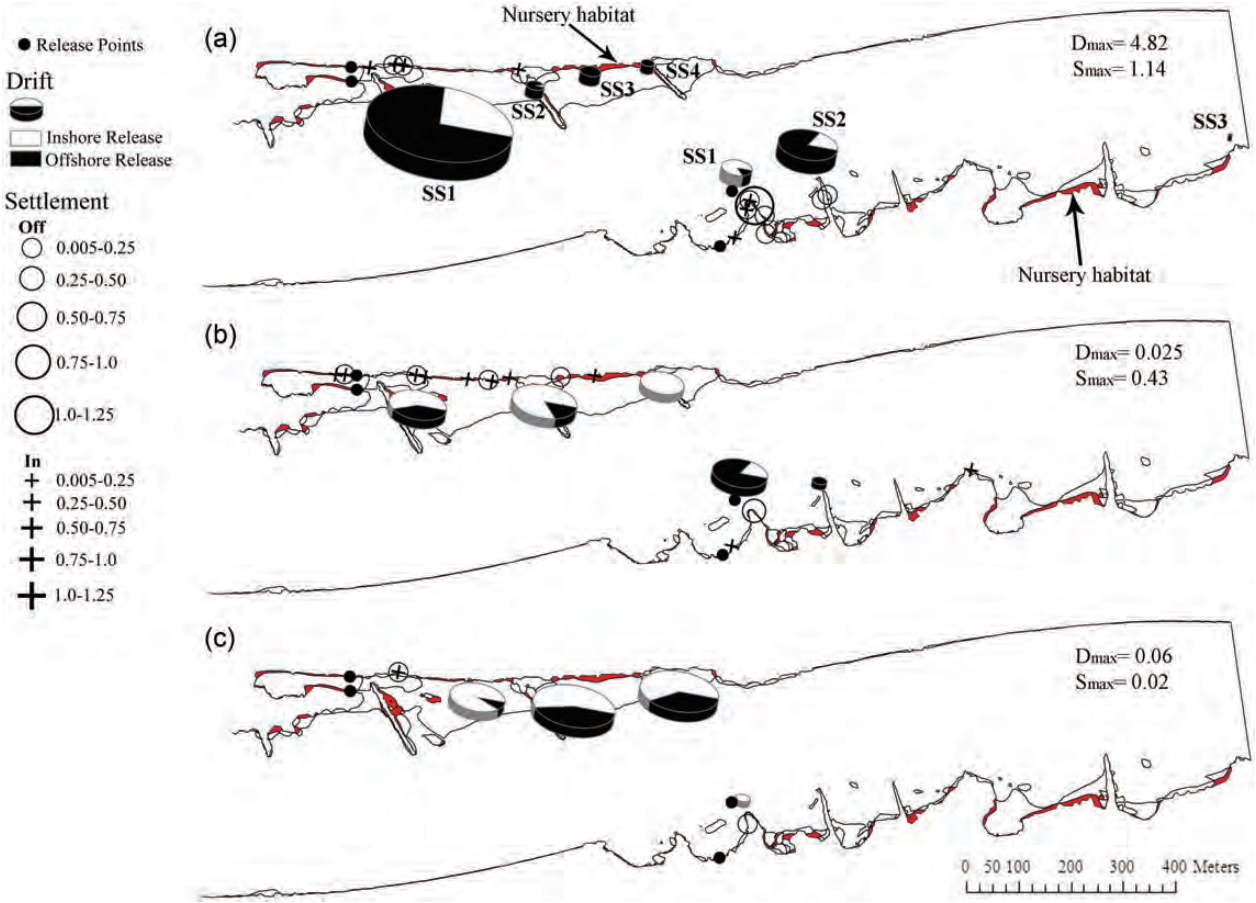

Figure 8. DRs (pies) and SRs (symbols) of L2-nase at all sampling stations (SS1 – SS4) are shown for the day of release (a) and subsequent samplings on day 2 (b) and day 5 (c). Pie sizes refer to the maximum mean DR on a given day. For comparisons between days, maximum values of mean DRs (D_{max}) are given. Maximum SRs (S_{max}) are given too. Red areas along the shorelines show suitable nurseries according to Keckeis *et al.* (1997).

retained larvae in GF1 and GF2 must pass groyne heads and enter high currents. Once in the drift, fish rather got lost to the main channel and rarely reached adjacent littoral zones by re-entering subsequent groyne fields due to poor accessibility.

Retention

The retention potential refers to the shoreline's capability of accommodating high larval population densities. The SRs of IR and OR larvae served as a base to analyse retention at the two shore configurations. The inshore "population" at the gravel bar was potentially composed of IR larvae that successfully stayed and moved along the shore as well as OR larvae that successfully reached these areas due to their high accessibility and connectivity. Here, larvae of both stages and release points were still detected drifting and settling until day 5. Although the investigated shoreline at the rip-rap was more than three times longer, the gravel bar provided a larger total area of suitable larval habitats. As a consequence, mean numbers of retained larvae per 100 m shoreline length were higher at the gravel bar each day (Table 2).

At the rip-rap, suitable larval habitats were patchily distributed at inshore gravel areas and within smaller bankside gyres which are known to have high retention capacities for passive particles (Tritthart *et al.*, 2009). This was indicated by larval settlement until day 5 in GF1 and longer/higher passive retention of floats. Nevertheless, the decrease in larval abundance over time at the rip-rap was steeper. The dominant hydraulic conditions for larvae in the groyne fields were harsh. High levels of turbulence can affect fish behaviour and physiology by challenging swimming speeds and increasing costs of locomotion (Utne-Palm and Stiansen, 2002; Liao, 2007). In combination with over-critical current speeds, these flows may have transported larvae from the centre of the large vortex towards the interface with the mixing layer and enhanced advection into the main channel. Additionally, the proximity to the shipping channel presumably enhances negative effects of navigation induced wave wash on young fish at the rip-rap. By altering the direction and speed of currents and dislocating microhabitats (Guhr, 2002; Wolter *et al.*, 2004; Kucera-Hirzinger *et al.*, 2009), wave wash may have increased larval displacement from the observed groyne fields. As drifting fish rarely re-entered and settled in adjacent nurseries, the probability of retention downstream of GF2 was very low.

Conclusion

The large, shallow, low-flow areas and the modified, newly created groyne structures along the left shore of the River Danube in the Danube Alluvial Zone National Park enabled dynamic dispersal processes of nase larvae. Cutting the groyne roots improved habitat diversity and quality by increasing connectivity of inshore

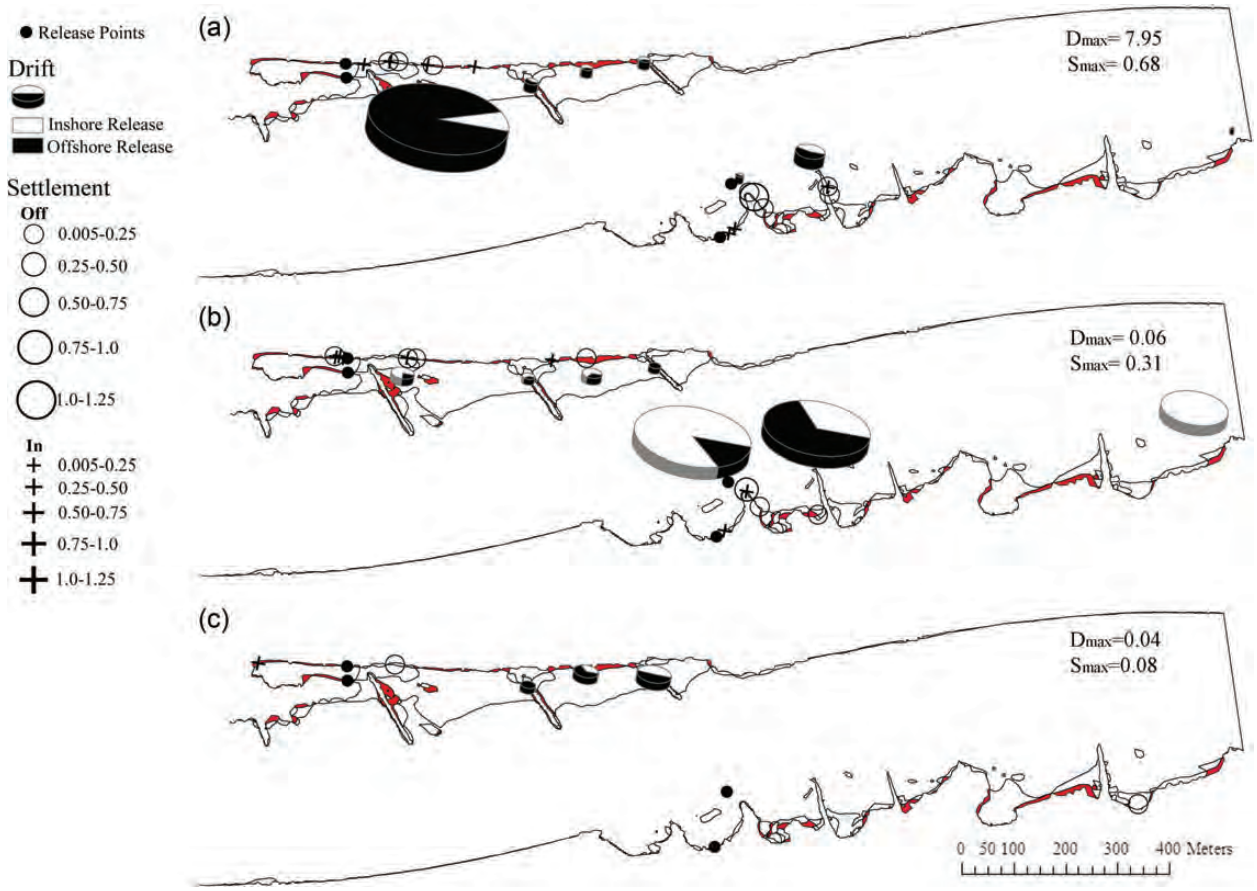

Figure 9. DRs (pies) and SRs (symbols) of L4-nase at all sampling stations (SS1 – SS3) are shown for the day of release (a) and subsequent samplings on day 2 (b) and day 5 (c). Pie sizes refer to the maximum mean DR on a given day. For comparisons between days, maximum values of mean DRs (D_{max}) are given. Maximum SRs (S_{max}) are given too. Red areas along the shorelines show suitable nurseries according to Keckeis *et al.* (1997).

nursery areas and directing a substantial part of the flow to the shore. Large lentic areas behind the remaining groynes became connected by this bankside flow, next to suitable inshore nursery habitats, presumably providing a safe route for larval dispersal. Larval DRs in the re-established bankside flow were high but these population losses were probably lowered by the hydraulic conditions and bank geomorphology which matched larval requirements and boosted shoreline accessibility, connectivity, and retention.

The conventional groyne fields along the right bank were found to be suboptimal nursery habitats for young fish due to stronger currents, higher turbulence, and greater water depths. Fish larvae may drift into groyne fields, but this seems to be more likely a stochastic event depending on several factors such as structural properties of the groynes, distinct flow patterns at the interface of river and groyne field, size and intensity of the mixing layer, as well as discharge- and navigation-induced currents. Active or passive movements of larvae out of these groyne fields are attended by strong currents at the groyne heads and a concomitant passive dislodgement of fish larvae downstream. Overall, this may lead to high mortalities and population losses, especially because the hydraulic and morphological features of the right shore seemed to inhibit re-entering subsequent groyne fields and nurseries. This study shows that these structures are disadvantageous by potentially interrupting dispersal pathways and settlement of riverine fish larvae.

Acknowledgements

The authors would like to thank P. Abel, M. Jung, S. Singer, W. Obruca, N. Savio, B. Zens, R. Krusch, M. Gruber, M. Humphries, and G. Össer for their help in the field and in the laboratory. M. Stachowitsch improved the English. Gabriel Singer improved the statistics. M. N. Martinz improved the first author's life. The study was financed by the Austrian Science Fund (FWF; www.fwf.ac.at) project no. P 22631-21 B17.

References

Basterretxea, G., Jordi, A., Catalan, I. A., and Sabates, A. 2012. Model-based assessment of local-scale fish larval connectivity in a network of marine protected areas. Fisheries Oceanography, 21: 291–306.

Beckman, D. W., and Schulz, R. G. 1996. A simple method for marking fish otoliths with alizarin compounds. Transactions of the American Fisheries Society, 125: 146–149.

Bennetts, R. E. N., Nichols, J. D., Pradel, R., Lebreton, J.-D., and Kitchens, W. M. 2001. Methods for estimating dispersal probabilities and related parameters using marked animals. *In* Dispersal, pp. 3–17. Ed. by J. D. Clobert, D. Etienne, A. Andre, and J. D. Nichols. Oxford University Press, Oxford.

Bischoff, A., and Wolter, C. 2001. Groyne-heads as potential summer habitats for juvenile rheophilic fishes in the Lower Oder, Germany. Limnologica, 31: 17–26.

Brown, A. V., and Armstrong, M. L. 1985. Propensity to drift downstream among various species of fish. Journal of Freshwater Ecology, 3: 3–17.

Dalley, E. L., Anderson, J. T., and deYoung, B. 2002. Atmospheric forcing, larval drift, and recruitment of capelin (*Mallotus villosus*). ICES Journal of Marine Science, 59: 929–941.

Dickey-Collas, M., Bolle, L. J., van Beek, J. K. L., and Erftemeijer, P. L. A. 2009. Variability in transport of fish eggs and larvae. II. Effects of hydrodynamics on the transport of Downs herring larvae. Marine Ecology Progress Series, 390: 183–194.

Dynesius, M., and Nilsson, C. 1994. Fragmentation and flow regulation of river systems in the northern 3rd of the world. Science, 266: 753–762.

Engelhardt, C., Kruger, A., Sukhodolov, A., and Nicklisch, A. 2004. A study of phytoplankton spatial distributions, flow structure and characteristics of mixing in a river reach with groynes. Journal of Plankton Research, 26: 1351–1366.

Flore, L., and Keckeis, H. 1998. The effect of water current on foraging behaviour of the rheophilic cyprinid *Chondrostoma nasus* (L.) during ontogeny: evidence of a trade-off between energetic gain and swimming costs. Regulated Rivers: Research and Management, 14: 141–154.

Guhr, H. 2002. Stoffdynamik in Buhnenfeldern der Elbe-Erste Ergebnisse. *In* Neue Erkentnisse über physikalische und ökologische Prozesse an Buhnenfeldern, pp. 9–16. Ed. by A. Mazijk van, and V. Weitbrecht. Karlsruhe (D)/Delft (NL).

Harvey, B. C. 1987. Susceptibility of young-of-the-year fishes to downstream displacement by flooding. Transactions of the American Fisheries Society, 116: 851–855.

Hinrichsen, H. H., John, M. S., Aro, E., Gronkjaer, P., and Voss, R. 2001. Testing the larval drift hypothesis in the Baltic Sea: retention versus dispersion caused by wind-driven circulation. ICES Journal of Marine Science, 58: 973–984.

Hjort, J. 1926. Fluctuations in the year classes of important food fishes. Journal du Conseil International pour l'Exploration de la Mer, 1: 5–38.

Hogan, J. D., and Mora, C. 2005. Experimental analysis of the contribution of swimming and drifting to the displacement of reef fish larvae. Marine Biology, 147: 1213–1220.

Houde, E. D. 2002. Mortality. *In* Fishery Science, pp. 64–87. Ed. by L. A. Fuiman, and R. G. Werner. Blackwell Publishing, Oxford.

Humphries, P. 2005. Spawning time and early life history of Murray cod, *Maccullochella peelii* (Mitchell) in an Australian river. Environmental Biology of Fishes, 72: 393–407.

Huret, M., Runge, J. A., Chen, C. S., Cowles, G., Xu, Q. C., and Pringle, J. M. 2007. Dispersal modeling of fish early life stages: sensitivity with application to Atlantic cod in the western Gulf of Maine. Marine Ecology Progress Series, 347: 261–274.

Kamler, E., Keckeis, H., and Bauer-Nemeschkal, E. 1998. Temperature-induced changes of survival, development and yolk partitioning in *Chondrostoma nasus*. Journal of Fish Biology, 53: 658–682.

Keckeis, H., BauerNemeschkal, E., and Kamler, E. 1996. Effects of reduced oxygen level on the mortality and hatching rate of *Chondrostoma nasus* embryos. Journal of Fish Biology, 49: 430–440.

Keckeis, H., Kamler, E., Bauer-Nemeschkal, E., and Schneeweiss, K. 2001. Survival, development and food energy partitioning of nase larvae and early juveniles at different temperatures. Journal of Fish Biology, 59: 763–763.

Keckeis, H., Winkler, G., Flore, L., Reckendorfer, W., and Schiemer, F. 1997. Spatial and seasonal characteristics of O+ fish nursery habitats of nase, *Chondrostoma nasus* in the River Danube, Austria. Folia Zoologica, 46: 133–150.

Korman, J., Wiele, S. M., and Torizzo, M. 2004. Modelling effects of discharge on habitat quality and dispersal of juvenile humpback chub (*Gila cypha*) in the Colorado River, Grand Canyon. River Research and Applications, 20: 379–400.

Kucera-Hirzinger, V., Schludermann, E., Zornig, H., Weissenbacher, A., Schabuss, M., and Schiemer, F. 2009. Potential effects of navigation-induced wave wash on the early life history stages of riverine fish. Aquatic Sciences, 71: 94–102.

Launder, B. E., and Spalding, D. B. 1974. The numerical computation of turbulent flows. Computer Methods in Applied Mechanics and Engineering, 3: 269–289.

Leavy, T. R., and Bonner, T. H. 2009. Relationships among swimming ability, current velocity association, and morphology for freshwater lotic fishes. North American Journal of Fisheries Management, 29: 72–83.

Lechner, A., Keckeis, H., Schludermann, E., Humphries, P., McCasker, N., and Tritthart, M. 2013. Hydraulic forces impact larval fish drift in the free flowing section of a large European river. Ecohydrology, DOI: 10.1002/eco.1386.

Leis, J. M. 2007. Behaviour as input for modelling dispersal of fish larvae: behaviour, biogeography, hydrodynamics, ontogeny, physiology and phylogeny meet hydrography. Marine Ecology Progress Series, 347: 185–193.

Liao, J. C. 2007. A review of fish swimming mechanics and behaviour in altered flows. Philosophical Transactions of the Royal Society B: Biological Sciences, 362: 1973–1993.

Patankar, S. V., and Spalding, D. B. 1972. A calculation procedure for heat, mass and momentum transfer in three-dimensional parabolic flows. International Journal of Heat and Mass Transfer, 15: 1787–1806.

Pavlov, D. S. 1994. The downstream migration of young fishes in rivers - mechanisms and distribution. Folia Zoologica, 43: 193–208.

Pavlov, D. S., Pakuhorukov, G. N., Kuragina, G. N., Nezdoliy, V. K., Nekrasova, N. P., Brodskiy, D. A., and Ersler, A. L. 1978. Some features of the downstream migrations of juvenile fishes in the Volga and Kuban Rivers. Journal of Ichthyology, 17: 63–374.

Peck, M. A., and Hufnagl, M. 2012. Can IBMs tell us why most larvae die in the sea? Model sensitivities and scenarios reveal research needs. Journal of Marine Systems, 93: 77–93.

Peck, M. A., Kuhn, W., Hinrichsen, H. H., and Pohlmann, T. 2009. Inter-annual and inter-specific differences in the drift of fish eggs and yolksac larvae in the North Sea: a biophysical modeling approach. Scientia Marina, 73: 23–36.

Penaz, M. 2001. A general framework of fish ontogeny: a review of the ongoing debate. Folia Zoologica, 50: 241–256.

Persat, H., and Copp, G. H. 1990. Electric fishing and point abundance sampling for the ichthyology of large rivers. *In* Developments in Electric Fishing, pp. 197–209. Ed. by I. G. Cowx. Blackwell Scientific Publications Ltd, Oxford, England.

Reichard, M., Jurajda, P., and Ondrackova, M. 2002a. The effect of light intensity on the drift of young-of-the-year cyprinid fishes. Journal of Fish Biology, 61: 1063–1066.

Reichard, M., Jurajda, P., and Ondrackova, M. 2002b. Interannual variability in seasonal dynamics and species composition of drifting young-of-the-year fishes in two European lowland rivers. Journal of Fish Biology, 60: 87–101.

Robinson, A. T., Clarkson, R. W., and Forrest, R. E. 1998. Dispersal of larval fishes in a regulated river tributary. Transactions of the American Fisheries Society, 127: 772–786.

Rochette, S., Huret, M., Rivot, E., and Le Pape, O. 2012. Coupling hydrodynamic and individual-based models to simulate long-term larval supply to coastal nursery areas. Fisheries Oceanography, 21: 229–242.

Savina, M., Lacroix, G., and Ruddick, K. 2010. Modelling the transport of common sole larvae in the southern North Sea: influence of hydrodynamics and larval vertical movements. Journal of Marine Systems, 81: 86–98.

Schiemer, F., Keckeis, H., Reckendorfer, W., and Winkler, G. 2001. The inshore retention concept and its significance for large rivers. Archiv für Hydrobiologie, Supplement, 135: 509–516.

Schiemer, F., Keckeis, H., Spindler, T., Wintersberger, H., Schneider, A., and Chovanec, A. 1991. Fish fry associations: important indicators for the ecological status of large rivers. Verhandlungen des Internationalen Verein Limnologie, 24: 2497–2500.

Schiemer, F., Keckeis, H., and Kamler, E. 2002. The early life history stages of riverine fish: ecophysiological and environmental bottlenecks. Comparative Biochemistry and Physiology A: Molecular and Integrative Physiology, 133: 439–449.

Schludermann, E., Keckeis, H., and Nemeschkal, H. L. 2009. Effect of initial size on daily growth and survival in freshwater *Chondrostoma nasus* larvae: a field survey. Journal of Fish Biology, 74: 939–955.

Schludermann, E., Tritthart, M., Humphries, P., and Keckeis, H. 2012. Dispersal and retention of larval fish in a potential nursery habitat of a large temperate river: an experimental study. Canadian Journal of Fisheries and Aquatic Sciences, 69: 1302–1315.

Schwartz, R., and Kozerski, H.-P. 2003. Entry and deposits of suspended particulate matter in groyne fields of the middle elbe and its ecological relevance. Acta Hydrochimica et Hydrobiologica, 31: 391–399.

Shields, F. D., Cooper, C. M., and Testa, S. 1995. Towards greener riprap: environmental considerations from microscale to macroscale. *In* River, Coastal and Shoreline Protection: Erosion Control using Riprap and Amourstone, pp. 557–574. Ed. by C. R. Thorne, S. R. Abt, F. B. S. Barends, S. T. Maynard and K. W. Pilarczyk. John Wiley and Sons.

Staaterman, E., Paris, C. B., and Helgers, J. 2012. Orientation behavior in fish larvae: a missing piece to Hjort's critical period hypothesis. Journal of Theoretical Biology, 304: 188–196.

Stevens, V. M., Trochet, A., Van Dyck, H., Clobert, J., and Baguette, M. 2012. How is dispersal integrated in life histories: a quantitative analysis using butterflies. Ecology Letters, 15: 74–86.

Stoll, S., and Beeck, P. 2012. Larval fish in troubled waters—is the behavioural response of larval fish to hydrodynamic impacts active or passive? Canadian Journal of Fisheries and Aquatic Sciences, 69: 1576–1584.

Sukhodolov, A., Uijttewaal, W. S. J., and Engelhardt, C. 2002. On the correspondence between morphological and hydrodynamical patterns of groyne fields. Earth Surface Processes and Landforms, 27: 289–305.

Tauber, M. J., Tauber, C. A., and Masaki, S. 1986. Seasonal Adaptation of Insects. Oxford University Press, Oxford.

Tritthart, M. 2005. Three-Dimensional Numerical Modelling of Turbulent River Flow using Polyhedral Finite Volumes. Wiener Mitteilungen Wasser-Abwasser-Gewässer, 193: 1–179.

Tritthart, M., and Gutknecht, D. 2007. Three-dimensional simulation of free-surface flows using polyhedral finite volumes. Engineering Applications of Computational Fluid Mechanics, 1: 1–14.

Tritthart, M., Liedermann, M., and Habersack, H. 2009. Modelling spatio-temporal flow characteristics in groyne fields. River Research and Applications, 25: 62–81.

Uijttewaal, W. S. J., Lehmann, D., and van Mazijk, A. 2001. Exchange processes between a river and its groyne fields: model experiments. Journal of Hydraulic Engineering (ASCE), 127: 928–936.

Urho, L. 1999. Relationship between dispersal of larvae and nursery areas in the Baltic Sea. ICES Journal of Marine Science, 56: 114–121.

Utne-Palm, A. C., and Stiansen, J. E. 2002. Effect of larval ontogeny, turbulence and light on prey attack rate and swimming activity in herring larvae. Journal of Experimental Marine Biology and Ecology, 268: 147–170.

Webb, P. W., and Cotel, A. J. 2011. Assessing possible effects of fish-culture systems on fish swimming: the role of stability in turbulent flows. Fish Physiology and Biochemistry, 37: 297–305.

White, K., Gerken, J., Paukert, C., and Makinster, A. 2010. Fish community structure in natural and engineered habitats in the Kansas River. River Research and Applications, 26: 797–805.

Wolter, C., Arlinghaus, R., Sukhodolov, A., and Engelhardt, C. 2004. A model of navigation-induced currents in inland waterways and implications for juvenile fish displacement. Environmental Management, 34: 656–668.

Wolter, C., and Sukhodolov, A. 2008. Random displacement versus habitat choice of fish larvae in rivers. River Research and Applications, 24: 661–672.

Handling editor: Claire Paris

ICES Journal of Marine Science

ICES International Council for the Exploration of the Sea
CIEM Conseil International pour l'Exploration de la Mer

ICES Journal of Marine Science (2014), 71(4), 943–956. doi:10.1093/icesjms/fst113

Contribution to the Themed Section: 'Larval Fish Conference'

Original Article

Effects of river regulations on fjord dynamics and retention of coastal cod eggs

Mari S. Myksvoll[1,2]*, Anne D. Sandvik[1,2], Lars Asplin[1,2], and Svein Sundby[1,2]

[1]*Institute of Marine Research, P.O. Box 1870 Nordnes, N-5817 Bergen, Norway*
[2]*Bjerknes Center for Climate Research, Bergen, Norway*

**Corresponding author: tel: +47 55 23 86 28; e-mail: mari.myksvoll@imr.no*

Myksvoll, M. S., Sandvik, A. D., Asplin, L., and Sundby, S. 2014. Effects of river regulations on fjord dynamics and retention of coastal cod eggs. – ICES Journal of Marine Science, 71: 943–956.

Received 6 November 2012; accepted 13 June 2013; advance access publication 21 July 2013.

High annual precipitation and steep mountains make Norway especially suited for the extraction of potential energy from waterfalls and is the country with largest production of hydroelectric power in Europe. The power production may affect both the position of river outlets and the seasonal cycle of freshwater discharge. To study the impact of river regulation on fjord dynamics and the transport of cod eggs, a numerical model is applied for the year 2009. We investigate two cases; the first case with only the natural seasonal cycle of freshwater discharge, whereas the second case includes all river regulations in the fjord system. The results show stronger surface outflow in the main part of the fjord when applying river regulations compared with natural run-off. The transport of cod eggs out of the fjord system increased with regulated run-off compared with the natural run-off, which correspondingly caused a reduced local retention of eggs within the various fjord branches. Changes in the seasonal cycle of freshwater discharge due to hydroelectric power production cannot be neglected as a contributing factor to the observed decline in coastal and fjord cod subpopulations.

Keywords: estuarine circulation, fjord modelling, *Gadus morhua* L., retention, river regulation, subpopulations.

Introduction

People have regulated rivers for thousands of years, mainly for irrigation purpose, freshwater supply and as an industrial energy source. High annual precipitation and steep mountains make Norway especially suited for extracting the potential energy in waterfalls and is the country with largest production of hydroelectric power in Europe. The theoretical annual potential of hydroelectric power is ~600 TWh of which 205 TWh is economical-technical exploitable (NVE, 2011). Through the mid-1900s, the Norwegian hydroelectric power production increased rapidly, and by 1979, the degree of regulation was 12.3% based on annual freshwater discharge (Kaartvedt, 1984). In 2009, the annual mean energy production was 127.1 TWh (NVE, 2011); hence, the degree of regulation has increased to 21.2%. The production is distributed among 1250 power stations all around Norway. Of the total hydroelectric power potential of 205 TWh, 60.2% is utilized, 23.7% is preserved, and 16% includes small power stations and projects in progress. Locally, there are substantial differences in the degree of regulations; in some fjords, more than half of the river input is controlled by power stations whereas others remain totally unaffected.

The anthropogenic influence on freshwater discharge through regulations causes a major change in the seasonal cycle. The general difference between a regulated river and a natural river is increased run-off during winter and decreased during summer (Pytte Asvall, 1976). The natural streamflow is low through winter as precipitation accumulates as snow and ice. At the same time, the demand for energy is high during the cold months and therefore will power production cause high discharge during a time of natural weak discharge, specifically in mountainous regions. Naturally, the discharge increases rapidly during spring, as the melting season starts, and reaches a distinct maximum in June/July (Saelen, 1976). The power production is lower during summer, with the result that run-off is reduced compared with the natural cycle. Hence, river regulations even out the natural seasonal variations (Pytte Asvall, 1976).

A large project was initiated in the 1970s to investigate the impacts of modified river run-off on the physical environment and ecosystems

in two fjord systems, Skjomen in northern Norway and Ryfylke in western Norway (Kaartvedt, 1984). In Skjomen, the wind was predominantly blowing out of the fjord through winter and early spring, which originated an outflow in the surface layer when the fjord was unaffected by regulations (Svendsen, 1983). An outflow in the upper 20–30 m was also measured after the power station started operating. However, the current measurements were not sufficient to make any precise conclusion about the effect of the river regulations (Svendsen, 1983). Significant differences in hydrography were observed, specifically lower salinity through winter and spring, most probably explained by modifications in the river run-off. Large river run-off during winter was observed by Skreslet and Loeng (1977), which caused the surface water to become colder and the basin water to become warmer. In Ryfylke, the building of a hydroelectric power station caused freshwater to be guided away from Jøsenfjorden and into Hylsfjorden (Kaartvedt and Svendsen, 1990a). A controlled discharge from the station generated an estuarine circulation with high velocities in the surface layer and increased surface salinity due to extensive mixing. High concentrations of euphausiids were detected in the upper 10 m, overlapping with the freshwater-driven currents and largely affected by the regulation (Kaartvedt and Svendsen, 1990b). Measurements also suggest that turbulent mixing close to the freshwater release cause mortality of zooplankton, as they are mixed into low-salinity water and subjected to osmotic stress (Kaartvedt and Aksnes, 1992). The spreading of the toxin-producing *Prymnesium parvum* was associated with a freshwater release from a hydroelectric power station in 1989 (Kaartvedt *et al.*, 1991).

Only a few studies have investigated the impacts of altered freshwater discharge from hydroelectric power production on marine ecosystems since the projects in the 1970s, most research has been on aquatic ecosystems within the river (Murchie *et al.*, 2008). Skreslet (1976) hypothesized that abnormal winter discharges will affect biological processes in fjords and coastal waters and possibly alter recruitment to fish stocks. He found a positive correlation between freshwater outflow and larval survival index of Arcto-Norwegian Cod (*Gadus morhua* L.) the following year and tried to explain the relationship by claiming that rich plankton production succeeds a year of high larval survival. However, the mechanisms causing the significant correlation are not fully understood and are probably influenced by several environmental variables (Kaartvedt, 1984). In the Gulf of St Lawrence, there was also found evidence that interannual variability in run-off has an impact on fisheries production, but again the underlying mechanisms are not understood (Sinclair *et al.*, 1986). They also argue that any effect of river regulations on fisheries is masked by the large interannual variability in run-off and high fishing intensity. Freshwater regulation for hydroelectric power production changes the seasonal discharge cycle and causes shifts in timing of flood waters. Drinkwater and Frank (1994) discuss the potential negative effect of asynchrony between run-off and spawning time. Fish species have adapted their spawning behaviour to ensure favourable transport or retention of life stages to nursery grounds and might be affected by changes to the natural run-off cycle. The natural seasonal run-off cycle varies considerably along the Norwegian coast (Tollan, 1976). Especially in northern Norway, the seasonal amplitude is large, with low run-off during autumn, winter and spring and high during summer. Hence, it can be expected that the potential impacts of hydroelectric power production on fjord dynamics and ecology will be large in northern Norwegian fjords. Since river regulations give highest deviation from the natural cycle during winter and early spring, is it particularly interesting to explore possible impacts on marine ecosystems during this period.

Fish eggs have developed distinct and separate values of specific gravity which relate to salinity (Solemdal, 1973). Vertical differences in salinity may therefore regulate the depth distribution of planktonic fish eggs (Sundby, 1991). This is the case with eggs of a local spawning stock of cod in Folda, a fjord system in northern Norway. According to a numerical model applied on this system by Myksvoll *et al.* (2011), the horizontal transport of a cod egg depends on its buoyancy, in addition to the local fjord hydrography and circulation. Depending on local differences in temperature during the ontogeny of cod embryos, the eggs hatch in a matter of about 3 weeks (Myksvoll *et al.*, 2014). After hatching, the cod larvae may perform vertical migration due to diurnal phototaxis, which may cause the larvae to be transported in ways that differ from what the eggs do. When the larvae metamorphose into juveniles with a full set of fins, they become more independent of horizontal advection of water and their behaviour is more controlled by predator avoidance and search for food. Thus, the final settlement of local 0-group cod in fjords depends on a combination of geophysical and biological factors.

The objective of this paper is to investigate the effect of river regulations on the horizontal transport of cod eggs in the fjord system of Folda in northern Norway. The Folda fjord has been subject to substantial river regulations for hydroelectric power production over the past 44 years, which may have caused deviations from the natural advection of fjord water and transport of cod eggs from local spawning areas. A regulated river differs from a natural river mainly through changes in the seasonal cycle. Hydroelectric power production during winter gives rise to increased freshwater discharge through the cold season and correspondingly reduced discharge during summer dampening the high flows during melting season. To study the impact of river regulation on fjord dynamics and transport of cod eggs, a numerical model is applied for the year 2009. Two scenarios are simulated; both cases utilize external forcing from 2009. The first scenario uses a natural seasonal cycle of freshwater discharge, whereas the second scenario includes all river regulations currently operating in the fjord system.

Material and methods

The study area

The fjord system of Sørfolda and Nordfolda in northern Norway is used in this study. These are two fjords with a joint opening towards Vestfjorden, located at 14.5–16°E 67.3–67.9°N (Figure 1). Both Sørfolda and Nordfolda have deep basins (up to 574 m) and are surrounded by steep mountains, which are characteristic for Norwegian fjords. The sill depths are 265 and 225 m, respectively. The freshwater input to the fjord system has large seasonal variability. During winter, the precipitation accumulates in the mountains as snow and ice. The melting starts in April and the run-off reach maximum in June. At the coast, a secondary run-off maximum is observed during fall, especially in years with discharges above average (Myksvoll *et al.*, 2011).

Four hydroelectric power stations are currently operating in the fjord system; all of them are located in Sørfolda (Figure 1). The two largest power stations started operating in 1968 and 1987, and together they control a drainage area of 688.7 km^2. Totally, 58% of the river run-off entering the fjord system passes through the four power stations, namely 93.15 $m^3 s^{-1}$ of a total 160.44 $m^3 s^{-1}$. In Sørfolda specifically, 78% of the river input is regulated. The power station built in 1968 diverted water away from a nearby fjord branch, where another power station was built in 1999. The

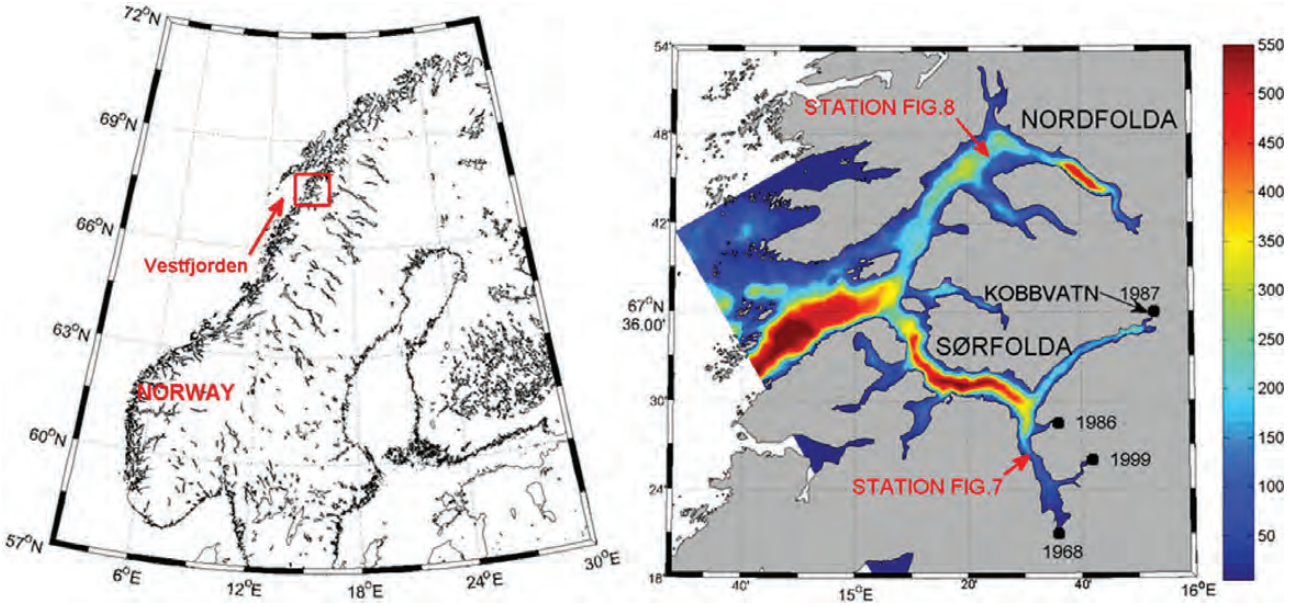

Figure 1. Location of the study area Sørfolda and Nordfolda in northern Norway nearby Vestfjorden. The right panel shows the model area with the bathymetry, and black dots show hydroelectric power stations with the year they started operating.

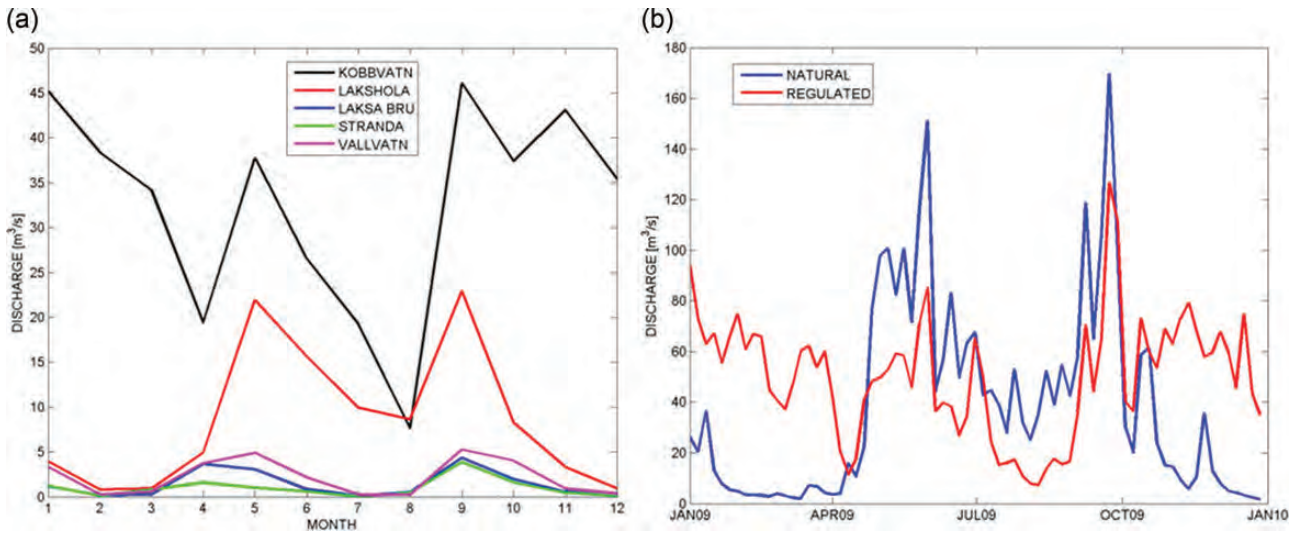

Figure 2. River data (a) provided by NVE and calculated river run-off to the model (b) for the entire drainage area discharging at Kobbvatn. (a) Monthly mean river run-off from one regulated river (Kobbvatn) and four natural rivers in 2009. (b) River forcing applied by the model for the whole drainage area of Kobbvatn.

result is that a large amount of water previously released further outwards now discharges at the innermost end of Sørfolda.

In a fjord with large river run-off compared with the surface area, an estuarine circulation is expected to dominate the dynamics of the surface layer during melting season (Svendsen, 1995). The estuarine circulation is characterized by a low-saline surface layer flowing out of the fjord and a compensating inflow below. Hydrographic monitoring by the Institute of Marine Research confirms the existence of a low-salinity surface layer with large interannual variability (Aure and Pettersen, 2004). Mohus and Haakstad (1984) measured currents in the inner part of Sørfolda in November 1978. They found a circulation pattern similar to an estuarine circulation, and the surface current was found to vary strongly with the local wind.

There are several known spawning areas for Norwegian coastal cod in Sørfolda and Nordfolda, as was shown in Myksvoll *et al.* (2011). Most of them are located in the inner part and near the heads of the various branches of the fjord system. Recent recordings of cod eggs prove the presence of a spawning population and indicating retention close to the spawning area (Myksvoll *et al.*, 2011).

Freshwater discharge

The Norwegian Water Resources and Energy Directorate (NVE) provided data from five rivers in the region. The monthly mean discharges from these rivers for 2009 are shown in Figure 2a. The measurements from Kobbvatn are taken downstream of a power station; the others are not directly affected by regulations. All rivers have

peak run-off during spring (May) and during fall (September); the regulated river Kobbvatn has several other peaks in addition. The regulated river does not show the same seasonal pattern as the other rivers, primarily due to high run-off all through winter season.

Total annual mean discharge to the fjord system was calculated to be 160.44 $m^3 s^{-1}$ for the period 1961–1990 in Myksvoll *et al.* (2011), distributed among 17 drainage areas. The drainage areas were classified in different run-off regimes; coastal, inland/transition, and mountain/glacier, depending on the elevation above sea level and the distance from the coast. The coastal regions have high run-off during autumn/winter and low run-off during summer, represented by the river Stranda (Figure 2a). The mountain/glacier regions are characterized by peak run-off during summer and low run-off through winter due to the accumulation of precipitation, represented by the river Lakshola. The inland/transition regimes, located in between the coastal and mountainous regions, have high run-off during spring/autumn and low run-off during summer/winter and are represented by the rivers Laksa Bru and Vallvatn. The river Kobbvatn represents a regulated mountain/glacier regime. The annual mean discharges for all five rivers were calculated for the period 1961–1990. A factor was calculated for all drainage areas to scale the river data relative to the total annual mean discharge within each drainage area. Then, this scaling factor was applied to the river data from 2009 (shown in Figure 2a), providing the total discharge within each drainage area for 2009 as the example in Figure 2b. The drainage area shown here is a mountain/glacier region and is therefore scaled with the river Lakshola in the natural case and the river Kobbvatn in the regulated case.

A limitation with this method is the assumption of a consistent river time-series from 1961 until 2009, which is not correct for Kobbvatn and Lakshola. The hydroelectric power station at Kobbvatn started operating in 1987 and the river run-off was affected the previous years during construction. The drainage area to this power station expanded from 406 to 455 km^2 (+12%). The annual mean discharge was therefore calculated for the period 1961–1980 and increased by 12% in 2009. In 1999, another hydroelectric power station guided water away from the river Lakshola, causing an abrupt decrease in annual mean discharge. Therefore, the annual mean discharge was calculated for the period 2000–2009, and thus, the scaling factor was based on this period. A trend in the time-series can also cause errors when using this method. However, data from the other rivers (Stranda, Laksa Bru, and Vallvatn) show no evidence of either decreasing or increasing run-off in the period 1953–2009.

Circulation model and forcing

The model used for these simulations is the Regional Ocean Modeling System (ROMS) version 3.5, with algorithms described by Shchepetkin and McWilliams (2005). This is a free-surface, hydrostatic, primitive equation ocean model that uses stretched terrain following *s*-coordinates in the vertical and curvilinear coordinates in the horizontal (Haidvogel *et al.*, 2008). The primitive equations are solved by a finite differences method on an Arakawa C-grid. The generic length scale closure scheme using the special case of Mellor-Yamada 2.5 is used for the turbulence parameterization (Umlauf and Burchard, 2003).

The model domain covers the fjord system of Sørfolda and Nordfolda in northern Norway at 67.5°N. The grid length is 200 m with 257 points in ξ direction and 282 points in η direction. In the vertical, there are 35 sigma layers, with higher resolution towards the surface. The initial and boundary conditions were provided by an 800-m coastal model (Albretsen *et al.*, 2011), as described in Myksvoll *et al.* (2014). The boundary variables are temperature, salinity, current, and surface elevation, updated every hour. The simulation was initiated on 1 January 2009 and continued through February with atmospheric forcing extracted from the ERA-interim reanalysis. Then, the model was restarted on 1 March 2009 continuing until June 30, with atmospheric forcing provided by the Weather Research and Forecasting (WRF) model. The WRF model, developed by the National Center of Atmospheric Research (NCAR), is a state-of-the-art numerical weather prediction model. It is also used for climatological studies and other purposes by a rapidly growing user community. A detailed description of the model might be found in Skamarock *et al.* (2008). The WRF simulation was performed with 31 terrain-following sigma levels and the model top at 50 hPa. Fine horizontal resolution was 1 km and default settings were used for the physical options. Static fields as land use and topographical data have been provided by the US Geological Survey in a horizontal resolution of 30″ (0.9 km in N–S direction).

Individual-based cod egg model

The cod egg model is a simple individual-based model included to the particle-tracking routines of ROMS as described by Narvaez *et al.* (2012), and based on Sundby (1983, 1991). The input parameters are egg diameter (1.4 mm) and mean egg neutral buoyancy (30.57) with standard deviation (1.27), in terms of salinity. Details about the individual-based cod egg model and measurements of the neutral buoyancy of the eggs can be found in Myksvoll *et al.* (2014).

Totally, 35 420 cod eggs were released into the model domain for each of the model simulations. The spawning areas where chosen based on information from the Norwegian Directorate of Fisheries (Myksvoll *et al.*, 2011). One egg was released daily at every ocean grid cell between 1 March and 30 April at 20-m depth, as shown in Figure 3.

Results

Spatial wind variations

The high-resolution atmospheric forcing used in these simulations reveal a highly complex wind pattern within the fjord. Windspeed and prevailing directions are shown in Figure 4 through March and April 2009, at specific locations. Locations are chosen based on spawning areas or areas of general interest. The wind generally follows the direction of the fjord, blowing either into or out of the fjord. This is especially seen in the inner part of the fjord which is surrounded by steep mountains, Figure 4c–g. Two main wind directions are dominating in the mouth area, Figure 4a; southeasterly and southwesterly. Winds from southeast are usually associated with a high air pressure developing over land causing cold-air flowing out of the fjord. This is a common winter situation that can persist for many days. Southwesterly winds are normally caused by the passage of low-pressure systems. Under such conditions, the winds can be particularly strong but normally of short duration, only 2–3 d.

We find from the atmospheric model results that most of the fjord branches in the inner part of Sørfolda are characterized by frequent winds out of the fjord (Figure 4c, d, and f), whereas the small fjord branch in the western part is dominated by wind blowing into the fjord (Figure 4b). During cold-air drainage, the wind follows the

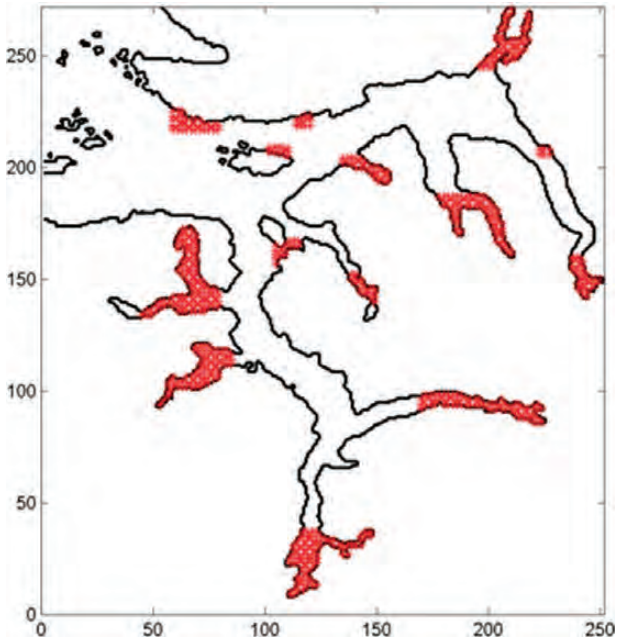

Figure 3. Release location of cod eggs in the model at the known spawning areas of Norwegian coastal cod, based on data provided by Gyda Lorås at the Norwegian Directorate of Fisheries (Myksvoll *et al.*, 2011).

topography of Sørfolda and is therefore directed towards the mouth of this fjord branch.

In the inner part of Nordfolda (Figure 4g), the wind is strictly aligned with the fjord axis, with the highest frequency of winds from southeast. The predominant wind direction in the whole of Nordfolda is southeasterly. Due to the complex topography in the fjord system, this circulation pattern causes the wind to be directed out of the southern branch (Figure 4h) and into the northern branch (Figure 4i). This is important for local dynamics and water exchange with the main fjord, and correspondingly, the southern branch is openly connected while the northern branch is more restricted.

Hydrography and circulation

The estuarine circulation is considered the most important semi-permanent density current in fjords (Gade, 1976). Svendsen (1995) classifies fjords in relation to width and freshwater supply, and the estuarine circulation is considered important in fjords with large freshwater supply relative to their surface area. In most fjords, the river outlets are located near the head, causing a density-driven current flowing out of the fjord towards the mouth following the curvature of the topography. Monthly mean surface current speed for March was calculated for both simulations in Folda (Figure 5). The mean freshwater run-off to the drainage area of Kobbvatn was 4.20 $m^3\ s^{-1}$ in the natural and 52.77 $m^3\ s^{-1}$ in the regulated cases for this period (from Figure 2). In the case with river regulations, the surface current in Sørfolda is considerably stronger than in the non-regulated case. The surface outflow in Sørfolda, characterized as the estuarine circulation, is up to 0.2 $m\ s^{-1}$ stronger in March when the river outflow is regulated. The upper layer circulation separates in the junction between the two fjords; one branch enters Nordfolda whereas the other flows out of the fjord system along the north coast at the mouth. In April, the difference between the two simulations is smaller, $\sim$0.08 $m\ s^{-1}$ (not shown).

Regulated freshwater run-off causes a reduction in the surface temperature for March in a large part of the fjord system compared with the natural discharge, the difference between the simulations is shown in Figure 6a. Especially in Nordfolda, the temperature is reduced with $\sim$3°C. In the innermost branches of southern and western Sørfolda, the temperature has increased. At the same time, the salinity is significantly reduced in Sørfolda ($\sim$5 units) and slightly reduced in Nordfolda (Figure 6b). The large reduction in the south is caused by locally increased river run-off through January, February, and March. During these months, low-saline water is advected into the northern part, and thereby causing the well distributed low surface salinity. In April, the overall salinity differences are low (Figure 6c), but specific fjord branches can have large local variations, mainly due to rivers being diverted into other fjord branches. Further into the melting season, the salinity difference turns positive in the southern part where all the large rivers are located (Figure 6d). In this period, the high summer flow is dampened by reduced freshwater release and the surface salinity is higher in the simulation with river regulations.

Monthly mean vertical profiles of salinity, temperature, and current speed from March are shown in Figure 7 in Sørfolda at the location shown in Figure 1, both with natural (blue) and regulated (red) rivers. The station is located in the narrowest part of Sørfolda, where there are only small variations across the fjord, and within the core of the outflow. In the case with natural river run-off, the salinity and temperature profiles are nearly vertically homogeneous. With river regulations, the surface salinity is reduced from 33.2 to 28.1 and below 20-m depth the salinity increases, up to 0.3 units in the lower layers. The surface temperature is also reduced in the regulated simulation, but below 2-m depth the temperature has increased by $\sim$1°. The surface outflow has increased with regulations to $\sim$0.39 $m\ s^{-1}$ from 0.15 $m\ s^{-1}$ in the natural case. The regulations cause a shallowing of the surface outflow; therefore, the current speed below 5 m is weaker with regulated run-off compared with natural run-off.

Salinity and temperature profiles from the central part of Nordfolda are shown in Figure 8, a monthly mean covering March with natural (blue) and regulated (red) rivers. Both salinity and temperature are significantly reduced in the upper 40 m when regulated rivers are used. Strong stability in the upper layer inhibits vertical transfer of energy and heat, causing the lower layer to be warmer and saltier. The depth of the mixed layer is $\sim$100 m when using natural rivers, compared with $\sim$40 m in the regulated case.

The surface temperature, current, and windfield on 4 March 2009 is shown in Figure 9, focusing specifically on Sørfolda and adjacent fjord branches. The windfield is identical for both cases, but the temperature and current are from the simulation with natural rivers (a) and regulated rivers (b). In both cases, the main pattern is outflowing water with corresponding low temperatures. A cyclonic eddy is located in the main part of the fjord and is stationary for $\sim$10–15 d (Figure 9a). This eddy is not present in the case with regulated rivers. Further out of the fjord, the wind direction is mainly easterly, directly blowing from the main fjord into the two small branches in the western part. When using natural river run-off, the surface current is highly influenced by the wind and surface water is flowing into the fjord branches, with outflow below. This circulation pattern is reversed compared with the regular estuarine circulation with the outflowing surface layer, directed away from the head and towards the mouth. The reversed

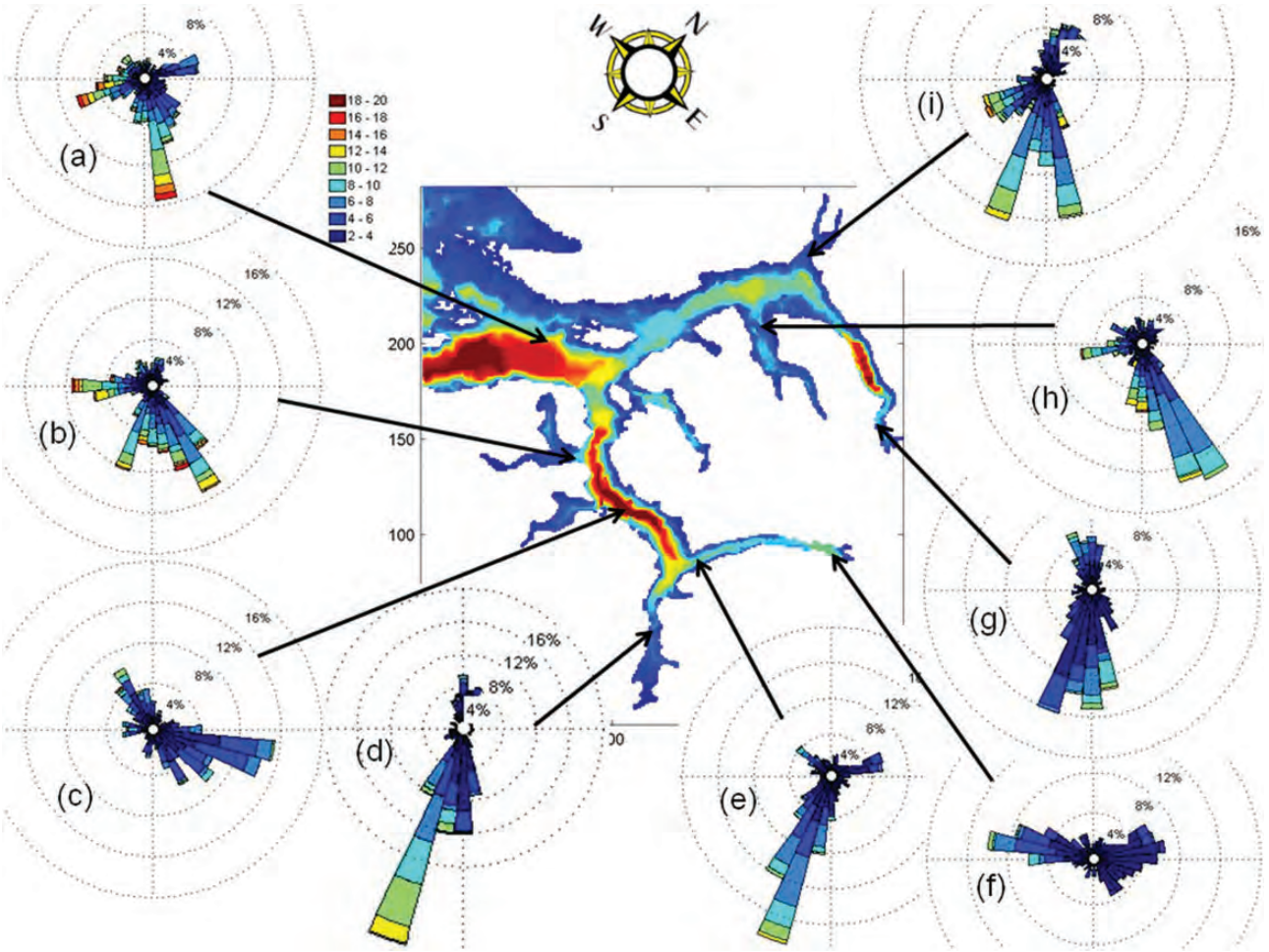

Figure 4. Windspeed and direction provided by the atmospheric model (WRF) for the period March and April 2009, used as forcing to the model.

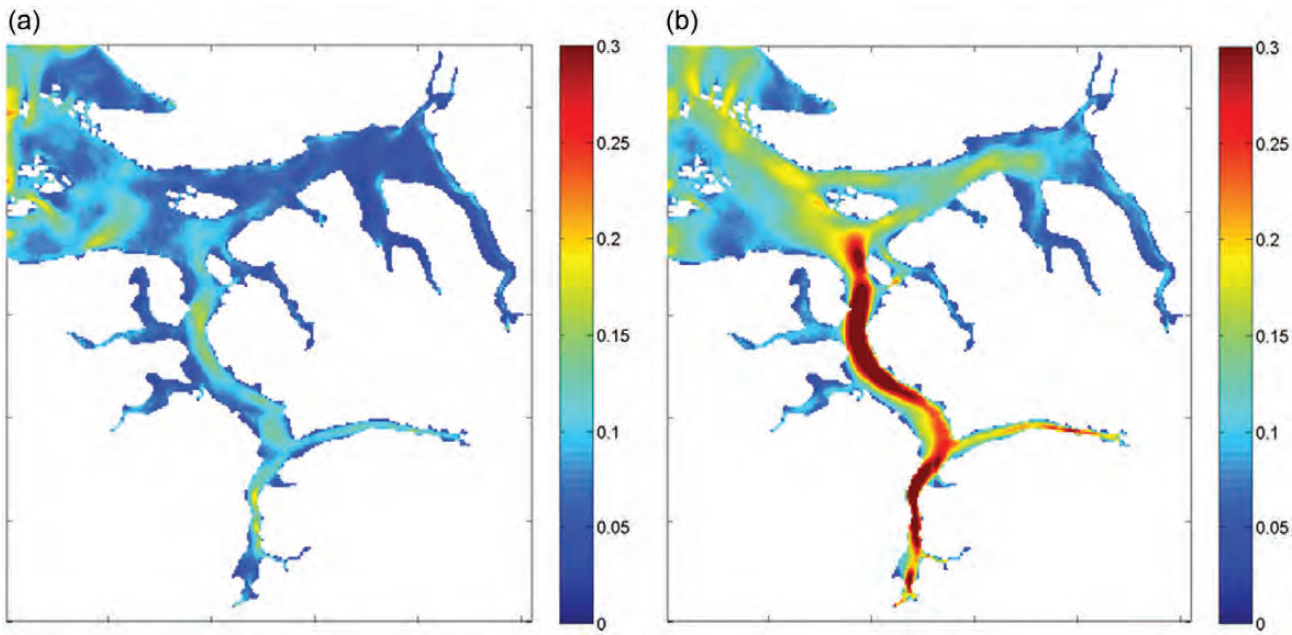

Figure 5. Monthly mean surface current speed for March 2009 when using natural rivers (a) and regulated rivers (b).

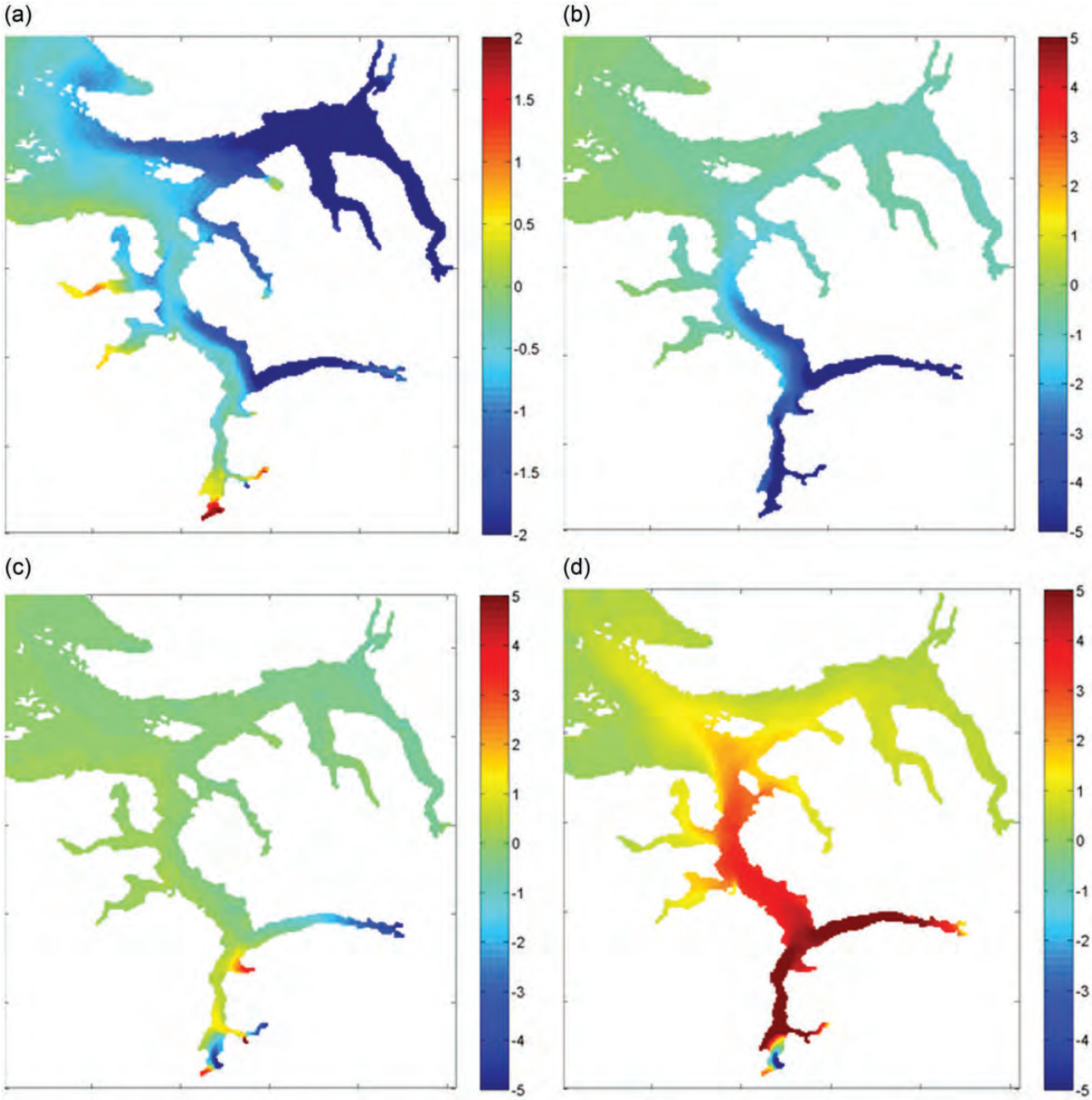

Figure 6. Difference between natural and regulated river run-off for monthly mean temperature (March) and salinity (March, April, and May). (a) Temperature March, (b) Salinity March, (c) Salinity April, and (d) Salinity May

circulation at the mouth of these fjord branches strongly affects the water exchange with the main fjord. However, with regulated run-off, the surface current is mainly controlled by the estuarine circulation which follows the curvature of the main fjord and is constricted to the north coastline due to rotation effects (right relative to the direction of the flow).

Transport and retention of cod eggs

Cod eggs were released into the domain at the positions shown in Figure 3. Eggs and larvae that stay inside the fjord will most likely recruit to the local fjord population, while if transported out of the fjord they might contribute to the coastal or oceanic populations. Therefore is the main focus here to calculate the number of eggs that stay inside the fjord until hatching. The corresponding retention can be defined in several ways; here, eggs are regarded as retained if they hatch within a 25-km radius from their respective spawning area.

The overall retention of eggs within all spawning areas is shown in Figure 10a when using natural rivers (solid lines) and regulated rivers (dashed lines). The eggs were divided into three groups according to their neutral buoyancy distribution, in reference to salinity: group 1, 28.00–29.62; group 2, 29.62–31.52; and group 3, 31.52–33.10. In natural conditions, without the influence of hydroelectric power production, the retention is high at the beginning of

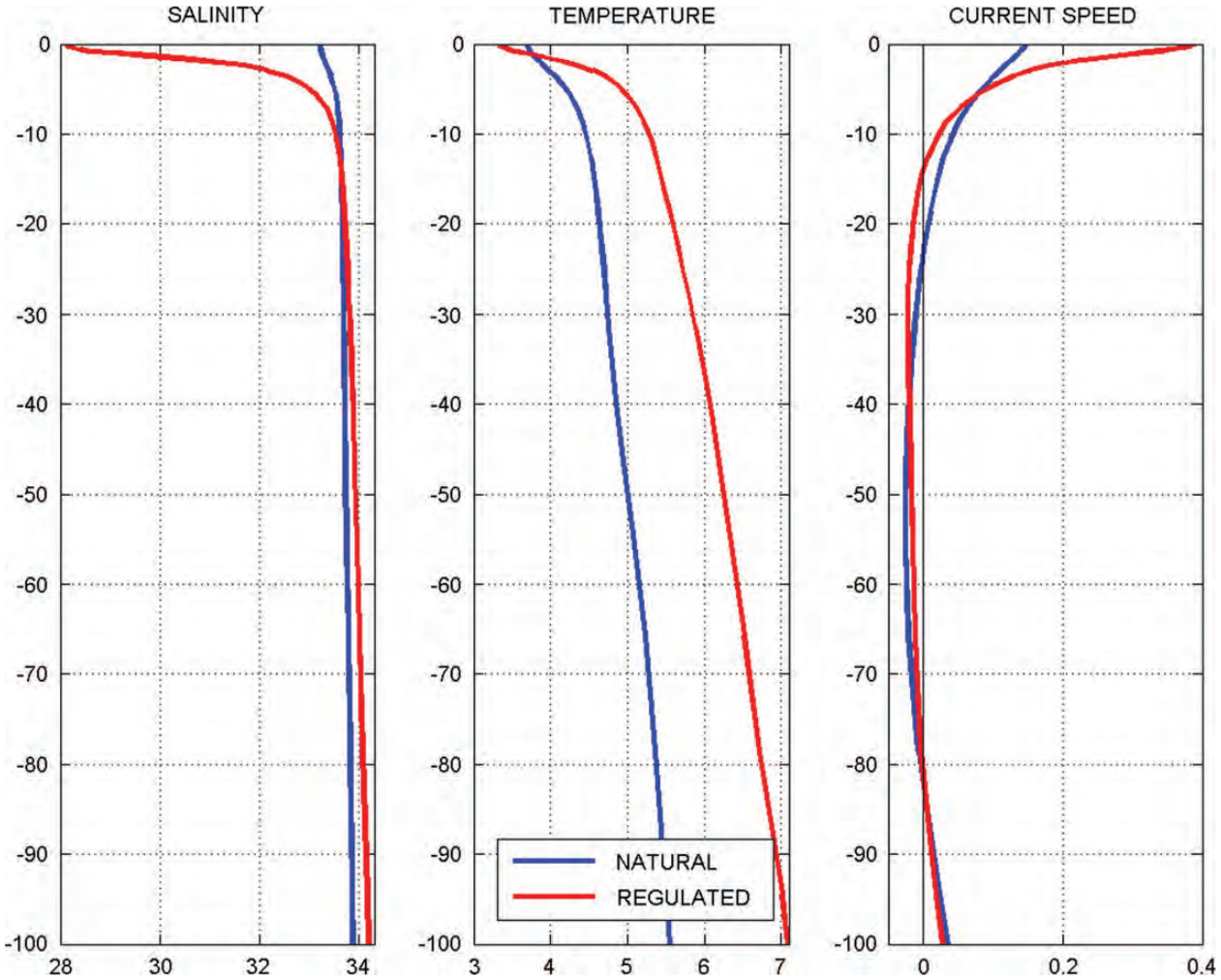

Figure 7. Monthly mean vertical profile in March of salinity, temperature, and current speed (positive direction is out of the fjord) in Sørfolda location is shown in Figure 1.

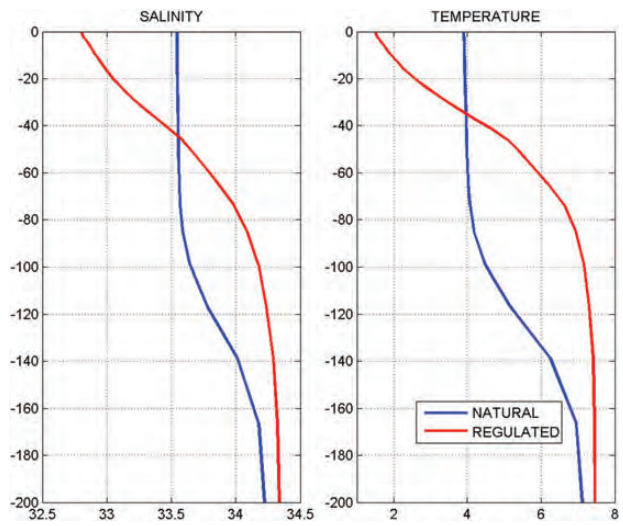

Figure 8. Monthly mean vertical salinity and temperature profiles in the central part of Nordfolda in March location is shown in Figure 1.

the period (above 90%) and decreases through spring and approaches 60% in late April. There are only minor differences in retention between the buoyancy groups, except for late April when group 3 has slightly higher retention than the other groups. The retention is lower when the rivers are regulated compared with the natural conditions, except for the last part of April. For regulated rivers, there is no obvious seasonal trend, and the retention stays at around 50–60% through the whole period.

The other panels in Figure 10 show the retention of cod eggs from specific spawning regions, as a function of neutral buoyancy and river run-off. The seasonal variability of retention in Sørfolda (Figure 10b) shows a completely different pattern compared with the overall spatial average. During March, the retention drops from ~80 to 20% during 15–20 d in the simulation with natural rivers. In this specific period, there are differences between the buoyancy groups, as the heaviest portion of eggs (group 3) has the highest retention. After March 28, the retention increases for all groups and in both run-off cases and with a further increase in the middle of April. Towards the end of the spawning period, there is hardly any difference between the cases with different river run-off, but there

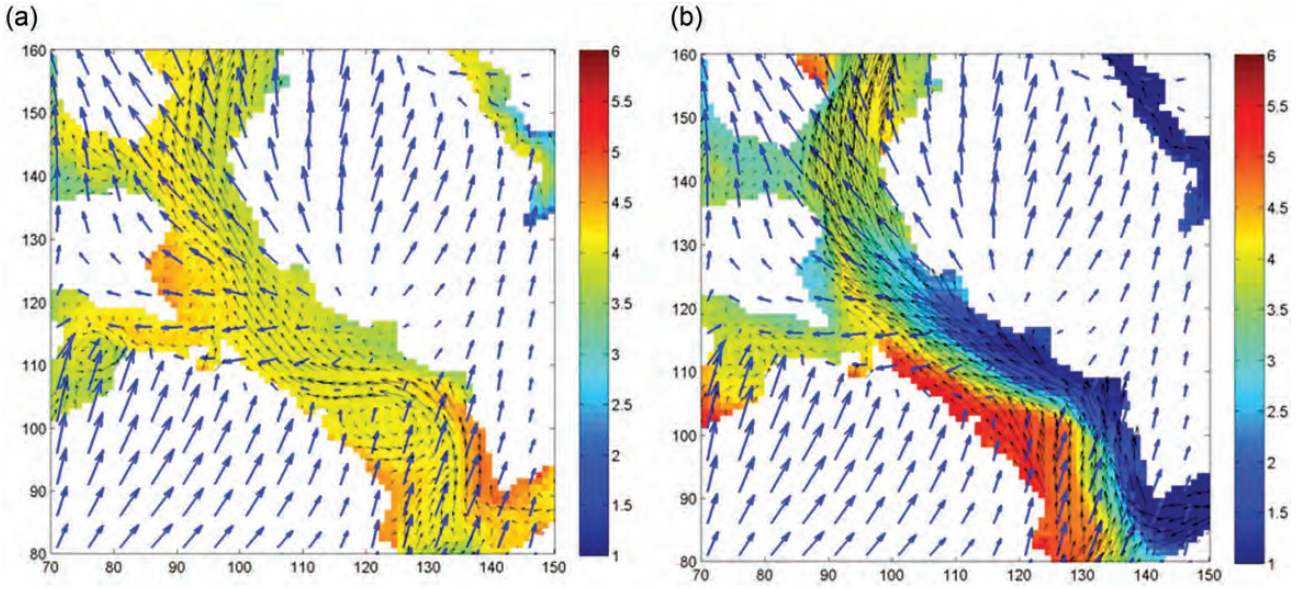

Figure 9. Surface temperature (colour scale), current (black arrows), and wind (blue arrows) on 4 March 2009 in Sørfolda, when using natural rivers (a) and regulated rivers (b).

is a difference between the buoyancy groups, highest retention for the heaviest eggs.

Figure 10c shows the transport of cod eggs from the two fjord branches in the western part of the fjord. When using natural rivers, almost all the eggs stay close to the spawning area through March, but the retention decreases through April. The retention is significantly lower when using regulated rivers, for all buoyancy groups. Especially for the heaviest group which is most likely of being transported away from the spawning area through the entire period. The decreasing trend in retention in April is also seen in the regulated case, and within this period, the highest retention is seen for the lightest buoyancy group regardless of run-off characteristics.

The retention related to the spawning areas in Nordfolda is shown in Figure 10d. In the natural run-off case, the retention is constantly high (90–100%) during March but intermediate (30–90%) during April with considerable variability. With regulations, the variability in retention is high through the whole spawning season, and there are also variations between the buoyancy groups. Buoyancy group 3 has lowest retention through March, whereas buoyancy group 1 has lowest retention through April.

The ambient temperature of the cod eggs are recorded along their pathways. The mean temperature as a function of spawning time is shown in Figure 11a averaged over all areas (black lines), only spawning areas in Sørfolda (blue) and Nordfolda (magenta), with both natural (solid lines) and regulated rivers (dashed lines). The corresponding incubation time based on the temperature is shown in Figure 11b, calculated from Equation (8). The average temperature experienced by cod eggs in the simulation with natural river run-off stays constantly between 3 and 4°C through the whole spawning period. Towards the end of April, the seasonal warming is clearly seen in Sørfolda with a rapid increase of 1.5°C within 5 d. When using regulated river run-off, the overall temperature is lower compared with the non-regulated case until April 6. In Sørfolda, there are only small temperature differences in the beginning, but after March 23, the temperature is higher in the regulated case. In Nordfolda, the ambient temperature of cod eggs is up to 2°C lower with regulations than with natural rivers. This large difference is present through March, then it decreases and disappears by April 12. The impact of temperature on incubation time increases exponentially towards low temperatures and, therefore, will have strongest effect in Nordfolda as seen in Figure 11b. For all areas, the incubation time of cod eggs is 6–7 d higher during March for the regulated case compared with the non-regulated, whereas specifically in Nordfolda, the difference is 15–20 d. Further into April, the difference diminishes, following the temperature difference. A small decrease in incubation time is seen in Sørfolda. The temperature difference has smaller impact here since the temperature is higher.

Discussion

Study design

In this study, we used a numerical model to investigate the impact of river regulations on hydrography, circulation, and transport of cod eggs in a fjord system. The model setup has shown to realistically reproduce hydrography in Sørfolda and Nordfolda (Myksvoll *et al.*, 2011) but the results were limited by insufficient external forcing, basically boundary conditions and atmospheric forcing. Comparisons with temperature and salinity sections in the fjord showed that the surface salinity was lower in the model compared with the observations, but the thickness of the low-salinity layer was similar. Myksvoll *et al.* (2011) also showed that the difference in surface salinity did not affect the vertical distribution of cod eggs. To improve the model setup, an 800-m coastal model provided hourly boundary conditions to the fjord model (Albretsen and Røed, 2010; Myksvoll *et al.*, 2014). This significantly improved the circulation in the intermediate and deep layer of the fjord, by increased supply of warm and saline coastal water. Aure *et al.* (1996) argue that density fluctuations in the coastal water are the dominating mode of water exchange in fjords (Asplin *et al.*, 1999). According to Stigebrandt (1976), inflowing coastal water also generates a strong velocity shear at the interface between the surface

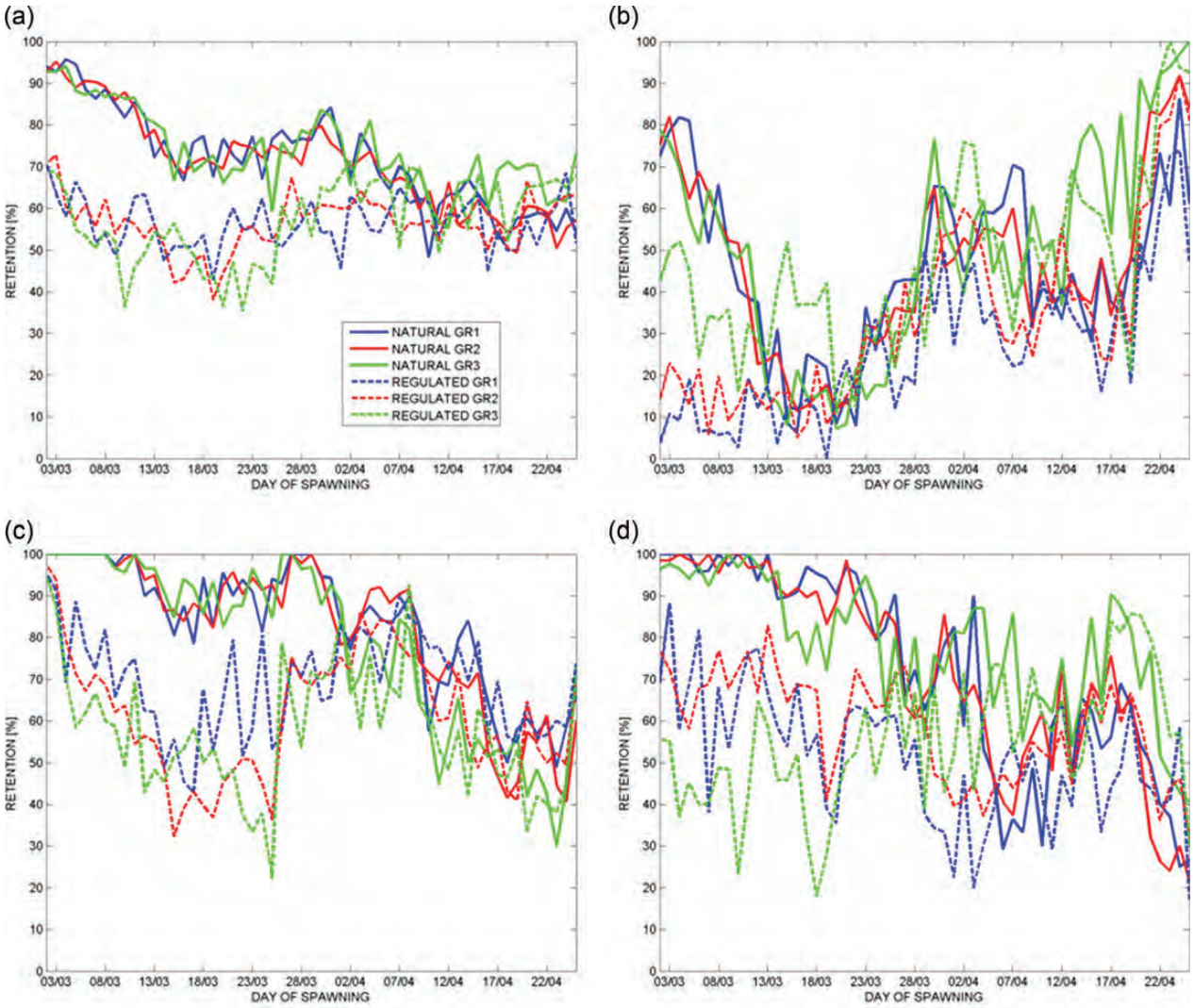

Figure 10. Retention (%) of cod eggs within 25 km with both natural (solid lines) and regulated (dashed lines) run-off, divided into three buoyancy groups: group 1 (28.00 – 29.62), group 2 (29.62 – 31.52), and group 3 (31.52 – 33.10), from different parts of the fjord. (a) All spawning areas, (b) Sørfolda, (c) Western Folda, and (d) Nordfolda.

and intermediate layer, creating internal waves and causing mixing across the interface. The atmospheric forcing was improved by running WRF with 1 km horizontal resolution. Especially, the wind pattern inside fjords has substantial spatial variability, not correlated with the coastal wind, and has strong influence on the surface circulation and mixing (Svendsen and Thompson, 1978). The importance of high-resolution windforcing on circulation and particle dispersion was illustrated by Myksvoll *et al.* (2012) in Porsangerfjorden.

This model experiment allows us to study the total effect of river regulations within the fjord system independent of interannual variability. The fjord projects in the 1970s investigated the impact of modified river run-off by performing hydrographic surveys before and after the operation of a power station (Kaartvedt, 1984). Svendsen (1983) described changes in the physical environment after river regulations in Skjomen, a smaller fjord ~150 km north of Folda, but encountered difficulties distinguishing between interannual variability and impacts of the regulation. Kaartvedt and Svendsen (1990b) studied impacts of altered freshwater discharge in the fjords of Ryfylke in southwestern Norway, but the power station was not running on full capacity. Numerical models have limitations like resolution, advection schemes, vertical mixing schemes, fictitious boundaries, diapycnal mixing, and internal pressure gradients near steep topography, but are well suited for our experiment where only one physical factor is altered and all other variables are held constant. This is because we want to investigate the relative differences rather than absolute values. Also the integrated effect of all power stations within a fjord system can be analysed, not only a single regulated river. The impact of a single power station can be negligible while a large degree of regulation within a fjord may have considerable impacts.

A controlled discharge from the power plant in Hylsfjorden in Ryfylke caused increased surface salinity due to intensive mixing near the outlet (Kaartvedt and Svendsen, 1990a). The initial mixing in the immediate vicinity of the power plant depends on the depth of water release and speed of the freshwater jet and can be fatal for zooplankton (Kaartvedt and Aksnes, 1992). This kind of freshwater discharge is fundamentally different from a river

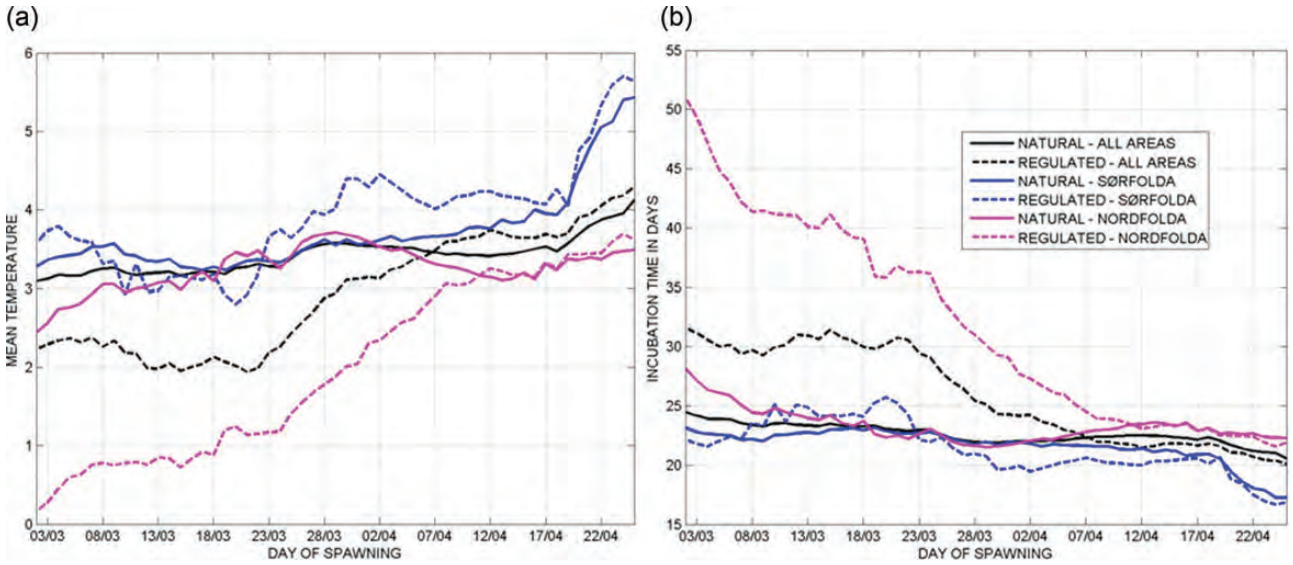

Figure 11. Mean ambient temperature (a) experienced by cod eggs in the model and calculated incubation time (b) with natural (solid lines) and regulated (dashed lines) run-off for all areas (black), Sørfolda (blue), and Nordfolda (magenta).

outlet and will possibly change the impact of regulations on the physical environment in the fjord. A submerged outlet will enhance mixing and possibly reduce the impact of river regulations. In the fjord system of Sørfolda and Nordfolda, freshwater from the power stations is released into freshwater lakes upstream of the river outlet to the fjord, meaning that the increased discharge enters the fjord through a normal river. This is easily represented in the model by just increasing the river transport, whereas the model might have difficulties representing the extensive mixing caused by submerged outlets. It is therefore important to assess the location and design of the hydroelectric power station when evaluating the impact on fjord dynamics.

Hydrography and circulation

Modified freshwater discharge from regulated rivers generates a strong surface outflow during winter. The difference in current speed is largest during winter and early spring, mainly because the difference between natural and regulated run-off is largest in this period (Pytte Asvall, 1976). These changes in circulation are a direct effect of river input which accelerates the estuarine circulation and will be largest nearby the river outlets and diminish downstream since the brackish layer is being more and more mixed on its way out of the fjord. The model results show largest changes in current speed in Sørfolda, directly downstream of the power stations, whereas at the junction between the northern and the southern part, the differences diminish. It is therefore likely that such changes in current speed will not propagate out of the fjord system. Kaartvedt and Nordby (1992) also observed increased current velocities as a consequence of a freshwater discharge, which resulted in increased transport of brackish zooplankton species out of the fjord. Large freshwater discharge throughout winter cause the advection of low-saline water from the fjord branches with power stations and into the neighbouring fjord branches. With time, the inner fjord is filled up with low-saline water and correspondingly causing a higher surface elevation. The strong surface outflow is then restricted from entering the branches and accelerates towards the coast. For the non-regulated case, not enough freshwater is released during spring to achieve the same effect which causes the surface outflow to be more easily deflected into nearby fjord branches.

Strong stratification confines the windstress to a shallow surface layer, which is thinner in the regulated run-off case compared with the natural run-off case and spins up the surface current. A considerable amount of energy is necessary to mix the freshwater down; increased freshwater run-off will therefore decrease the depth of the upper layer (Pickard and Emery, 1982). Due to the difference in vertical density structure, the wind input will have different contributions to the surface circulation. Svendsen and Thompson (1978) also found that stratification is important for trapping the windstress response to the near-surface layers. A strong pycnocline limits the energy transfer from the surface into the deeper layer. During March, the prevailing wind direction is out of the fjord, which therefore contributes to a strong surface outflow.

Reduced temperatures in the surface layer are a consequence of stronger stratification caused by high freshwater discharge during winter. Normally, the water column has weak stability during winter caused by surface cooling, strong wind mixing, and convection. The heat loss to the atmosphere is therefore distributed through the entire mixed layer which can reach a depth of several hundred metres. The release of freshwater from power stations during winter generates a low-saline surface layer and a strong stratification independent of temperature. The heat loss to the atmosphere is then confined to a surface layer less than 50 m deep, with the result of significantly lower than normal temperatures in the surface layer. At the same time, the surface layer insolates the intermediate layer below giving rise to higher than normal temperatures in this layer. The same pattern was observed in Skjomen by Skreslet and Loeng (1977) during a winter with naturally large freshwater outflow causing low surface temperatures and warm basin water.

Higher salinities in the intermediate layer can only be explained through increased inflow of salty coastal water below the low-saline surface layer. High temperatures in the intermediate layer is probably caused by both redistribution of heat, as discussed above, and increased inflow of coastal water. Mixing of salty water into the surface layer deepens the pycnocline in the inner part of the fjord compared with the outer part, which sets up a pressure gradient

and corresponding current directed into the fjord. Increased, freshwater discharge causing more mixing and increased inflow of coastal water might explain the salinity difference between natural and regulated run-off. According to Sælen (1967), the outflow in the surface layer will be between 2 and 6 times larger than the river input, a volume that has to be replaced from below.

A limitation of this study is that only the year 2009 is used for comparison between natural and regulated run-off. This means that the results strongly depend on the power production and corresponding freshwater discharge from the power station close to Kobbvatn during this specific year. The production at this power station is not necessarily correlated with the others in the fjord system; however, all external factors affecting the energy production would be the same. It is also important to emphasize that 2009 was not an extreme year regarding winter discharge. In the period from 2000 to 2009, there are 5 years with low winter discharge (<15 $m^3 s^{-1}$) and 5 years with high winter discharge (>35 $m^3 s^{-1}$) unevenly distributed, where 2009 is close to the average of the high discharge years. The energy production has large interannual variability depending both on natural variability (precipitation and temperature) and economical profit.

Retention mechanisms and spatial variations

The retention of cod eggs within a radius of 25 km from the spawning site was lower in the case with regulated river run-off compared with the case with natural river run-off. The main difference between natural and regulated run-off is the seasonal cycle, where the regulation causes increased run-off during winter and early spring. Therefore, it is not unexpected that the largest difference in retention is seen during March, and only minor differences can be seen during April. The spatial variations within the fjord system are large, due to different mechanisms controlling dispersion of cod eggs. The discussion further will therefore focus on specific spawning areas.

Sørfolda

The retention variability in Sørfolda is fundamentally different from the other branches of the fjord system. The average retention for the whole fjord system shows a decreasing trend during spawning season when using natural run-off, but Sørfolda has a period of low retention between two periods of high retention. This seasonality fits well with the results obtained in Myksvoll *et al.* (2011), where it was hypothesized that cod eggs were allowed to leave the fjord system during a short period in spring, a so-called "window of leakage". The "window" is open before the estuarine circulation is well established and coincides with relatively high surface salinities. As the seasonal melting begins, high river run-off gives rise to low surface salinities and the cod eggs attain a subsurface distribution which induces retention. The timing is depending on precipitation and temperature which both affect the river run-off and is therefore subject to interannual variability. The year 2009 is used in the present study, which is close to an average run-off year compared with the extreme years 1960 and 1989 used in the previous study. The timing of offshore transport is therefore earlier than the dry year 1960 (late April) and later than the wet year 1989 (late March).

The period of high retention in the beginning of March with natural run-off is related to the cyclonic eddy in the central part of Sørfolda (Figure 9a), persisting for $\sim$12 d. This eddy efficiently increases the residence time of cod eggs released in the inner part of the fjord.

Sørfolda is also the only spawning area with differences in retention between buoyancy groups, with highest retention for the heaviest eggs. The retention is reduced when using regulated run-off compared with natural for the first part of the spawning period; the differences in retention are largest for lightest eggs (Figure 10b). The heavy eggs have a deeper vertical distribution and are less susceptible for changes in the outflowing surface layer. Strong surface currents caused by freshwater discharge from the power stations increase the dispersal of the lightest portion of the eggs that are positioned closer to the surface. Towards the end of the spawning period, the surface salinity is sufficiently low for both buoyancy groups 2 and 3 to be submerged below the strong outflow and the heaviest eggs are correspondingly retained within the fjord in both cases.

Western Folda

The small fjord branches in the western part of Folda show persisting high retention during March in the simulation with natural rivers, which is mainly due to interaction between frequent wind and surface current directed into the fjord branches at the mouth. With natural run-off, the surface current in the central part of Sørfolda is easily deflected towards the west and into the fjord arms. With increased freshwater discharge, the low-saline outflow is trapped to the north coast and not as influenced by the wind, as seen in Figure 9. This explains the decrease in retention when using regulated river run-off. Different buoyancy groups have only minor differences in retention in this part of the fjord system. There is a small tendency that heavy cod eggs have lower retention, which may be caused by the reversed circulation at the mouth. This mechanism is opposite of what was seen in Sørfolda, where the estuarine circulation contributes to high retention of heavy cod eggs.

A negative trend in retention develops through April. This is related to the local increase of river run-off within the fjord, generating a surface outflow. However, the surface salinity is not low enough for the eggs to be submerged and the transport out of the fjord increases correspondingly.

Nordfolda

The retention in Nordfolda is reduced from the simulation with natural to regulated run-off, mainly due to the decrease in temperature resulting in considerably longer incubation times (Figure 11). High retention in the natural run-off case is caused by a reversed circulation as in the western part of Folda. Both frequent winds directed into the fjord and outflow from Sørfolda entering Nordfolda contribute to a surface inflow and outflow below. But this mechanism is not stable enough to keep the retention high when the incubation time is almost doubled. As the temperature decreases the incubation time increases exponentially and therefore causing especially large differences within the low temperature range.

With natural rivers, there is no significant difference in retention between buoyancy groups, but when the rivers are regulated the retention is low for heavy eggs. This is related to the reversed circulation which was also present in the western fjord branches.

General considerations

The year-class strength of Norwegian coastal cod has been declining since 1984 and is currently at a low level. However, the local variations in abundance are large. In some fjords, the stock is in good condition while the neighbouring fjord is in poor condition (Berg and Albert, 2003). Of many possible explanations for reduced spawning

stock and recruitment are overfishing, predation, loss of nursery habitat, aquaculture, climate variability, and river regulations. Some fjords have a large degree of freshwater regulation whereas some are unaffected, and this is unevenly distributed among nearby locations just like the decline in cod. Fish species in Norwegian fjords are adapted to a spring bloom system, where recruitment processes depend on the timing of larval feeding with maximum food availability (Ellertsen *et al*., 1989). Freshwater discharge during winter and early spring disturbs the natural seasonal cycle and increases the transport of fish eggs out of the fjord during the main spawning period (Drinkwater and Frank, 1994). The consequence of this is lower densities of early life stages left in the fjord to potentially recruit to the local population. Fewer offspring means higher vulnerability for a mismatch with high zooplankton abundance. Small populations of coastal cod specialized to their respective fjords are especially susceptible to changes in the local environment like river regulations (Dahle *et al*., 2006; Otterå *et al*., 2006). Changes in the seasonal pattern due to hydroelectric power production cannot be neglected as a contributing factor to the decline in coastal and fjord cod subpopulations as the present results clearly indicate.

The retention mechanisms operating in this fjord system can be described within two categories; discharge retention and downstream retention. Discharge retention is directly related to the freshwater discharge in the inner part of the fjord, which reduces the surface salinity and cause the cod eggs to sink below the surface layer (Sørfolda). A subsurface distribution of eggs, situated just below the surface outflow, counteracts dispersion and increase local retention. This mechanism is only efficient within a narrow fjord branch with large river input. The downstream retention is a non-local effect in nearby fjord branches caused by inflowing surface water and outflow below (Western Folda and Nordfolda). In these areas, the surface salinity is relatively high, meaning that the cod eggs float near the surface and as the surface current is directed into the fjord the eggs are retained. This mechanism is only active in a fjord with negligible river input locally but near a fjord with large river input, or wind directed into the fjord. Another important retention mechanism, only briefly mentioned here, is eddy retention. Eddy activity in a fjord system increases the residence time of passive particles which enhances retention. Early in the spawning season, a stationary eddy in Sørfolda accumulated eggs within the central part, but usually eddy retention is more important in wide fjords with low river run-off, like Porsangerfjorden (Myksvoll *et al*., 2012). The importance of eddy retention is reduced as the freshwater discharge increase. Generally, there are large variations in retention mechanisms within a fjord and between different fjords. Discharge retention is important in narrow fjords with large river run-off, downstream retention in fjords with complex topography and eddy retention in wide fjords with low river run-off. All these processes can interact within a fjord and also have seasonal variability as run-off varies. Discharge retention did not change very much between the cases, but the other two retention mechanisms were weakened by river regulations. In addition, indirect effects of regulations like decreased temperatures causing increased incubation time also reduced retention. Discharge retention could become stronger with regulations due to lower surface salinity, but in this fjord, the overall area of sufficiently low surface salinity was too small to counteract the total decline in retention, meaning that regulations probably will have a negative effect on the retention of cod eggs in other fjords as well.

In conclusion, the results show stronger surface outflow in the main part of the fjord when applying river regulations compared with natural run-off. This difference is most pronounced during winter and early spring and is therefore coinciding with the spawning season for coastal cod. Increased freshwater discharge during winter causes reduced temperatures in the surface layer. Strong stratification confines the heat loss to the upper layer and insolates the layers below. A combination of the redistribution of heat and increased inflow of coastal water give rise to higher temperatures in the intermediate layer when using regulated run-off. The transport of cod eggs out of the fjord system increased with regulated run-off compared with the natural run-off, which correspondingly reduced the local retention within the various fjord branches. Different retention mechanisms were important in different regions of the fjord system and can be divided into two categories; discharge retention and downstream retention. In addition, low temperatures in some regions increased the incubation time of egg which also contributed to weakened retention. Despite the range of retention mechanisms, most of them became less efficient when the run-off was regulated. Therefore cannot river regulations, causing changes in the seasonal run-off pattern, be neglected as a contributing factor to the decline in coastal and fjord cod subpopulations.

References

Albretsen, J., and Røed, L. P. 2010. Decadal long simulations of mesoscale structures in the northern North Sea/Skagerrak using two ocean models. Ocean Dynamics, 60: 933–955.

Albretsen, J., Sperrevik, A. K., Staalstrøm, A., Sandvik, A. D., Vikebø, F., and Asplin, L. 2011. NorKyst-800 Report No.1, User manual and technical descriptions. Tech. rept. 2. Fisken og Havet, Institute of Marine Research.

Asplin, L., Salvanes, A. G. V., and Kristoffersen, J. B. 1999. Nonlocal wind-driven fjord-coast advection and its potential effect on plankton and fish recruitment. Fisheries Oceanography, 8: 255–263.

Aure, J., Molvær, J., and Stigebrandt, A. 1996. Observations of inshore water exchange forced by a fluctuating offshore density field. Marine Pollution Bulletin, 33: 112–119.

Aure, J., and Pettersen, R. 2004. Miljøundersøkelser i norske fjorder 1975–2000 [Environmental investigations in Norwegian fjords 1975–2000]. Fisken og Havet, 8: 1–176 (in Norwegian).

Berg, E., and Albert, O. T. 2003. Cod in fjords and coastal waters of North Norway: distribution and variation in length and maturity at age. ICES Journal of Marine Science, 60: 787–797.

Dahle, G., Jørstad, K. E., Rusaas, H. E., and Otterå, H. 2006. Genetic characteristics of broodstock collected from four Norwegian coastal cod (*Gadus morhua*) populations. ICES Journal of Marine Science, 63: 209–215.

Drinkwater, K., and Frank, K. T. 1994. Effects of river regulation and diversion on marine fish and invertebrates. Aquatic Conservation: Freshwater and Marine Ecosystem, 4: 135–151.

Ellertsen, B., Fossum, P., Solemdal, P., and Sundby, S. 1989. Relation between temperature and survival of eggs and first-feeding larvae of northeast Arctic cod (*Gadus morhua* L.). Rapports et Procès-Verbaux des Réunions du Conseil International pour l'Exploration de la Mer, 191: 209–219.

Gade, H. G. 1976. Transport mechanisms in fjords. *In* Fresh Water on the Sea, pp. 51–56. Ed. by S. Skreslet, R. Leinebø, J. B. L. Matthews, and E. Sakshaug. The Association of Norwegian Oceanographers, Oslo.

Haidvogel, D. B., Arango, H., Budgell, W. P., Cornuelle, B. D., Curchitser, E., Di Lorenzo, E., Fennel, K., *et al.* 2008. Ocean forecasting in terrain-following coordinates: formulation and skill assessment of the Regional Ocean Modeling System. Journal of Computational Physics, 227: 3595–3624.

Kaartvedt, S. 1984. Vassdragsreguleringers virkning på fjorder [Effects on fjord of modified freshwater discharge due to hydroelectric power production]. Fisken Hav., 3: 1–104 (in Norwegian).

Kaartvedt, S., and Aksnes, D. L. 1992. Does freshwater discharge cause mortality of fjord-living zooplankton? Estuarine, Coastal and Shelf Science, 34: 305–313.

Kaartvedt, S., Johnsen, T. M., Aksnes, D. L., Lie, U., and Svendsen, H. 1991. Occurrence of the toxic phytoflagellate *Prymnesium Parvum* and associated fish mortality in a Norwegian fjord system. Canadian Journal of Fisheries and Aquatic Sciences, 48: 2316–2323.

Kaartvedt, S., and Nordby, E. 1992. Impact of a controlled freshwater discharge on zooplankton distribution in a Norwegian fjord. Journal of Experimental Marine Biology and Ecology, 162: 279–293.

Kaartvedt, S., and Svendsen, H. 1990a. Impact of freshwater runoff on physical oceanography and plankton distribution in a western Norwegian fjord: an experiment with a controlled discharge from a hydroelectric power plant. Estuarine Coastal and Shelf Science, 31: 381–395.

Kaartvedt, S., and Svendsen, H. 1990b. Advection of euphausiids in a Norwegian fjord system subject to altered freshwater input by hydroelectric power production. Journal of Plankton Research, 12: 1263–1277.

Mohus, Å., and Haakstad, M. 1984. Straumbukta i Sørfold, en kortfattet hydrografisk og hydrokjemisk kartlegging [Straumbukta in Sørfold a brief hydrographic and hydrochemical survey]. Nordland distriktshøgskole, Bodø (in Norwegian).

Murchie, K. J., Hair, K. P. E., Pullen, C. E., Redpath, T. D., Stephens, H. R., and Cooke, S. J. 2008. Fish response to modified flow regimes in regulated rivers: research methods, effects and opportunities. River Research and Applications, 24: 197–217.

Myksvoll, M. S., Jung, K-M., Albretsen, J., and Sundby, S. 2014. Modeling dispersal of eggs and quantifying connectivity among Norwegian Coastal cod subpopulations. ICES Journal of Marine Science, 71: 957–969.

Myksvoll, M. S., Sandvik, A. D., Skarðhamar, J., and Sundby, S. 2012. Importance of high resolution wind forcing on eddy activity and particle dispersion in a Norwegian fjord. Estuarine, Coastal and Shelf Science, 113: 293–304.

Myksvoll, M. S., Sundby, S., Ådlandsvik, B., and Vikebø, F. B. 2011. Retention of coastal cod eggs in a fjord caused by interactions between egg buoyancy and circulation pattern. Marine and Coastal Fisheries, 3: 279–294.

Narvaez, D. A., Klinck, J. M., Powell, E. N., Hofmann, E. E., Wilkin, J., and Haidvogel, D. B. 2012. Modeling the dispersal of Eastern Oyster (*Crassostrea virginica*) larvae in Delaware Bay. Journal of Marine Research, 70: 381–409

NVE. 2011. Energistatus 2010 [Energy state 2010]. Norwegian Water Resources and Energy Directorate.

Otterå, H., Agnalt, A. L., and Jørstad, K. E. 2006. Differences in spawning time of captive Atlantic cod from four regions of Norway, kept under identical conditions. ICES Journal of Marine Science, 63: 216–223.

Pickard, G. L., and Emery, W. J. 1982. Descriptive Physical Oceanography—an Introduction, 4th (SI) Enlarged Edn. Pergamon Press, Oxford. 249 pp.

Pytte Asvall, R. 1976. Effects of regulation on freshwater runoff. *In* Fresh Water on the Sea, pp. 15–20. Ed. by S. Skreslet, R. Leinebø, J.B.L. Matthews, and E. Sakshaug The Association of Norwegian Oceanographers, Oslo.

Saelen, O. H. 1967. Some features of the hydrography of Norwegian fjords. *In* Estuaries, pp. 63–70. Ed. by G.H. Lauff. AAAC, Washington, DC.

Saelen, O. H. 1976. General hydrography of fjords. *In* Fresh Water on the Sea, pp. 43–49. Ed. by S. Skreslet, R. Leinebø, J.B.L. Matthews, and E. Sakshaug, The Association of Norwegian Oceanographers, Oslo.

Shchepetkin, A. F., and McWilliams, J. C. 2005. The regional oceanic modeling system (ROMS): a split-explicit, free-surface, topography-following-coordinate oceanic model. Ocean Modeling, 9: 347–404.

Sinclair, M., Budgen, G. L., Tang, C. L., Therriault, J. C., and Yeats, P. A. 1986. Assessment of effects of freshwater runoff variability on fisheries production in coastal waters. *In* The Role of Freshwater Outflow in Coastal Marine Ecosystem. NATO ASI Series G, Vol. 7, pp. 59–94. Ed. by S. Skreslet. Springer-Verlag, Berlin.

Skamarock, W., Klemp, J., Dudhia, J., Gill, D., Barker, D., Duda, M., Huang, X. Y., *et al.* 2008. A description of the advanced research WRF version 3. NCAR Technical Note, NCAR/TN-475+STR. 113 pp.

Skreslet, S. 1976. Influence of freshwater outflow on recruitment to the stock of Arcto-Norwegian cod (*Gadus morhua*). *In* Fresh Water on the Sea, pp. 233–237. Ed. by S. Skreslet, R. Leinebø, J.B.L. Matthews, and E. Sakshaug. The Association of Norwegian Oceanographers, Oslo.

Skreslet, S., and Loeng, H. 1977. Deep water renewal and associated processes in Skjomen, a fjord in north Norway. Estuarine and Coastal Marine Science, 5: 383–398.

Solemdal, P. 1973. Transfer of Baltic flat fish to a marine environment and the long term effects on reproduction. Oikos Supplement, 15: 268–276.

Stigebrandt, A. 1976. Vertical diffusion driven by internal waves in a sill fjord. Journal of Physical Oceanography, 6: 486–495.

Sundby, S. 1983. A one-dimensional model for the vertical distribution of pelagic fish eggs in the mixed layer. Deep Sea Research, 30: 645–661.

Sundby, S. 1991. Factors affecting the vertical distribution of eggs. ICES Marine Science Symposia, 192: 33–38.

Svendsen, H. 1983. Hydrofysiske forhold i Skjomen etter vassdragsreguleringene [The hydrophysical environment in Skjomen after river regulations]. Rådgivende utvalg for fjordundersøkelser Skjomenprosjektet, Rapport nr.3, Oslo (in Norwegian).

Svendsen, H. 1995. Physical oceanography of coupled fjord-coast systems in northern Norway with special focus on frontal dynamics and tides. *In* Ecology of Fjords and Coastal Waters, pp. 149–164. Ed. by H. R. Skjoldal, C. Hopkins, K. E. Erikstad, and H. P. Leinaas. Elsevier.

Svendsen, H., and Thompson, R. O. R. Y. 1978. Wind-driven circulation in a fjord. Journal of Physical Oceanography, 8: 703–712.

Tollan, A. 1976. River runoff in Norway. *In* Fresh Water on the Sea, pp. 11–13. Ed. by S. Skreslet, R. Leinebø, J. B. L. Matthews, and E. Sakshaug, The Association of Norwegian Oceanographers, Oslo.

Umlauf, L., and Burchard, H. 2003. A generic length-scale equation for geophysical turbulence models. Journal of Marine Research, 61: 235–265.

Handling editor: Claire Paris

ICES Journal of Marine Science

ICES International Council for the Exploration of the Sea
CIEM Conseil International pour l'Exploration de la Mer

ICES Journal of Marine Science (2014), 71(4), 957–969. doi:10.1093/icesjms/fst022

Contribution to the Themed Section: 'Larval Fish Conference'

Original Article

Modelling dispersal of eggs and quantifying connectivity among Norwegian coastal cod subpopulations

Mari S. Myksvoll[1,2]*, Kyung-Mi Jung[1], Jon Albretsen[1], and Svein Sundby[1,2]

[1]*Institute of Marine Research, P.O. Box 1870, Nordnes, Bergen, Norway N-5817*
[2]*Bjerknes Center for Climate Research, Bergen, Norway*

**Corresponding author: tel: +47 55 23 86 28; e-mail: mari.myksvoll@imr.no*

Myksvol, M. S., Jung, K-M., Albretsen, J., and Sundby, S. 2014. Modelling dispersal of eggs and quantifying connectivity among Norwegian coastal cod subpopulations. – ICES Journal of Marine Science, 71: 957–969.

Received 28 September 2012; accepted 26 January 2013; advance access publication 14 February 2013.

The Norwegian coast is populated by two cod populations: Northeast Arctic cod and Norwegian Coastal cod. In this paper, we use a further division based on life history: oceanic cod, coastal cod, and fjord cod. A numerical ocean model was implemented for the northern Norwegian coast where all these populations have spawning areas. The model results were used to simulate connectivity and retention of cod eggs from the different subpopulations. The model reproduced the observed variability and mesoscale activity in the Norwegian Coastal Current. Eggs released at an oceanic spawning area were transported northwards along the coastline. Coastal cod eggs had intermediate connectivity with each other and fjord cod eggs had high local retention. Although the high retention of eggs in fjord areas is mainly caused by a subsurface distribution of eggs, the intermediate retention of eggs from coastal spawning areas is caused by small-scale eddies in-between many small islands. The high-resolution ocean model made it possible to reveal these specific dispersal patterns. The high retention of early life stages in fjords combined with strong homing to spawning areas indicates that fjord subpopulations may be described as a metapopulation.

Keywords: eddy activity, egg buoyancy, *Gadus morhua* L., metapopulation, Norwegian Coastal Current, particle tracking.

Introduction

The Norwegian coast is populated by two main cod populations (*Gadus morhua* L.), which are managed as two separate stocks, the Northeast Arctic cod (NEAC) and the Norwegian coastal cod (NCC). The NEAC is a large oceanic stock with spawning area in Vestfjorden (VE), in addition to several areas along the coast from 60 to 71°N (Sundby and Nakken, 2008). The eggs and larvae are transported northwards with the Norwegian Coastal Current, to the juvenile feeding and nursery areas in the Barents Sea, travelling a distance of up to 1200 km (Bergstad *et al.*, 1987). The NCC has a very different life history, with both spawning and nursery areas at the coast. Several studies have indicated that the NCC consists of several subpopulations with separated life histories. NCC can be categorized into two major components: stationary NCC and migratory NCC. Stationary NCC spawns and feeds inside the fjords and does not migrate far from their local habitat. Jakobsen (1987) even claimed that each fjord has its own cod population. Migratory NCC spawns at the coast and migrates short distances along the coast for feeding at coastal banks and bays. Altogether, there are three cod populations with different life histories spawning near VE: oceanic cod (NEAC), coastal cod (migratory NCC), and fjord cod (stationary NCC). Several authors have reported genetic differences between NEAC and NCC (e.g. Fevolden and Pogson, 1997; Pogson and Fevolden, 2003). Recently, also genetically separated subpopulations within NCC are recognized (Dahle *et al.*, 2006; Jorde *et al.*, 2007). Dispersal and mixing among early life stages from different spawning areas could counteract the build-up of genetic differentiation. This implies that the maintenance of this differentiation is depending on the retention of early life stages and/or strong homing of juveniles and adults (Knutsen *et al.*, 2007). Retention mechanisms of cod eggs within

the fjords have been investigated, showing a large degree of isolation during the early life stages (Ciannelli *et al.*, 2010; Myksvoll *et al.*, 2011). Also the transport of NEAC eggs and larvae from Lofoten into the Barents Sea is well known by observations (Bergstad *et al.*, 1987) and by modelling (Ådlandsvik and Sundby, 1994; Vikebø *et al.*, 2005). However, the transport of early life stages from coastal spawning areas is not well characterized. Specifically, we want to investigate the potential for retention at the coast and quantify the connectivity among subpopulations spawning in coastal areas and among subpopulations spawning in fjords and coastal areas.

Smedbol and Wroblewski (2002) discussed the subpopulation structure of northern cod in a metapopulation perspective. Metapopulation means a "population of populations", where individual populations are connected through migration, extinction, and recolonization events (Smedbol *et al.*, 2002). The theory was introduced by Levins (1970) consisting of three assumptions: (i) subpopulations have the same geographic extent and degree of isolation, (ii) each subpopulation has separate local population dynamics, and (iii) the rate of exchange of individuals among subpopulations is too low to affect local population dynamics (Smedbol and Wroblewski, 2002). The subpopulations are not necessarily genetically different, but an observed difference would indicate low exchange rates among subpopulations. Smedbol *et al.* (2002) emphasize that metapopulations have to be a set of semi-independent subpopulations where at least one must have a non-zero probability of extinction, not caused by anthropogenic influence such as fishing. One issue addressed when applying the metapopulation theory to marine populations is connectivity. Many species, such as cod, have pelagic eggs and larvae with potential for long-distance dispersal. Because of this, marine populations have traditionally been considered "open". However, Cowen *et al.* (2000) showed that larval behaviour might enhance retention and that coastal marine populations were not as "open" as previously assumed.

The objective of this paper is to investigate the degree of isolation among several coastal spawning areas by analysing the dispersal pattern during the pelagic egg stages. Biological data will be used as input to an individual-based model coupled to a circulation model covering Helgeland county in northern Norway. The results will be used to evaluate connectivity among fjord cod and coastal cod populations and will be discussed within a metapopulation framework. The focus in this paper will be on the egg stage, although the larval dispersal may also have a significant impact. Available knowledge regarding the vertical distribution of cod larvae state that the larvae avoid the upper 5–10 m of the water column (Ellertsen *et al.*, 1984, 1989; Sundby and Fossum, 1990). The consequence of a subsurface larval distribution is a considerable reduction in spatial dispersion. It is therefore likely that the distribution pattern described for cod eggs will continue also for cod larvae. Dispersing eggs will continue to disperse, whereas eggs that are retained will continue to be retained as larvae.

Material and methods

The study area

The area of interest is shown in Figure 1, mainly covering the coastal areas of Nordland County in northern Norway from ~64.5 to 70.0°N. The coloured area shows the model domain with bathymetry, in relation to the Norwegian Costal Current and the Norwegian Atlantic Current. The Norwegian Coastal Current originates from the outflow of brackish water from the Baltic Sea through Kattegat, the North Sea coastal water, and freshwater run-off from Norwegian rivers and follows the entire Norwegian coast (Sætre, 2007b). The low-saline current mixes initially with North Sea water and subsequently with Atlantic water northwards, becoming more saline. The Norwegian Coastal Current is mainly driven by the wind pattern and the density structure and forms a wedge-shaped current bordered by the Norwegian coast. The Norwegian Atlantic Current is located offshore of the coastal current and is characterized by warm saline water (Orvik and Niiler, 2002).

The model area was divided into seven subareas, called zones, representing different spawning areas and geographical regions as shown in Figure 2. The names of the zones with corresponding abbreviation are shown in Table 1, including geographical information and spawning population. Vikna (VI) is a known spawning area for NEAC (Sundby and Nakken, 2008) and is located offshore. The three coastal zones, Rørvik-Vega (RV), Vega-Træna (VT), and Træna-Bodø (TB), are known spawning areas for the NCC and

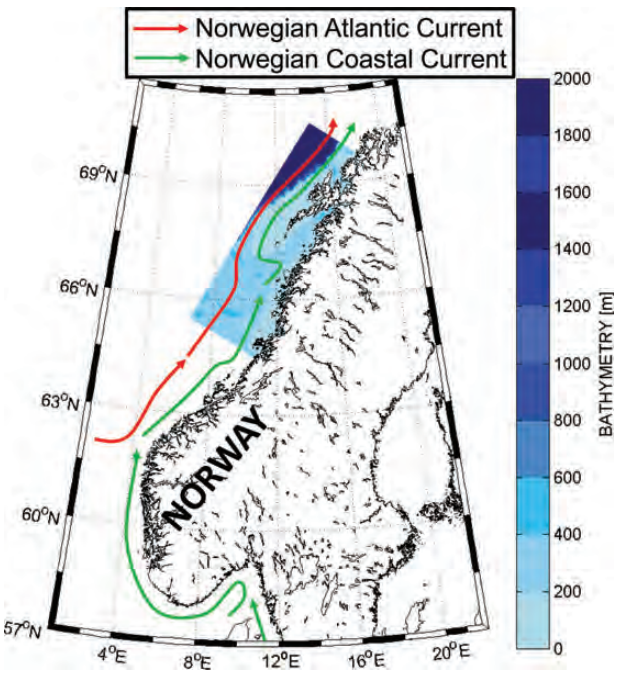

Figure 1. The location of the study area in Nordland County in northern Norway, in relation to the Norwegian Atlantic Current and the Norwegian Coastal Current.

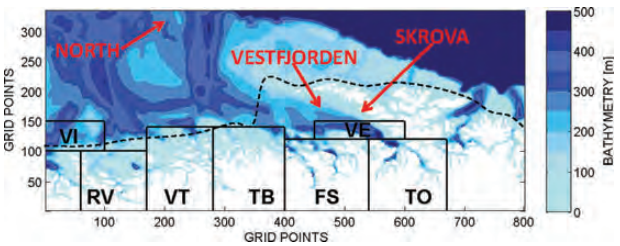

Figure 2. The model area with bathymetry and subdivision into seven zones representing different spawning areas and geographical regions: VI, RV, VT, TB, FS, TO, and VE. The location of VE, the main spawning area of NEAC, and the coastal station Skrova are shown on the map, and the dashed line is the baseline.

Table 1. Names of zones including information about the geographical region, spawning population by oceanic cod (NEAC), coastal cod (migratory NCC), or fjord cod (stationary NCC), and colour scheme used in Figure 7.

Abb.	Name	Region	Spawning population	Colour
VI	Vikna	Oceanic	Oceanic cod	Red
RV	Rørvik-Vega	Coastal	Coastal cod	Blue
VT	Vega-Træna	Coastal	Coastal cod	Green
TB	Træna-Bodø	Coastal	Coastal cod	Magenta
FS	Folda-Skjerstadfjord	Fjordic	Fjord cod	Cyan
TO	Tysfjord-Ofotfjord	Fjordic	Fjord cod	Blue (- -)
VE	Vestfjorden	Coastal	Oceanic/coastal cod	Red (- -)

named Helgeland stock in Dahle *et al.* (2006) and Otterå *et al.* (2006). The two fjordic zones, Folda-Skjerstadfjord (FS) and Tysfjord-Ofotfjord (TO), are inhabited by the stationary component of NCC and are genetically separated from the Helgeland population (Dahle *et al.*, 2006). Myksvoll *et al.* (2011) showed how spawning in a fjord system enhance retention and therefore contribute to sustain the subpopulations within fjords. VE is the most important spawning area for NEAC, in addition to substantial spawning by NCC (Nordeide, 1998).

The transport of cod eggs is discussed in relation to the zones. The degree of retention is hereby defined as the percentage of eggs that hatch in the zone they were released. Connectivity is used to describe the degree of transport of cod eggs from one zone to another.

Egg specific gravity measurements

The egg specific gravity is one of the input parameters for the model of egg vertical distribution. Hence, we obtained the experimental data of the egg specific gravity examined by Jung *et al.* (2012) with Tysfjord and Helgeland origin cod populations, assuming that Tysfjord and Helgeland populations represent typical fjord-spawning cod and coastal-spawning cod, respectively. Eggs were naturally spawned during 2 months (March and April), and they were collected from seven and three different female cod for Tysfjord and Helgeland, respectively. See the study of Jung *et al.* (2012) for the detailed information of raised broodfish, egg collection, and the determination of the egg specific gravity.

Experiments for the measurements of the egg specific gravity were designed for two purposes: one was "point measurements" to obtain all possible phenotypes of the egg specific gravity only at the morula stage (2-d old; Fridgeirsson, 1978), and the other was "continuous measurements" to track ontogenetic changes in the egg specific gravity during development. (i) For the point measurements, up to four egg batches per broodfish were used. The total number of egg batches was ten for Tysfjord and eight for Helgeland, using ~50 eggs per batch. As there was no significant difference between Tysfjord and Helgeland (t-test, $P = 0.12$, Figure 3), all the measured values of specific gravities were merged to generate a normal distribution of the egg specific gravity at the morula stage (the mean egg specific gravity expressed in salinity units: 30.57; 1 s.d.: 1.27). (ii) Continuous measurements used a single egg batch for each population. About 50 eggs at the morula stage were used, and the eggs were monitored for 2 weeks until hatching. The positions of eggs and glass floats were noted every day. As seen in Figure 4, fertilized eggs showed a slight

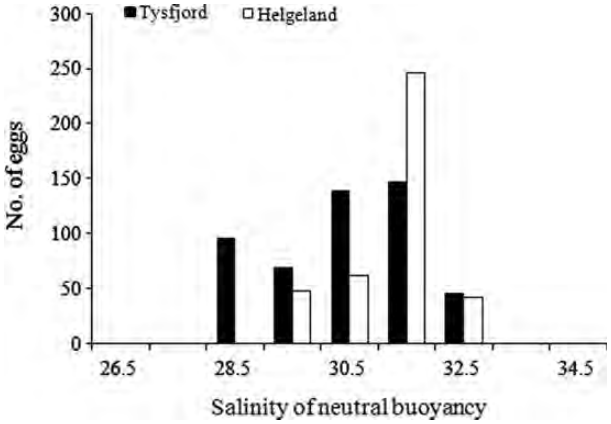

Figure 3. Point measurements. Frequencies of the egg specific gravity at the morula stage measured from Tysfjord and Helgeland populations during spawning season (March to April). The egg specific gravity was expressed by the salinity of neutral buoyancy at 6°C. Then total number of egg batches per population was ten for Tysfjord and eight for Helgeland. The total number of eggs per batch was ~50.

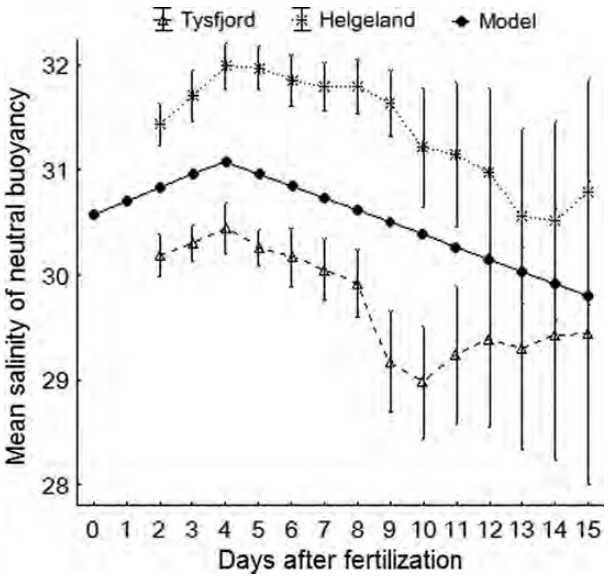

Figure 4. Continuous measurements. Ontogenetic changes in the mean salinity of neutral buoyancy for Tysfjord and Helgeland populations during development. Three transition points (i.e. morula stage, day 4, and day 15) were used to develop a simplified linear model in the present study. Vertical bars denote 1 s.d.

increase in their specific gravity until day 4, then a gradual decrease during the rest of the incubation time. To develop a simplified linear model during development, the specific gravity at the morula stage is assumed as the value at fertilization. The values on days 4 and 15 are assumed as maximum and minimum specific gravities, respectively. The ontogenetic variability was larger among individual eggs, but the degree of changes were limited between the maximum and minimum (Jung *et al.* 2012). Hence, we chose the trend of Helgeland because Helgeland showed much smoother changes in the egg specific gravity throughout the development.

Circulation model

The model used for the ocean current simulation is the Regional Ocean Modeling System (ROMS) version 3.4, algorithms described by Shchepetkin and McWilliams (2005). This is a free-surface, hydrostatic, primitive equation ocean model that uses stretched terrain-following *s*-coordinates in the vertical and curvilinear coordinates in the horizontal (Haidvogel *et al.*, 2008). The primitive equations are solved by the finite differences method on an Arakawa C-grid, including a generic length scale turbulence closure scheme (Umlauf and Burchard, 2003) using the special case of Mellor-Yamada 2.5. Vikebø *et al.* (2010) used the ROMS model to simulate the transport of herring larvae and found that the ocean model reproduced observed variability within the Norwegian Coastal Current and the Norwegian Atlantic Current.

The model domain covers the Norwegian coast from 64.5 to 70°N (Figure 1; Albretsen *et al.*, 2011). The Norwegian Mapping Authority, the hydrographic service, provided the bathymetric data. To avoid model instabilities, the bathymetry was smoothed to a maximum *r* factor of 0.33. The grid resolution is 800 m with 801 points in the ξ direction and 335 points in the η direction. In the vertical, there are 35 sigma layers, stacked together at the surface with a reduced resolution towards the bottom. The atmospheric forcing was extracted from the ERA-Interim reanalysis with 75-km resolution prepared at European Centre for Medium Range Weather Forecasts, including wind, temperature, pressure, cloud cover, humidity, and precipitation. Initial and boundary conditions were collected from the operational model Meteorological Institute's Princeton Ocean Model, operated by the Norwegian Meteorological Institute, covering the Nordic Seas with 4-km resolution. The input is updated with daily averaged currents, salinity, and temperature at ten vertical levels. A global barotropic model of ocean tides, TPXO7.2, provides eight primary harmonic constituents (M_2, S_2, N_2, K_1, K_2, O_1, P_1, and Q_1). The river input is provided by NVE (Norwegian Water Resources and Energy Directorate) and based on the Hydrologiska ByrûËns Vattenbalanssektions model hydrological model with 1-km horizontal resolution. Details about the model setup and external forcing may be found in Albretsen *et al.* (2011).

Individual-based cod egg model

The cod egg model is a simple individual-based model included to the particle-tracking routines of ROMS as described by Narvaez *et al.* (2012) and based on Sundby (1983, 1991). The input parameters are egg diameter (1.4 mm) and mean egg neutral buoyancy (30.57) with s.d.(1.27), in terms of salinity. Each egg is assigned a specific gravity based on a normally distributed random number generator with zero mean and unit variance. The eggs attain a vertical velocity depending on the egg size and the density difference between the egg and the surrounding water. Stokes' formula is used to calculate the terminal velocity:

$$w = \frac{1}{18}\frac{gd^2\Delta\rho}{\mu}, \tag{1}$$

where g is the acceleration due to gravity, d the diameter of the egg, $\Delta\rho = \rho_w - \rho_e$ the density difference between the surrounding water and the egg, and μ the molecular viscosity. Stokes' formula is only valid when the Reynolds number is low, $\mathrm{Re} < 0.5$:

$$\mathrm{Re} = \frac{\rho_w dw}{\mu}, \tag{2}$$

When combining Equations (1) and (2), an expression for the maximum diameter D within Stokes' regime appears:

$$D^3 = \frac{9\mu^2}{\rho_w g\Delta\rho}, \tag{3}$$

For larger Reynolds numbers, Dallavalle's formula is used:

$$w = K_I(d - \zeta D)\Delta\rho^{2/3}\mu^{-1/3}, \tag{4}$$

where $\zeta = 0.4$ for a sphere. The coefficient K_I is derived by combining the two equations inserting $\mathrm{Re} = 0.5$ and $d = D$.

$$K_I = \frac{5}{54}9^{1/3}g^{2/3}\rho^{-1/3} = 0.0875\,\mathrm{kg}^{-1/3}m^{5/3}s^{-4/3}. \tag{5}$$

Both Stokes' and Dallavalle's formulae are included in the simulation, and for every time-step, the maximum diameter D is calculated to determine which regime the egg is within. The dynamic molecular viscosity of seawater is computed by the equation (Ådlandsvik, 2000):

$$\mu = 10^{-3}\,(1.7915 - 0.0538\,T + 0.0007\,T^2 + 0.0023\,S)\,\mathrm{kg\,m^{-1}\,s^{-1}}. \tag{6}$$

The incubation time of the eggs is calculated as a function of temperature and integrated as degree-days until hatching. The relationship is assumed to have the shape of a power-curve, as showed by Page and Frank (1989):

$$\mathrm{DS} = a(T + 2)^b, \tag{7}$$

where DS is the days and T the temperature. The parameters chosen here are reported in Table 9 for stage IV in Page and Frank (1989), $\log(a) = 1.88$ and $b = -0.85$.

$$\mathrm{DS}(T + 2)^{0.85} = a \times \mathrm{const} = C. \tag{8}$$

A controlled experiment showed that the eggs hatch after 16 d at a constant temperature of 6°C. By using this information, we can adjust the right-hand side of Equation (8) and calculate a new constant $C = 93.70$.

The measurements described in "Egg specific gravity measurements" showed that the egg specific gravity increases just after spawning, reaching a maximum after 4 d (at 6°C) then declining to a minimum just before hatching as shown in Figure 4. The maximum specific gravity was 0.515 salinity units higher than the initial value resulting in an increase of 0.103 units per day until degree-days is 29.28. The difference between maximum and minimum specific gravities was 1.29 salinity units occurring from day 4 until day 16, causing a decrease of 0.117 units/day until degree-days is 93.70. This simplified linear approach was included in the individual-based model to include the variations in the egg specific gravity, as seen in Figure 4.

In total, 183 427 cod eggs were released into the model domain during the whole model simulation. Eggs were released in every fifth ocean grid cell reaching as far out as grid cell 150 in the *y*-direction (westwards, see Figure 2) all at 20-m depth, once every day through March and April 2009. Initial depth does not affect the horizontal distribution of eggs when the model calculates

the vertical distribution internally (Sundby, 1991; Myksvoll *et al.*, 2011). The egg specific gravity was equal for all the spawning areas, since Jung *et al.* (2012) found no significant population difference between NCC and NEAC.

Results

Hydrography and model evaluation

Hydrographic data are collected by the Institute of Marine Research at the coastal station at Skrova (Figure 2) in VE. Temperature and salinity are sampled irregularly, usually 2–4 times per month, at 12 fixed depths between 1 and 250 m. The frequency distributions of the temperature and salinity measurements are plotted in Figure 5 from eight profiles taken during March and April 2009. Model results from the approximate location are retrieved at the corresponding dates.

The temperature variations are reproduced well in the model compared with the observations. Temperatures between 3 and 4°C are most frequent both in the observations and in the model results. However, the highest observed temperatures (above 6°C) are not present in the model output, meaning that the temperatures are slightly underestimated. The distribution of salinity values in the model also deviates from the observations. The observations show two peak abundances, at 32.8 and 33.3, whereas the model shows only one peak at 33.5. The largest offset between the peaks is therefore 0.7, which is then an estimate of the maximum salinity error in the model. The salinity range in the model is narrower (33.2–34.1) than the range covered by the observations (32.3–34.6).

Figure 6 shows the surface temperature on 5 March and 25 March 2009. The Norwegian Coastal Current enters the model domain in the south, follows the shelf break and turns westward just south of VE. A small branch of the coastal current enters VE, seen as a tongue of warm water close to the coast. A temperature front between Atlantic and coastal water is positioned at the baseline on 5 March, where the outermost islands are located. Several mesoscale meanders characterize the flow pattern in the coastal current, enhancing the production of eddies. On 25 March, the front between Norwegian Atlantic Current and Norwegian Coastal Current is shifted offshore compared with 5 March.

Retention within and connectivity between areas

Trajectories from a selection of cod eggs released on 31 March and 20 April are shown in Figure 7, where colours correspond to different zones (Table 1). The drift pathways from the spawning area at VI, located offshore to the south, are clearly distinguished from the others due to the long and more offshore transport route. The eggs are caught in the Norwegian Coastal Current, follow the shelf break, and flow around the Lofoten archipelago. Most of the eggs released in the coastal area (RV–VT–TB) stay inside of the baseline and have a weak northwards component. Within the fjords (FS–TO), the retention is large and only a small number of eggs are transported out into VE. A large part of the eggs spawned in VE stay within the area, whereas a few is transported through the small straits towards north.

Figure 8 shows the retention of cod eggs within each of the zones, meaning percentage of eggs that hatch within the zone they were released, through the spawning season. The spatial variability between the locations is large, varying from 0% at VI to 90% at TO. The oceanic zone at VI has zero retention during the whole spawning period, as these eggs are captured by the coastal current jet (Saetre, 1999) and transported rapidly northwards. The highest retention is found in the fjordic zones. TO has high retention during the whole period (70–90%), whereas FS experience some temporal variability (50–90%). Regarding the coastal zones (RV–VT–TB), RV always has highest retention for all days through March and April followed by TB and VT with the lowest percentage. All three show similar temporal variability during the 2 months and the difference between them stays constant through the whole period. There is no obvious trend through the spawning season or any specific time that is specifically favourable for retention. VE has large variability in the retention, between 15 and 65%, and is occasionally negatively correlated with the other zones.

Transport of cod eggs between zones is illustrated in Figure 9 for eggs released at six different times during the spawning

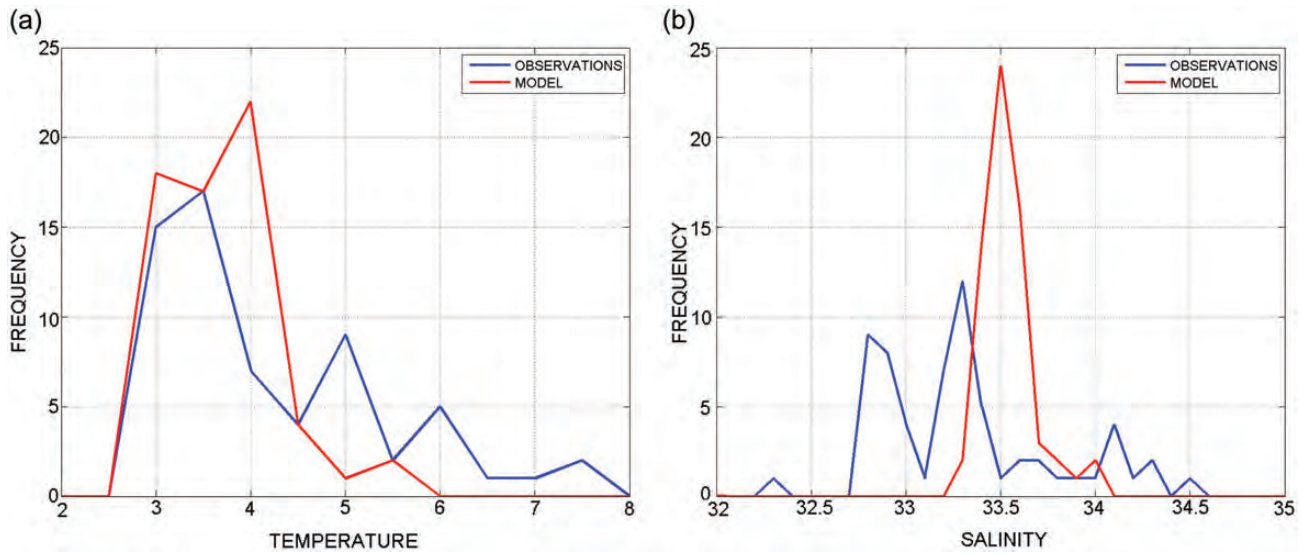

Figure 5. Eight observed (blue) profiles of temperature (a) and salinity (b) was compared with the model (red) results at the coastal station Skrova (Figure 1) during March and April 2009.

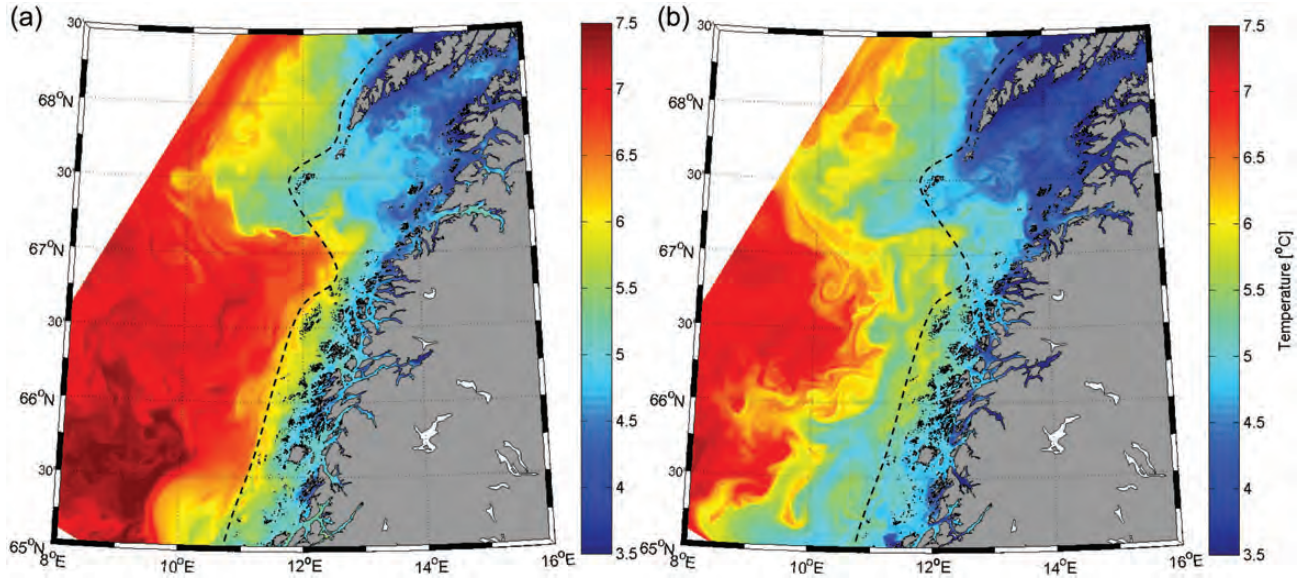

Figure 6. The daily mean sea surface temperature on two specific days in 2009. (a) 5 March and (b) 25 March.

season: 11 March, 21 March, 31 March, 10 April, 20 April, and 30 April. The *x*-axes represents the initial zone where the eggs were released at spawning and the *y*-axes shows the zones where the eggs are located at hatching time, starting from south moving northwards. The diagonal shows retention within the respective zones, the same values that was shown in the time-series in Figure 8. All numbers are the percentage of the initial number of eggs within this spawning zone.

The results show that the transport of eggs is directed northwards following the Norwegian Coastal Current, only a small number of eggs is transported southwards (values below the diagonal). The spawning area VI has low retention and highest connectivity with VT; otherwise most of the eggs have been transported offshore. The two following coastal zones (RV–VT) have medium retention within the zone, in addition to comparable transport into the neighbouring zone to the north (VT–TB). The third coastal-zone TB shows only small transport into the neighbouring fjord zone (FS) and VE. The two fjord zones (FS–TO) have little connectivity with the other zones, few eggs leave the spawning areas inside the fjords and those that do will most probably enter VE. Eggs spawned inside VE have medium retention during March, whereas in April, a considerable amount of eggs are transported into TO. Considering the whole period through March and April, the connectivity pattern is similar but the magnitude of transport varies, consistent with the variable mesoscale activity and the strength of the Norwegian Coastal Current.

Physical–biological interactions

The temperature experienced by the cod eggs was recorded from spawning to hatching, and a mean representing the entire egg stage in each zone was calculated (Figure 10a). Calculated hatching time, as a function of spawning date and temperature starting on 1 March continuing until 30 April, is shown in Figure 10b. The highest temperatures (5.5–6.5°C) were experienced by cod eggs spawned at VI, ~0.5–1°C warmer than the coastal area. The decrease in temperature at the beginning of the period is associated with the offshore shift of the coastal current, as seen in Figure 6. All the coastal zones (RV–VT–TB) are similar to each other, from 5 to 6°C, whereas VT is the warmest of these during the last part of March. The northern fjordic areas are coldest (below 4°C) during the whole period, ~1°C colder than the coastal areas further south. All the areas experience small fluctuations in temperature initially, followed by the seasonal warming in mid-April. The fjordic regions have strongest warming, starting around 4°C increasing above 5°C during 20 d. The two southernmost zones, VI and RV, are geographically close together but a temperature difference of ~1° is seen for the major part of the spawning period. The same difference is seen between TB and FS, which are neighbouring areas but represent coastal and fjordic regions.

Hatching time for cod eggs is a function of temperature experienced by the eggs along their trajectories [Equation (8)] and, therefore, depends on spawning zones and time (Figure 10b). The hatching time stays constant during the main part of the spawning period and decreasing towards the end of April when the seasonal warming starts. The fjord zones (FS and TO) show similar variability and are staying at ~21 d during March while decreasing below 18 d in the end of April. The coastal areas further south have shorter hatching times starting at ~18 d and decreasing towards 16 d. VI has the lowest hatching time during the whole spawning period, with a minimum of 15.5 d. The variability between the zones is largest at the beginning of the season and is reduced towards the end of April.

The mean transport depth of eggs released at VT on 31 March is shown in Figure 11a, in the upper panel, together with the temperature experienced by the eggs. The lower panel shows the salinity together with egg neutral buoyancy as a function of degree-days. The eggs in this figure represent the mean neutral buoyancy range from 29.62 to 31.52 and are surrounded by water with salinity of ~33.5. This large salinity difference causes all the eggs to float towards the surface, being pelagically distributed. The eggs are confined to the surface through the whole egg stage with only small variations due to changes in water elevation. The temperature stays at around 5°C through egg development.

Figure 11b shows the eggs released at RV on 31 March and with neutral buoyancy ranging from 31.52 to 33.1. The salinity in this

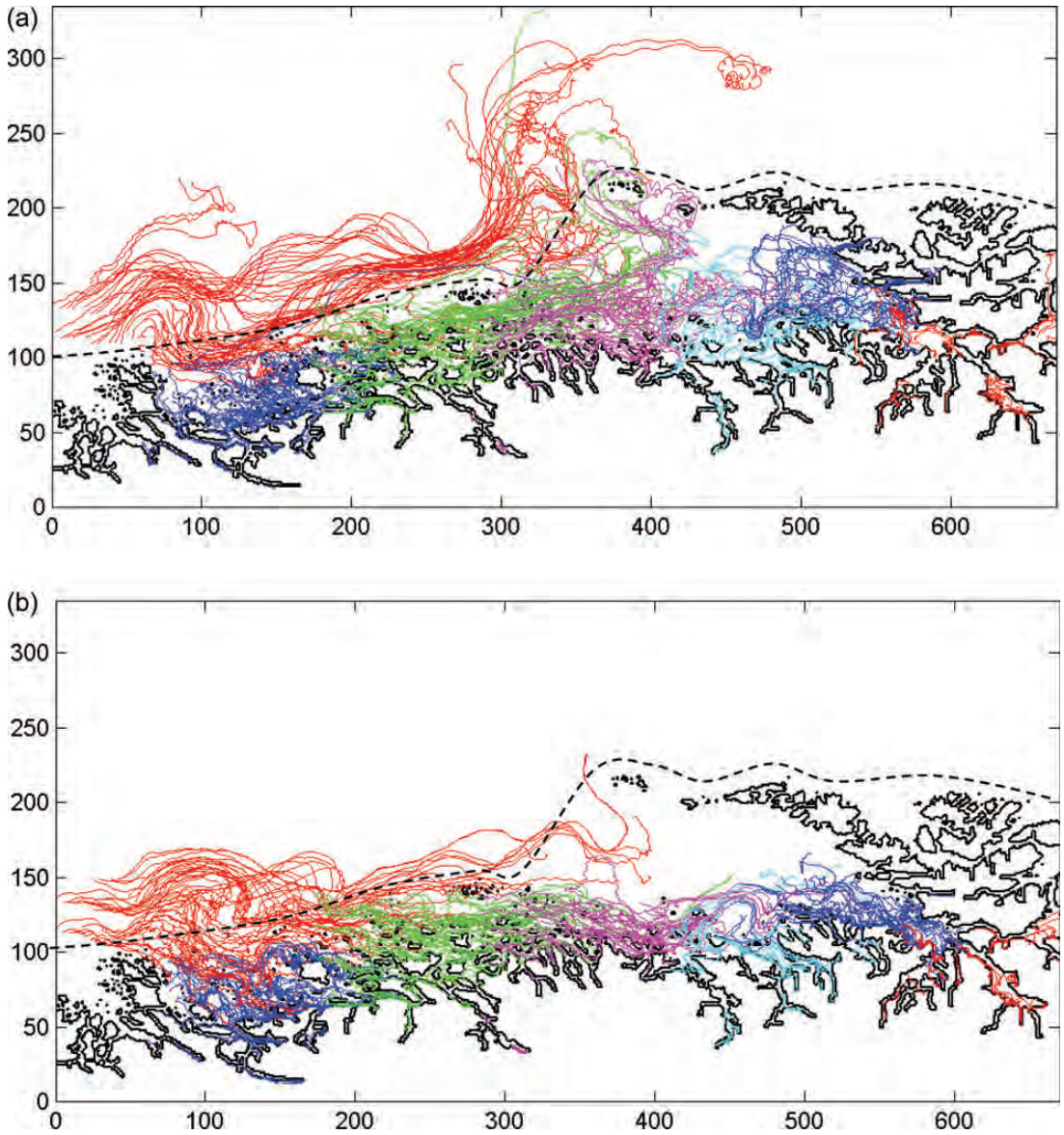

Figure 7. Trajectories of cod eggs from all spawning areas, colour coding is based on the zonal subdivision as seen in Table 1. All eggs are released simultaneously and advected for ~18 d, which is the time when 50% of the eggs are hatched. The two dates, (a) 31 March and (b) 20 April, are examples of different dispersal patterns.

region is slightly lower than VT. For a short period, around degree-days 30, the neutral buoyancy approaches the surface salinity and the eggs become negatively buoyant. The corresponding impact on vertical distribution is seen in the upper panel, where the eggs sink to ~13-m depth between degree-days 30 and 40. A small negative salinity difference between the egg and the surrounding water results in a weak descending speed [Equation (1)], this causes a delay in maximum depth related to the minimum salinity difference.

Discussion

Hydrography and model evaluation

The model reproduced the observed temperature distribution well, but the salinity to a lesser degree. The temperature variations within this region are basically controlled by the local air-sea exchange, whereas salinity variations are controlled by water masses advected by the Norwegian Coastal Current (Mork, 1981). The model domain is of limited geographical extent and upstream variations can only be included through the boundary conditions. A 4-km model provides the external forcing on the southern boundary where the coastal current enters the domain. The outer model includes the whole Norwegian coast and the input of low-saline water from the Baltic Sea, which is the most important freshwater source influencing hydrography (Røed and Albretsen, 2007). It is therefore likely that the 800-m model in this study is limited by low-resolution boundary conditions, which is not resolving the mesoscale structure of the coastal current. Albretsen and Røed (2010) showed that an eddy-resolving model is required to capture the mesoscale circulation along the southern Norwegian coast due to improved representation of the topography.

Higher salinity in the model than in the observations during winter can be caused by limitations in the river run-off to the model. Many hydroelectric power stations along the coast affect the seasonal cycle of river run-off through regulations (Pytte Asvall, 1976). The major difference is increased run-off during winter compared with naturally low discharge. The modelled run-off is not corrected for this shift, which might contribute to the difference in salinity between model and observations. Skarðhamar and Svendsen (2005) also acknowledged the importance of accurate freshwater discharge, as the strength of stratification controls the influence of wind, tides, and topography on surface circulation. However, Albretsen (2007) showed for the Skagerrak that realistic river run-off is not required when the focus is on modelling mesoscale activity, meaning that the current pattern may be simulated realistically despite an offset in the modelled density or salinity.

The salinity was higher in the model compared with the observations, on the same order as the spatial differences between the zones in the model. The specific gravity of cod eggs used in this study was significantly lower than spatial density variations in the model, which means that most of the eggs have a pelagic vertical distribution and is only affected by the model error to a limited degree. However, the heaviest portions of eggs located in regions of low salinity are very near their level of equilibrium. These are more influenced by the salinity discrepancy in the model and might attain a subsurface distribution in a realistic physical environment (Sundby, 1991). The effect of this discrepancy is largest in the fjord regions, since this is where the salinity is lowest. A subsurface distribution of cod eggs here would further reduce offshore transport and increase retention. This would therefore support the main connectivity pattern already described here.

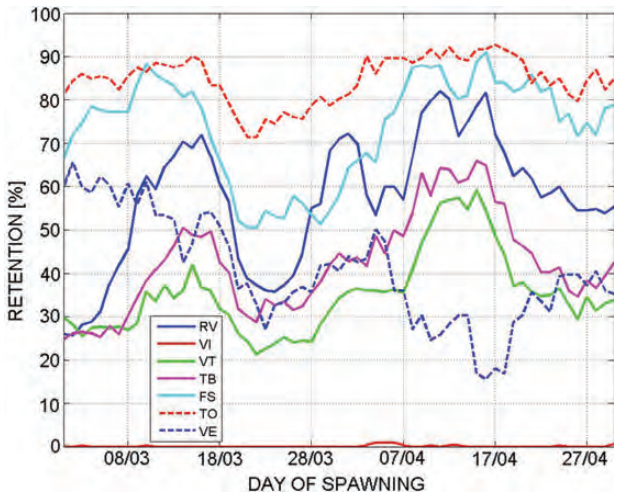

Figure 8. Retention of cod eggs, meaning the percentage that hatch within the zone they were spawned, in each of the zones; V), RV, VT, TB, Folda-Sagfjord (FS), TO, and VE through spawning season. The same number of eggs is released every day through March and April.

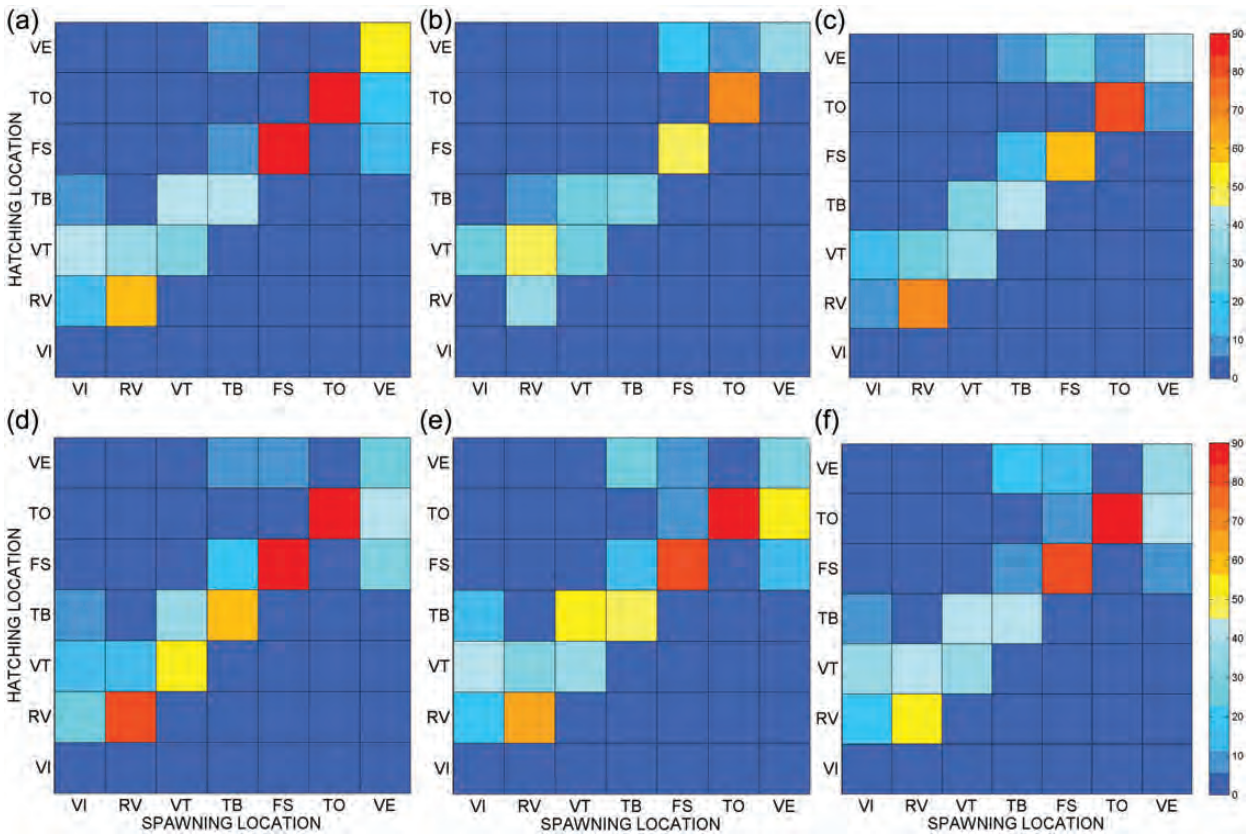

Figure 9. Connectivity matrices showing transport from spawning location (*x*-axes) to hatching location (*y*-axes), colour coding showing the percentage of the initial number of eggs released in the spawning zone. The diagonal shows retention within the respective zones. (a) 11 March, (b) 21 March, (c) 31 March, (d) 10 April, (e) 20 April, and (f) 30 April.

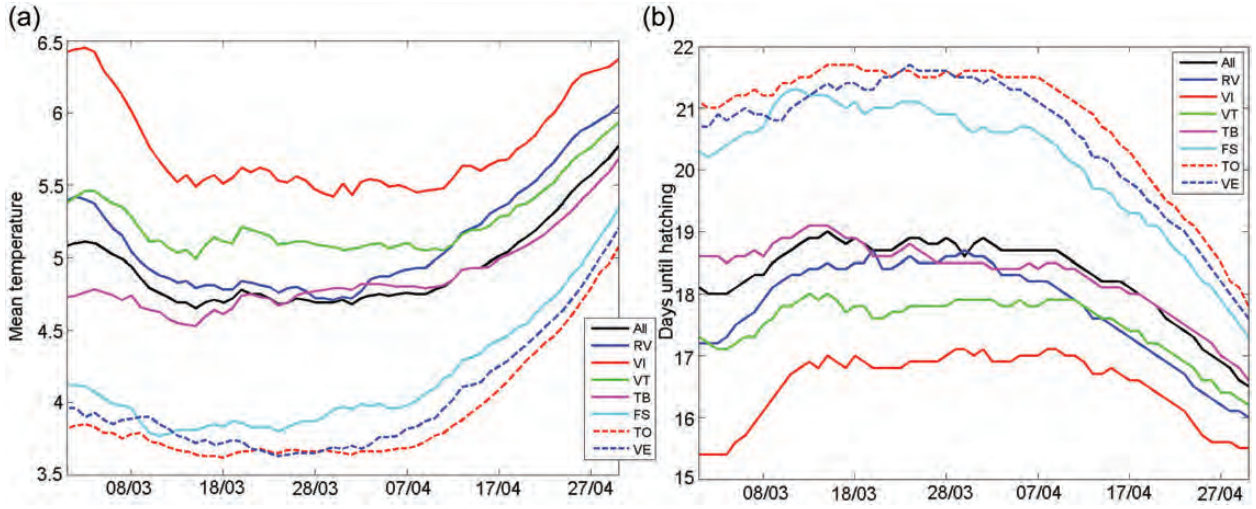

Figure 10. The mean temperature (a) experienced by cod eggs during development and calculated hatching time (b), as a function of spawning time, for all areas (black) and in each of the zones; VI, RV, VT, TB, Folda-Sagfjord (FS), TO, and VE. (a) Mean temperature and (b) days until hatching.

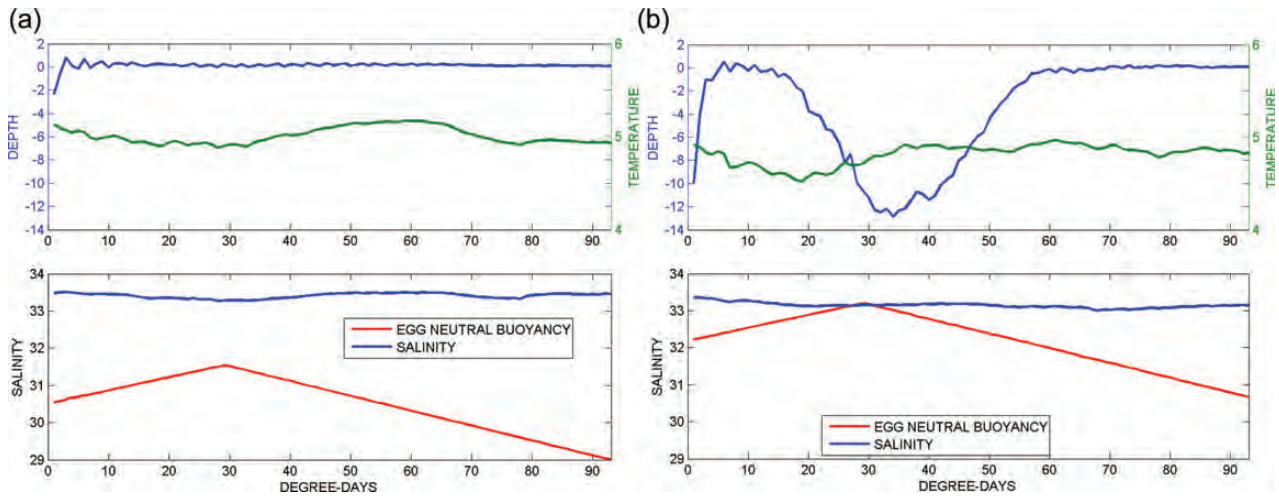

Figure 11. Evolution of the mean depth (blue, upper panel), temperature (green, upper panel), salinity (blue, lower panel), and egg neutral buoyancy (red, lower panel) through egg development as a function of degree-days for two specific zones, both released 31 March 2009. (a) VT, average for eggs with neutral buoyancy: 29.62 – 31.52, (b) RV, average for eggs with neutral buoyancy: 31.52 – 33.1.

The model used in these simulations is not well suited for detailed studies on fjord dynamics, because of the 800-m horizontal resolution and the regionally scaled run-off used in the model. The river run-off is an important mechanism controlling the estuarine circulation (Saelen, 1967), but is not realistically represented within each fjord in this model setup resulting in higher salinities within the fjords. However, river input is scaled to match the total freshwater contribution to the coastal current. Myksvoll *et al.* (2011) showed strong retention mechanisms inside the fjord system of Folda. The model simulations shown here focus more on possible transport pathways between coastal and fjord populations, showing that the connectivity is very low. This was hypothesized by Myksvoll *et al.* (2011) and confirmed by the present paper.

Observed seasonal variations in the horizontal extent of the coastal current were well reproduced by the model. It is well known that the width of the coastal current is affected by monsoon like wind variations (Saere *et al.*, 1988; Mitchelson-Jacob and Sundby, 2001; Saetre, 2007a). North/northwesterly winds during summer typically advect the low salinity water offshore and the coastal current broadens. Southerly winds during winter push the coastal wedge towards the coast and cause a narrowing of the current. The model recreates this seasonal pattern, as illustrated in Figure 6, where the coastal current is broadening towards summer.

Retention within and connectivity between areas

The eggs spawned at VI are captured by the coastal current jet and dispersed rapidly northwards which favours transport into the Barents Sea. NEAC occupies several offshore spawning areas along the coast of Helgeland (Bergstad *et al.*, 1987; Sundby and Nakken, 2008), including VI and Vega. Opdal *et al.* (2008) showed that larval trajectories from these two spawning grounds

spread northwards along the Norwegian coast just offshore of the baseline. The model results show that spawning at VI results in a significantly different dispersal pattern than all the other spawning areas in this study, mainly due to persistent zero retention. This is consistent with being populated by another cod stock than the inshore spawning areas, which has a different life history.

There is no trend in retention during the spawning season; the variability is high but consistent between the zones. The exception is VE, which is occasionally negatively correlated with the others, probably influenced by wind interacting with local topography (Ellertsen *et al.*, 1981; Furnes and Sundby, 1981). The spawning areas can be classified into different retention regimes: large retention in fjords, medium retention at the coast, and no retention offshore. The transition from zero to medium retention occurs at the baseline, which is marked by the outermost islands. The complex bathymetry of the Norwegian coast causes persistent mesoscale meanders and eddies along the path of the coastal current (Oey and Chen, 1992; Mitchelson-Jacob and Sundby, 2001). This might explain the persistent connectivity pattern through the spawning season, as retention is mainly caused by topographic features (Moseidjord *et al.*, 1999; Saetre, 1999). Retention of cod eggs inshore of the baseline is mainly caused by interaction with small islands. High horizontal resolution is needed in such regions to model dispersion of particles, where strong tidal flow interacts with topographic features (Lynge *et al.*, 2010). It is also important to emphasize that the conclusions made here are only based on simulations from 2009. However, the respective period in 2009 covers the seasonal transition from winter to spring and corresponding offshore shift in the coastal front. The connectivity pattern is stable through these seasonal shifts (Figure 8). The topographic features in the region controls the transport and the system is less sensitive to seasonal and interannual variability.

Transport from a coastal zone into the neighbouring zone to the north is of comparable magnitude as retention within the zone. Further northwards beyond the neighbouring zone, the connectivity is significantly lower. Saetre *et al.* (2002) studied larval transport from Norwegian spring-spawning herring in the same area. They found that larvae was temporarily retained due to topographically trapped eddies and good recruitment coincided with slow northwards drift.

Physical–biological interactions

Differences in temperature between the zones reflect the different dynamic regions and distance from the coast. The temperature gradient from inshore to offshore is larger than from north to south (Haakstad *et al.*, 1994), at least within this part of the Norwegian coast. The highest temperatures are seen at the offshore spawning ground at VI, which was also shown in Opdal *et al.* (2008), whereas the lowest temperatures are seen inside the fjords. The coastal banks experience intermediate temperatures as an average between the open ocean and the fjords. The temperature differences are also reflected in the differences in hatching time, clearly showing a geographic pattern. It is therefore interesting that the pattern in hatching time is opposite of the connectivity pattern, meaning that fjord zones have long hatching time and high retention and at the same time VI has short hatching time and low retention. This illustrates the persistence of the connectivity pattern described in "Retention within and connectivity between areas", since it is working against the indirect effect of temperature on transport.

The egg specific gravities used in these calculations, relative to the coastal density structure, result in a pelagic vertical distribution with highest concentration at the surface and exponentially decreasing downwards (Sundby, 1991). Only the proportion with the highest specific gravity located in specific areas with low salinities attain a subsurface distribution. The cod eggs only experience these low salinities inside the fjords (Myksvoll *et al.*, 2011), meaning that there is no difference in vertical distribution between oceanic and coastal cod in the coastal region. And the difference in vertical distribution between fjord cod and coastal cod is caused by the local salinity profile. Variations in the vertical distribution of cod eggs have two causes: (i) variations in the local salinity profile determined by the ocean physics and (ii) variations in the egg specific gravity determined by the phenotypic and genotypic characteristics of the spawners. Since the average specific gravity of eggs in a population appears to be remarkably constant through time, it is likely to assume that it is a long-term ecological adaptation to the average ambient environmental factors. But also the variation in the specific gravity around the mean value, expressed as, for example, by the s.d., must be considered to be a long-term ecological adaptation to the variation in the ambient environmental factor. However, variability, in general, caused by biotic as well as abiotic factors is a source to connectivity among populations, and variability in biotic factors is a source to the potential for adaptation to a variable and changing environment.

The observed variations in the egg specific gravity through development (Figure 4) affect the vertical distribution only for a limited period and are therefore not important for horizontal distribution. The only effect is for eggs that are situated in waters with approximately the same density as the egg, but for pelagic eggs the effect is negligible.

The connectivity matrices (Figure 9) show that offspring from different areas remain physically separated during the egg stages, and hence this result is not contradicting investigations, showing that coastal cod populations are genetically separated (Pogson and Fevolden, 2003). Myksvoll *et al.* (2011) showed high retention within a fjord system and here we show that transport from coastal areas into fjords is negligible. As larvae are known to obtain a subsurface distribution (Ellertsen *et al.*, 1984), the described connectivity pattern is also representative for the larval stages. This means that fjord populations with stationary individuals are partly isolated and have low genetic connectivity (Jorde *et al.*, 2007). The largest possibility for the exchange of genes is when juveniles and subsequently adults migrate into or out of the fjord and spawn together with another population.

Metapopulation perspective

We provide new knowledge of the degree of connectivity during egg stages among different cod habitats. Eggs spawned in typical fjords with a narrow entrance (FS and TO) were likely to be retained in their birth places until hatching (50–90% retention). Once hatched in the fjords, larvae would keep staying inside the fjords by active vertical movement against outflowing currents (Ellertsen *et al.*, 1984). The hypothesis of larval retention has been confirmed by the study of Øresland and André (2008) showing genetic differences in cod larvae between inside and outside fjord. Besides, fjord cod had very low mixing rates with eggs originating from neighbouring coastal and fjord areas (Figure 9), indicating low connectivity of egg/larval stages to neighbouring areas. Recently, one study demonstrates that adult

cod have strong tendency of homing to their nursery fjord to spawn (Skjæraasen *et al.*, 2011). Hence, with the evidence of egg/larval retention and spawning site fidelity, it is conceivable that each single fjord cod population may evolve a disparate subpopulation. On the contrary, the egg retention in successive coastal areas (RV, VT, and TB) varied from 20 up to 80%. The remaining eggs were transported to the north by the Norwegian Coastal Current. Under this condition, the RV, VT, and TB might share a common larval pool so that self-recruitment occurs regionally on a larger geographical scale than the fjord population. Therefore, dispersal patterns of early life-history stages are clearly different between fjords and coastal areas, and hence this difference can enhance substructuring among cod populations along the Norwegian coast.

Levins (1970) postulated that subpopulations within a metapopulation would have the same geographic extent and a degree of isolation. The Norwegian coast consists of many fjords, which are all possible habitats for local cod populations, but the fjords do not have the same geographical extent. Some common features exist in many fjords, like large depth, small width, seasonal river run-off, and a sill near the mouth (Wassmann *et al.*, 1996). Large variations occur within these categories, e.g. differences in sill depth will affect the water exchange and correspondingly the habitat suitability. Large differences in cod abundance between neighbouring fjords (Berg and Albert, 2003) suggest uncorrelated recruitment mechanisms and potentially one subpopulation could go extinct, while another subpopulation nearby is sustained. For the coastal regions, the habitats are not as well delimited as in the fjords. While spawning inshore of the baseline increase the residence time of eggs, the retention is intermediate and mainly caused by small-scale eddies between the many islands.

Each subpopulation in a metapopulation should have its own dynamics, meaning that individuals spend their entire life cycle within the local habitat. Tagging experiments of cod show only short migrations mainly within the respective fjord (Karlsson and Mork, 2003; Knutsen *et al.*, 2011). Strong homing has also been detected for local populations in Skagerrak (Svedäng *et al.*, 2007) and several other places in the North Atlantic (Robichaud and Rose, 2004). This supports the assumption that fjord populations can have their own population dynamics. A study from Trondheimsfjorden in the middle of Norway shows that only 1.5% of tagged fish was recaptured outside of the fjord 5 years after the release (Karlsson and Mork, 2003). Migration on this scale is too low to affect the local dynamics and genetic structure, but is sufficient to allow a rescue or recolonization event in a neighbouring fjord following the so-called stepping-stone dispersal model.

Another important aspect of the metapopulation theory is that at least one subpopulation must have a non-zero probability of extinction (non-anthropogenic), followed by a recolonization event. Low abundance of cod in some fjords has been reported (Berg and Albert, 2003), but it is difficult to distinguish between natural and anthropogenic influence as they may occur at the same time. Extinctions have occurred in several subpopulations, but recolonizing is more seldom and possibly hard to detect. The large volume of a fjord makes it hard to know for sure that a population has gone extinct. It is also likely that the population is too low to be detected by fisheries and scientific surveys and might apparently recolonize itself in the absence of fishing.

Our study is the first report of egg connectivity among different cod habitats. Demographic exchanges by egg dispersal could be low not only between fjords and coastal areas but also among neighbouring fjords. With the evidence of resident behaviour in fjord populations, we argue that a fjord might have its own cod subpopulation. Regarding the coastal spawning populations it is not as clear due to less available knowledge and the weaker retention mechanism operating at the coast. Retention of early life stages within fjords, stationary juveniles, and spawning site fidelity indicate the existence of subpopulations in fjords similar to what is described as a metapopulation. And as the exchange of individuals between local habitats is low, the time-scale for natural recolonization events may be very long. This is very important to consider in fisheries management, as the growth and harvest potential could be overestimated, and for a collapse the recovery will be slow (Sterner, 2007).

Acknowledgements

We would like to thank two anonymous reviewers for constructive comments that significantly improved the manuscript.

References

Ådlandsvik, B. 2000. VertEgg: a Toolbox for Simulation of Vertical Distribution of Fish Eggs. Institute of Marine Research, Bergen, Norway.

Ådlandsvik, B., and Sundby, S. 1994. Modeling the transport of cod larvae from the Lofoten area. ICES Marine Science Symposia, 198: 379–392.

Albretsen, J. 2007. The impact of freshwater discharges on the ocean circulation in the Skagerrak/northern North Sea area. Part II: energy analysis. Ocean Dynamics, 57: 287–304.

Albretsen, J., and Røed, L. P. 2010. Decadal long simulations of mesoscale structures in the northern North Sea/Skagerrak using two ocean models. Ocean Dynamics, 60: 933–955.

Albretsen, J., Sperrevik, A. K., Staalstrøm, A., Sandvik, A. D., Vikebø, F., and Asplin, L. 2011. NorKyst-800 Report No.1, User Manual and Technical Descriptions. Technical Report 2, Fisken og Havet, Institute of Marine Research.

Berg, E., and Albert, O. T. 2003. Cod in fjords and coastal waters of North Norway: distribution and variation in length and maturity at age. ICES Journal of Marine Science, 60: 787–797.

Bergstad, O. A., Jørgensen, T., and Dragesund, O. 1987. Life history and ecology of the gadoid resources of the Barents Sea. Fisheries Research, 5: 119–161.

Ciannelli, L., Knutsen, H., Olsen, E. M., Espeland, S. H., Asplin, L., Jelmert, A., Knutsen, J. A., *et al.* 2010. Small-scale genetic structure in a marine population in relation to water circulation and egg characteristics. Ecology, 91: 2918–2930.

Cowen, R. K., Lwiza, K. M. M., Sponaugle, S., Paris, C. B., and Olson, D. B. 2000. Connectivity of marine populations: open or closed? Science, 287: 857–859.

Dahle, G., Jørstad, K. E., Rusaas, H. E., and Otterå, H. 2006. Genetic characteristics of broodstock collected from four Norwegian coastal cod (*Gadus morhua*) populations. ICES Journal of Marine Science, 63: 209–215.

Ellertsen, B., Fossum, P., Solemdal, P., and Sundby, S. 1989. Relation between temperature and survival of eggs and first-feeding larvae of Northeast Arctic cod (*Gadus morhua* L.). Rapports et Procès-Verbaux des Réunions du Conseil International pour l'Exploration de la Mer, 191: 209–219.

Ellertsen, B., Fossum, P., Sundby, S., and Tilseth, S. 1984. A case study on the distribution of cod larvae and availability of prey organisms in relation to physical processes in Lofoten. *In* The Propagation of Cod (*Gadus morhua* L.), pp. 453–477. Ed. by E. Dahl, D. S. Danielsen, E. Moksness, and P. Solemdal. Flødevigen Rapportserie 1, Arendal.

Ellertsen, B., Furnes, G. K., Solemdal, P., and Sundby, S. 1981. Influence of wind induced currents on the distribution of cod eggs and zooplankton in Vestfjorden. *In* The Norwegian Coastal Current, Proceedings from the Norwegian Coastal Current Symposium, Geilo, 9–12 September 1980, pp. 604–628. Ed. by R. Sætre, and M. Mork. University of Bergen.

Fevolden, S. E., and Pogson, G. H. 1997. Genetic divergence at the synaptophysin (Syp I) locus among Norwegian coastal and north-east Arctic populations of Atlantic cod. Journal of Fish Biology, 51: 895–908.

Fridgeirsson, E. 1978. Embryonic development of five species of gadoid fishes in Icelandic waters. Rit Fiskideildar, 5: 1–68.

Furnes, G. K., and Sundby, S. 1981. Upwelling and wind induced circulation in Vestfjorden. *In* The Norwegian Coastal Current, Proceedings from the Norwegian Coastal Current Symposium, Geilo, 9–12 September 1980, pp. 152–177. Ed. by R. Sætre, and M. Mork. University of Bergen.

Haakstad, M., Kögeler, J. W., and Dahle, S. 1994. Studies of sea surface temperatures in selected northern Norwegian fjords using Landsat TM data. Polar Research, 13: 95–103.

Haidvogel, D. B., Arango, H., Budgell, W. P., Cornuelle, B. D., Curchitser, E., Di Lorenzo, E., Fennel, K., *et al.* 2008. Ocean forecasting in terrain-following coordinates: formulation and skill assessment of the Regional Ocean Modeling System. Journal of Computational Physics, 227: 3595–3624.

Jakobsen, T. 1987. Coastal cod in northern Norway. Fisheries Research, 5: 223–234.

Jorde, P. E., Knutsen, H., Espeland, S. H., and Stenseth, N. C. 2007. Spatial scale of genetic structuring in coastal cod (*Gadus morhua*) and geographic extent of local populations. Marine Ecology Progress Series, 343: 229–237.

Jung, K-M., Folkvord, A., Kjesbu, O. S., Agnalt, A. L., Thorsen, A., and Sundby, S. 2012. Egg buoyancy variability in local populations of Atlantic cod (*Gadus morhua*). Marine Biology, 159: 1969–1980.

Karlsson, S., and Mork, J. 2003. Selection-induced variation at the pantophysin locus (PanI) in a Norwegian fjord population of cod (*Gadus morhua* L.). Molecular Ecology, 12: 3265–3274.

Knutsen, H., Olsen, E. M., Cianneli, L., Espeland, S. H., Knutsen, J. A., Simonsen, J. H., Skreslet, S., *et al.* 2007. Egg distribution, bottom topography and small-scale cod population structure in a coastal marine system. Marine Ecology Progress Series, 333: 249–255.

Knutsen, H., Olsen, E. M., Jorde, P. E., Espeland, S. H., André, C., and Stenseth, N. C. 2011. Are low but statistically significant levels of genetic differentiation in marine fishes 'biologically meaningful'? A case study of coastal Atlantic cod. Molecular Ecology, 20: 768–783.

Levins, R. 1970. Extinction. *In* Some Mathematical Problems in Biology, pp. 77–107. Ed. by M. Desternhaber. American Mathematical Society, Providence.

Lynge, B. K., Berntsen, J., and Gjevik, B. 2010. Numerical studies of dispersion due to tidal flow through Moskstraumen, northern Norway. Ocean Dynamics, 60: 907–920.

Mitchelson-Jacob, G., and Sundby, S. 2001. Eddies of Vestfjorden, Norway. Continental Shelf Research, 21: 1901–1918.

Mork, M. 1981. Circulation phenomena and frontal dynamics of the Norwegian Coastal Current. Philosophical Transactions of the Royal Society of London, 302A: 635–647.

Moseidjord, H., Svendsen, H., and Slagstad, D. 1999. Sensitivity studies of circulation and ocean-shelf exchange off northern Norway. Sarsia, 84: 191–198.

Myksvoll, M. S., Sundby, S., Ådlandsvik, B., and Vikebø, F. B. 2011. Retention of coastal cod eggs in a fjord caused by interactions between egg buoyancy and circulation pattern. Marine and Coastal Fisheries, 3: 279–294.

Narvaez, D. A., Klinck, J. M., Powell, E. N., Hofmann, E. E., Wilkin, J., and Haidvogel, D. B. 2012. Modeling the dispersal of Eastern Oyster (*Crassostrea virginica*) larvae in Delaware Bay. Journal of Marine Research, 70: 381–409.

Nordeide, J. T. 1998. Coastal cod and north-east Arctic cod—do they mingle at the spawning grounds in Lofoten. Sarsia, 83: 373–379.

Oey, L-Y., and Chen, P. 1992. A nested-grid ocean model: with application to the simulation of meanders and eddies in the Norwegian Coastal Current. Journal of Geophysical Research, 97: 20063–20086.

Opdal, A. F., Vikebø, F. B., and Fiksen, Ø. 2008. Relationships between spawning ground identity, latitude and early life thermal exposure in Northeast Arctic cod. Journal of Northwest Atlantic Fishery Science, 41: 13–22.

Øresland, V., and André, C. 2008. Larval group differentiation in Atlantic cod. Fisheries Research, 90: 9–16.

Orvik, K. A., and Niiler, P. 2002. Major pathways of Atlantic water in the northern North Atlantic and Nordic Seas towards Arctic. Geophysical Research Letter, 29: 1896–1899.

Otterå, H., Agnalt, A. L., and Jørstad, K. E. 2006. Differences in spawning time of captive Atlantic cod from four regions of Norway, kept under identical conditions. ICES Journal of Marine Science, 63: 216–223.

Page, F. H., and Frank, K. T. 1989. Spawning time and egg stage duration in Northwest Atlantic Haddock (*Melanogrammus eaglefinus*) stocks with emphasis on Georges Bank and Browns bank. Canadian Journal of Fisheries and Aquatic Sciences, 46(Suppl.1): 68–81.

Pogson, G. H., and Fevolden, S. E. 2003. Natural selection and the genetic differentiation of coastal and Arctic populations of the Atlantic cod in northern Norway: a test involving nucleotide sequence variation at the pantophysin (PanI) locus. Molecular Ecology, 12: 63–74.

Pytte Asvall, R. 1976. Effects of regulation on freshwater runoff. *In* Fresh Water on the Sea, pp. 15–20. Ed. by S. Skreslet, R. Leinebø, J. B. L. Matthews, and E. Sakshaug. The Association of Norwegian Oceanographers, Oslo.

Robichaud, D., and Rose, G. A. 2004. Migratory behavior and range in Atlantic cod: inference from a century of tagging. Fish and Fisheries, 5: 185–214.

Røed, L. P., and Albretsen, J. 2007. The impact of freshwater discharges on the ocean circulation in the Skagerrak/northern North Sea area. Part I: model validation. Ocean Dynamics, 57: 269–285.

Saelen, O. H. 1967. Some features of the hydrography of Norwegian fjords. *In* Estuaries, pp. 63–70. Ed. by G. H. Lauff. AAAC, Washington, DC.

Saetre, R. 1999. Features of the central Norwegian shelf circulation. Continental Shelf Research, 19: 1809–1831.

Saetre, R. 2007a. Driving forces. *In* The Norwegian Coastal Current—Oceanography and Climate, pp. 45–58. Ed. by R. Sætre. Tapir Academic Press, Trondheim.

Saetre, R. 2007b. Introduction. *In* The Norwegian Coastal Current—Oceanography and Climate, pp. 9–18. Ed. by R. Sætre. Tapir Academic Press, Trondheim.

Saetre, R., Aure, J., and Ljøen, R. 1988. Wind effects on the lateral extension of the Norwegian Coastal Water. Continental Shelf Research, 8: 239–253.

Saetre, R., Toresen, R., Søiland, H., and Fossum, P. 2002. The Norwegian spring spawning herring - spawning, larval drift and larval retention. Sarsia, 87: 167–178.

Shchepetkin, A. F., and McWilliams, J. C. 2005. The regional oceanic modeling system (ROMS): a split-explicit, free-surface, topography-following-coordinate oceanic model. Ocean Modeling, 9: 347–404.

Skarðhamar, J., and Svendsen, H. 2005. Circulation and shelf-ocean interaction off North Norway. Continental Shelf Research, 25: 1541–1560.

Skjæraasen, J. E., Meager, J. J., Karlsen, Ø., Hutchings, J. A., and Ferno, A. 2011. Extreme spawning site-fidelity in Atlantic cod. ICES Journal of Marine Science, 68: 1472–1477.

Smedbol, R. K., McPherson, A., Hansen, M. M., and Kenchington, E. 2002. Myths and moderation in marine metapopulations. Fish and Fisheries, 3: 20–35.

Smedbol, R. K., and Wroblewski, J. S. 2002. Metapopulation theory and northern cod population structure: interdependency of subpopulations in recovery of a groundfish population. Fisheries Research, 55: 161–174.

Sterner, T. 2007. Unobserved diversity, depletion and irreversibility: the importance of subpopulations for management of cod stocks. Ecological Economics, 61: 566–574.

Sundby, S. 1983. A one-dimensional model for the vertical distribution of pelagic fish eggs in the mixed layer. Deep-Sea Research Part A: Oceanographic Research Papers, 30: 645–661.

Sundby, S. 1991. Factors affecting the vertical distribution of eggs. ICES Marine Science Symposia, 192: 33–38.

Sundby, S., and Fossum, P. 1990. Feeding conditions of Arcto-Norwegian cod larvae compared with the Rotschild-Osborn theory on small-scale turbulence and plankton contact rates. Journal of Plankton Research, 12: 1153–1162.

Sundby, S., and Nakken, O. 2008. Spatial shifts in spawning habitats of Arcto-Norwegian cod related to multidecadal climate oscillations and climate change. ICES Journal of Marine Science, 65: 953–962.

Svedäng, H., Righton, D., and Jonsson, P. 2007. Migratory behavior of Atlantic cod Gadus morhua: natal homing is the prime stock-separating mechanism. Marine Ecology Progress Series, 345: 1–12.

Umlauf, L., and Burchard, H. 2003. A generic length-scale equation for geophysical turbulence models. Journal of Marine Research, 61: 235–265.

Vikebø, F., Sundby, S., Ådlandsvik, B., and Fiksen, Ø. 2005. The combined effect of transport and temperature on distribution and growth of larvae and pelagic juveniles of Arcto-Norwegian cod. ICES Journal of Marine Science, 62: 1375–1386.

Vikebø, F. B., Husebø, Å., Slotte, A., Stenevik, E. K., and Lien, V. S. 2010. Effect of hatching date, vertical distribution, and interannual variation in physical forcing on northward displacement and temperature conditions of Norwegian spring-spawning herring larvae. ICES Journal of Marine Science, 67: 1948–1956.

Wassmann, P., Svendsen, H., Keck, A., and Reigstad, M. 1996. Selected aspects of the physical oceanography and particle fluxes in fjords of northern Norway. Journal of Marine Systems, 8: 53–71.

Handling editor: Claire Paris

ICES Journal of Marine Science

ICES Journal of Marine Science (2014), 71(4), 970–981. doi:10.1093/icesjms/fst131

Contribution to the Themed Section: 'Larval Fish Conference'

Original Article

Spatio-temporal overlap of oil spills and early life stages of fish

Frode B. Vikebø[1]*, Petter Rønningen[2], Vidar S. Lien[1], Sonnich Meier[1], Mark Reed[2], Bjørn Ådlandsvik[1], and Trond Kristiansen[1]

[1]*Institute of Marine Research, Box 1870 Nordnes, N-5817, Bergen, Norway*
[2]*SINTEF, Strindvegen 4, 7465 Trondheim, Norway*

**Corresponding Author: e-mail: frovik@imr.no*

Vikebø, F. B., Rønningen, P., Lien, V. S., Meier, S., Reed, M., Ådlandsvik, B., and Kristiansen, T. 2014. Spatio-temporal overlap of oil spills and early life stages of fish. – ICES Journal of Marine Science, 71: 970–981.

Received 21 December 2012; accepted 4 July 2013; advance access publication 14 October 2013.

Coupling an oil drift and fates model (Oscar) in an offline environment with an individual-based model (IBM) for Northeast Arctic cod (*Gadus morhua*) eggs and larvae enables us to quantify the exposure of eggs and larvae to oil from various oil spill scenarios. Oscar describes the spatio-temporal dispersal and fate of hydrocarbons, whereas the egg and larval IBM integrates the exposure of each individual. We can thus evaluate the effects of the time and location of an oil spill on the degree of exposure for individuals from different spawning grounds (SGs). In addition, we quantify how this effect is modified by the dynamic vertical positioning of eggs and the vertical behaviour of larvae. The principal findings of the study indicate that the mean egg and larval exposures for individuals from different SGs are highly dependent on the time and location of the spill and the vertical distribution of the offspring. Approximately 9.9, 4.7, 3.5, and 0.4% of the offspring would experience total polycyclic aromatic hydrocarbon (TPAH) concentrations above 1 $\mu g\ l^{-1}$ (parts per billion, ppb) for oil spill scenarios situated at Haltenbanken, Lofoten, and Vesterålen near the coast and near the shelf edge, respectively, based on the maximum TPAH concentrations in the water column along the individual offspring trajectories.

Keywords: exposure, ichthyoplankton, individual-based model, Lofoten, Northeast Arctic cod, oil-drift model, Oscar, polycyclic aromatic hydrocarbons, toxicity.

Introduction

The Lofoten–Barents Sea is the habitat for several commercially important fish stocks, such as the Northeast Arctic (NEA) cod (Olsen *et al.*, 2010). NEA cod migrate from their winter feeding grounds in the Barents Sea (a shelf sea of ~1.4 million km^2, with an average depth of 230 m) to spawning grounds (SGs) distributed at the continental shelf along the Norwegian Coast from Møre to the Finnmark coast, with the principal SGs located in the Lofoten area. Spawning occurs from early March until late April, and the peak spawning date varies little among years (Sundby and Nakken, 2008). However, the spawning intensity at different SGs varies among years. It has been demonstrated that this variation is related to climate fluctuations (Sundby and Nakken, 2008) and spawning–migration capability through fisheries-induced changes in the age of maturation (Jørgensen *et al.*, 2008; Opdal, 2010). NEA cod eggs are pelagically distributed and exhibit a near-exponential decay in abundance with increasing depth (Sundby, 1991). The duration of the egg stage is ~3 weeks. Newly hatched larvae, distributed between ~5 and 40 m, depend on match with the zooplankton production, which is triggered by the spring bloom and delayed, on average, by ~37 d from Møre towards Lofoten (Vikebø *et al.*, 2012). Trade-offs between successful feeding and predator avoidance motivate vertical migration (Fiksen *et al.*, 2007), which affects horizontal dispersal (Vikebø *et al.*, 2007). After metamorphosis (the transition from larvae to juvenile fish), juvenile NEA cod gradually move deeper in the water column until bottom settlement begins during August and September (Sundby and Nakken, 2008).

A potential oil spill on the Norwegian continental shelf may affect the pelagic stages of NEA cod and thereby affect recruitment to the stock. However, the degree of this effect has proven difficult to quantify. Among the uncertainties are (i) the spatio-temporal variability

in natural mortality, affecting the contribution of offspring from different areas to the recruitment (Hjermann *et al.*, 2007); (ii) the effect of specific oil concentrations on the growth, survival, and motility of different stages and sizes of young fish; and (iii) the long-term effect of exposure to non-lethal oil concentrations. Ongoing research activities are attempting to address these issues, with an overall goal of assessing the impact of different oil spill scenarios on fish recruitment for optimal planning of joint activities in fisheries and the petroleum industry. However, there is a need to combine numerical models representing the different parts of this process with existing relevant observational data from field and laboratory studies.

Documentation from both laboratory studies and field observations after the Exxon Valdez oil spill furnished good evidence that the embryonic and larval stages of fish are particularly sensitive to oil exposure, especially to polycyclic aromatic hydrocarbons (PAHs; Carls and Meador, 2009). In weathered oils, the toxicity is primarily explained by the concentration of PAHs, but there are also significant contributions of unknown and more polar compounds (Neff *et al.*, 2000). Although PAHs do not explain the total toxicity, the measurement of total PAH (TPAH) nonetheless appears to be the best estimate to predict the toxicity of an oil spill to the early life stages of marine fish (Barron *et al.*, 2004; Wu *et al.*, 2012). Several studies of relevant marine cold-water species document that oil exposure induces increased mortality in fish embryos/larvae even at very low water concentrations of PAHs. Atlantic herring larvae (*Clupea harengus*) exhibited a clearly increased mortality after 12 d of exposure to 6 $\mu g\,l^{-1}$ (parts per billion, ppb) TPAH (Ingvarsdottir *et al.*, 2012); larvae of NEA cod had increased mortality after 4 d of exposure to 38 $\mu g\,l^{-1}$ TPAH (Nordtug *et al.*, 2011) and 90 d of 1.8 $\mu g\,l^{-1}$ TPAH (Meier *et al.*, 2010); and in capelin (*Mallotus villosus*), 40 $\mu g\,l^{-1}$ TPAH increased the mortality after 32 d of exposure at the embryo stages (Frantzen *et al.*, 2012). Sublethal effects, including morphological deformation and reduced feeding rates, were found in several studies at even lower concentrations (0.13–2 $\mu g\,l^{-1}$ TPAH) (Carls *et al.*, 1999; Heintz *et al.*, 1999; Nordtug *et al.*, 2011; Ingvarsdottir *et al.*, 2012). The concentration and composition of PAHs that are released after an oil spill are highly dependent on the oil type and also vary over time during the weathering of the oil. However, crude oil normally contains between 0.1 and 5% TPAH (Neff *et al.*, 2000), and this content also agrees with the fact that the acute toxicity on fish embryos/larvae measured as total hydrocarbons is $\sim$1–2 $mg\,l^{-1}$ (parts per million, ppm; Solberg *et al.*, 1982; Paine *et al.*, 1992).

In this study, we address part of the overall goal of describing the effect of an oil spill on fish recruitment by quantifying the spatio-temporal exposure of individual NEA cod eggs and larvae to TPAH from a set of specific oil spill scenarios located along the Norwegian continental shelf. The main objectives are to quantify the potential overlap between NEA cod offspring and TPAH and how it varies with (i) the spatial location of the oil spill, (ii) the timing of the oil spill relative to the time of spawning, and (iii) larval vertical behaviour. Furthermore, we discuss the results in the context of the documented effects of various durations and concentrations of exposure on the early stages of fish.

Methods and material

Evaluation of all future potential release sites, times of the year, durations, and rates is impossible; therefore, we selected four scenarios that represent contrasting areas of the Norwegian shelf with respect to ocean dynamics: the wide shelf at Haltenbanken

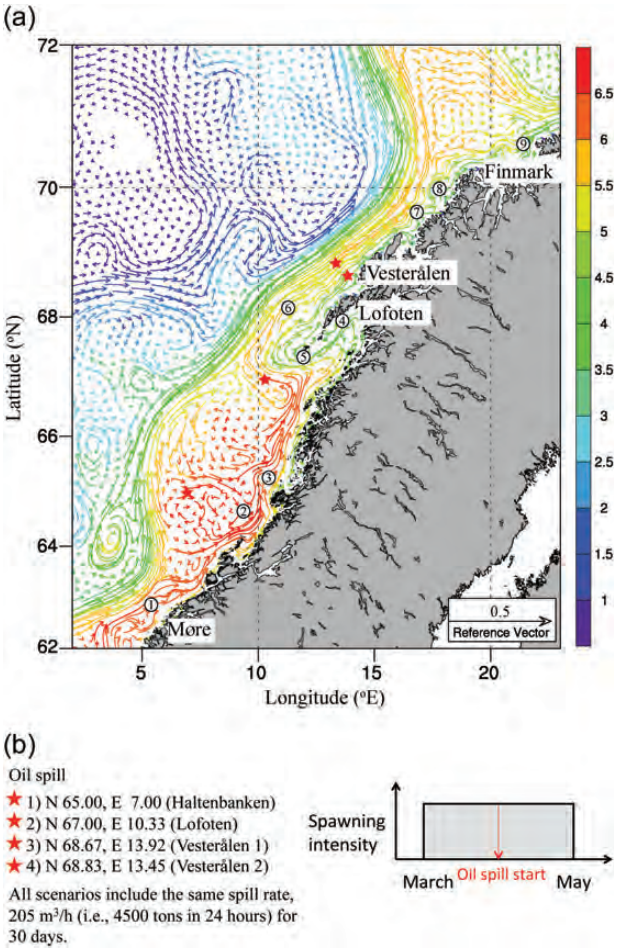

Figure 1. (a) SGs (1–9) and potential oil spill locations (red stars). The map shows the monthly mean circulation at 20-m depth for April during 1989–2008, and the colours indicate temperatures. (b) Oil spill rates and durations (left) and the spawning duration of NEA cod (right) (idealized; in reality, the shape of the relational data is Gaussian).

(65.00°N 7.00°E), Røst south of Lofoten (67.00°N 10.33°E), and two sites at the narrow shelf off Vesterålen (68.67°N 13.92°E and 68.83°N 13.45°E; Figure 1). The beginning of the spill is set to 1 April, with a rate of 4500 $m^3\,d^{-1}$ and a duration of 30 d yielding a total spill of 135 000 m^3 (Statfjord light crude). In contrast, the deep-water horizon spill produced a total of 780 000 m^3 over a period of 86 d. Together, the four scenarios represent a wide span of overlap studies that may aid in our search for answers addressing the main objectives listed above.

In accordance with the winter North Atlantic Oscillation (NAO; December–February) and spring NAO (March–April), we have chosen an average climatic year with respect to the NAO and, correspondingly, the large-scale atmospheric forcing in the region where the early stages of NEA cod appear in the pelagic zone. The NAO is the first mode of the North Atlantic sea level pressure variability (Hurrell, 1995) and is defined to be the normalized sea level pressure difference between the Azorean high and the Icelandic low. A strong and positive NAO implies a strong control of storm tracks across the North Atlantic (Bader *et al.*, 2011). Persistent southwesterly winds in the North Atlantic result in a strengthened Norwegian Coastal Current (NCC; Skagseth *et al.*, 2011). The winter and spring NAO values for 1997 were 0.18 and −0.08, respectively.

As a first approach, we assume that the eggs and larvae are exposed to the maximum concentration of oil in the water column along their individual trajectories. This pattern defines the maximum potential exposure for individuals from the different SGs given the oil spill scenarios specified here but will certainly represent an overestimate of exposure because both eggs and larvae are, at times, distributed deeper than the maximum concentration of spilled oil. Second, we incorporate the modelled hourly vertical distribution of the individual ichthyoplankton and recalculate overlap estimates with the actual concentration of TPAH at the egg and larval depths. Larvae typically perform diel migrations and spend part of the night closer to the surface than during the daytime. Hence, larvae may migrate vertically through a gradient of TPAHs. Overall, this method enables a quantification of the sensitivity of the exposure to the vertical distribution of ichthyoplankton.

Ocean model

The ocean-model archive is produced with the Regional Ocean Modelling System (ROMS; Haidvogel *et al.*, 2008; www.myroms.org). Daily mean currents, temperatures, and salinities in three-dimensions are stored on a local disk for use in the offline oil-drift model Oscar and in the individual-based egg and larvae model. The archive covers the period 1989–2008 and includes 30 vertical topography-following *s*-coordinate layers with a horizontal resolution of 4 by 4 km. The incorporated boundary forcing includes river influx, monthly mean three-dimensional currents, temperatures, and salinities with a spatial horizontal resolution of 20 by 20 km on the lateral boundaries and 6-hourly ERA Interim (Uppala *et al.*, 2008) windstress, precipitation, humidity, air temperature, and longwave and shortwave radiation in the vertical dimension. Eight tidal constituents are included in the lateral boundary forcing. Details of the model setup and performance are reported by Vikebø *et al.* (2010) and Lien *et al.* (2013), indicating that the main circulation features in the habitat of NEA cod are captured.

Oil-drift model Oscar

The SINTEF OSCAR (Oil Spill Contingency And Response) model is a three-dimensional model system that calculates and records the fates and effects of oil contaminants in the marine environment. The fates of contaminants are tracked as the mass and concentrations in four different compartments: the water surface, shorelines, in the water column, and in sediments.

For subsurface releases (e.g. blowouts or pipeline leakages), the nearfield part of the simulation is computed with a multiphase integral plume model (Johansen, 2000, 2003). The nearfield model incorporates the buoyancy effects of oil and gas, hydrocarbon dissolution, hydrate formation, and gas expansion as well as the effects of ambient stratification and cross flow on the dilution and rise time of the plume.

Surface releases and far-field behaviour are computed using a pseudo-Lagrangian model in which each element of the released contaminants is tracked through a flowfield, incorporating buoyancy and sinking due to density differences.

The model computes surface spreading, slick transport, entrainment into the water column, evaporation, emulsification, and shoreline interactions to determine the oil drift and fate at the surface. Weathering processes are computed using data from standardized laboratory weathering procedures. In the water column, the horizontal and vertical transport by currents, dissolution, adsorption, settling, and degradation are simulated. The varying solubility, volatility, and aquatic toxicity of oil components are incorporated by representing the oil in terms of 25 pseudo-components (Reed *et al.*, 2000), but only the four pseudo-component groups representing TPAH were included for this study: naphtalenes (C0-C1-alkylated), naphtalenes (C2-C3-alkylated), PAH 1 (3 rings, non-alkylated), and PAH 2 (3 rings-alkylated, 4–5+ rings). Changes in the oil composition due to evaporation, dissolution, and degradation are represented in each of the 25 pseudo-components.

The outputs of these surface blowouts are recorded as three-dimensional grids of TPAH concentrations for the water column compartment (see example in Figure 2) and as two-dimensional grids for the water-surface, sediment, and shoreline compartments.

Individual-based egg and larval model

The dispersal of NEA cod spawning products is simulated with a Lagrangian particle-tracking model including a module resolving the dynamic vertical positioning of eggs according to density differences with the surrounding water masses and spatio-temporally varying turbulence (Thygesen and Ådlandsvik, 2007). Additionally, temperature-dependent larval growth, according to Folkvord (2005), and diel vertical larval migration are included in this module (see

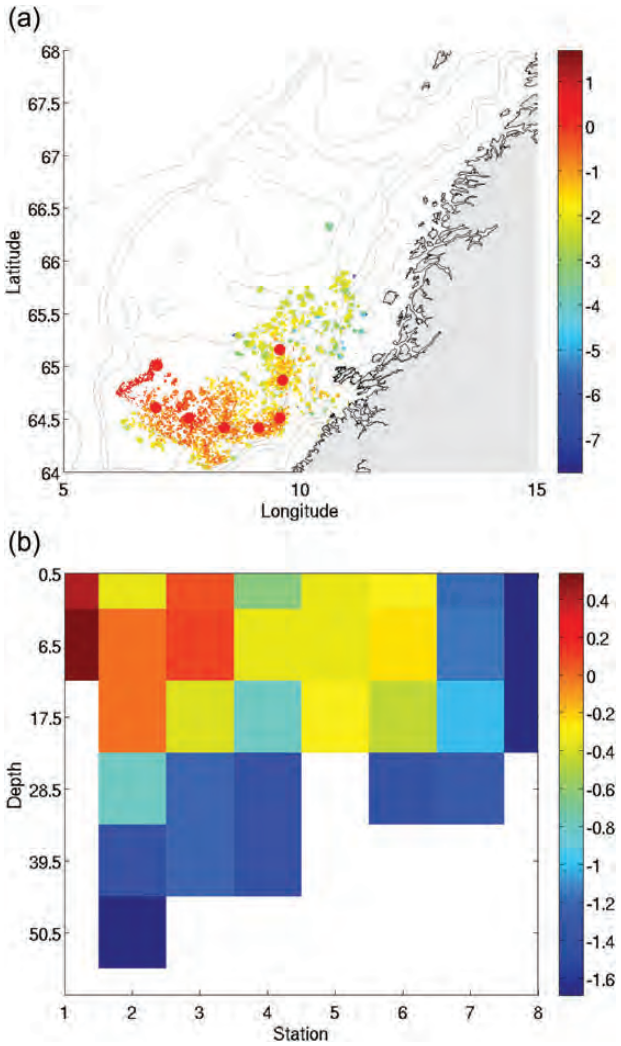

Figure 2. (a) TPAH in the top layer (0–1 m) at day 30 for the oil spill scenario with the spill location at Haltenbanken (log_{10}, ppb). (b) The red dots indicate the stations where the vertical distribution of oil was extracted for an illustrative view (log_{10}, ppb).

Opdal *et al.*, 2011 for details). The egg-stage duration is set to 21 d. For up-scaling to realistic temporal and spatial spawning intensities, the contributions from the selected SGs 1–9 are based on Sundby *et al.* (1989) and Vikebø *et al.* (2011) as follows: 5, 5, 5, 20, 10, 20, 15, 10, and 10% for SGs 1 through 9, respectively.

Coupling of oil- and ichthyoplankton-drift models

Oscar operates on a grid different from that of the individual-based model (IBM) for eggs and larvae but is forced with the same hydrodynamics. In all, 20 000 particles represent oil dispersal at the surface on a fixed grid of 400 by 400 m horizontal resolution and 10 vertical layers with mid-centre points at 0.5, 6.5, 17.5, 28.5, 39.5, 50.5, 61.5, 72.5, 83.5, and 94.5 m. The overlap estimates are therefore quantified by translating the Oscar spatial coordinates to the egg and larval coordinate system and thereafter using these coordinates to sample the TPAH concentration at the individual egg or larvae positions at a daily time-step. In all, 94 500 particles are distributed equally among the nine SGs and released every 3rd day between 1 March and 30 April, a total of 500 particles each day per SG.

Results

TPAH exposure as a function of the date, oil spill scenario, and SG

Figure 3a shows the mean temporal overlap from 1 April to 1 June for 10 500 individual offspring from each of the nine different SGs in terms of the maximum TPAH concentration (ppb) in the water column along the individual offspring trajectories as a result of an oil spill at Haltenbanken. The offspring from SG2 are, on average, exposed to much higher TPAH concentrations than those of the other eight SGs. The elevated levels last for more than 20 d and peak at 0.116 ppb in early May. The exposures of the individuals from SG1 and SG3 peak, on average, at 0.005 and 0.009 ppb, whereas the exposures of the individuals from SG4–SG9 remain, on average, well below this exposure level.

Consideration of only the 10 or 50% of individuals that are most severely exposed (the composition varies with time) results in elevated mean ambient TPAH concentrations (Figure 3b). The pattern is similar to the result for all the individuals concerning duration and relative exposure among the SGs. The 10% (or 50%) most exposed individuals from SG2 at any given time experience, on

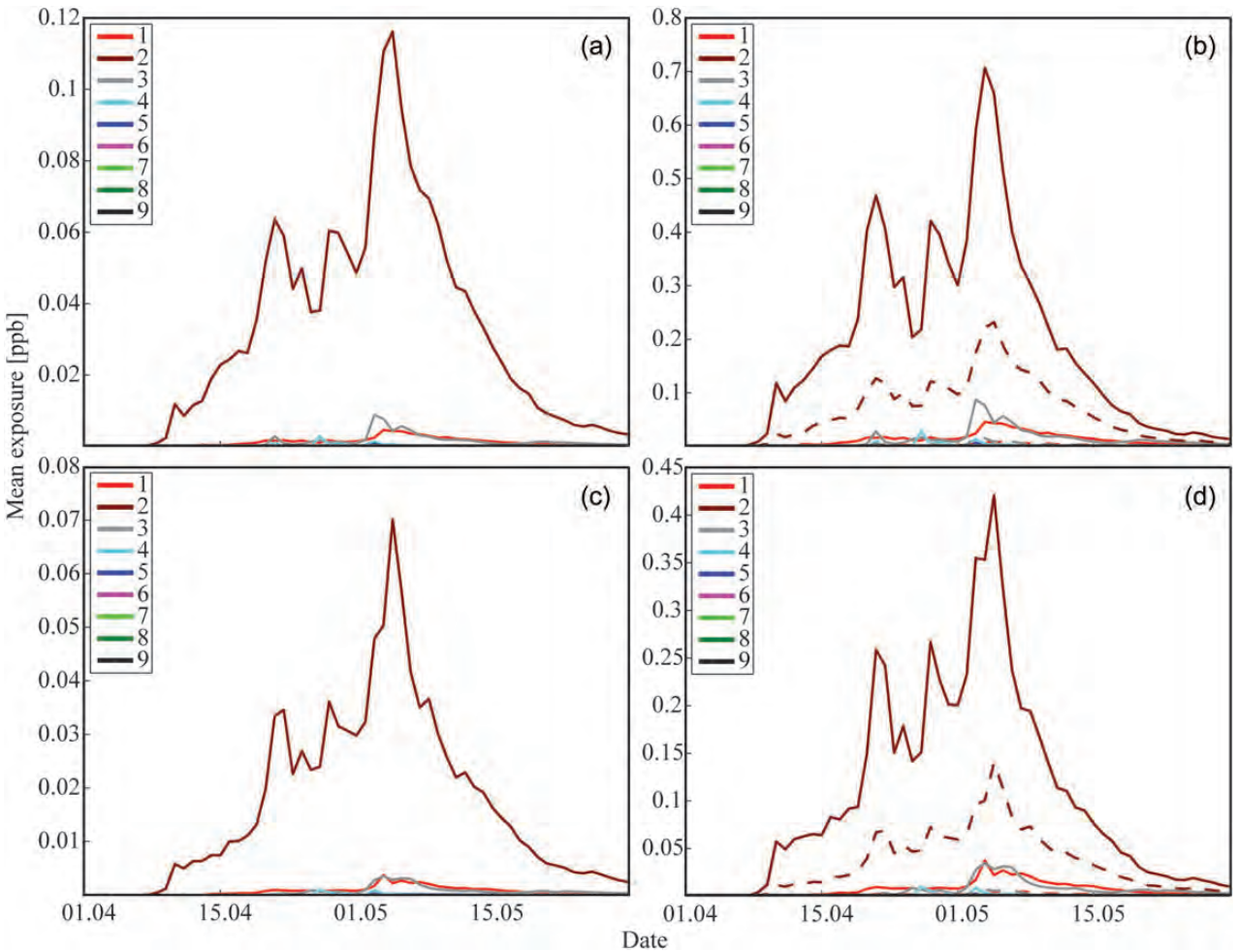

Figure 3. (a) Mean overlap between individual offspring and maximum concentrations of TPAH (ppb) in the water column corresponding to the horizontal position of the offspring per SG as a function of time for the oil spill scenario at Haltenbanken. (b) Similar to (a) but calculated for the 10% (solid line) and 50% (broken line) of the offspring experiencing the highest exposure values. (c) Similar to (a) but calculated for the TPAH at the horizontal and vertical position of the offspring. (d) Similar to (c) but calculated for the 10% (solid line) and 50% (broken line) of the offspring exposed to the highest concentrations of TPAH.

average, peak TPAH concentrations of 0.707 (or 0.232) ppb in early May. The exposure of individuals from SG1 and SG3 peaks at 0.046 and 0.087 ppb, respectively, during early May.

If, instead, the TPAH concentrations at the hourly depths of the individual offspring along their respective trajectories are considered, the mean ambient exposures are markedly reduced (Figure 3c). The mean ambient exposure for SG2 then peaks at 0.070 ppb. The exposure of individuals from all the other SGs stays well below this level. Based only on the 10% (or 50%) most exposed individuals from SG2, the individual exposure peaks at 0.421 (or 0.140) ppb, on average, during early May (Figure 3d).

If an oil spill occurs at Lofoten, the offspring from SG1–SG5 are affected most severely (Figure 4a). The average TPAH exposure for offspring from SG3, based on the maximum oil concentrations in the water column along the individual offspring trajectories, peaks at 0.181 ppb less than 2 weeks after the spill starts. Individuals from SG1, SG2, SG4, and SG5 peak later than individuals from SG3 at less than half the maximum level. Almost identical features can be seen if only the 10% (or 50%) most exposed individuals are considered, although the exposure levels are almost an order of magnitude higher. The exposure of offspring from SG3 peaks at 1.792 ppb, whereas the values at SG1, SG2, SG4, and SG5 peak at 0.868, 0.823, 0.335, and 0.174 ppb, respectively. The exposures of individuals from all the other SGs remain below 0.1 ppb (Figure 4b). A clear decrease in mean ambient exposure is evident from the analysis of oil concentrations at the same hourly depth levels as the offspring (Figure 4c). The results for the 10% of the individuals with the highest exposure when accounting for the oil concentrations at the hourly depth of the offspring are similar to the result obtained by averaging over all individuals when accounting for the maximum oil concentrations, although the exposure values are approximately an order of a magnitude higher. In this case, offspring from SG1–SG3 all experience TPAH concentrations well above 0.1 ppb on average (Figure 4d).

Although the two northernmost oil spill locations are at approximately the same latitude and are near each other (either towards the coast or the shelf edge), they result in different TPAH exposures for individual offspring from the SGs addressed here (Figures 5a–d and 6a–d). The highest average exposure rates, when considering TPAH concentrations at the hourly depths of the larvae, occur as a result of oil spill scenario 4, although the order of magnitude is the same as that for the other oil spill scenarios. Considering the average TPAH concentrations at the hourly depths of the 10% most exposed individuals show

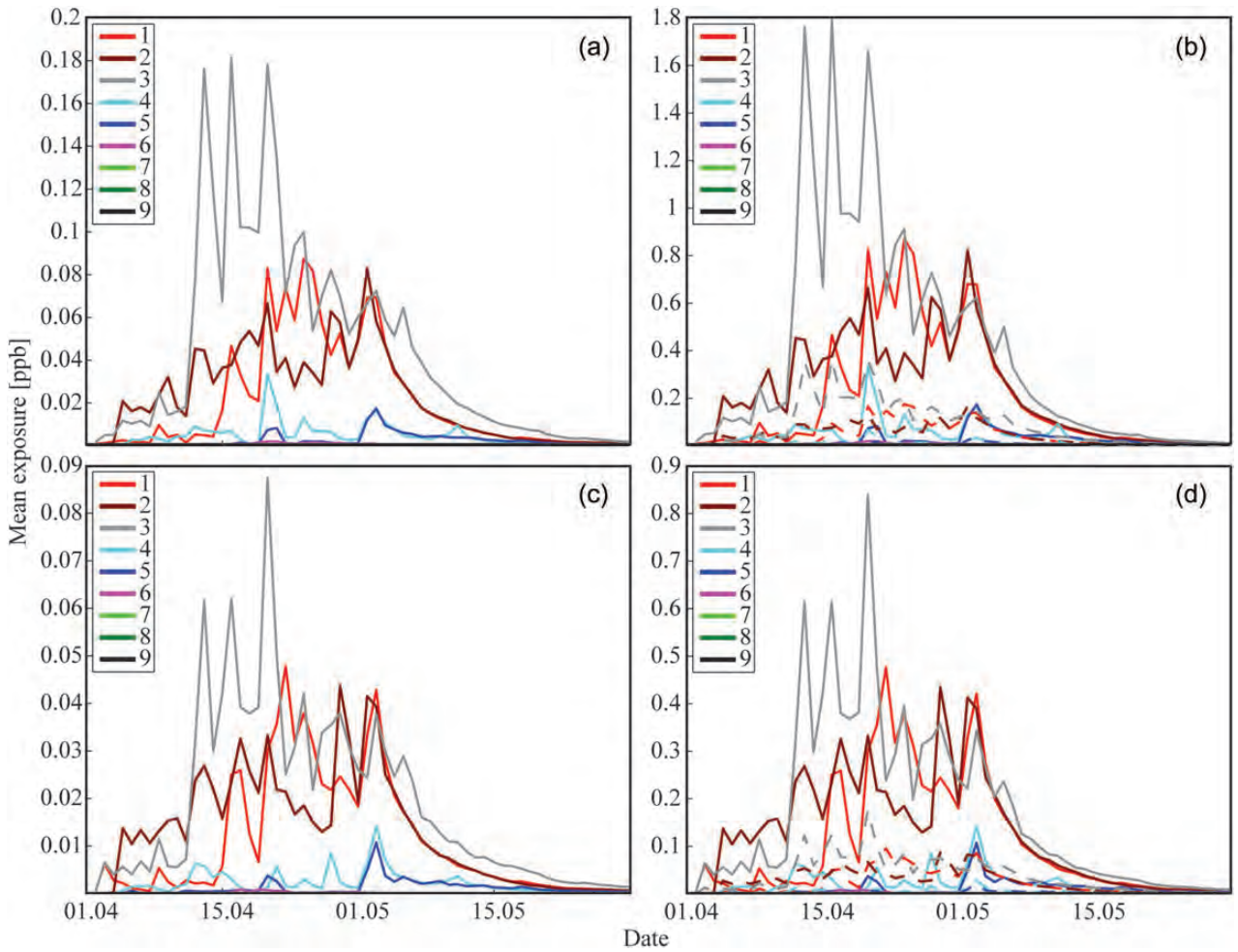

Figure 4. (a) Mean overlap between individual offspring and maximum concentrations of TPAH (ppb) in the water column corresponding to the horizontal position of the offspring per SG as a function of time for the oil spill scenario at Lofoten. (b) Similar to (a) but calculated for the 10% (solid line) and 50% (broken line) of the offspring experiencing the highest exposure values. (c) Similar to (a) but calculated for the TPAH at the horizontal and vertical position of the offspring. (d) Similar to (c) but calculated for the 10% (solid line) and 50% (broken line) of the offspring exposed to the highest concentrations of TPAH.

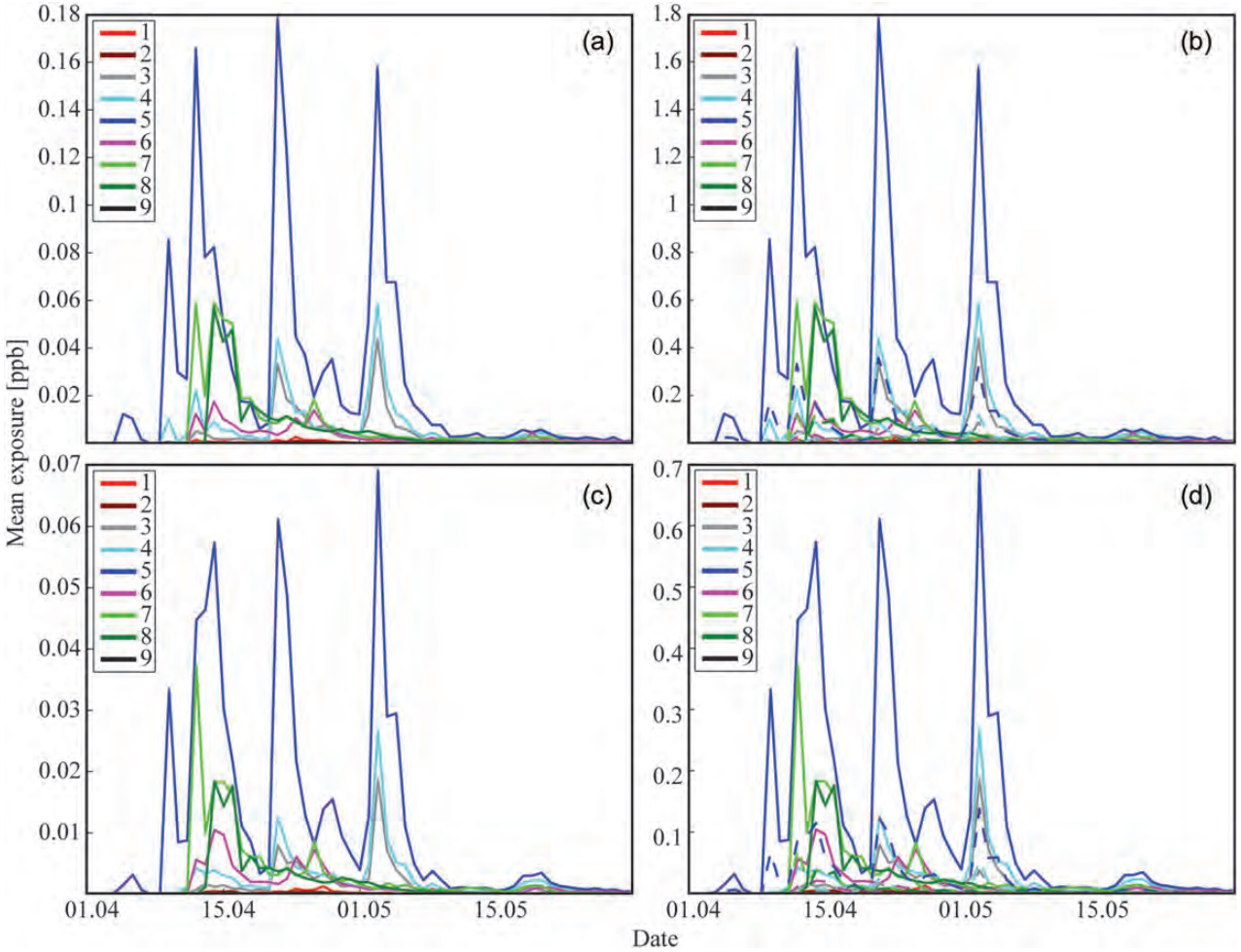

Figure 5. (a) Mean overlap between individual offspring and maximum concentrations of TPAH (ppb) in the water column corresponding to the horizontal position of the offspring per SG as a function of time for the oil spill scenario near the coast at Vesterålen. (b) Similar to (a) but calculated for the 10% (solid line) and 50% (broken line) of the offspring experiencing the highest exposure values. (c) Similar to (a) but calculated for the TPAH at the horizontal and vertical position of the offspring. (d) Similar to (c) but calculated for the 10% (solid line) and 50% (broken line) of the offspring exposed to the highest concentrations of TPAH.

that only offspring from SG1–SG4 experience TPAH concentrations above 0.1 ppb for an oil spill at Lofoten, this is the case for SG3–SG8 and for SG1 and SG3–SG7 for oil spill scenarios 3 and 4, respectively.

Integrated exposure

Although peak oil exposure is essential to evaluate acute toxicity, the integrated exposure over time may be critical for evaluating sub-lethal effects. Figure 7 displays the mean integrated exposure (ppb) over 60 d as a function of the oil spill scenario (*x*-axis) and SG (1–9, different colours), based on the maximum TPAH concentration in the water column along the offspring drift trajectories (Figure 7a) and the actual TPAH concentration at the individual hourly depth at which the offspring occur (Figure 7b). The highest integrated mean exposure is experienced by the offspring from SG3 during an oil spill at Lofoten. This pattern is also the case for TPAH concentrations at the hourly depth of the individuals. As the location of the oil spill scenario moves north, the integrated exposure level increases for individuals from the northern SGs and decreases for the southern SGs. However, although a southern oil spill scenario results in negligible exposure of the offspring from northern SGs, this pattern is not the case for oil spill locations located to the north where both northern and southern SGs become exposed.

Impact of the spawning time and time of oil spill

Figure 8a–d shows the mean integrated exposure of individual offspring based on the maximum TPAH concentration (ppb) in the water column following a spill at Haltenbanken, Lofoten, and at Vesterålen near the shore and near the shelf edge as a function of the time of spawning (*x*-axis) and SG (*y*-axis). Because the analysis of the oil concentrations at the hourly depth of the larvae results in similar features but consistently lower values, these levels are not shown here. There are substantial differences in exposure levels with varying spawning dates for most combinations of oil spill scenario, spawning date, and location. Clearly, southern SGs upstream from the spill site result in higher levels of exposure for the early spawned offspring relative to the late-spawned offspring. SGs in the proximity of the spill site experience similar exposures across the different spawning times, and northern SGs downstream from the spill site result in higher levels of exposure for the late-spawned offspring. In certain

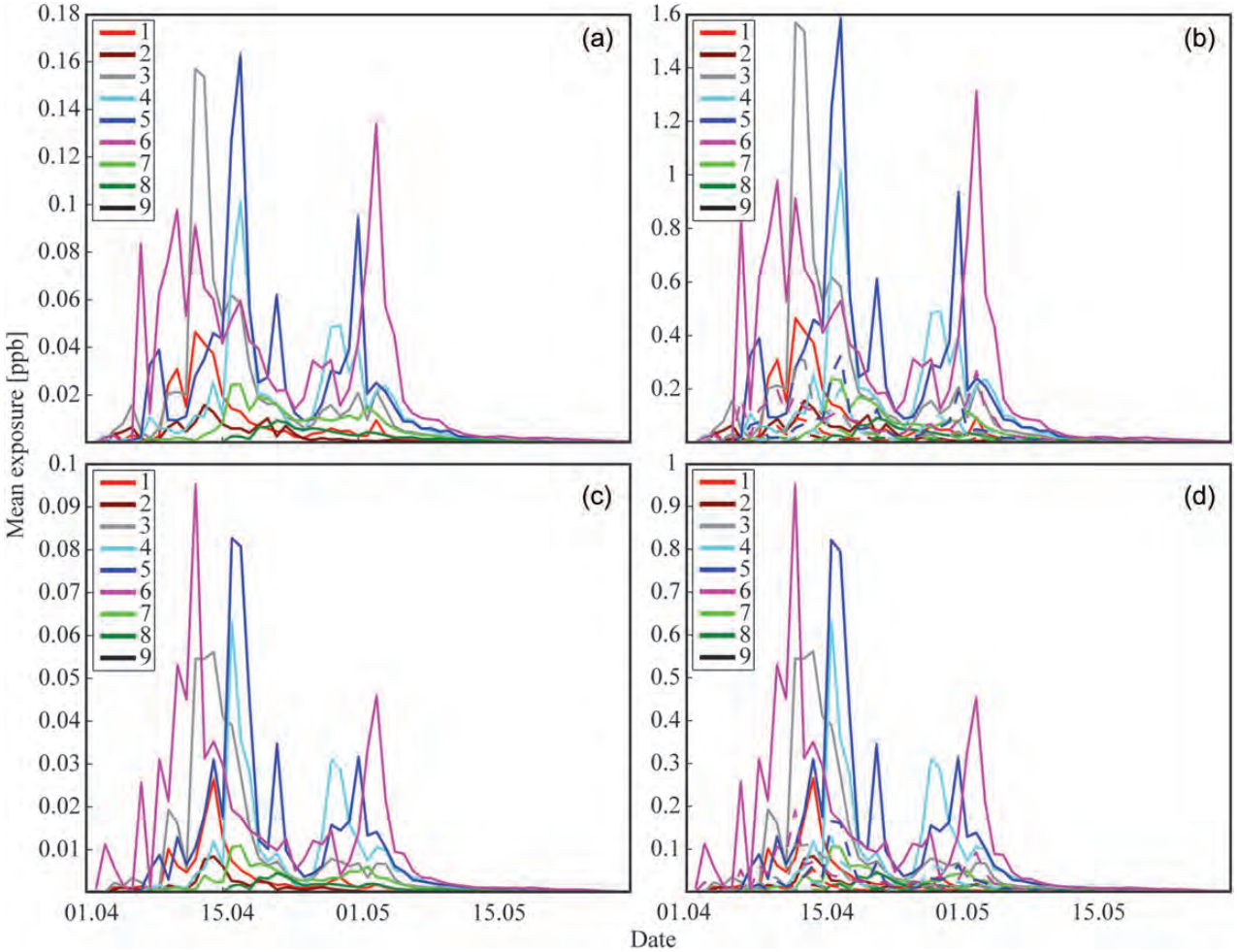

Figure 6. (a) Mean overlap between individual offspring and maximum concentrations of TPAH (ppb) in the water column corresponding to the horizontal position of the offspring per SG as a function of time for the oil spill scenario near the shelf edge at Vesterålen. (b) Similar to (a) but calculated for the 10% (solid line) and 50% (broken line) of the offspring experiencing the highest exposure values. (c) Similar to (a) but calculated for the TPAH at the horizontal and vertical position of the offspring. (d) Similar to (c) but calculated for the 10% (solid line) and 50% (broken line) of the offspring exposed to the highest concentrations of TPAH.

cases, there are no exposure at all, e.g. late-spawned offspring at SG1–SG4 during the oil spill scenarios in Vesterålen.

Fraction of the offspring exposed to oil concentrations above threshold values

As described earlier in the paper, there are different thresholds for different effects (acute compared with sublethal effects). Also, it is to be expected that early larval stages, as the ones studied here, are more sensitive to contamination than older larvae. Acute toxicity in relevant species has been found at TPAH concentrations ~1 ppb, whereas TPAH concentrations ~0.1 ppb are related to sublethal effects. For this reason, we quantified the fraction of offspring from the different SGs that experienced TPAH levels above 1.0 or 0.1 ppb at least once during the first 60 d after the beginning of the oil spill. Tables 1 and 2 provide the fractions of offspring that are exposed to above 1 ppb once during the oil spill scenarios. Tables 3 and 4 are corresponding analyses but apply to values of 0.1 ppb. Offspring originating in SG3–6 during oil spill scenario 4 along with offspring from SG5 during oil spill scenario 3 and SG1 and SG3 during oil spill 2 all result in overlap with values greater than 1.0 ppb that are 1 s.d. (5.79) above the mean (4.06) for all the SGs and scenarios relative to the maximum TPAH concentrations in the water column. Based on the TPAH concentrations at the hourly larval depths, the SG and oil spill scenario-specific mean overlaps with values greater than 1.0 ppb that are 1 s.d. (3.86) above the mean (2.44) result from a combination of offspring from SG3–SG6 during oil spill scenario 4, SG5 during oil spill scenario 3, and SG1–SG3 during oil spill scenario 2. Similar combinations of SG and oil spill scenario are elevated compared with the others for a threshold of 0.1 ppb instead of 1.0 ppb, although the percentage of overlap is much higher overall. For example, the number of individuals from SG2 during oil spill 1 that overlap with a minimum of 1 ppb once during the 60 d is 6.22% for the maximum TPAH in the water column, but increases to 58.05% if the TPAH concentration threshold is 0.1 ppb.

Treating particles as super-individuals, i.e. representing more than one individual offspring, enables the results to be scaled upwards to a realistic temporal and spatial spawning intensity. Before averaging the estimates of the fraction of offspring exposed to above-threshold

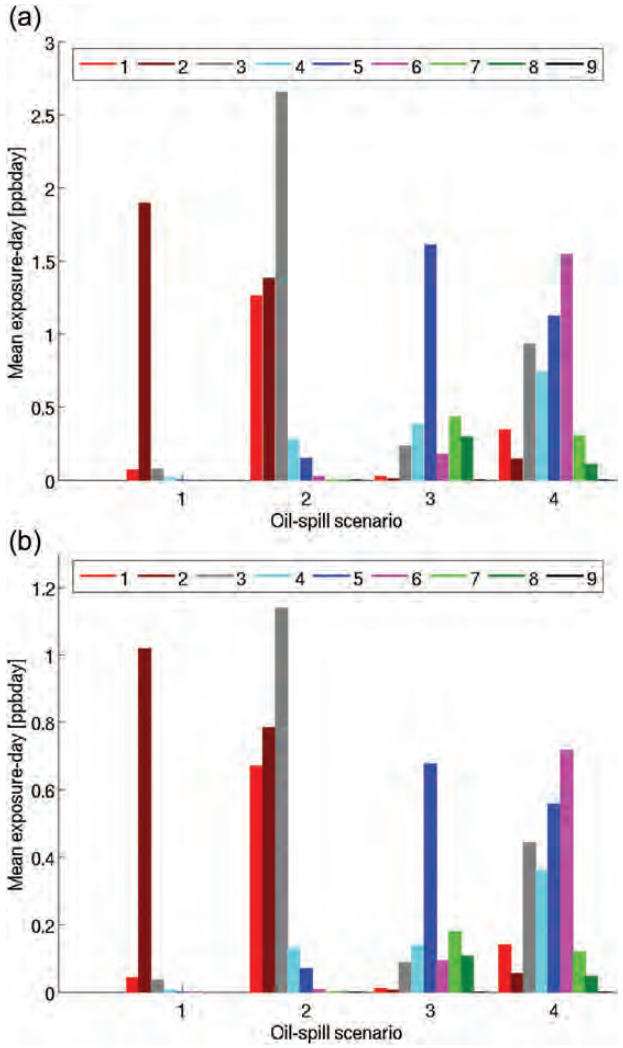

Figure 7. Mean integrated exposure (ppb) over 60 d as a function of the SG (1–7) and oil spill scenario (1–4) based on (a) the maximum TPAH concentration in the water column and (b) the TPAH concentration at the depth of the individual offspring.

values of TPAH concentrations, we included seasonal variation in spawning by scaling (i) with a Gaussian curve with the mean at 1 April and a standard deviation of 15 d and (ii) by the weights specified previously in this paper. The total fractions of offspring experiencing TPAH concentrations above 1.0 or 0.1 ppb at least once during the oil spill scenarios based on both the maximum TPAH in the water column and the TPAH at the hourly depth of the individuals are summarized in Table 5. Interestingly, the exposures based on the maximum TPAH concentrations in the water column as opposed to the concentrations at the larval hourly depths, result in a greater decrease in the exposure in strong advective areas, e.g. northern compared with southern oils spill scenarios.

Discussion

Summary of the principal results

A model system allowing an assessment of the effects of various oil spill scenarios on the early stages of fish is useful for both a pre-evaluation of risk in selecting locations for future petroleum activity, determining where and when to allow the use of dispersants, and post-evaluation of the effect of accidents whenever oil and dispersants enter the ocean. This risk could be related to exploratory drilling, normal production, or an oil tanker casualty. It is therefore crucial to develop generic model systems enabling the risk evaluation of potential and existing sites for petroleum activities with respect to fisheries resources.

In this study, we use the daily mean ocean circulation, hydrography, and turbulence from a three-dimensional ocean model to simulate the dispersal and fate of oil from four different spill scenarios and the corresponding exposure of spawning products from well-known spawning sites of NEA cod. The principal results show that the mean egg and larval exposures for individuals from different SGs are highly dependent on the time and location of the spill and the vertical distribution of the offspring. Oil spill scenarios 2–4 generally create higher levels of exposure than oil spill scenario 1, except for individuals from SG2. Oil spill scenario 2 generally indicates a prolonged duration of exposure, although this increase is partly compensated by repeated peak exposures for oil spill scenarios 3 and 4. As the latitude of the oil spill scenario increases, the integrated exposures tend to decrease slightly, but the elevated levels of exposure include more SGs than those associated with oil spills farther south. If observations are used to weight the contribution from the different SGs and the individuals released during the spawning period from early March through April, an oil spill at the narrow shelf of the Vesterålen has a much greater impact on the offspring than a similar spill on the extensive shelf farther south. The narrow northern shelf is also particularly sensitive to the location of a spill across the shelf because the topographic steering of currents limits the cross-shelf dispersal of offspring and oil. From these results, it becomes obvious that a realistic dynamic vertical distribution of the offspring is essential to obtain realistic estimates of exposure, and the levels reported here represent best approximations and the upper limits.

Bottom topography affects circulation and is the principal reason that certain areas experience prolonged periods of high exposure and other areas undergo either low exposure or short-term peaks of high exposure. The oil spills at Haltenbanken and Lofoten are both good examples of the first category. Due to a semi-permanent eddy-like structure located on top of Haltenbanken (Sætre, 1999), both a part of the oil spill and, particularly, offspring from the nearby SG2 are retained and overlap. Pulses of water masses shed from the bank contain both oil and offspring. This pattern results in a prolonged overlap of a substantial part of the offspring and high concentrations of TPAH. In contrast, offspring from the upstream SG1 and downstream SGs are not entrained into this eddy-like structure. Instead, these offspring ride the core of the NCC northward, avoiding patches of water containing high concentrations of oil. As for the Haltenbanken release, a release at Lofoten implies a partial retention of the spill at and near the site due to complex circulation features. This area represents a meeting point for the NCC and the Norwegian Atlantic slope current. This hydrographic pattern results in a particularly dynamic ocean state, with a meandering flow and high degree of mixing across water masses of different characteristics. Immediately downstream from the potential spill site, the shelf narrows to ~10 km in width, concentrating everything advected in this direction. Oil dispersal at the narrow shelf off Vesterålen is particularly sensitive to the location across the shelf. Oil from spill sites near the shelf edge would be caught by the rapid, topographically locked current. Closer to the coast, the oil has a greater probability of reaching the shore and being deposited. This area

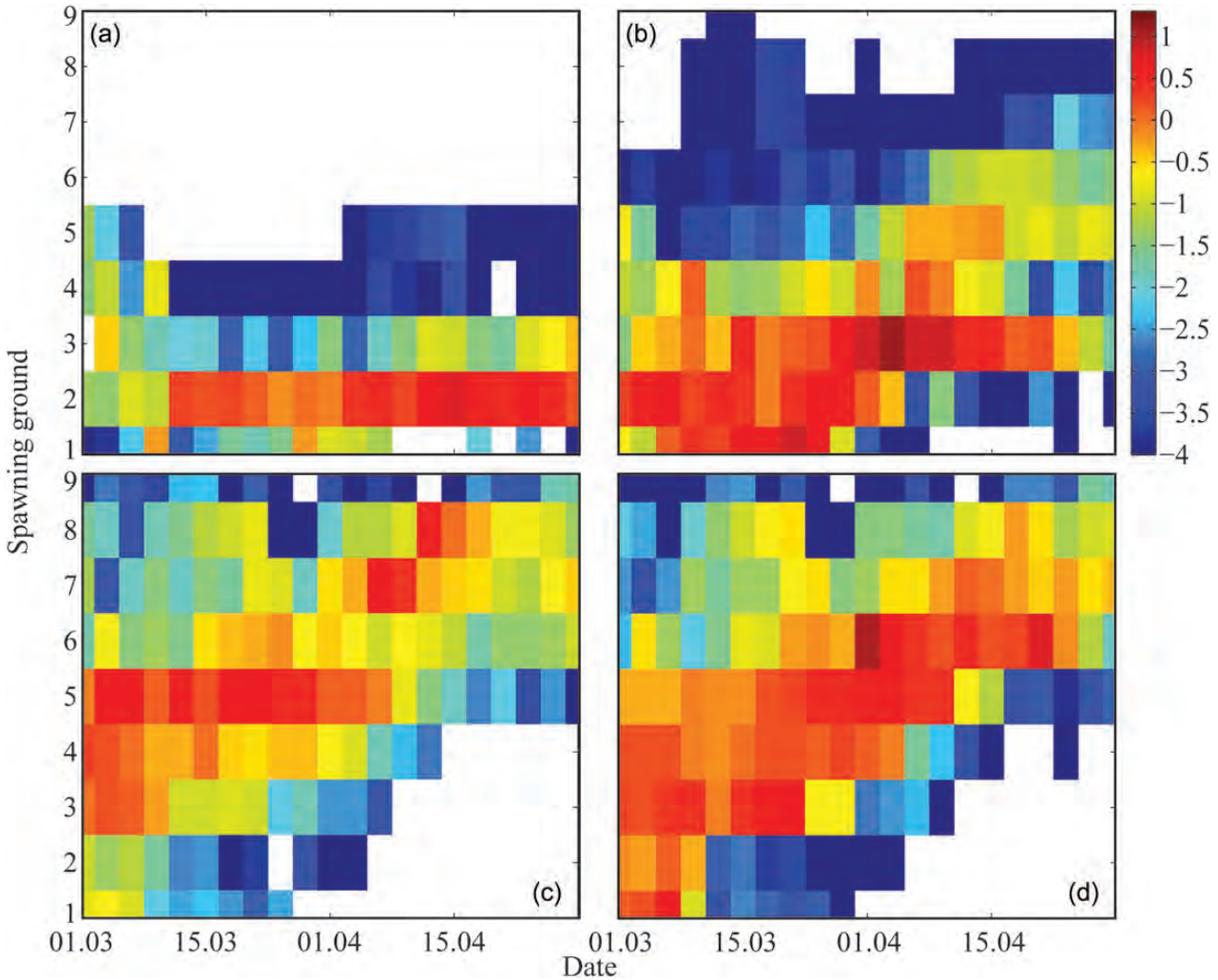

Figure 8. Mean integrated exposure (log_{10}, ppb) over 60 d as a function of the SG (*y*-axis) and spawning date (*x*-axis) for oil spill scenarios 1–4 (a–d) based on the maximum TPAH in the water column along the individual offspring trajectories. The blank areas indicate no overlap.

Table 1. Percentage overlap of the spawning products with TPAH concentrations above 1 ppb at least once during the first 60 d after the beginning of the oil spill, based on the maximum TPAH concentrations in the water column.

	SG1	SG2	SG3	SG4	SG5	SG6	SG7	SG8	SG9
Oil spill scenario 4	4.13	2.01	12.21	10.55	15.30	16.99	0.67	0.00	0.00
Oil spill scenario 3	0.25	0.10	2.40	3.74	14.62	2.04	6.50	3.07	0.00
Oil spill scenario 2	11.65	9.60	20.07	2.18	1.05	0.00	0.00	0.00	0.00
Oil spill scenario 1	0.44	6.22	0.21	0.06	0.02	0.00	0.00	0.00	0.00

The grey cells are values of 1 s.d. above the mean of all the values in the table.

Table 2. Percentage overlap of offspring with TPAH concentrations above 1 ppb at least once during the first 60 d after the beginning of the oil spill, based on the TPAH concentrations at the individual depth of the offspring.

	SG1	SG2	SG3	SG4	SG5	SG6	SG7	SG8	SG9
Oil spill scenario 4	2.36	0.92	7.47	6.47	10.20	12.08	0.11	0.00	0.00
Oil spill scenario 3	0.01	0.04	1.11	1.70	9.69	1.10	2.70	1.23	0.00
Oil spill scenario 2	8.08	6.84	12.60	1.22	0.65	0.00	0.00	0.00	0.00
Oil spill scenario 1	0.13	1.04	0.08	0.04	0.01	0.00	0.00	0.00	0.00

The grey cells are values of 1 s.d. above the mean of all the values in the table.

also represents a divergence zone for tracers distributed at different depths due to strong vertical gradients. However, several small banks immediately downstream from Vesterålen may retain and concentrate oil and cod offspring. In addition, Tromsøflaket, even farther downstream, is well known to concentrate cod offspring before they drift into the nursery grounds of the Barents Sea.

Table 3. Percentage overlap of the spawning products with TPAH concentrations above 0.1 ppb at least once during the first 60 d after the beginning of the oil spill, based on the maximum TPAH concentrations in the water column.

	SG1	SG2	SG3	SG4	SG5	SG6	SG7	SG8	SG9
Oil spill scenario 4	7.24	3.57	21.72	18.81	35.10	42.41	29.20	9.02	0.01
Oil spill scenario 3	2.35	1.14	7.60	12.33	31.62	18.29	21.69	17.74	0.07
Oil spill scenario 2	21.14	19.20	44.44	9.22	3.93	0.86	0.00	0.00	0.00
Oil spill scenario 1	3.70	58.05	5.39	0.18	0.11	0.00	0.00	0.00	0.00

The grey cells are values of 1 s.d. above the mean of all the values in the table.

Table 4. Percentage overlap of offspring with TPAH concentrations above 0.1 ppb at least once during the first 60 d after the beginning of the oil spill based on the TPAH concentrations at the individual depth of the offspring.

	SG1	SG2	SG3	SG4	SG5	SG6	SG7	SG8	SG9
Oil spill scenario 4	6.42	3.26	17.77	16.24	27.80	30.45	12.48	3.47	0.01
Oil spill scenario 3	1.27	0.55	4.95	7.87	24.91	9.98	14.38	8.39	0.00
Oil spill scenario 2	19.36	17.98	38.20	3.73	2.08	0.18	0.00	0.00	0.00
Oil spill scenario 1	2.66	51.70	2.65	0.13	0.08	0.00	0.00	0.00	0.00

Grey cells are values of 1 s.d. above the mean of all values in the table.

Table 5. Percentage overlap of offspring with TPAH concentrations above 1.0 or 0.1 ppb at least once during the first 60 d after the beginning of the oil spill, based on either the maximum TPAH concentrations in the water column (A) or the TPAH concentrations at the individual depths of the offspring (B).

	A, 1.0 ppb	B, 1.0 ppb	A, 0.1 ppb	B, 0.1 ppb
Oil spill scenario 4	9.90	6.93	27.16	18.68
Oil spill scenario 3	4.68	2.39	16.93	10.91
Oil spill scenario 2	3.51	2.22	8.10	6.01
Oil spill scenario 1	0.35	0.06	3.33	2.80

Note that the seasonal and spatial spawning intensity are incorporated in the analysis.

Limitations and sources of errors

We acknowledge that the vertical behaviour of larvae is still a source of uncertainty and is not yet fully understood. Several potential cues could motivate larval vertical behaviour, and the actual movement is a combination of these effects. Earlier attempts to assess this process show how feeding and predator avoidance represent a trade-off dependent on individual larval risk awareness, which may affect growth, survival probability, and drift trajectories (Fiksen *et al.*, 2007; Vikebø *et al.*, 2007; Kristiansen *et al.*, 2009, 2014). Likewise, this study demonstrates that egg and larval vertical distributions affect the organism's exposure to oil due to the different vertical distributions of egg/larvae and oil.

Another serious concern is that the presence of oil in the water column could also represent a cue for larval vertical behaviour. Larvae are visual feeders and depend on light to detect their prey. If oil is present in the water column, the availability of light for visual feeding decreases, and the larvae may respond by moving higher in the water column. To the authors' knowledge, this effect has not been studied in controlled experiments. However, Arild Folkvord *et al.* (pers. comm.) have detected changes in larval vertical behaviour as a response to the presence of vegetal oil at the surface. An up-scaling of the findings from an experiment with vertical columns in a laboratory to the open ocean is not straight forward, but the study documented that changes in larval vertical behaviour due to the presence of oil in the open ocean are to be expected.

Whenever a numerical ocean model is involved in a study, it is valid to question whether the model sufficiently resolves all the relevant ocean physics. Typically, the answer is no. The horizontal resolution of an ocean model is limited by the geographical extent of the model domain, the length of the integration, the maximum depth of the ocean involved, and the computing resources available. In this study, we selected a model that is eddy permitting and therefore suitable for resolving the main features of the circulation determining the dispersal of oil and offspring (Vikebø *et al.*, 2010). However, an enhanced resolution will, most likely, affect the results (Mahadevan, 2006), and the results should therefore be interpreted with care and viewed as indications of the order of exposure rather than as detailed predictions.

It is also relevant to ask whether the year selected for our analysis gives results that may be used to discuss general trends in the exposure of offspring from different SGs under various oil spill scenarios or whether the studied time represents an anomalous year relative to ocean physics. The NAO indices for both winter and spring identified the selected time as an average year, but the only way to be certain is to re-simulate all the scenarios for several years. Hence, again, the present results must be interpreted with care if they are to be generalized.

Another important issue relevant to assessing the effects of oil contamination on eggs and larvae is the spatio-temporal variability in natural mortality. It is probable that mortality is not evenly distributed in time and space but is rather highly variable due to gradients in prey and predators (Hjermann *et al.*, 2007). This pattern remains as one of the key knowledge gaps in the early life history of fish and has great significance in terms of the assessment of the impact of an overlap between offspring and oil on recruitment. Would the offspring exposed to above-threshold values of contaminants die in any case due to natural causes or could it be that the oil spill unfortunately harmed most of the individuals that could have contributed to recruitment in that particular year? This question is currently being investigated by combining numerical models and observations of different stages of fish, but is hampered by the limited amount of observational data and capabilities of the numerical models.

It has been reported that it is primarily the dissolved oil compounds that are bioavailable and that therefore contribute to the

toxicity of oil to fish (Carls *et al.*, 2009; Nordtug *et al.*, 2011), but we have also observed that oil drops from dispersed oil can be eaten by or physically adhere to zooplankton and that first-feeding fish larvae eat the polluted zooplankton, resulting in oral exposure (unpublished results). The copepod *Calanus finmarchicus* is very lipid rich and is therefore efficient at accumulating PAHs both from bioconcentration of PAHs from seawater (Jensen *et al.*, 2012) and direct filter-feeding on oil droplets (Hansen *et al.*, 2012). *Calanus finmarchicus* is therefore an important candidate for the trophic transfer of oil compounds to fish larvae and this exposure route must also be considered.

Early stages of fish development show different sensitivities to oil exposure throughout their development. Hence, it is crucial to develop body-burden models based on laboratory experiments that may interact with an IBM of egg and larval stages, enabling the assessment of the integrated effect of time-varying exposure to various levels of oil. This research should include acute toxic oil, as well as non-acute toxic oil that may produce changes in development and behaviour that can be incorporated into the IBM. Again, a prerequisite for the development of such a system is the systematic testing of different stages of fish development with different body-burden histories in response to various concentrations of oil.

If a spill occurred tomorrow, it would be necessary to decide whether to use dispersants to reduce the droplet size of the oil, and thereby its buoyancy, to remove it from the sea surface. For the GOM Deepwater Horizon, the use of dispersants may have led to less oil being displaced onto the shelf of the southern US states and, therefore, to less interaction with coastal marshlands because the oil was distributed deeper than the shelf depths. Wu *et al.* (2012) describe the toxicity of several dispersed and undispersed types of oil and conclude that the use of dispersants increases the bioavailability of TPAHs due to smaller droplets and a greater amount of oil dissolved in water. If, at the same time, the use of dispersants increases the vertical overlap of TPAHs and offspring, this process may substantially increase the impact of an oil spill. However, it is important to assess the combined effects of several processes to better understand the potential consequences of using dispersants to reduce the droplet size of oil and to enable sound decisions on when and where to allow the use of dispersants. For example, will the use of dispersants increase or decrease the concentration of oil at the depth of eggs and larvae? How will this distribution affect the bioavailability relative to direct and indirect (e.g. through prey) uptake? These and many other questions remain for future studies to resolve.

Acknowledgements

We thank the Norwegian Research Council (NRC) for support through the PRIBASE (project number 191698/S40) and SYMBIOSES (PETROMAKS BIP project #ES468602) programmes. The SYMBIOSES project is a cooperation of 15 research partners, financed by the NRC, BP Exploration Operating Company Limited, ConocoPhillips Skandinavia, ExxonMobil Upstream Research Company, Eni Norway, Shell Technology Norway, Statoil Petroleum, and Total E&P Norway.

References

Bader, J., Mesquita, M. d. S., Hodges, K. I., Miles, M., Østerhus, S., and Keenlyside, N. 2011. A review on northern hemisphere sea-ice, storminess and teleconnection patterns: observations and projected changes. Atmospheric Research, doi:10.1016/j.atmosres.2011.04.007.

Barron, M. G., Carls, M. G., Heintz, R., and Rice, S. D. 2004. Evaluation of fish early life-stage toxicity models of chronic embryonic exposures to complex polycyclic aromatic hydrocarbon mixtures. Toxicological Sciences, 78: 60–67.

Carls, M. G., and Meador, J. P. 2009. A perspective on the toxicity of petrogenic PAHs to developing fish embryos related to environmental chemistry. Human and Ecological Risk Assessment, 15: 1084–1098.

Carls, M. G., Rice, S. D., and Hose, J. E. 1999. Sensitivity of fish embryos to weathered crude oil: part I. Low-level exposure during incubation causes malformations, genetic damage, and mortality in larval Pacific herring (*Clupea pallasii*). Environmental Toxicology and Chemistry, 18: 481–493.

Fiksen, Ø., Jørgensen, C., Kristiansen, T., Vikebø, F., and Huse, G. 2007. Linking behavioural ecology and oceanography: larval behaviour determines growth, mortality and dispersal. Marine Ecology Progress Series, 347: 195–205.

Folkvord, A. 2005. Comparison of size-at-age of larval cod (*Gadus morhua* L.) from different populations based on size- and temperature-dependent models. Canadian Journal of Fisheries and Aquatic Sciences, 62: 1037–1052.

Frantzen, M., Falk-Petersen, I. B., Nahrgang, J., Smith, T. J., Olsen, G. H., Hangstad, T. A., and Camus, L. 2012. Toxicity of crude oil and pyrene to the embryos of beach spawning capelin (*Mallotus villosus*). Aquatic Toxicology, 108: 42–52.

Haidvogel, D., Arango, H., Budgell, W., Cornuelle, B., Curchitser, E., Lorenzo, E. D., Fennel, K., *et al.* 2008. Ocean forecasting in terrain-following coordinates: formulation and skill assessment of the regional ocean modelling system. Dynamics of Atmospheres and Oceans, 227: 3595–3624.

Hansen, B. H., Altin, D., Olsen, A. J., and Nordtug, T. 2012. Acute toxicity of naturally and chemically dispersed oil on the filter-feeding copepod *Calanus finmarchicus*. Ecotoxicology and Environmental Safety, 86: 38–46.

Heintz, R. A., Short, J. W., and Rice, S. D. 1999. Sensitivity of fish embryos to weathered crude oil: part II. Increased mortality of pink salmon (*Oncorhynchus gorbuscha*) embryos incubating downstream from weathered Exxon Valdez crude oil. Environmental Toxicology and Chemistry, 18: 494–503.

Hjermann, D. Ø., Melsom, A., Dingsør, G. E., Durant, J. M., Eikeset, A. M., Røed, L. P., Ottersen, G., *et al.* 2007. Fish and oil in the Lofoten-Barents Sea system: synoptic review of the effect of oil spills on fish populations. Marine Ecology Progress Series, 339: 283–299.

Hurrell, J. W. 1995. Decadal trends in the North Atlantic Oscillation: regional temperatures and precipitation. Science, 269: 676–679.

Ingvarsdottir, A., Bjorkblom, C., Ravagnan, E., Godal, B. F., Arnberg, M., Joachim, D. L., and Sanni, S. 2012. Effects of different concentrations of crude oil on first feeding larvae of Atlantic herring (*Clupea harengus*). Journal of Marine Systems, 93: 69–76.

Jensen, L. K., Honkanen, J. O., Jæger, I., and Carroll, J. 2012. Bioaccumulation of phenanthrene and benzo[a]pyrene in *Calanus finmarchicus*. Ecotoxicology and Environmental Safety, 78: 225–231.

Johansen, Ø. 2000. DeepBlow—a Lagrangian plume model for deep water blowouts. Spill Science and Technology Bulletin, 6: 103–111.

Johansen, Ø. 2003. Development and verification of deep-water blowout models. Marine Pollution Bulletin, 47: 360–368.

Jørgensen, C., Dunlop, E. S., Opdal, A. F., and Fiksen, Ø. 2008. The evolution of spawning migrations: state dependence and fishing-induced changes. Ecology, 89: 3436–3448.

Kristiansen, T., Jørgensen, C., Lough, R. G., Vikebø, F. B., and Fiksen, Ø. 2009. Modeling rule based behavior: habitat selection and the growth-survival trade-off in larval cod. Behavioral Ecology, 20: 1–11.

Kristiansen, T., Vollset, K., Sundby, S., and Vikebø, F. 2014. Turbulence enhances feeding of larval cod at low prey densities. ICES Journal of Marine Science. doi: 10.1093/icesjms/fsu051.

Lien, V. S., Vikebø, F. B., and Skagseth, Ø. 2013. One mechanism contributing to co-variability of the Atlantic inflow branches to the Arctic. Nature Communications, 4: 1488, doi:10.1038/ncomms2505.

Mahadevan, A. 2006. Modeling vertical motion at ocean fronts: are non-hydrostatic effects relevant at submesoscales? Ocean Modeling, 14: 222–240.

Meier, S., Craig Morton, H., Nyhammer, G., Grosvik, B. E., Makhotin, V., Geffen, A., Boitsov, S., *et al.* 2010. Development of Atlantic cod (*Gadus morhua*) exposed to produced water during early life stage. I. Effects on embryos, larvae, and juvenile fish. Marine Environmental Research, 70: 383–394.

Neff, J. M., Ostazeski, S., Gardiner, W., and Stejskal, I. 2000. Effects of weathering on the toxicity of three offshore Australian crude oils and a diesel fuel to marine animals. Environmental Toxicology and Chemistry, 19: 1809–1821.

Nordtug, T., Olsen, A. J., Altin, D., Overrein, I., Storoy, W., Hansen, B. H., and De Laender, F. 2011. Oil droplets do not affect assimilation and survival probability of first feeding larvae of North-East Arctic cod. Science of the Total Environment, 412: 148–153.

Olsen, E., Aanes, S., Mehl, S., Holst, J. C., Aglen, A., and Gjøsæter, H. 2010. Cod, haddock, saithe, herring, and capelin in the Barents Sea and adjacent waters: a review of the biological value of the area. ICES Journal of Marine Science, 67: 87–101.

Opdal, A. F. 2010. Fisheries change spawning ground distribution of northeast. Arctic cod Biology Letters, 6: 261–264.

Opdal, A. F, Vikebø, F. B., and Fiksen, Ø. 2011. Parental migration, climate and thermal exposure of larvae: spawning in southern regions gives Northeast Arctic cod a warm start. Marine Ecology Progress Service, 439, 255–262.

Paine, M. D., Leggett, W. C., McRuer, J. K., and Frank, K. T. 1992. Effects of Hibernia crude-oil on capelin (*Mallotus villosus*) embryos and larvae. Marine Environmental Research, 33: 159–187.

Reed, M., Daling, P. S., Singsaas, I., Brakstad, O. G., Faksnes, L. G., Hetland, B., and Ekrol, N. 2000. OSCAR2000: a multi-component 3-dimensional oil spill contingency and response model. *In* Proceedings of the AMOP Seminar, Vancouver, 2000, pp. 663–680.

Sætre, R. 1999. Features of the central Norwegian shelf circulation. Continental Shelf Research, 19: 1809–1831.

Skagseth, Ø., Drinkwater, K. F., and Terrile, E. 2011. Wind- and buoyancy-induced of the Norwegian Coastal Current in the Barents Sea. Journal of Geophysical Research, 116: C08007. doi:10.1029/2011JC006996.

Solberg, T. S., Barth, T., and Westrheim, K. 1982. Effects of illuminated Ekofisk crude oil on yolksac larvae of cod (*Gadus morhua* L.). ICES Document CM 1982/E: 52: 1–8.

Sundby, S., Bjørke, H., Soldal, A. V., and Olsen, S. 1989. Mortality rates during the early life stages and year-class strength of Northeast Arctic cod (Gadus morhua L.). Rapports et Proces-verbaux des Réunions. Conseil International pour l'Exploration de la Mer, 191: 351–358.

Sundby, S. 1991. Factors affecting the vertical distribution of eggs. ICES Marine Science Symposia, 192: 33–38.

Sundby, S., and Nakken, O. 2008. Spatial shifts in spawning habitat of Arcto-Norwegian cod related to multi-decadal climatic oscillations and climate change. ICES Journal of Marine Science, 65: 953–962.

Thygesen, U. H., and Ådlandsvik, B. 2007. Simulating vertical turbulent dispersal with finite volumes and binned random walks. Marine Ecology Progress Series, 347: 145–153.

Uppala, S., Dee, D., Kobayashi, S., Berrisford, P., and Simmons, A. 2008. Towards a climate data assimilation system: status update of ERA-Interim. ECMWF Newsletter, 115: 7.

Vikebø, F., Jørgensen, C., Kristiansen, T., and Fiksen, Ø. 2007. Drift, growth and survival of larval Northeast Arctic cod with simple rules of behavior. Marine Ecology Progress Series, 347: 207–219. doi:10.3354/meps06979.

Vikebø, F. B., Husebø, Å., Slotte, A., Stenevik, E. K., and Lien, V. S. 2010. Impact of hatching date, vertical distribution and inter-annual variation in physical forcing on northward displacement and temperature conditions of Norwegian spring spawning herring larvae (*Clupea harengus* L.). ICES Journal of Marine Science, 67: 1710–1717.

Vikebø, F. B., Ådlandsvik, B., Albretsen, J., Sundby, S., Stenevik, E. K., Huse, G., Svendsen, E., Kristiansen, T., and Eriksen, E. 2011. Real-time ichthyoplankton drift in northeast arctic cod and norwegian spring-spawning herring PLoS ONE, 6, e27367.

Vikebø, F. B., Korosov, A., Stenevik, E. K., and Slotte, A. 2012. Match-mismatch in Norwegian spring spawning herring and spring phytoplankton bloom—observational records from herring larval surveys and SeaWIFS. ICES Journal of Marine Science, 69: 1298–1302.

Wu, D., Zhendi, W., Hollebone, B., McIntosh, S., Knig, T., and Hodson, V. 2012. Comparative toxicity of four chemically dispersed and undispersed crude oils to rainbow trout embryos. Environmental Toxicology and Chemistry, 31: 754–765. doi:10.1002/etc.1739.

Handling editor: C. Brock Woodson

ICES Journal of Marine Science

ICES Journal of Marine Science (2014), 71(4), 982–990. doi:10.1093/icesjms/fst050

Contribution to the Themed Section: 'Larval Fish Conference'

Original Article

Survival bottlenecks in the early ontogenesis of Atlantic herring (*Clupea harengus*, L.) in coastal lagoon spawning areas of the western Baltic Sea

Patrick Polte*, Paul Kotterba, Cornelius Hammer, and Tomas Gröhsler

Thünen-Institute of Baltic Sea Fisheries, Alter Hafen Süd, D-18069 Rostock, Germany

**Corresponding Author: tel: +49 381 8116 103; fax: +49 381 8116 199; e-mail: patrick.polte@ti.bund.de*

Polte, P., Kotterba, P., Hammer C., and Gröhsler, T. 2014. Survival bottlenecks in the early ontogenesis of Atlantic herring (*Clupea harengus*, L.) in coastal lagoon spawning areas of the western Baltic Sea. – ICES Journal of Marine Science, 71: 982–990.

Received 16 November 2012; accepted 20 March 2013; advance access publication 22 May 2013.

Dominant drivers of larval survival are considered to include oceanographic dispersal, sea temperatures, and food availability in the phase of first-feeding. However, research progress on larval herring survival dynamics indicates that multiple factors might act on differing larval developmental stages. Hypothesizing that in inshore systems of the western Baltic Sea bottlenecks of herring development occur before the point of first-feeding, we analysed an extensive time-series of weekly abundances of early stage larvae in Greifswald Bay, an important spawning area for Western Baltic herring. Additionally, we investigated whether distinct hatching cohorts contribute differently to established survival indices on the level of (i) later larval stages in Greifswald Bay and (ii) 1+ group juveniles in the overall western Baltic Sea. Results revealed that abundances of the earliest larval stage explain 62% of the variability of later stage larvae and 61% of the variability of surviving juveniles, indicating pre-hatching survival bottlenecks. Hatching cohorts occurring later during the spawning season contribute most to the surviving year class. Earlier hatching cohorts were not found to result in significant amounts of growing larvae, indicating a bottleneck phase at the critical period when larvae start feeding.

Keywords: Atlantic herring, Baltic Sea, *Clupea harengus*, Greifswald Bay, spring spawning.

Introduction

Investigating the mechanisms of North Atlantic herring (*Clupea harengus*, Linné, 1758) recruitment variability is a major task of fishery science since its early beginnings. Although herring is exploited for human consumption since medieval times, the current understanding of natural factors driving annual reproduction success is rather limited. There is, however, scientific consensus that many important influences structuring on the number of recruits in a year class are affecting the fish's larval stage (Hjort, 1914, 1926; Cushing, 1975; Houde, 2008). According to this, larval herring ecology and behaviour became a focus of marine research in the second half of the last century (e.g. Blaxter, 1953; Holliday and Blaxter, 1960; Hempel and Blaxter, 1961), providing most of the knowledge to build on today. For coastal shelf spawning herring, stocks of the North Atlantic Ocean major causes of larval mortality are considered to be related to the variability of broad scale oceanography and temperature regimes (Fässler *et al.*, 2010; Gröger *et al.*, 2010) or food limitation at the particular period when larvae convert from yolk consumption to active feeding (Hjort, 1914, 1926; Cushing, 1975, 1990). A considerable amount of current knowledge of early herring larvae dispersal is based on the oceanographic modelling of climatic drivers (Gröger *et al.*, 2010) or on the application of particle-tracking models along major current regimes and windfields (e.g. Fox and Aldridge, 2002).

On the transition of North Sea and Baltic Sea ecotones, Western Baltic spring-spawning (WBSS) herring represents a meta-population composed of multiple spawning components recruiting from various inshore spawning grounds in estuaries, bays, and lagoons along coastal transitional waters (Bekkevold *et al.*, 2005; Clausen *et al.*, 2007; Gaggiotti *et al.*, 2009). The population structure documented for WBSS herring supports the assumption of natal homing in this species (e.g. Iles and Sinclair,

1982; Ruzzante *et al.*, 2006) thus underlining the importance of particular spawning grounds or even particular functions of small-scale spawning sites on the population level.

Besides distinct phylogenetic population structures, Baltic Sea herring stocks differ from commercially relevant North Sea herring according to their spawning mode. Spring and autumn spawning herring both occur in the North Sea as well as in the Baltic Sea but their contribution to commercially relevant fishery stocks differ conversely in that North Sea fishery relies on autumn and winter spawning stocks (Dickey-Collas *et al.*, 2010), whereas Baltic Sea fishery nowadays focuses on spring-spawning herring (Parmanne *et al.*, 1994). Additionally to spawning season, reproduction modes differ significantly according to spawning site selection. Autumn spawning North Sea herring frequents outer coastal shelf banks and gravel beds for spawning (Cushing, 1967, and citations therein), whereas Baltic Sea spring-spawning herring immigrates inshore to spawn on complex littoral substrates such as aquatic vegetation (Klinkhardt, 1986; Rajasilta *et al.*, 1989, 1999).

Among WBSS herring, the particular population spawning in shallow brackish lagoons near the Island of Rügen, Germany, is considered a major component (Klinkhardt, 1996; ICES, 2012). The so-called "Rügen-herring" performs annual spawning migrations towards inshore spawning grounds from about March to late May (Bekkevold *et al.*, 2005). After hatching, the sheltered, brackish lagoons (German: "Bodden") represent particular retention areas where larvae are considered to perform most of the critical early life stage development (Oeberst *et al.*, 2009). Although those retention systems are not *per se* subjected to large-scale current regimes (Lehmann *et al.*, 2002) and larvae are therefore not exposed to passive export by major hydrodynamics, the recruitment of WBSS herring is subjected to an interannual year class variability of similar magnitudes to coastal shelf spawning stocks of the North Atlantic Ocean. Additionally, there is in general a decreasing trend in WBSS herring recruitment demonstrated by monitoring programmes over the last two decades (Oeberst *et al.*, 2008, 2009).

Verifying larval dispersal and survival models by field data is complicated due to logistical, financial, or simply methodological limitations in tracking successive larval stages over space and time. Seasonal delineation of bottleneck periods of larval survival in nearshore retention areas would help to focus research on structuring variables effective on the small spatial scales of individual spawning sites (Heath and McLachlan, 1987). Studying early life-history ecology of Rügen herring on the limited scale of a lagoonal or estuarine retention area, however, over a relatively wide range of developmental stages might offer a particular opportunity to increase the understanding of major drivers and the stressors of herring recruitment. A crucial requirement for mechanistic research might be to locate phases in the early herring life cycle where major mortalities occur. Linking these ontogenetic bottleneck phases to environmental and biological variables explicit at the relatively narrow periods might significantly increase the explanatory power of variables and accelerate the understanding of critical factors of herring recruitment.

In the effort to identify significant bottleneck phases in early Rügen herring life history, we combined time-series analysis on larval herring abundance with abundance indices of the corresponding juvenile 1+ group, hypothesizing that (i) Rügen herring recruitment variability in inshore retention areas is structured by survival bottlenecks on the pre-hatching and early larval level, before larvae start feeding actively and (ii) during the spawning season distinct hatching cohorts contribute differently to the year-class strength of surviving recruits.

Material and methods

Study sites

Greifswald Bay is a semi-enclosed, inshore basin formed by the Southern Baltic mainland coast and the Island of Rügen, Germany. The bay covers an area of ~514 km^2 (Reinicke, 1989) and opens to the east into the Baltic Sea by a shallow, fringing shoal interrupted by individual shipping canals. To the west, the bay connects to the coastal Baltic Sea by a narrow sound, separating the Island of Rügen from the mainland. The average water depth of Greifswald Bay is 5.8 m with a maximum of 13.6 m (Reinicke, 1989). An exchange of the entire water body of Greifswald Bay with Baltic Sea water occurs about eight times a year (Stigge, 1989) and is predominantly wind-driven since tidal amplitudes are marginal (<10 cm, semi-diurnal) in the inner Baltic Sea region. Salinity of the mesohaline system varies seasonally with precipitation intensity and wind drift of lower saline surface waters at a range of ~8 (winter) to ~6 in spring and summer. The annual mean salinity is 7.3 (Kell, 1989). Vertical haline stratification is rather scarce, limited to the drainage areas of small rivers. Seasonal temperature fluctuations are large, ranging from regular sub-zero degree Celsius sea surface temperatures (SSTs) with a closed ice sheet in winter to more than 20°C SST during summer. Due to the shallow seabed and frequent strong winds, thermoclines are rare but might occur in summer during periods of exceptionally calm weather (Schoknecht, 1973).

Although the system is largely affected by eutrophication (e.g. Munkes, 2005) extensive mixing by wind force regularly results in suitable aeration and dissolved oxygen contents at the bottom are usually close to 100% during the herring spawning season. Spawning substrates in terms of submerged aquatic vegetation are abundant in the littoral zone, dominated by communities of flowering plants including pondweeds (Potamogetonaceae) and eelgrass (*Zostera marina*) as well as a diverse macroalgal community.

Ichthyoplankton sampling and the larval herring time-series

Sampling of herring larvae in Greifswald Bay and the adjacent Strelasund as a predictive proxy for the stock assessment started in 1979 (Oeberst *et al.*, 2008, 2009). A corrected, validated database of larval densities currently dates back to 1991. Regular ichthyoplankton surveys include a grid of 35 stations sampled weekly throughout Greifswald Bay and Strelasund. The present study is focused on the 30 stations located in Greifswald Bay (Figure 1). From 1991 to 2006, the survey duration was from mid-April to late June. From 2007 to present, the survey starts as soon in spring as regular ice cover retreats (usually mid-March) and ends in the last week of June. During the

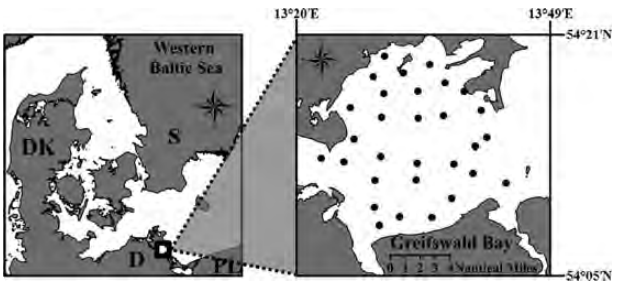

Figure 1. Location of Greifswald Bay in the Southwest Baltic Sea including the sampling grid of 30 stations homogenously distributed within the shallow lagoon.

respective periods, herring larvae were sampled weekly using a Bongo net consisting of two parallel mounted frames carrying nets with different mesh sizes (335 and 780 μm) to account for size-dependent catch efficiency. For the present analyses on early larval stages, only larvae caught by the smaller mesh size were considered. Samples were taken performing stepwise oblique tows (surface and each subsequent 1-m depth step for a 30-s towing time) down to 1 m above ground. Consequently, the total time for each oblique haul depends on the particular water depth at the station. To measure the water volume filtered, the Bongo-frame was equipped with mechanical flowmeters (HYDRO-BIOS). To evaluate differing clogging effects due to mesh size, each centre of both net rings was equipped with an individual flowmeter. Data of the individual flowmeters were used to calibrate for the particular water volume filtered by the particular mesh size.

The volume of water filtered was calculated from flowmeter data as follows:

$$\text{Filtered volume}\,(\text{m}^3) = 0.28\,(\text{m}^2) \times \text{flowmeter difference} \times 0.3\,(\text{m}),$$

where 0.28 m^2 is the opening area of the used plankton net (Ø 0.6 m), the flowmeter difference taken from readings at the beginning and the end of trawl, 0.3 is a constant calibration factor for the flowmeter type used. On board, samples were preserved in 4% buffered (Borax) formalin. In the laboratory, all herring larvae were counted for each sample. Larvae were measured to the nearest millimetre total length (TL). If the number of larvae in the samples exceeded 1000 individuals, a random subsample of 600 larvae was measured for length distribution. For analyses of survival dynamics, length classes of 5 mm were used. Besides the determination of the larval TL, the abundance of development stages was separated according to yolk-sac or post-yolk-sac stages since the year 2007.

Data analysis

During the spawning season, the periods of major larval hatching were identified based on the results of weekly sampling. This analysis had to be limited to the most recent years because before 2007 the ichthyoplankton surveys started later in the season not including potential hatching peaks before mid-April. An exception was the year 1995 when the survey already started in early April [calendar week (cw) 14]. This year was additionally included in the analyses as a reference to former recruitment patterns. Variations in survey duration along the time-series were compensated by focusing on cw 19–23 sampled in all years. Of the larval time-series, the years 1995 and 2007–2011 containing the entire spawning period (cw 14–23) were used to correlate distinct hatching cohorts with two different survival indices: (i) the "N20 larval herring index" which is an annual estimate of the sum of larvae reaching a critical length of 20 mm TL considered to represent year-class strength (see Oeberst *et al.*, 2009, for details). For the current analysis, a modified index was used further referred to as $N20_{GWB}$. This index excludes five of the original N20 stations located in the connecting sound (Strelasund) to avoid potential effects caused by differing water body hydrology. (ii) The single otolith winter ring index (1 − wr) of juvenile herring in the outer western Baltic Sea from the Southern Kattegat area to the Arkona basin (ICES Subdivisions 21–24) reflecting the number of 1-year-old individuals derived by regular hydro acoustic surveys (see for details, ICES, 2012; German acoustic survey, GERAS).

The amount of yolk-sac larvae identified during the sampling campaigns from 2007 to 2011 was correlated with the $N20_{GWB}$ of those years. Because the identification of yolk-sac stages became initiated in 2007, there are only 5 years to correlate with later larval stages and 4 years to correlate with 1 − wr juvenile stages. To cope for this limitation, the analyses were extended to individuals of the length group of 5–9 mm (TL), considering their majority to represent pre-feeding life stages. Using this size class as a proxy, the entire valid time-series on larval herring from 1994 to 2011 was correlated with the $N20_{GWB}$ derived from the Rügen herring survey and the 1 − wr index.

Larval herring abundance (m^{-3}) was presented as the median values of the weekly station grid. The median was considered to be the most representative metric for larval abundance compensating for temporal and spatial patchiness of larval abundance. For interannual analyses, the sum of weekly median values was used for comparisons with the above outlined indices.

$$C_{14-18} = \sum_{i=14}^{18} \tilde{a}_i,$$

$$C_{19-23} = \sum_{i=19}^{23} \tilde{\alpha}_i,$$

$$C_{14-23} = \sum_{i=14}^{23} \tilde{\alpha}_i,$$

$$\tilde{\alpha} = \text{median}\,(\alpha_j),$$

where C_{14-18} is the sum of weekly medians between cw 14 and 18 (first hatching cohort), $C_{19-23}$is the sum of weekly medians between cw 19 and 23 (second hatching cohort), C_{14-23} is the sum of weekly medians between cw 14 and 23, $\tilde{\alpha}$ is the weekly median herring larvae abundance, α is the herring larvae (5–9 mm TL) abundance (m^{-3}) at 1 of the 30 stations, i is the week index, and j is the station index.

Data were analysed using linear regression represented by Pearson's correlation coefficient (r) and the respective coefficient of determination (R^2). The significance level was set at $\alpha < 0.05$.

Results

Relation of yolk-sac larvae abundance and numbers of later larval stages

In general, abundances of yolk-sac larvae *per se* identified were very low. The highest amount of particularly determined yolk-sac larvae of all investigated years was found to be a median value of 0.07 ind. m^{-3} in cw 16, 2009. In contrast, the abundance of actively feeding larvae in this particular week was 0.96 ind. m^{-3}.The annual amounts of yolk-sac larvae derived by the summation of median values per week (cw 14–23) resulted in highest abundance in 2009 (0.36 ind. m^{-3}) and lowest in 2008 (0.03 ind. m^{-3}). The yolk-sac larvae abundance found during the years 2007–2011 correlated significantly with the $N20_{GWB}$ (Table 1). The correlation of yolk-sac larvae abundance of the particular period (2007–2011) with the respective 1 − wr index of the period from 2007 to 2010 (1-year lag phase, $n = 4$) resulted in no significant correlation (Table 1). Compensating for the limited sample size, the 5–9-mm (TL) length group abundance used as a proxy for pre-feeding stages analysed along the entire time-series (1994–2011) revealed a significant correlation with both indices (Table 1).

Table 1. Linear regression including R^2.

		Larvae between 5 and 9 mm (TL)		
	Yolk-sac larvae 2007–2011 (weeks 14–23)	1995 and 2007–2011		1994–2011
		C_{14-18}	C_{19-23}	C_{14-23}
$N20_{GWB}$	$n = 5$	$n = 6$	$n = 6$	$n = 18$
	$R^2 = 0.87$	$R^2 = 0.37$	$R^2 = 0.88$	$R^2 = 0.62$
	$p = 0.021$	$p = 0.196$	$p = 0.005$	$P < 0.001$
1 − wr	$n = 4$	$n = 5$	$n = 5$	$n = 17$
	$R^2 = 0.40$	$R^2 = 0.05$	$R^2 = 0.67$	$R^2 = 0.61$
	$p = 0.370$	$p = 0.721$	$p = 0.091$	$p < 0.001$

The sample size (n) and the significance level (p) of the $N20_{GWB}$ larval herring index and the 1 − wr juvenile herring index with the amount of yolk-sac larvae of the years 2007–2011; and the two distinct hatching cohorts (C_{14-18} and C_{19-23}) for the years 1995 and 2007–2011 and for the second cohort from 1994 to 2011, respectively.
Due to the 1-year lag phase from larvae to 1+ group juveniles, the sample size for the regression with the 1 − wr index is reduced for 1 year ($n = 4$).

Seasonal hatching cohorts and larval survival

An overview of the annual abundance (median m^{-3}) of the larval length group 5–9 mm (TL) according to cw demonstrates high variability between stations (Figure 2).

According to peak abundances of hatching larvae, the extended survey duration of recent years (2007–2011) and the reference year 1995 can be divided into two distinct hatching cohorts annually recurring during (i) cw 14–18 (cohort C_{14-18}) and (ii) 19–23 (cohort C_{19-23}) (Figure 3). Whereas the first cohort (C_{14-18}) constantly did not result in survival as indicated by larger larvae found in consecutive weeks, the second hatching cohort (C_{19-23}) was found to be followed by larger numbers of later larval stages (Figure 3). To compare the two distinct hatching cohorts with the annual survival indices ($N20_{GWB}$ and 1 − wr), the weekly median values for each hatching cohort were summarized for each year. In contrast to the C_{14-18} cohort, only the trend of the C_{19-23} hatching cohort reflects that of the $N20_{GWB}$ and 1 − wr indices, respectively (Figure 4). This is underlined by the results of linear regression of the two cohorts with both indices of later ontogenetic stages. In contrast to the C_{14-18} cohort, the C_{19-23} hatching cohort significantly correlates with the $N20_{GWB}$ (Table 1). With respect of the 1 − *wr* index, there is no significant correlation with either the first or the second hatching cohort. Nevertheless, the second cohort shows a much stronger trend for a relation with the juvenile index than the first hatching cohort. This trend becomes highly significant if the entire time-series (1994–2011) is taken into account (Table 1). However, for C_{14-18}, these data are limited to certain years.

Discussion

Implications of larval Rügen herring dynamics for the WBSS herring stock

The rationale of comparing the Rügen herring spawning component with the abundance o juveniles on the level of the entire WBSS herring stock is based on current assessment practice where the Rügen herring larval index (N20) is used as the only fishery-independent metric for 0-group WBSS herring year-class strength (ICES, 2012). This in turn is based on the observation on recurring correlations of the particular indices also used (with a slightly modified N20) in this study. Although those correlations are not suitable to test for the causal linkage, they strongly indicate that the WBSS herring recruitment is not independent of the year class of the Rügen spawning component. Critical phases in herring life history were displayed for North Sea herring using Paulik diagrams (Nash and Dickey-Collas, 2005). Their results indicate that the amount of spawning-stock biomass (SSB) as a primary factor drives the recruitment success of herring in the North Sea. This is in contrast to WBSS herring, where no SSB index is incorporated as a predictor variable into current stock assessments (ICES, 2012). Cardinale et al. (2009) concluded that SSB does not represent a strong explanatory variable for WBSS herring recruitment strength. Since the Rügen herring is considered a major WBSS herring stock component, SSB-induced recruitment variability would probably be reflected on the WBSS herring stock level and is therefore not considered a main driver. However, there are no reliable estimates available on the biomass of the particular spawning components of the stock. It cannot be empirically excluded that SSB might affect individual populations of WBSS herring. However, although no explicit data on SSB on the Rügen stock component are available, own systematical observations on seasonal egg deposition on standardized spawning bed transects (P. Kotterba, unpubl. data) reveal two distinct spawning peaks corresponding to the hatching cohorts as demonstrated in this study. Our results indicate multiple mortality mechanisms acting differently on differing hatching cohorts emerging from one particular spawning area during the spring-spawning season.

Bottleneck phase from egg stage to yolk-sac larvae

The significant positive correlation of interannual variability patterns among yolk-sac larvae densities and the $N20_{GWB}$ derived in the spawning area points on a potential linkage between the initial amount of hatching larvae and the eventual survival rate of the year class. The non-significant result of the correlation of yolk-sac larvae abundance and the 1 − wr index derived in the outer western Baltic Sea is probably due to the limited number of years ($n = 4$) available for the analyses. Furthermore, own observations indicate that abundances of early yolk-sac stages are underestimated in this study. This is considered a sampling artefact related to a high susceptibility against the mechanical detachment of larval yolk sacs. Therefore, the low relative abundances of yolk-sac larvae actually identified as such might severely under represent the *in situ* abundance not allowing for conclusions on recruitment success based on a certain initial abundance of yolk-sac larvae. However, since that sampling bias is considered a systematical error, it would not affect comparisons of between-year variability. To compensate for the above limitations, the size class of 5–9 mm (TL) was selected as a proxy of pre-feeding larval stages. This size class is strongly correlated with either the $N20_{GWB}$ or the 1 − wr index. These findings are considered neither trivial nor are they unimportant in the process of understanding the driving mechanisms in herring recruitment: since Hjort (1914) postulated his "critical period hypotheses" that research on early life-history mortality of fish is focused on the particular larval stage when larvae exhausted their yolk reservoir and start feeding actively (Hjort, 1914, 1926). A potential mismatch of that critical period with the availability of suitable food is considered as the major bottleneck of herring ontogenesis as well as that of many other pelagic fish species (Cushing, 1975, 1990). However, Houde (2008) summarized case studies and evidence from multiple species in various systems showing recruitment bottlenecks in the egg or early larval stage. In respect of herring in particular,

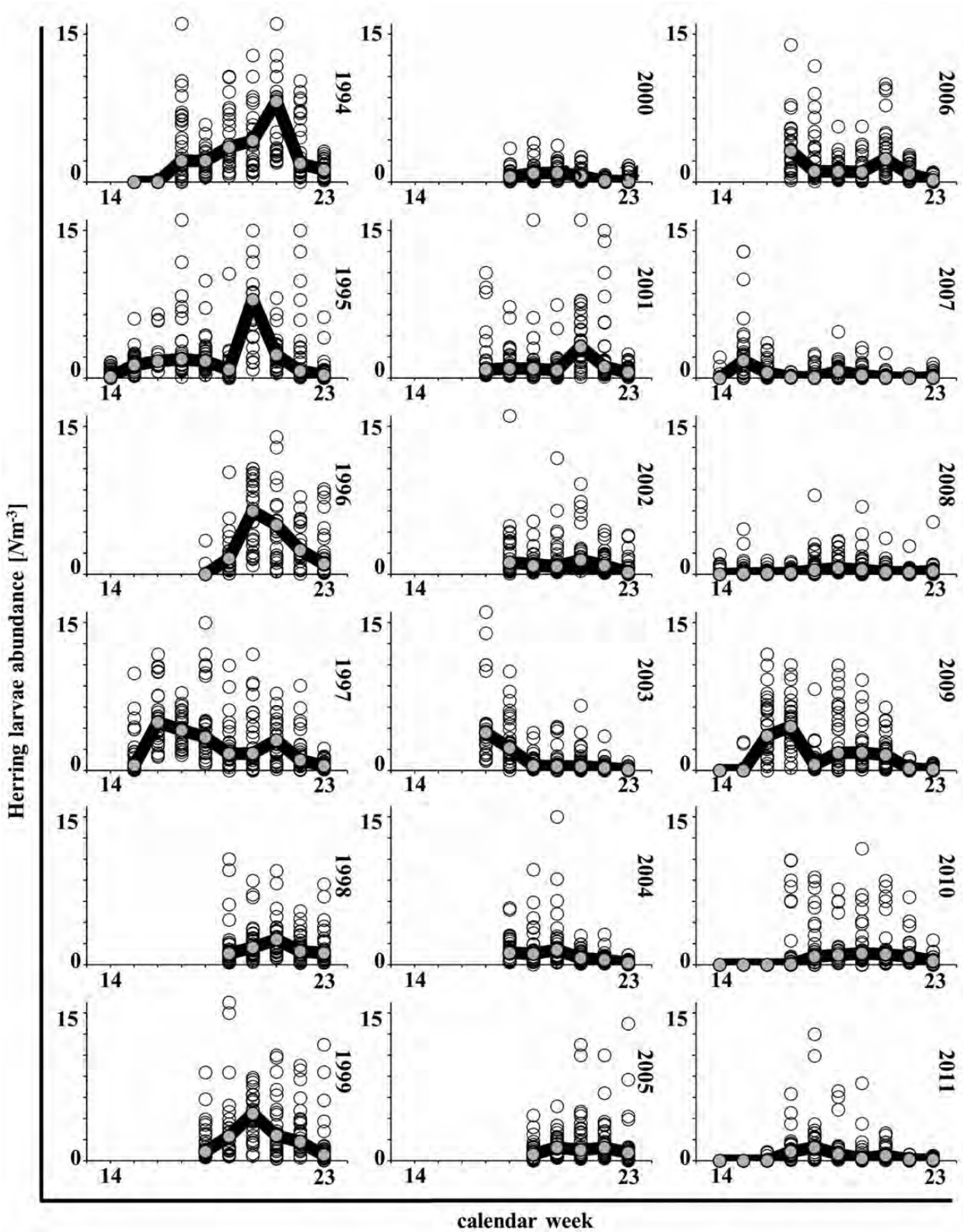

Figure 2. Larval herring abundance m^{-3} of the length group 5–9 mm (TL) of cw 14–23 from 1994 to 2011. White circles indicate larval numbers on the individual stations of the 30 stations grid; grey circles indicate the weekly median of larval numbers. Data from most years before 2007 are limited due to a shorter survey duration starting at cw 17 or later.

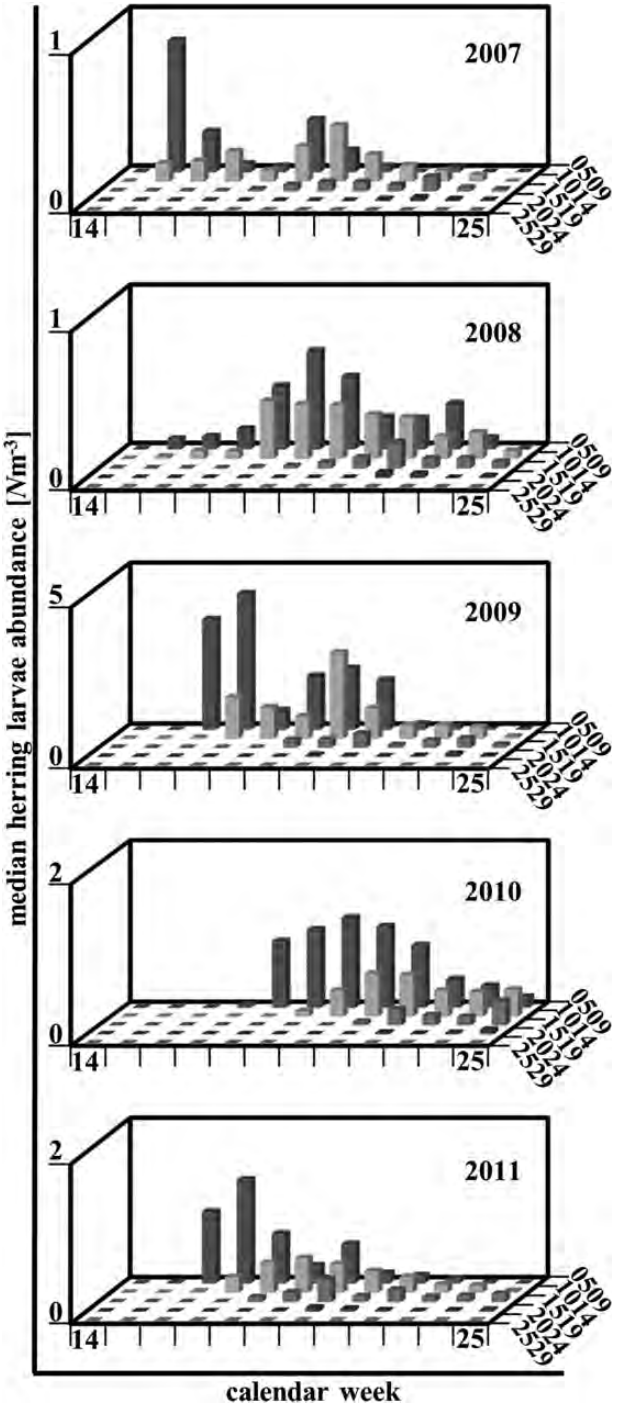

Figure 3. Seasonal larval survival dynamics demonstrated by median abundance m^{-3} (30 stations) of selected larval length classes ("0509", TL 5–9 mm; "1014", TL 10–14 mm; "1519", TL 15–19 mm; "2024", TL 20–24 mm; "2529", TL 25–29 mm) according to cw for the years 2007–2011. Note: *y*-axis values were adjusted to larval numbers to visualize growth dynamics in years with low larval abundance (2007 and 2008).

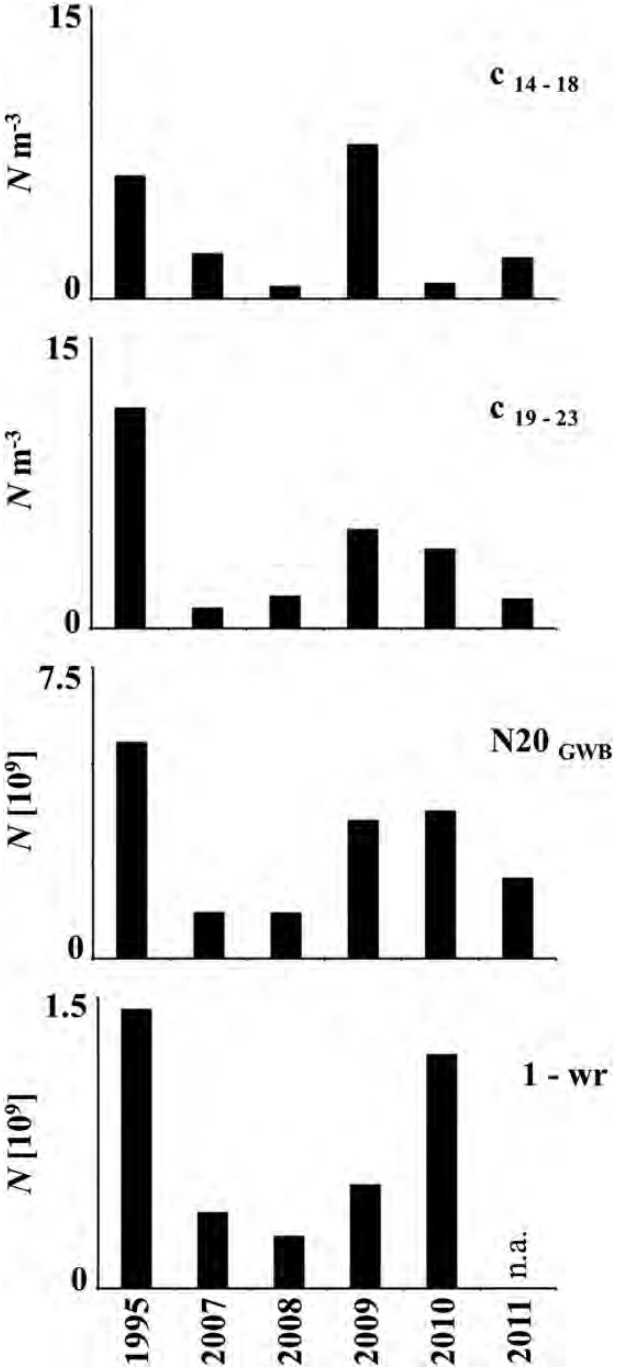

Figure 4. Median values of larval abundance m^{-3} of the years 1995 and 2007–2011 separated according to distinct hatching cohorts represented by C_{14-18} and C_{19-23}, respectively. Additionally, the corresponding values for the $N20_{GWB}$ index and the 1 − wr index are presented. Note: Due to the 1-year lag phase from larvae to 1+ group juveniles, no data (n.a.) were available for the 2012 1 − wr index representing surviving juveniles of the 2011 year class.

larval mortality is widely attributed to later larval stages of length groups >10 mm (TL) (e.g. Nash and Dickey-Collas, 2005). In the nutrient-rich (eutrophic) waters of Greifswald Bay, survival bottlenecks along the concept of Cushing's (1975) match–mismatch hypothesis might still be important when spawning occurs significantly before spring plankton blooms. This is indicated by the minor contribution of the earlier hatching cohort to numbers of surviving older stages. In addition to this, our results indicate structuring mechanisms that apply in the sensitive ontogenetic period before active feeding occurs. However, all ontogenetic

stages from spawning over egg fertilization and development to the survival of hatchlings before yolk exhaustion should receive further attention. All this stages are susceptible to a variety of potential stressors and most probably one or multiple of those very early stages represent an important survival bottleneck for WBSS herring.

The effect of particular mortality mechanisms during this phase might well vary between years, and at this state, we can only speculate on their very nature. In Greifswald Bay, egg mortalities on the shallow spawning beds in the littoral zone are the most likely cause for the early survival bottleneck indicated by our results. For other herring populations, it is documented that pre-hatching effects might significantly influence herring reproduction. Rankine and Morrison (1989) described predation on herring eggs and larvae by sandeel species (*Ammodytes marinus*, Raitt 1934, *Hyperoplus lanceolatus*, Le Sauvage 1824). For Northeast Atlantic herring stocks, it was recently documented that egg predation by haddock (*Melanogrammus aeglefinus*, L. 1758) significantly structured herring recruitment patterns (Richardson *et al.*, 2011). Although those gadoid fish are rare in the brackish lagoons of the western Baltic Sea, intense herring egg predation by three-spined sticklebacks (*Gasterosteus aculeatus,* L. 1758) was observed and is subject of current research efforts. Embryonic development within the demersal eggs is affected by a variety of environmental factors including, i.e. climate regimes (Rosenthal, 1967; Peck *et al.*, 2012), toxins (Rosenthal and Sperling, 1974; von Westernhagen *et al.*, 1979, 1988), and spawning substrate (Aneer, 1987; Kääriä *et al.*, 1988; Rajasilta *et al.*, 1989, 2006). At the earliest phase in the reproductive cycle, the fecundity of the spawning stock might trigger the number of fertilized eggs and possible amounts of hatchlings. For Pacific herring (*Clupea pallasii*, Valenciennes 1847), Tanasichuk and Ware (1987) showed that fecundity increased with temperature. For populations of central Baltic herring (*C. harengus membras*, L. 1761) such as, that is, the Gulf of Riga herring, fecundity fluctuations are considered to be compensated by the abundance of fertile fish and recruitment variability is rather attributed to larval survival than to the condition of the spawning stock (Raid *et al.*, 2010).

Role of distinct hatching cohorts for herring recruitment

Research on larval herring dynamics in Greifswald Bay became established in the late 1970's. However, a standardized, validated time-series on quantitative larval dynamics dates back to 1991. Except particular years (1994, 1995, 1997), the ichthyoplankton survey started later in the season (early April) not including the first hatching cohort investigated in the present study. Recently, in 2007, the survey duration was expanded starting as early in the season as ice covers allows (mid-March), providing a direct comparison of the distinct hatching cohorts to the overall Rügen herring year class. Until 2006, the N20 larval index (Oeberst *et al.*, 2009) was solely a product of the second hatching cohort. Investigating the particular importance of the second hatching cohort but avoiding the autocorrelation with the $N20_{GWB,}$ we correlated the entire time-series with the year class of 1+-group juveniles in the western Baltic Sea (1 − wr) as a proxy for fish surviving early life stage mortalities. The 0-group of young-of-the-year herring had to be neglected, since those early juveniles are considered to stay in the nearshore area where they are difficult to sample quantitatively by hydro acoustic means and ocean-going vessels (Oeberst *et al.*, 2009). Overall, the results indicate two distinct hatching cohorts during the herring spring-spawning period in the Greifswald Bay area. The early cohort (C_{14-18}) hatching in March/April constantly collapses not reflecting significant growth or larval survival, whereas the later cohort (C_{19-23}) hatching in April/May seems to contribute the majority to Rügen herring recruitment strength. The second cohort hatches in a more suitable environment because it regularly appears during the spring plankton bloom. The physicochemical environment, i.e. temperatures, might as well effect the differing success of hatching cohorts. Laboratory experiments by Peck *et al.* (2012) recently revealed that successful hatching of WBSS herring takes place from eggs incubated at 5–17°C (with low hatching success at 2.9 and 19°C), indicating a broad temperature tolerance of the embryo. However, their findings also revealed a distinct effect of incubation temperatures on hatchling size, indicating that hatching at lower ambient temperatures resulted in a size at hatch of ∼5.5 mm standard length (SL), whereas at higher temperatures hatchling length was ∼7.5 mm (Peck *et al.*, 2012). This underlines that the length group 5–9 mm TL delineated in our study is considered adequately representing pre-feeding stages. In general, larval size at first active feeding is considered to vary on the herring population level (Blaxter and Hempel, 1963). According to this, literature reports differ regionally. Examples include North Sea winter spawning (Downs) herring that are reported to start feeding at 10–11 mm (Rosenthal and Hempel, 1970); North Sea spring-spawning (Clyde) herring exhaust their yolk with (SL) 10 mm (Batty, 1984) and start feeding at 8–11 mm (Blaxter, 1968); WBSS herring begins exogenous feeding at 8.6 mm (Kiørboe *et al.*, 1985). Since larvae in our study were measured in TL according to the standards of the N20 larval index assessment, the size range chosen representing first-feeding stages is considered to correspond to observations of those earlier studies. Whether larval length at hatch affects growth and early life stage mortality is subject of some controversy. Based on laboratory experimentation, Geffen (2002) concludes that smaller, earlier hatched larvae display similar growth than larger, later hatched larvae. A possible explanation might be that they experience a longer adaptation phase to active feeding encountering suitable prey while still consuming their yolk reservoir (Geffen, 2002). Although the above studies outline important parameters for larval herring growth, we can still not explain the reason for the existence of an early cohort spawned in Greifswald Bay. Potentially this might be linked to behavioural aspects of spawning adults but this must remain subject of further research.

The significance of our findings on larval recruitment dynamics of western Baltic herring is twofold:

(i) the interannual variability of pre-feeding larvae abundance explains the majority of the $N20_{GWB}$ and 1 − wr index variability;

(ii) the pronounced contribution of the second hatching cohort to herring survival underlines the importance of survival bottlenecks before yolk-sac consumption since the particular length class of 5–9 mm (TL) larvae represent predominantly pre-feeding stages. At the same time, the minor contribution of the earlier hatching cohort points on the potential significance of a second bottleneck period related to the availability of food during the critical period which might be limited before the spring plankton bloom.

Correlative time-series analyses of larval abundance are not suitable to explain the explicit mechanisms of early life stage

mortality. However, it can well be used as the baseline to precisely direct research to particular development stages and cohorts important for reproductive success. This will fuel further research on the drivers of early life stage mortality and indicates the need to increase research efforts on spawning ecology and egg development of WBSS herring.

Acknowledgements

This work was funded and conducted as part of the European Union Data Collection Framework and the Femern Bælt A/S Science Provision Project. The authors wish to thank the crew of the research vessel FFS CLUPEA and the laboratory staff of the Institute of Baltic Sea fisheries particularly Heike Peters, Norbert Proetel, and Dagmar Stephan. Furthermore, the authors wish to thank Rainer Oeberst for his input on an earlier version of the manuscript. Thanks are extended to two anonymous reviewers for their constructive comments and suggestions that greatly helped to improve the manuscript.

References

Aneer, G. 1987. High natural mortality of Baltic herring (*Clupea harengus*) eggs caused by algal exudates. Marine Biology, 94: 163–167.

Batty, R. S. 1984. Development of swimming movements and musculature of larval herring (*Clupea harengus*). Journal of Experimental Biology, 110: 217–229.

Bekkevold, D., André, C., Dahlgren, T. G., Clausen, L. A. W., Torstensen, E., Mosegaard, H., Carvalho, G. R., *et al.* 2005. Environmental correlates of population differentiation in Atlantic Herring. Evolution, 59: 2656–2668.

Blaxter, J. H. S. 1953. Sperm storage and cross fertilization of spring and autumn spawning herring. Nature, 172: 1189–1190.

Blaxter, J. H. S., and Hempel, G. 1963. The influence of egg size on herring larvae (*Clupea harengus* L.). Journal du Conseil International pour l'Exploration de la Mer. 28: 211–240.

Blaxter, J. H. S. 1968. Visual thresholds and spectral sensitivity of herring larvae. Journal of Experimental Biology, 48: 39–53.

Cardinale, M., Möllmann, C., Bartolino, V., Casini, M., Kornilovs, G., Raid, T., Margonski, P., *et al.* 2009. Effect of environmental variability and spawner characteristics on the recruitment of Baltic herring *Clupea harengus* populations. Marine Ecology Progress Series, 388: 221–234.

Clausen, L. A. W., Bekkevold, D., Hatfield, E. M. C., and Mosegaard, H. 2007. Application and validation of otolith microstructure as a stock identification method in mixed Atlantic herring (*Clupea harengus*) stocks in the North Sea and western Baltic. ICES Journal of Marine Science, 64: 1–9.

Cushing, D. H. 1967. The grouping of herring populations. Journal of the Marine Biology Association of the UK, 47: 193–208.

Cushing, D. H. 1975. Marine Ecology and Fisheries. Cambridge University Press, London. 292 pp.

Cushing, D. H. 1990. Plankton production and year-class strength in fish populations: an update of the match/mismatch hypothesis. Advances of Marine Biology, 26: 249–294.

Dickey-Collas, M., Nash, R. D. M., Brunel, T., van Damme, C. J. G., Marshall, T., Payne, M. R., Corten, A., *et al.* 2010. Lessons learned from stock collapse and recovery of North Sea herring: a review. ICES Journal of Marine Science, 67: 1875–1886.

Fässler, S. M. M., Payne, M. R., Brunel, T., and Dickey-Collas, M. 2010. Does larval mortality influence population dynamics? An analysis of North Sea herring (*Clupea harengus*) time series. Fisheries Oceanography, 20: 530–543.

Fox, C. J., and Aldridge, J. N. 2002. Hydrographic circulation and the dispersal of yolk-sac herring (*Clupea harengus*) larvae in the Blackwater Estuary. Journal of the Marine Biology Association of the UK, 80: 921–928.

Gaggiotti, O. E., Bekkevold, D., Jørgensen, H. B. H., Foll, M., Carvalho, G. R., Andre, C., and Ruzzante, D. E. 2009. Disentangling the effects of evolutionary, demographic, and environmental factors influencing genetic structure of natural populations: Atlantic herring as a case study. Evolution, 63: 2939–2951.

Geffen, A. J. 2002. Length of herring larvae in relation to age and time of hatching. Journal of Fish Biology, 60: 479–485.

Gröger, J. P., Kruse, G. H., and Rohlf, N. 2010. Slave to the rhythm: how large-scale climate cycles trigger herring (*Clupea harengus*) regeneration in the North Sea. ICES Journal of Marine Science, 67: 454–465.

Heath, M. R., and McLachlan, P. 1987. Dispersion and mortality of yolk-sac herring (*Clupea harengus* L.) larvae from a spawning ground to the west of the Outer Hebrides. Journal of Plankton Research, 9: 613–630.

Hempel, G., and Blaxter, J. H. S. 1961. The experimental modification of meristic characters in herring (*Clupea harengus* L.). Journal du Conseil International pour l'Exploration de la Mer, 36: 336–346.

Hjort, J. 1914. Fluctuations in the great fisheries of northern Europe viewed in the light of biological research. Rapports et Proce's-Verbaux des Re'unions du Conseil Permanent International pour l'Exploration de la Mer, 20: 1–228.

Hjort, J. 1926. Fluctuations in the year classes of important food fishes. ICES Journal of Marine Science, 1: 5–38.

Holliday, F. G. T., and Blaxter, J. H. S. 1960. The effects of salinity on the developing eggs and larvae of the herring. Journal of the Marine Biological Association of the UK, 39: 591–603.

Houde, E. D. 2008. Emerging from Hjort's shadow. Journal of Northwest Atlantic Fishery Science, 41: 53–70.

ICES. 2012. Report of the Herring Assessment Working Group for the Area South of 62° N (HAWG). ICES Document CM 2012/ACOM: 06.

Iles, T., and Sinclair, M. 1982. Atlantic herring: stock discreteness and abundance. Science, 215: 627–633.

Kääriä, J., Eklund, J., Hallikainen, S., Kääriä, R., and Rajasilta, M. 1988. Effects of coastal eutrophication on the spawning grounds of the Baltic herring in the SW Archipelago of Finland. Kieler Meeresforschung Sonderheft, 6: 348–356.

Kell, V. 1989. Das Phytoplankton des Greifswalder Boddens. Meer und Museum, 5: 25–35.

Klinkhardt, M. 1986. Ergebnisse von Untersuchungen zur Schlupf- und Dottersackphase der Larven von Rügenschen Frühjahrsheringen (*Clupea harengus* L.). Fischereiforschung, 24: 28–30.

Klinkhardt, M. 1996. Der Hering. Die Neue Brehm Bücherei. Bd. 199. Spektrum Akademischer, Verlag, Magdeburg. 230 pp. (in German).

Kiørboe, T., Munk, P., and Støttrup, J. G. 1985. First feeding by larval herring *Clupea harengus* L. Dana, 5: 95–107.

Lehmann, A., Krau, W., and Hinrichsen, H.-H. 2002. Effects of remote and local atmospheric forcing on circulation and upwelling in the Baltic Sea. Tellus A, 54: 299–316.

Munkes, B. 2005. Eutrophication, phase shift, the delay and the potential return in the Greifswalder Bodden, Baltic Sea. Aquatic Sciences, 67: 372–381.

Nash, R. D. M., and Dickey-Collas, M. 2005. The influence of life history dynamics and environment on the determination of year class strength in North Sea herring (*Clupea harengus* L.). Fisheries Oceanography, 14: 279–291.

Oeberst, R., Klenz, B., Dickey-Collas, M., and Nash, R. D. M. 2008. Variability of the year-class strength of western Baltic spring spawning herring (Rügen herring)—which factors determine the year-class strength? Theme Session on Evidence of global warming effects on zooplankton populations and communities, including larvae of benthic invertebrates and fish. ICES CM 2008/Q:07.

Oeberst, R., Klenz, B., Gröhsler, T., Dickey-Collas, M., Nash, R. D. M., and Zimmermann, C. 2009. When is the year class strength

determined in Western Baltic herring? ICES Journal of Marine Science, 66: 1667–1672.

Parmanne, R., Rechlin, O., and Sjörstrand, B. 1994. Status and future of herring and sprat stocks in the Baltic Sea. Dana, 10: 29–59.

Peck, M. A., Kanstinger, P., Holste, L., and Martin, M. 2012. Thermal windows supporting survival of the earliest life stages of Baltic herring (*Clupea harengus*). ICES Journal of Marine Science, 69: 529–536.

Raid, T., Kornilovs, G., Lankov, A., Nisumaa, A-M., Shpilev, H., and Järvik, A. 2010. Recruitment dynamics of the Gulf of Riga herring stock: density-dependent and environmental effects. ICES Journal of Marine Science, 67: 1914–1920.

Rajasilta, M., Eklund, J., Kääriä, J., and Ranta-Aho, K. 1989. The deposition and mortality of the eggs of the Baltic herring, *Clupea harengus membras* L., on different substrates in the south-west archipelago of Finland. Journal of Fish Biology, 34: 417–427.

Rajasilta, M., Eklund, J., Laine, P., Jönsson, N., and Lorenz, T. 2006. Intensive Monitoring of Spawning Populations of the Baltic Herring (*Clupea harengus membras* L.). Final Report of the Study Project ref. N. 96-068, 1997–1999. SEILI Archipelago Research. Institute Publications, 3: 1–75.

Rajasilta, M., Mankki, J., Ranta-Aho, K., and Vuorinen, I. 1999. Littoral fish communities in the Archipelago Sea, SW Finland: a preliminary study of changes over 20 years. Hydrobiologia, 393: 253–260.

Rankine, P. W., and Morrison, J. A. 1989. Predation on herring larvae and eggs by sand-eels *Ammodytes marinus* (Rait) and *Hyperoplus lanceolatus* (Lesauvage). Journal of the Marine Biological Association of the UK, 69: 493–498.

Reinicke, R. 1989. Der Greifswalder Bodden—geographisch-geologischer Überblick, Morphogenese und Küstendynamik. Meer und Museum, 5: 3–7.

Richardson, D. E., Hare, J. A., Fogarty, M. J., and Link, J. S. 2011. Role of egg predation by haddock in the decline of an Atlantic herring population. Proceedings of the National Academy of Sciences USA, 108: 13606–13611.

Rosenthal, H. 1967. Die Herztätigkeit von Heringsembryonen bei verschiedenen Temperaturen. Helgoländer Wissenschaftliche Meeresuntersuchungen, 16: 112–118.

Rosenthal, H., and Hempel, G. 1970. Experimental studies in feeding and food requirements of herring larvae (*Clupea harengus*, L.) *In* Marine Food Chains. Ed. by J. H. Steele. University of California Press, Berkeley. 552 pp.

Rosenthal, H., and Sperling, K. 1974. Effects of cadmium on development and survival of herring eggs. *In* The Early Life History of Fish, pp. 383–396. Ed. by J. H. S. Blaxter. Springer Verlag Berlin and New York.

Ruzzante, D. E., Mariani, S., Bekkevold, D., André, C., Mosegaard, H., Clausen, L. A. W., Gröhsler, T., *et al.* 2006. Biocomplexity in a highly migratory pelagic marine fish, Atlantic herring. Proceedings of the Royal Society of London, Series B: Biological Science, 273: 1459–1464.

Schoknecht, G. 1973. Einige Untersuchungsergebnisse über die Wasserbeschaffenheit des Greifswalder Boddens. Acta hydrochimica et hydrobiologica, 1: 387–395.

Stigge, H. J. 1989. Der Wasserkörper Bodden und seine Hdrodynamik. Meer und Museum, 5: 10–14.

Tanasichuk, R. W., and Ware, D. M. 1987. Influence of interannual variations in winter sea temperature on fecundity and egg size in Pacific herring (*Clupea harengus pallasii*). Canadian Journal of Fishery and Aquatic Sciences, 44: 1485–1495.

von Westernhagen, H. 1988. Sublethal effects of pollutants on fish eggs and larvae. Fish Physiology, 11: 253–346.

von Westernhagen, H., Dethlefsen, V., and Rosenthal, H. 1979. Combined effects of cadmium, copper and lead on developing herring eggs and larvae. Helgoländer Wissenschaftliche Meeresuntersuchungen, 32: 257–278.

Handling editor: Howard Browman

ICES Journal of Marine Science

ICES International Council for the Exploration of the Sea
CIEM Conseil International pour l'Exploration de la Mer

ICES Journal of Marine Science (2014), 71(4), 991–1000. doi:10.1093/icesjms/fst168

Contribution to the Themed Section: 'Larval Fish Conference'

Original Article

Nutritional situation for larval Atlantic herring (*Clupea harengus* L.) in two nursery areas in the western Baltic Sea

Matthias Paulsen[1,2]*‡, Cornelius Hammer[1], Arne M. Malzahn[3,4], Patrick Polte[1], Christian von Dorrien[1], and Catriona Clemmesen[2]

[1]*Thünen-Institute, Institute of Baltic Sea Fisheries, Alter Hafen Süd 2, 18069 Rostock, Germany*
[2]*Helmholtz Centre for Ocean Research (GEOMAR), Düsternbrooker Weg 20, 24105 Kiel, Germany*
[3]*Department of Marine Science and Fisheries, College of Agricultural and Marine Sciences, Sultan Qaboos University, PO Box 34, PC: 123 Al-Khod, Sultanate of Oman*
[4]*Alfred Wegener-Institute for Polar and Marine Research, Biologische Anstalt Helgoland, Postbox 180, 27483 Helgoland, Germany*

**Corresponding author: tel: +49 431 6004567; fax: +49 431 6004553; e-mail: mpaulsen@geomar.de*
‡Present address: Institute of Baltic Sea Fisheries, Alter Hafen Süd 2, 18069 Rostock.

Paulsen, M., Hammer, C., Malzahn, A. M., Polte, P., von Dorrien, C., and Clemmesen, C. 2014. Nutritional situation for larval Atlantic herring (*Clupea harengus* L.) in two nursery areas in the western Baltic Sea. – ICES Journal of Marine Science, 71: 991 – 1000.

Received 31 October 2012; accepted 11 September 2013; advance access publication 8 October 2013.

The Greifswalder Bodden (GWB) is considered to be the most important spawning and nursery area for the western Baltic spring-spawning herring. However, the biotic and abiotic reasons for this are still unclear. Consequently, we investigated larval growth conditions in the GWB and in the Kiel Canal (KC), another nursery and spawning area of Baltic herring. We investigated prey quantity and quality [copepod abundance and essential fatty acid (EFA) concentration] as well as biochemically derived growth rates and fatty acid content of larval herring in spring 2011. A significant correlation between larval growth and larval EFA concentration could be observed in the GWB. The highest growth rates and EFA concentrations in the larval herring coincided with high food quality. Compensating effects of food quality on food quantity and *vice versa* could be observed in both the GWB and the KC. While larval growth rates in the KC were high early in the season, highest growth rates in the GWB were achieved late in the season. In conclusion, neither area was superior to the other, indicating similar growth conditions for larval herring within the region.

Keywords: DHA, EPA, essential fatty acids, food quality, growth, prey density.

Introduction

Early life stages are crucial for the determination of year-class strengths. A hundred years ago, Hjort (1914) already hypothesised that large numbers of suitable prey items during the stage of first feeding are responsible for good recruitment in marine fish stocks. This has been the basis of recruitment research ever since, and his hypothesis was continually refined and supported by modelling, experimental, and field-workers alike (Rosenthal and Hempel, 1970; Cushing, 1974; Sinclair and Tremblay, 1984; Anderson, 1988; Sinclair, 1988; Cury and Roy, 1989; Cushing, 1990; Buckley and Durbin, 2006). However, it is still not possible to reliably predict recruitment simply based on biotic and abiotic parameters. Hence, other uninvestigated or only rarely investigated factors seem to play an important role as well.

Although the strong effects of food quality on larval rearing are well known from aquaculture as well as experimental work, this issue is mostly neglected in field studies. In particular, the effect of essential fatty acid (EFA) supply on the performance of marine fish larvae is well documented in experiments. Total amounts of docosahexaenoic acid (DHA) and eicosapentaenoic acid (EPA) as well as their ratio, along with arachidonic acid affect development, growth, and survival of marine larval fish (Mourente *et al.*, 1991; Bell *et al.*, 1995; Furuita *et al.*, 1998; Copeman *et al.*, 2002; Van Anholt *et al.*,

2004; Cutts *et al.*, 2006; Copeman and Laurel, 2010). These dietary components are mainly synthesized by the phytoplankton and subsequently transferred to higher trophic levels. Therefore, the basic EFA pattern in marine foodwebs is determined by the planktonic primary producers. Two of the most important and widespread phytoplankton classes, diatoms and dinoflagellates, differ basically in their EFA ratios. Diatoms are rich in EPA and poor in DHA, while dinoflagellates provide high amounts of DHA and substantially less EPA (Dalsgaard *et al.*, 2003). The relative amount of EFA is also higher in the exponential growth phase of the phytoplankton (e.g. during a spring bloom) when cell division occurs frequently and decreases as it reaches the growth plateau when storage lipids then accumulate (Morris, 1981; Kattner *et al.*, 1983; Falk-Petersen *et al.*, 1998). Within certain ranges, i.e. physiologically possible or tolerable limits, the EFA concentration of the fish larvae's food is determined by the phytoplankton. Significantly improved growth was observed in larval cod fed with copepod nauplii originating from adult copepods grown on dinoflagellates when compared with a diatom-based diet (St John *et al.*, 2001). Malzahn *et al.* (2007a) were also able to show nutritional effects that travelled up the food chain to larval fish. Since the total EFA concentration as well as the ratios between the different EFAs can differ strongly between habitats and during spring season, food quality is expected to vary for larval fish in space and time.

In current ICES stock assessment practice, Ruegen herring spawning in Greifswalder Bodden (GWB) is considered the major component for western Baltic spring-spawning herring. Oeberst *et al.* (2009a) found a strong correlation between the number of 20 mm larvae within the GWB and the number of recruits found in the western Baltic Sea during hydroacoustic surveys in autumn. It is characteristic for spring-spawning herring in the Baltic Sea to seek low saline, shallow coastal, and protected habitats for spawning like the GWB, the KC, or the Schlei Fjord (Neb, 1952; Weber, 1971; Aneer *et al.*, 1983; Aneer, 1989; Biester, 1989a). Höök *et al.* (2008) were able to show that nursery conditions for larval herring were better in coastal sheltered areas by judging the quality of the different habitats based on the RNA/DNA ratios of larval herring and the RNA content of *Eurytemora affinis*, an important larval herring food source (Schnack, 1972).

In the light of the apparent dominance of the GWB as a herring spawning ground, the question arises as to what the particular qualitative differences are between this major spawning ground and the many other quantitatively less important spawning grounds, such as the Kiel Canal (KC). In contrast to the natural habitat of the GWB, the KC is an artificial inland waterway. Despite the obvious differences between GWB and the KC, they have important hydrological features in common; for example, high nutrient load, no anoxia due to a well-mixed water column, and low salinity. The latter is especially important in order for a spawning ground to be suitable for Baltic herring. The question remains if both areas are similarly suitable as nursery grounds for herring hatchlings.

The principle of using RNA/DNA ratios as an indicator of condition is based on the assumption that the DNA content of a cell is constant, while the RNA content varies with the nutritional condition of the cell. The RNA/DNA ratio is a well-established biochemical method to determine the condition of fish larvae (Clemmesen, 1994; Caldarone *et al.*, 2003; Malzahn *et al.*, 2007b; Grote *et al.*, 2012; Meyer *et al.*, 2012). Standardizing the RNA/DNA ratios (Caldarone *et al.*, 2006) and using a multispecies fish larvae growth model allows for the calculation of instantaneous growth rates for a comparative approach (Buckley *et al.*, 2008). An increase in EFAs, especially in DHA, in the diet of laboratory-reared cod larvae was reflected in an increase in larval growth using this method (St John *et al.*, 2001).

Based on our observations that larval growth is affected by food quality in experimental work and that the GWB potentially provides more recruits than other spawning areas of the western Baltic spring-spawning herring, we defined the following two hypotheses: (i) food quality as determined by concentrations of EFAs significantly affects larval growth *in situ*, and (ii) the GWB provides better nutritional conditions for larval growth than the KC. To test this, we analysed and compared food quantity and quality in terms of DHA and EPA and investigated larval growth, based on larval RNA/DNA ratios, as well as DHA and EPA concentration of larval herring simultaneously from the GWB and KC.

Material and methods

Sampling

Herring larvae (*Clupea harengus* L.) were sampled along with mesozooplankton and abiotic parameters to compare the growth conditions of larval herring in different spawning sites. One sampling site was located in the KC at a station 15 km inland from the open Baltic Sea (ICES Subdivision 22; Figure 1a), whereas the other sampling site was located in the GWB (ICES Subdivision 24; Figure 1b). All samples were collected between April and June 2011 during the seasonal occurrence of larval herring.

Herring larvae were sampled with a bongo net (60 cm diameter, 335 and 500 μm mesh size, respectively) that was heaved in an oblique haul. All larvae were frozen on board within 30 min of the haul. Before further analysis, larval standard length was measured to the lower 0.1 mm and freeze-dried for 24 h using a freeze drier (CHRIST ALPHA 1–4 LSC). Thereafter, the larvae were weighed to the nearest 0.1 μg (SARTORIUS microbalance SC2). The prey field was sampled with a WP2-net (200 μm mesh size) that was

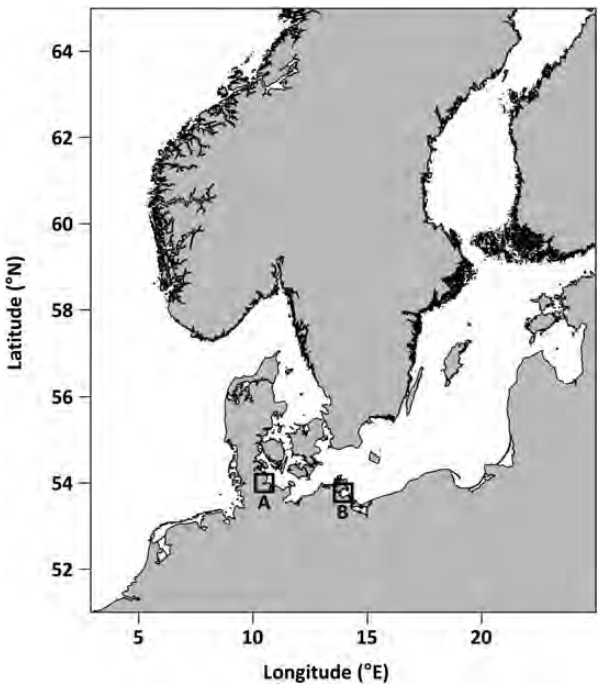

Figure 1. Sampling sites for larval herring and copepods in the western Baltic Sea during spring season. (a) KC; (b) GWB.

hauled once vertically from 3 m above the bottom to the surface in the KC, and from 1 m above the ground in the GWB.

Mesozooplankton abundance

The mesozooplankton samples, conserved with 4% formaldehyde, were separated in a plankton divider (Kott, 1953) up to the point where at least 100 individuals of the most abundant copepod species were available in the section that was counted. All copepods were determined to the species level where possible, although for *Acartia* species, some remained classified at the genus level.

Fatty acids

Fatty acids (FA) were measured as FA methyl esters by gas chromatography slightly modified after Malzahn *et al.* (2007a, b). Lipids were extracted with dichlormethane/methanol (vol. 2:1) for a minimum of 72 h at −80°C. After the extraction, larvae were removed and stored in a desiccator to vaporize the adhering dichlormethane/methanol. Copepod samples were treated similarly, but with an additional 30 min of ultrasound bath after the 72 h extraction at −80°C.

RNA/DNA analysis

For better comparability of the RNA/DNA ratio and the EFA concentration of the larvae, RNA/DNA ratio and FA were measured in the same larvae individuals. This was possible by first defatting the herring larvae and then homogenizing the defatted carcass for the RNA/DNA analysis according to Clemmesen (1993) and Belchier *et al.* (2004). For both analyses, complete larvae were used. Therefore, the ratio determined is a whole larva respond neglecting the fact that different tissue types respond differently to changes in food availability (Olivar *et al.*, 2009). Some modifications were necessary because of the increased elasticity of the larvae due to the missing lipids. The cells of the defatted larvae were homogenized in three steps: (i) freeze-dried larvae were placed in a cell mill for 15 min together with different sized glass beads (diameter 2.0 and 0.17–0.34 mm), (ii) supersonic treatment in Tris–sodium dodecyl sulphate (SDS) buffer (Tris 0.05 mol l^{-1}, NaCl 0.01 mol l^{-1}, ethylenediaminetetracetic acid 0.01 mol l^{-1}, SDS 0.01%), and (iii) larvae together with buffer and glass beads were placed in the cell mill for 15 min. Then, the homogenate was centrifuged at 3829*g* (6800 rpm) at 0°C for 8 min (Sigma Laboratories Centrifuge 3–18k). A combined fluorometric measurement of RNA and DNA in the homogenate in a microtiter fluorescence reader (Labsystems, Fluoroscan Ascent) followed. Next, RNase was added to the samples to digest the RNA (30 min at 37°C) and the remaining DNA was measured. The difference of the sum of total nucleic acids and the remaining DNA was assigned to be RNA. By using the calibration curve fitted to the standard measurements (23s r RNA Boerhinger), the amount of RNA was calculated. The RNA calibration was repeated every measurement day. The DNA concentrations were calculated using the relationship between RNA and DNA described by Le Pecq and Paoletti (1966) with a slope ratio of 2.2 for DNA to RNA.

Growth calculation

Larval instantaneous growth rates were calculated according to Buckley *et al.* (2008). The best-fit multispecies growth model that was chosen for further calculation was:

$$G_i = 0.0145 \times sRD + 0.0044 \times (sRD \times T) - 0.078,$$

where G_i is the instantaneous growth rate, *sRD* the standardized RNA/DNA ratio (Caldarone *et al.*, 2006), and T the temperature at the given date. Results have to be interpreted in the way that a value of 0 would mean no growth at all and a value of 1 would be a doubling of the weight of the larva per day.

Estimation of larval herring production in both nursery areas

To gain a rough estimation of the larval herring production of the KC and the GWB to relate the productivity of both systems, available larval abundance data (n m^{-3}) from the whole season were used to calculate the median of larval herring abundance. For the GWB (area: 512 km^2), abundance data of 36 stations were available and used to get the best approximation possible. Analyses of larval growth as well as chlorophyll *a* data from four stations in the GWB have shown limited spatial variability (Paulsen *et al.*, in prep.), indicating comparable conditions within the system. Owing to logistic

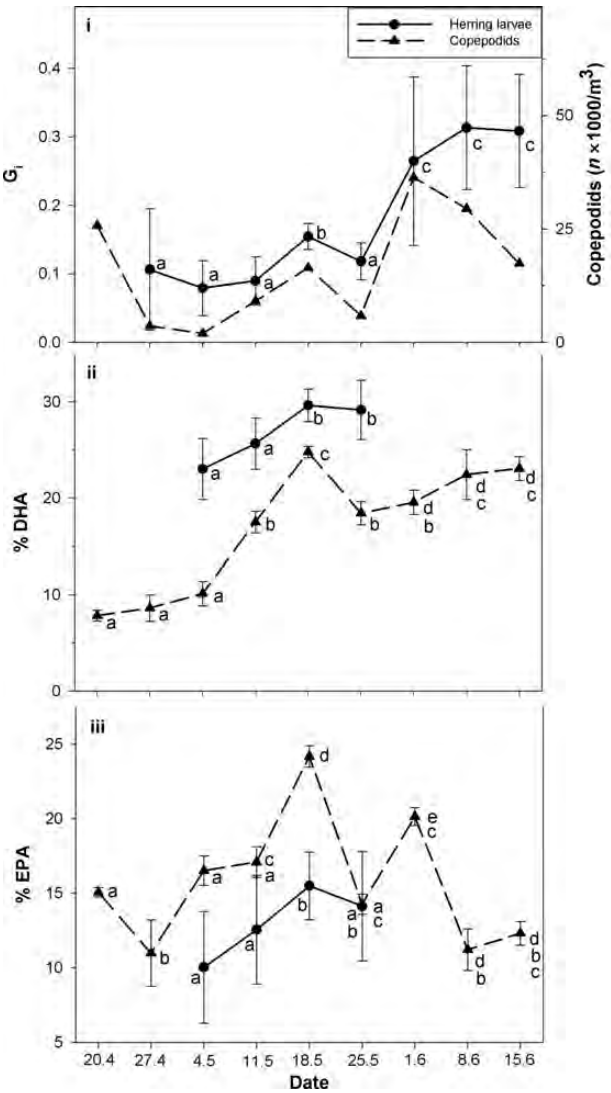

Figure 2. GWB. Error bars indicate standard deviations. (i) Instantaneous growth rate (G_i) of larval herring and copepodid abundance per cubic metre over time. (ii) DHA concentration of larval herring and copepods over time. (iii) EPA concentration in larval herring and in copepods over time. Different letters besides the data points denote significant differences.

Table 1. Average standard length per date in the GWB.

Date	27 April	4 May	11 May	18 May	25 May	1 June	8 June	15 June
Length	9.5 ± 2.0	9.8 ± 1.8	10.8 ± 2.4	12.4 ± 2.5	12.9 ± 3.4	15.3 ± 2.3	14.0 ± 2.8	13.1 ± 1.9

constraints, only a single sampling station was analysed in the KC with the assumption that this is representative for the relatively small nursery area (area: 6 km^2). The median of larval abundance was multiplied by the volume of water of the spawning sites. The value of the GWB was then divided by the KC's value to relate both areas. Since the sampling sites from which abundance data were used are spread over the whole area of the GWB, the whole water volume of the GWB was used for calculation. However, in the KC, only ~40 km of the total area is used for spawning and this was accounted for in the calculation.

Silica and chlorophyll *a* concentrations

Silica as well as chlorophyll *a* concentrations were analysed according to Grasshoff *et al.* (1999).

Statistics

Statistical analyses were performed using the statistic software package STATISTICA (version 6). The data were checked for normal distribution and homogeneity of variances using the Shapiro–Wilk and the Levene tests. When variances were heterogeneous, data were transformed by extracting the cube and fourth root, respectively. To check between sampling days, a one-way analysis of variance (ANOVA) was conducted and a Tukey honestly significant difference (HSD) test was used for *post hoc* comparison. Linear regressions were performed to test for effects of larval EFA on larval growth. To test for differences between the two habitats, the season was split into two time windows, where drastic changes in prey availability and larval growth were observed. Larval growth rates, larval and copepod EFA concentration, as well as copepod abundance within each time window and region were pooled. Thereafter, the different parameters were tested with a *t*-test between the two regions.

Results

Greifswalder Bodden

The mesozooplankton assemblage of the GWB consisted mainly of copepods. *Acartia* spp. was the dominant genus until 25 May, contributing 60–80% to the copepodid community. The strong increase in prey abundance on 1 June was driven by increasing *Eurytemora* abundance. This species contributed 70% of the copepodids on that day. Thereafter, the contribution of *Eurytemora* decreased strongly and *Acartia* became dominant again on 15 June (97% of all copepodids). In the GWB, instantaneous growth rates of larval herring followed the copepodid abundance (Figure 2i). An exception was the time window between 1 and 15 June, when growth remained constantly on a high level despite an approximate halving in prey abundance. Prey DHA concentration increased significantly between 4 and 18 May (ANOVA, Tukey HSD, $p < 0.05$), which was reflected in the significantly increasing DHA concentration of the larvae (ANOVA, Tukey HSD, $p < 0.05$, Figure 2ii). Growth rates increased significantly on 1 June (ANOVA, Tukey HSD, $p < 0.01$) when prey abundance increased sixfold. However, not only growth rates increased, but also average larval standard length (Table 1). This affects larval growth rates, since during adequate growth conditions, larger larvae generally have higher growth rates than smaller ones (Clemmesen, 1994). While copepodid abundance decreased by

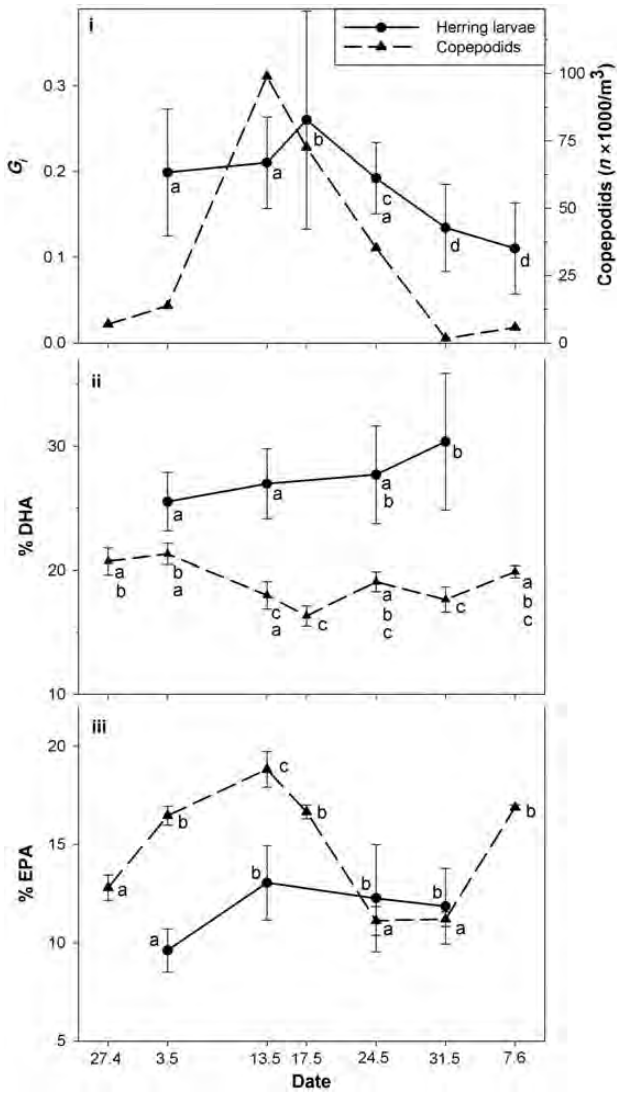

Figure 3. KC. Error bars indicate standard deviations. (i) Instantaneous growth rate (G_i) of larval herring and copepodid abundance per cubic meter over time. (ii) DHA concentration of larval herring and copepods over time. (iii) EPA content in larval herring and in copepods over time. Different letters besides the data points denote significant differences.

50% between 1 and 15 June, DHA concentration of the copepods showed an increasing trend and larval growth remained constant. Variance in growth and DHA concentration of the herring larvae was low when nutritional conditions were bad between 4 and 25 May. Although growth conditions in terms of prey abundance and copepod DHA concentration were similar between 18 May and 15 June, larval growth rates were significantly higher on 15 June. However, temperatures were 7°C higher on 8 June than on 11 May (Figure 8). The EPA concentration of the copepods increased similar to the DHA concentration between 27 April and 18 May. As a result, EPA concentrations increased in the larvae as well (Figure 2iii).

Table 2. Average standard length per date in the KC.

Date	3 May	13 May	17 May	24 May	31 May	7 June
Length	9.0 ± 1.1	11.1 ± 1.4	10.1 ± 2.0	12.5 ± 2.2	13.1 ± 1.5	18.6 ± 1.2

Kiel Canal

Eurytemora dominated the copepodite assemblage during late April and throughout May (90–100% of all copepodites sampled) in the KC. From late May on, *Acartia* dominated (70–80% of all copepodids). Similar to the GWB, growth rates of larval herring followed prey abundance in the KC (Figure 3i). However, growth rates remained constant, even when prey abundance increased eightfold on 13 May. This occurred when DHA concentration of the copepods decreased significantly (ANOVA, Tukey HSD, $p < 0.05$) and DHA of the larvae showed an increasing trend (Figure 3ii). Since larvae were larger on 13 May compared with 3 May (Table 2), a faster growth due to the increase in size would be expected. When food quantity abruptly became limited on 31 May, growth rates of the larvae decreased significantly. While DHA concentration in the larvae increased during the whole season (Figure 3ii), EPA remained constant after an initial increase (Figure 3iii).

Comparison of both areas

In the GWB, larval growth was significantly correlated with the DHA and EPA concentration in the larvae ($p < 0.01$, Figures 4 and 5). Highest growth rates were achieved at highest DHA and EPA concentrations in the larvae. When DHA and EPA concentrations in the copepods were highest on 18 May, larvae had the highest DHA and EPA concentrations and grew at the highest rates. In contrast to this, no significant correlation between DHA and larval growth was detected in the KC (Figure 6), though one between larval growth and EPA was found (Figure 7).

Over the whole season, chlorophyll *a* values were higher in the GWB when compared with the KC (Figures 8 and 9). Silica values were very low ($<1\ \mu mol\ l^{-1}$) in the GWB until 11 May, when silica values started to recover (Figure 8). In contrast, silica values were above 21 $\mu mol\ l^{-1}$ in the KC throughout the whole season (Figure 9).

As aforementioned, to better compare both habitats, the season was divided into two time windows according to drastic changes in prey availability and larval growth. The first time window reached from 27 April to 25 May, while the second one made up of two or three samplings from 31 May to 15 June, depending on the habitat. In contrast to significantly different prey abundances in both time windows ($p < 0.05$, Table 3), prey DHA concentration was only significantly different in the second time window ($p < 0.05$, GWB > KC, Table 3). In the first time window, larvae grew significantly faster in the KC, whereas growth rates were significantly higher in the GWB in the second time window (Table 4). This was true for all ontogenetic stages. Larval FA data were only available for the first time window. Contrary to larval growth rates, DHA and EPA concentrations were only significantly different in certain ontogenetic stages (Table 4). Yolk-sac larvae (<9 mm) had significantly higher DHA and EPA concentrations in the KC than larvae from the GWB. At first feeding, no differences could be detected, while EPA was significantly higher in pre-flexion larvae (11–14 mm) of the GWB. In post-flexion larvae, EPA as well as DHA were significantly higher in the GWB compared with the KC irrespective of the bad growth conditions in terms of prey abundance and prey EFA concentration during that time window.

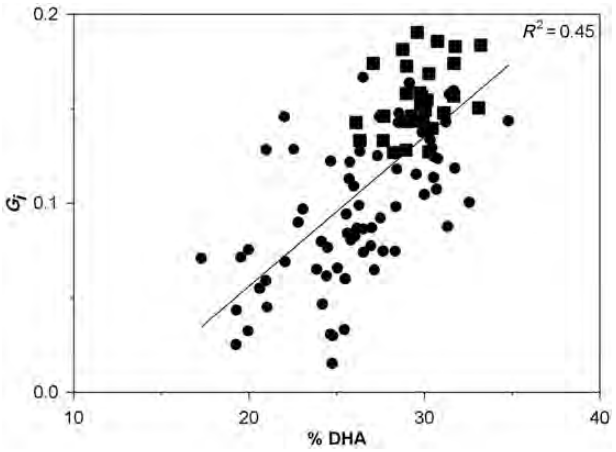

Figure 4. *GWB.* Significant correlation ($p < 0.01$) between instantaneous growth rates (G_i) of larval herring and their DHA concentration. Dots indicate all available data, and squares show data from 18 May, when DHA concentration in copepods was highest.

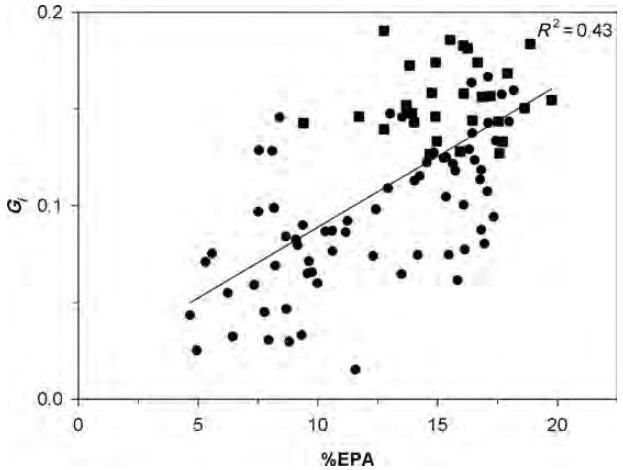

Figure 5. *GWB.* Significant correlation ($p < 0.01$) between instantaneous growth rates (G_i) of larval herring and their EPA concentration.

The calculation of the rough estimate of total larval production of the different spawning sites revealed a 24-fold higher production of larval herring in the GWB compared with the KC.

Discussion

Though growth of fish larvae is dominantly affected by food availability and temperature, other factors such as salinity, oxygen, and the larvae's interactions with other organisms are known to be influencing factors (Clemmesen, 1994; Johnes, 2002). Furthermore, it is known from experimental work that food quality can also be an important factor (Copeman *et al.*, 2002; Malzahn and Boersma, 2009). The present study shows that high food quality is able to compensate

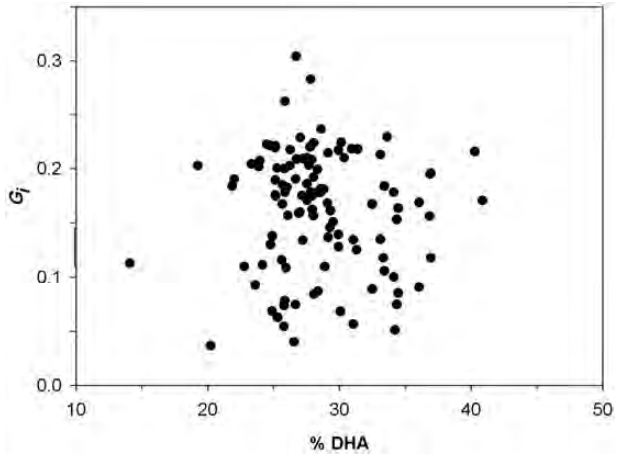

Figure 6. *KC.* Correlation between instantaneous growth rates (G_i) of larval herring and their DHA content. The correlation is not significant.

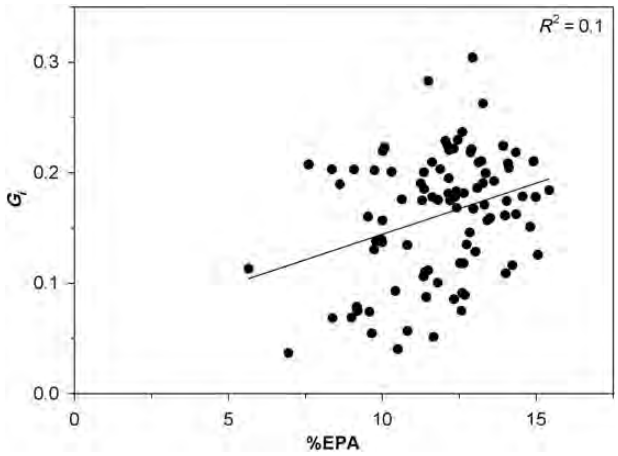

Figure 7. *KC.* Significant correlation ($p < 0.01$) between instantaneous growth rates (G_i) of larval herring and their EPA concentration.

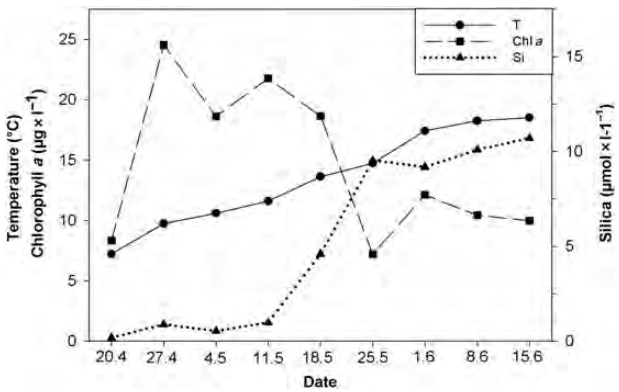

Figure 8. *GWB.* Temperature, silica, and chlorophyll *a* over time.

for low food quantity and *vice versa* for larval fish in the field. This can lead to constant growth rates in larval herring even when both parameters develop in opposing directions. Examples for these

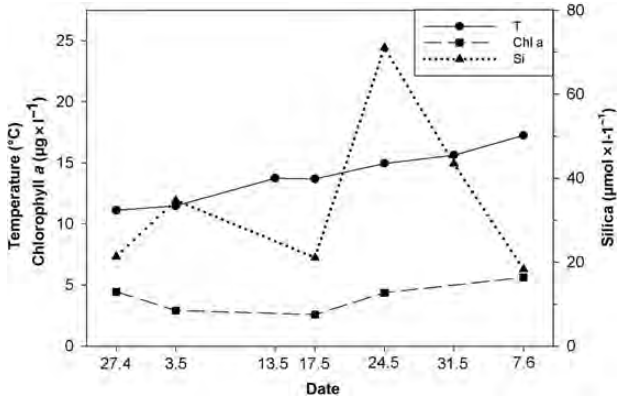

Figure 9. *KC.* Temperature, silica, and chlorophyll *a* over time.

effects can be found on 15 June in the GWB and on 13 May in the KC. However, the increase in copepod DHA was relatively modest compared with the decrease in prey abundance on 15 June in the GWB, which leads to the assumption that other uninvestigated factors, for instance, essential amino acids, vitamins, sterols (Cahu *et al.*, 2003), or abiotic factors, might have played a role in addition to the increase in DHA. A possible explanation for this compensatory effect is that the demand for essential components is assumed to be constant, depending on the developmental stage of the larva. When food quality decreases, the larva needs to capture more prey to accommodate this demand, which is an energy-consuming process. In addition, the EFA are needed as construction material and precursors to build-up neural tissue along with cell membranes and hormones (Sargent *et al.*, 1999). Therefore, growth is limited when essential component supply is limited.

Although it is possible to compensate for nutritional value and food quantity to a certain extent, this does not necessarily happen. During the early season in the GWB, very low food quantity was coupled with extremely low food quality, and this led to very low growth rates. Variances in larval growth data were very small during this period, apart from the first date when yolk-sac larvae appeared who had not begun to externally feed. Growth of aquatic larval organisms is at least partly genetically determined (Meyer and Manahan, 2010), and slow-growing individuals may have an advantage when growth conditions are poor. Fast-growing individuals starve during bad feeding conditions leading to small variances in larval growth. In contrast, variance of larval growth is high when growth conditions are moderate or good (Houde, 1987; Voss *et al.*, 2006). In this case, relatively slow- and fast-growing individuals occur simultaneously, although the fast-growing individuals may have an ecological advantage.

Growth of larval herring in the GWB increased significantly and remained on a constant high level from 1 June onwards. Here, different aspects might have played a role: first, food quantity increased strongly on 1 June, which enabled the larvae to take up more prey with a constant quality. Second, temperature increased more than 3°C between 25 May and 1 June. This enabled the larvae to take full advantage of the improved nutritional situation. Similarly, a temperature increase of 7°C is a possible reason for higher growth rates despite very similar food quality and quantity conditions between 18 May and 15 June.

We could show in the GWB that larval growth increases with increasing DHA and EPA concentration in the larvae. The highest DHA and EPA concentrations of the copepods were reflected in the

highest DHA and EPA concentrations of the larvae and both these concentrations were likely two important factors that led to the highest larval growth rates. Conversely, only larval EPA showed an effect on larval growth in the KC, while larval DHA did not affect larval growth in our correlation analysis. The reason for the pronounced effects of larval EFAs in the GWB and EPA in the KC is that the development of prey EFA was consistent while prey quantity remained constant over the course of several weeks consequently leading to an accumulation or dilution of EFA in the larvae. In the KC, no correlation between larval DHA and their growth rates existed. Here, high food quality was offset by low food quantity, and *vice versa*, and this might have been a reason for the very similar DHA values found in the larvae over a 4-week period. Nevertheless, prey DHA probably affected larval growth in the KC, for example, on 13 May, although the strong decrease in larval DHA did not lead to decreasing DHA concentrations in the larvae themselves due to high prey quantities. St John and Lund (1996) showed that it takes 13 days until larval cod FAs were in equilibrium with the prey. However, this is just the complete effect on the FA in the larvae themselves, and not related to larval growth. The larvae are not able to take up EFA selectively, but depend on the composition delivered by the food. FAs in the larvae change successively, starting at the point when food with a different FA composition is taken up. As a result, the larvae are able to grow faster when more essential components are delivered, leading to an up-regulating of their RNA content. Contrary to their FA metabolism, larval growth is actively regulated since they are able to build-up and catabolize RNA actively. Though we suppose that this is an ongoing process, we expect a detectable time delay between the DHA concentration of the prey and larval growth of ~3–4 days at the latest, according to experimental data regarding the time delay in herring larvae facing different prey quantities (Clemmesen, 1994). However during short time frames, significant effects in larval DHA are expected only when prey quality changes strongly. Even when the effect of a changing food quality or quantity on larval DHA is not significant yet, the process is nonetheless ongoing. This could explain the constancy of larval growth and EFA during adequate growth conditions in the KC, because contrary developments of EFA in the prey and prey abundance were occurring. Additionally, other parameters not investigated in this study influence larval growth, for instance, essential amino acids and sterols. In both areas, *Acartia* spp. as well as *Eurytemora* were by far the most dominant copepod genera. Interestingly, in both habitats, the highest abundances were reached by *Eurytemora*. Schnack (1972) as well as Donner (2006) and Busch (1996) showed that both genera in all developmental stages (nauplii, copepodids, and adults) are the preferred prey items of larval herring in the estuarine habitats Schlei Fjord, KC, and GWB. The different concentrations of especially DHA in the prey between both areas are likely due to differences in the taxonomic composition of the primary producers. In the KC, *Chlorophyceae* dominate the spring bloom while diatoms are negligible (A. Stuhr, pers. comm.). This is supported by high silica values over the season, because silica is an essential nutrient for diatoms and therefore is decreasing in the water column during a diatom bloom. *Chlorophyceae* are known to be DHA poor (Dalsgaard *et al.*, 2003). However, substantial amounts of DHA and EPA could be detected in the copepods of the KC. A possible explanation for this might be trophic upgrading by protists, as shown by Klein Breteler *et al.* (1999). The underlying process is the elongation of HUFA precursors which leads to the synthesis of EPA and DHA. In contrast to the *Chlorophyceae*-dominated KC, diatoms are the major phytoplankton taxon during the spring bloom in the GWB until the depletion of nutrients, and flagellates start to take over (Edler, 2008). Diatoms are a DHA-poor taxa, while dinoflagellates are rich in this EFA (Dalsgaard *et al.*, 2003). The extremely low silica values at the beginning of our sampling period indicate a constant uptake of silicate by diatoms. From the middle of May onwards, silica values started to recover strongly and remain on a high level thereafter which might indicate the succession from diatoms to dinoflagellates. The increasing DHA values of the copepods also support this assumption.

Interestingly, yolk-sac larvae from the KC grew significantly faster and had a significantly higher DHA as well as EPA concentration than in the GWB. Therefore, maternal effects in terms of increased levels of EFAs in the eggs seem to influence not only hatching rate (Navas *et al.*, 1997; Pickova *et al.*, 1997), but also larval growth, at least in the early phase when larvae do not feed yet. A possible explanation for the different EFA concentrations and growth rates in the yolk-sac larvae is that the females from both areas fed on different quality food. Izquierdo *et al.* (2001) concluded in their review that the amount of DHA in the eggs partly depends on the diet of the females.

Mesozooplankton samples in the KC were taken only on one station. But since the same succession of copepods has been observed in the KC since 2005, a single haul could be argued to be representative for observing prey field development in this area. In the GWB, similar patterns in larval growth rates were observed between 2010 and 2012 (data not shown), which indirectly shows that similar succession patterns of the prey field occur in the GWB interannually. The prey field was sampled over the whole water

Table 3. Results from *t*-tests between prey quantity and quality of GWB and KC.

	27 April – 25 May	31 May – 15 June
Prey abundance	$p < 0.05$; KC > GWB	$p < 0.05$; GWB > KC
% DHA	$p > 0.05$	$p < 0.05$, GWB > KC
% EPA	$p > 0.05$	$p > 0.05$

Table 4. Results from *t*-tests of larval herring originating in GWB and KC.

	<9 mm	9 – 11 mm	11 – 14 mm	>14 mm
G_i I	$p < 0.001$; KC > GWB	$p < 0.001$; KC > GWB	$p < 0.001$; KC > GWB	$p > 0.05$; KC > GWB
G_i II	–	–	$p < 0.001$; GWB > KC	$p < 0.001$; GWB > KC
% DHA	$p < 0.05$; KC > GWB	$p > 0.05$	$p > 0.05$	$p < 0.01$; GWB > KC
% EPA	$p < 0.05$; KC > GWB	$p > 0.05$	$p < 0.01$; GWB > KC	$p < 0.01$; GWB > KC

The length classes reflect different ontogenetic stages of the larvae: yolk-sac (<9 mm), first feeding (9 – 11 mm), pre-flexion (11 – 14 mm), and post flexion (>14 mm). The season is divided into two time windows, according to drastic changes in prey availability and larval growth in both habitats. G_i I and DHA and EPA are results from time window 1, reaching from 27 April to 25 May, while G_i II shows results from time window 2, 31 May to 15 June. Larval FA data to test exist only from time window 1, these results are shown

column, and it was not distinguished between prey quantity and prey availability. Copepods tend to accumulate in patches, e.g. in fine layers close to the thermocline. However, both areas, GWB and KC, are well mixed due to very shallow waters in the GWB (5.6 m in depth on average) or heavy shipping traffic for the KC. Though it is not expected that patchiness does not occur in these areas, it might be reduced due to the strong mixing. Since larval growth data from both areas follow quite well the observed prey field development, we are confident that our method is reliable to describe prey field development in our investigation areas. According to Schnack (1972), prey biomass of 14 mm estuarine western Baltic herring larvae consisted of 90% copepodids and adults, and only 10% of nauplii. At least at the first-feeding stage, it is expected that the larvae feed on nauplii and protists. However, because most of the analysed larvae were beyond that stage, it is assumed that samples taken with 200 μm mesh size sufficiently describe prey field conditions for estuarine larval herring.

In the KC, prey abundance was significantly higher and larval growth rates were significantly higher compared with the GWB up until 25 May. As the season proceeded, however, in the GWB, the larvae experienced favourable growth conditions with significantly higher prey abundance and DHA concentration of the prey that led to significantly higher growth rates than in the KC. In contrast, the KC growth conditions worsened late in the season due to a strong decline in prey abundance. Interestingly, at least in recent years, this pattern of larval growth conditions seems to be typical for both nursery areas. The time-series of the KC (Catriona Clemmesen, GEOMAR) shows the same trend in prey field succession since 2005 (Donner, 2006; Peschutter, 2008; Paulsen, 2010), indicating that recruits from the KC originate mainly from early in the season. In contrast, data from the GWB time-series (Institute of Baltic Sea Fisheries) revealed that the late season provided the most recruits in recent years (Polte *et al.*, 2014). At this time, growth rates of the larvae were also highest. Since predators selectively prey upon slow growing larvae (Takasuka *et al.*, 2003), larval growth data in the present study support the recruitment data mentioned above. Our results are also consistent with calculations by Houde (1987) where even relatively small changes in growth rates can lead to strongly increased mortality in larval Atlantic herring.

Since no strong differences in larval growth conditions of both areas could be detected, there have to be other reasons for the potential importance of the GWB as a nursery area (Oeberst *et al.*, 2009b). The rough estimate of total production of both GWB and KC showed that the GWB produced 24 times as many larvae as the KC did. Although our sampling site in the KC is at the edge of the main spawning area and the true production is probably higher than the calculated one, results indicate that a possible reason for the importance of the GWB as a nursery area is simply a size effect. Since the volume of water used for spawning of the GWB is 41 times larger than that of the KC, this is tenable. This would also mean that while the KC may provide more recruits per cubic metre of water available, in absolute numbers, the GWB is superior to the KC. We are well aware that this is a very rough estimate and not a precise calculation, but it does provide one possible reason for the GWB's importance.

In conclusion, we found support for our first hypothesis that food quality significantly affects larval fish growth *in situ*. Food quality was able to compensate food quantity effects, and *vice versa*. However, our second hypothesis that the GWB generally provides better nutritional conditions for larval herring than other nursery areas in this region do was rejected. Therefore, we propose that other factors, like habitat size, might be the reason for the great importance of the GWB as a nursery area for the western Baltic spring-spawning herring.

Acknowledgements

The authors want to thank Bettina Oppermann for measuring CHN of copepod samples. Thank you to the staff of the Institute for Baltic Sea Fisheries for participating in the sampling in the GWB. Thanks also to the research vessel crews of FB "Polarfuchs" and FFK "Clupea" for their help during sampling. We would like to thank Paul Kotterba for creating Figure 1, and Luke Phelps for improving the language of the text. Thank you very much to three unknown reviewers, who helped to improve the manuscript significantly. The research was partly financed and conducted as part of the Fehmarn Belt Science Provision Project.

References

Anderson, J. T. 1988. A review of size dependent survival during pre-recruit stages of fishes in relation to recruitment. Journal of Northwest Atlantic Fishery Science, 8: 55–66.

Aneer, G. 1989. Herring (*Clupea harengus* L.) spawning and spawning ground characteristics in the Baltic Sea. Fisheries Research, 8: 169–195.

Aneer, G., Florell, G., Kautsky, U., Nellbring, S., and Sjöstedt, L. 1983. *In-situ* observations of Baltic herring (*Clupea harengus membras*) spawning behaviour in the Askö-Landsort area, northern Baltic proper. Marine Biology, 74: 105–110.

Belchier, M., Clemmesen, C., Cortes, D., Doan, T., Folkvord, A., Garcia, A., Geffen, A., *et al.* 2004. Recruitment studies: manual on precision and accuracy of tools. ICES Techniques in Marine Environmental Sciences, 33: 35 pp.

Bell, M. V., Batty, R. S., Dick, J. R., Fretwell, K., Navarro, J. C., and Sargent, J. R. 1995. Dietary deficiency of docosahexaeonic acid impairs vision at low-light intensities in juvenile herring (*Clupea harengus* L). Lipids, 30: 443–449.

Biester, E. 1989a. The distribution of spring-spawning herring larvae in coastal waters of the German Democratic Republic. Rapports et Procès-Verbaux des Réunions du Conseil Permanent International pour l'Exploration de la Mer, 190: 109–112.

Buckley, L. J., Caldarone, E. M., and Clemmesen, C. 2008. Multi-species larval fish growth model based on temperature and fluorometrically derived RNA/DNA ratios: results from a meta-analysis. Marine Ecology Progress Series, 371: 221–232.

Buckley, L. J., and Durbin, E. G. 2006. Seasonal and inter-annual trends in the zooplankton prey and growth rate of Atlantic cod (*Gadus morhua*) and haddock (*Melanogrammus aeglefinus*) larvae on Georges Bank. Deep-Sea Research Part II—Topical Studies in Oceanography, 53: 2758–2770.

Busch, A. 1996. Nahrungsökologische Untersuchungen an den Larven des Rügenschen Frühjahrsherings (*Clupea hargengus* L.) im Greifswalder Bodden in den Jahren 1990 bis 1992. Dissertation, Universität Rostock.

Cahu, C., Infante, J. Z., and Takeuchi, T. 2003. Nutritional components affecting skeletal development in fish larvae. Aquaculture, 227: 245–258.

Caldarone, E. M., Clemmesen, C. M., Berdalet, E., Miller, T. J., Folkvord, A., Holt, G. J., Olivar, M. P., *et al.* 2006. Intercalibration of four spectrofluorometric protocols for measuring RNA/DNA ratios in larval and juvenile fish. Limnology and Oceanography: Methods, 4: 153–163.

Caldarone, E. M., Onge-Burns, J. M. S., and Buckley, L. J. 2003. Relationship of RNA/DNA ratio and temperature to growth in larvae of Atlantic cod *Gadus morhua*. Marine Ecology Progress Series, 262: 229–240.

Clemmesen, C. 1993. Improvements in the fluorimetric determination of the RNA and DNA content of individual marine fish larvae. Marine Ecology Progress Series, 100: 177–183.

Clemmesen, C. 1994. The effect of food availability, age or size on the RNA/DNA ratio of individually measured herring larvae—laboratory calibration. Marine Biology, 118: 377–382.

Copeman, L. A., and Laurel, B. J. 2010. Experimental evidence of fatty acid limited growth and survival in Pacific cod larvae. Marine Ecology Progress Series, 412: 259–272.

Copeman, L. A., Parrish, C. C., Brown, J. A., and Harel, M. 2002. Effects of docosahexaenoic, eicosapentaenoic, and arachidonic acids on the early growth, survival, lipid composition and pigmentation of yellowtail flounder (*Limanda ferruginea*): a live food enrichment experiment. Aquaculture, 210: 285–304.

Cury, P., and Roy, C. 1989. Optimal environmental window and pelagic fish recruitment success in upwelling areas. Canadian Journal of Fisheries and Aquatic Sciences, 46: 670–680.

Cushing, D. 1974. The natural regulation in fish populations. *In* Sea Fisheries Research, pp. 399–412. Ed. by F.R. Harden Jones. Elek Science, London.

Cushing, D. H. 1990. Plankton production and year-class strength in fish populations: an update of the match/mismatch hypothesis. Advances in Marine Biology, 26: 249–294.

Cutts, C. J., Sawanboonchun, J., de Quero, C. M., and Bell, J. G. 2006. Diet-induced differences in the essential fatty acid (EFA) compositions of larval Atlantic cod (*Gadus morhua* L.) with reference to possible effects of dietary EFAs on larval performance. ICES Journal of Marine Science, 63: 302–310.

Dalsgaard, J., St John, M., Kattner, G., Muller-Navarra, D., and Hagen, W. 2003. Fatty acid trophic markers in the pelagic marine environment. Advances in Marine Biology, 46: 225–340.

Donner, M. 2006. Wachstum und Kondition von Heringslarven (Clupea harengus L.) in der Kieler Förde und im Nord-Ostsee-Kanal. Diploma thesis, Kiel University.

Edler, L. 2008. Einfluss einer Warmwasserleitung auf das Phytoplankton im Greifswalder Bodden. UVU zur "Errichtung und Betrieb des Gas- und Dampfturbinenkraftwerks Lubmin III EWN", Anhang II/11.

Falk-Petersen, S., Sargent, J. R., Henderson, J., Hegseth, E. N., Hop, H., and Okolodkov, Y. B. 1998. Lipids and fatty acids in ice algae and phytoplankton from Marginal Ice Zone in the Barents Sea. Polar Biology, 20: 41–47.

Furuita, H., Takeuchi, T., and Uematsu, K. 1998. Effects of eicosapentaenoic and docosahexaenoic acids on growth, survival and brain development of larval Japanese flounder (*Paralichthys olivaceus*). Aquaculture, 161: 269–279.

Grasshoff, K., Kremling, K., and Ehrhardt, M. 1999. Methods of Seawater Analysis. Wiley-VCH Verlag, Weinheim. 600 pp.

Grote, B., Ekau, W., Stenevik, E. K., Clemmesen, C., Verheye, H. M., Lipinski, M. R., and Hagen, W. 2012. Characteristics of survivors: growth and nutritional condition of early stages of the hake species *Merluccius paradoxus* and *M.capensis* in the southern Benguella ecosystem. ICES Journal of Marine Science, 69: 553–562.

Hjort, J. 1914. Fluctuations in the great fisheries of northern Europe viewed in the light of biological research. Rapports et Procès-Verbaux des Réunions du Conseil Permanent International pour l'Exploration de la Mer, 20: 1–228.

Höök, T. O., Gorokhova, E., and Hansson, S. 2008. RNA:DNA ratios of Baltic Sea herring larvae and copepods in embayment and open sea habitats. Estuarine Coastal and Shelf Science, 76: 29–35.

Houde, E. D. 1987. Fish early life dynamics and recruitment variability. American Fisheries Society Symposium, 2.

Izquierdo, M. S., Fernandez-Palacios, H., and Tacon, A. G. J. 2001. Effect of broodstock nutrition on reproductive performance of fish. Aquaculture, 197: 25–42.

Johnes, C. M. 2002. Age and growth. *In* Fishery Science: the Unique Contributions of Early Life Stages, pp. 33–63. Ed. by L. A. Fuiman, and R. G. Werner. Blackwell Sciences Ltd, Oxford.

Kattner, G., Gercken, G., and Eberlein, K. 1983. Development of lipids during a spring plankton bloom in the northern North Sea. I. Particulate fatty acids. Marine Chemistry, 14: 149–162.

Klein Breteler, W., Schogt, N., Baas, M., Schouten, S., and Kraay, G. W. 1999. Trophic upgrading of food quality by protozoans enhancing copepod growth: role of essential lipids. Marine Biology, 135: 191–198.

Kott, P. 1953. Modified whirling apparatus for the subsampling of plankton. Australian Journal of Marine and Freshwater Research, 4: 387–393.

Le Pecq, J.-B., and Paoletti, C. 1966. A new fluorometric method for RNA and DNA determination. Analytical Biochemistry, 17: 100–107.

Malzahn, A. M., Aberle, N., Clemmesen, C., and Boersma, M. 2007a. Nutrient limitation of primary producers affects planktivorous fish condition. Limnology and Oceanography, 52: 2062–2071.

Malzahn, A. M., and Boersma, M. 2009. Trophic flexibility in larvae of two fish species (lesser sandeel, *Ammodytes marinus* and dab, *Limanda limanda*). Scientia Marina, 73: 131–139.

Malzahn, A. M., Clemmesen, C., Wiltshire, K. H., Laakmann, S., and Boersma, M. 2007b. Comparative nutritional condition of larval dab *Limanda limanda* and lesser sandeel *Ammodytes marinus* in a highly variable environment. Marine Ecology Progress Series, 334: 205–212.

Meyer, E., and Manahan, D. T. 2010. Gene expression profiling of genetically determined growth variation in bivalve larvae (*Crassostrea gigas*). The Journal of Experimental Biology, 213: 749–758.

Meyer, S., Caldarone, E. M., Chicharo, M. A., Clemmesen, C., Faria, A. M., Faulk, C., Folkvord, A., *et al.* 2012. On the edge of death: rates of decline and lower thresholds of biochemical condition in food-deprived fish larvae and juveniles. Journal of Marine Systems, 93: 11–24.

Morris, I. 1981. Photosynthetic products, physiological state, and phytoplankton growth. Canadian Bulletin of Fisheries and Aquatic Sciences, 210: 83–102.

Mourente, G., Tocher, D. R., and Sargent, J. R. 1991. Specific accumulation of docosahexaenoic acid 22:6*n*-3 in brain lipids during development of juvenile turbot *Scophthalmus maximus* L. Lipids, 26: 871–877.

Navas, J. M., Bruce, M., Thrush, M., Farndale, B. M., Bromage, N., Zanuy, S., Carrillo, R., *et al.* 1997. The impact of seasonal alteration in the lipid composition of broodstock diets on egg quality in the European sea bass. Journal of Fish Biology, 51: 760–773.

Neb, K-E. 1952. Untersuchungen über Fortpflanzung und Wachstum an den Heringen in der westlichen Ostsee mit besonderer Berücksichtigung der Kieler Förde als Laichgebiet und Fangplatz. Dissertation, Universität Kiel, 145 pp.

Oeberst, R., Dickey-Collas, M., and Nash, R. D. M. 2009a. Mean daily growth of herring larvae in relation to temperature over a range of 5–20°C, based on weekly repeated cruises in the Greifswalder Bodden. ICES Journal of Marine Science, 66: 1696–1701.

Oeberst, R., Klenz, B., Gröhsler, T., Dickey-Collas, M., Nash, R. D. M., and Zimmermann, C. 2009b. When is year-class strength determined in western Baltic herring? ICES Journal of Marine Science, 66: 1667–1672.

Olivar, M. P., Diaz, M. V., and Chicharo, M. A. 2009. Tissue effect on RNA:DNA ratios of marine fish larvae. Scientia Marina, 73: 171–182.

Paulsen, M. 2010. Einfluss der Fettsäuren auf die Kondition von Heringslarven. Diploma thesis, Kiel University.

Peschutter, J. 2008. Ernährungszustand von Fischlarven in der Kieler Förde und im Nord-Ostsee-Kanal. Diploma thesis, Kiel University.

Pickova, J., Dutta, P. C., Larsson, P. O., and Kiessling, A. 1997. Early embryonic cleavage pattern, hatching success, and egg-lipid fatty acid composition: comparison between two cod (*Gadus morhua*) stocks. Canadian Journal of Fisheries and Aquatic Sciences, 54: 2410–2416.

Polte, P., Kotterba, P., Hammer, C., and Gröhsler, T. 2014. Survival bottlenecks in the early ontogenesis of Atlantic herring (*Clupea harengus*, L.) in coastal lagoon spawning areas of the western Baltic Sea. ICES Journal of Marine Science, 71: 982–990.

Rosenthal, H., and Hempel, G. 1970. Experimental studies in feeding and food requirements of herring larvae (*Clupea harengus* L.). *In* Marine Food Chains. Ed. by J. H. Steele. University of California Press, Berkeley and Los Angeles, CA.

Sargent, J., Bell, G., McEvoy, L., Tocher, D., and Estevez, A. 1999. Recent developments in the essential fatty acid nutrition of fish. Aquaculture, 177: 191–199.

Schnack, D. 1972. Nahrungsökologische Untersuchungen an Heringslarven. Ber dt wiss Kommn Meeresforsch, 22: 273–343.

Sinclair, M. 1988. Marine Populations: an Essay on Population Reulation and Speciation. University of Washington Press, Seattle.

Sinclair, M., and Tremblay, M. J. 1984. Timing of spawning of Atlantic herring (*Clupea harengus harengus*) populations and the match–mismatch theory. Canadian Journal of Fisheries and Aquatic Sciences, 41: 888–898.

St John, M., and Lund, T. 1996. Lipid biomarkers: linking the utilization of frontal plankton biomass to enhanced condition of juvenile North Sea cod. Marine Ecology Progress Series, 131: 75–85.

St John, M. A. S., Clemmesen, C., Lund, T., and Koester, T. 2001. Diatom production in the marine environment: implications for larval fish growth and condition. ICES Journal of Marine Science, 58: 1106–1113.

Takasuka, A., Aoki, I., and Mitani, I. 2003. Evidence of growth-selective predation on larval Japanese anchovy *Engraulis japonicus* in Sagami Bay. Marine Ecology Progress Series, 252: 223–238.

Van Anholt, R. D., Spanings, E. A. T., Koven, W. M., Nixon, O., and Bonga, S. E. W. 2004. Arachidonic acid reduces the stress response of gilthead seabream *Sparus aurata* L. Journal of Experimental Biology, 207: 3419–3430.

Voss, R., Clemmesen, C., Baumann, H., and Hinrichsen, H. H. 2006. Baltic sprat larvae: coupling food availability, larval condition and survival. Marine Ecology Progress Series, 308: 243–254.

Weber, W. 1971. Die Laichplätze des Herings (*Clupea harengus* L.) der westlichen Ostsee. Kieler Meeresforsch, 27: 194–208.

Handling editor: Claire Paris

ICES Journal of Marine Science

ICES Journal of Marine Science (2014), 71(4), 1001–1009. doi:10.1093/icesjms/fst011

Contribution to the Themed Section: 'Larval Fish Conference'

Original Article

Individual growth history of larval Atlantic mackerel is reflected in daily condition indices

Dominique Robert[1]*, Pierre Pepin[2], John F. Dower[3], and Louis Fortier[4]

[1]*Centre for Fisheries Ecosystems Research, Fisheries and Marine Institute, Memorial University of Newfoundland, PO Box 4920, St John's, NL, Canada A1C 5R3*
[2]*Fisheries and Oceans Canada, Northwest Atlantic Fisheries Centre, PO Box 5667, St John's, NL, Canada A1C 5X1*
[3]*School of Earth and Ocean Sciences, University of Victoria, PO Box 1700, STN CSC Victoria, BC, Canada V8W 3N5*
[4]*Québec-Océan, Département de Biologie, Université Laval, 1045 avenue de la Médecine, Québec, QC, Canada G1V 0A6*

**Corresponding author: tel: +1 709 778 0499; fax: +1 709 778 0669; e-mail: dominique.robert@mi.mun.ca*

Robert, D., Pepin, P., Dower, J. F., and Fortier, L. 2014. Individual growth history of larval Atlantic mackerel is reflected in daily condition indices. – ICES Journal of Marine Science, 71: 1001–1009.

Received 25 September 2012; accepted 15 January 2013; advance access publication 8 February 2013.

We tested the hypothesis that faster-growing Atlantic mackerel (*Scomber scombrus*) larvae generally achieve better feeding success than their slower-growing counterparts. Feeding success and growth were derived from the analysis of gut content and otolith microstructure of larvae from four cohorts (1997–2000) from the southern Gulf of St Lawrence. We observed a high degree of serial correlation in otolith growth (OG) from hatching, suggesting that events occurring early in life have long-standing effects on future growth potential. The diet of fast-growing individuals was dominated by large prey, such as cladocerans and fish larvae (including conspecifics), while slow-growing larvae foraged primarily on smaller copepod naupliar stages. Both feeding success (stomach content) and an index of condition (body depth) were positively correlated with OG, and these relationships explained approximately three times more variance in mackerel than in larval radiated shanny (*Ulvaria subbifurcata*) of similar size. Relationships linking age-dependent scores of body depth to feeding success and growth were ~3.5–4 times stronger than those based on length-dependent indices, suggesting that differences in energy allocation during early ontogeny may play a significant role in determining an individual's capacity to cope with variations in feeding conditions.

Keywords: feeding, growth, larval fish, otolith microstructure, *Scomber scombrus*, stomach content.

Introduction

The availability of adequate prey during the early larval stage is considered one of the main sources of year-class fluctuations in marine fish populations (Hjort, 1914; Cushing, 1990; Houde, 2008). It is widely accepted that poor feeding success leads to increased larval mortality through suboptimal growth (Anderson, 1988), as slow-growing individuals generally suffer higher vulnerability to predation (e.g. Miller *et al.*, 1988; Takasuka *et al.*, 2003) for an extended period (e.g. Chambers and Leggett, 1987). However, despite being a key assumption of the growth-survival paradigm, the link between feeding success and growth at the individual level remains poorly characterized in the field (Dower *et al.*, 2009). The main problem when linking feeding and growth in larvae captured at sea is that both vital rates are not sampled on the same temporal scale. Feeding success is estimated from stomach content, representing at most the last few hours of foraging before capture (e.g. Llopiz and Cowen, 2008), while growth derived from otolith microstructure integrates events experienced during the days before capture (e.g. Pepin *et al.*, 2001).

Despite the temporal resolution mismatch between stomach content and otolith microstructure, a positive relationship linking feeding success to growth is to be expected. The strong serial correlation usually found in larval daily growth trajectories (Pepin *et al.*, 2001; Dower *et al.*, 2009) implies that events

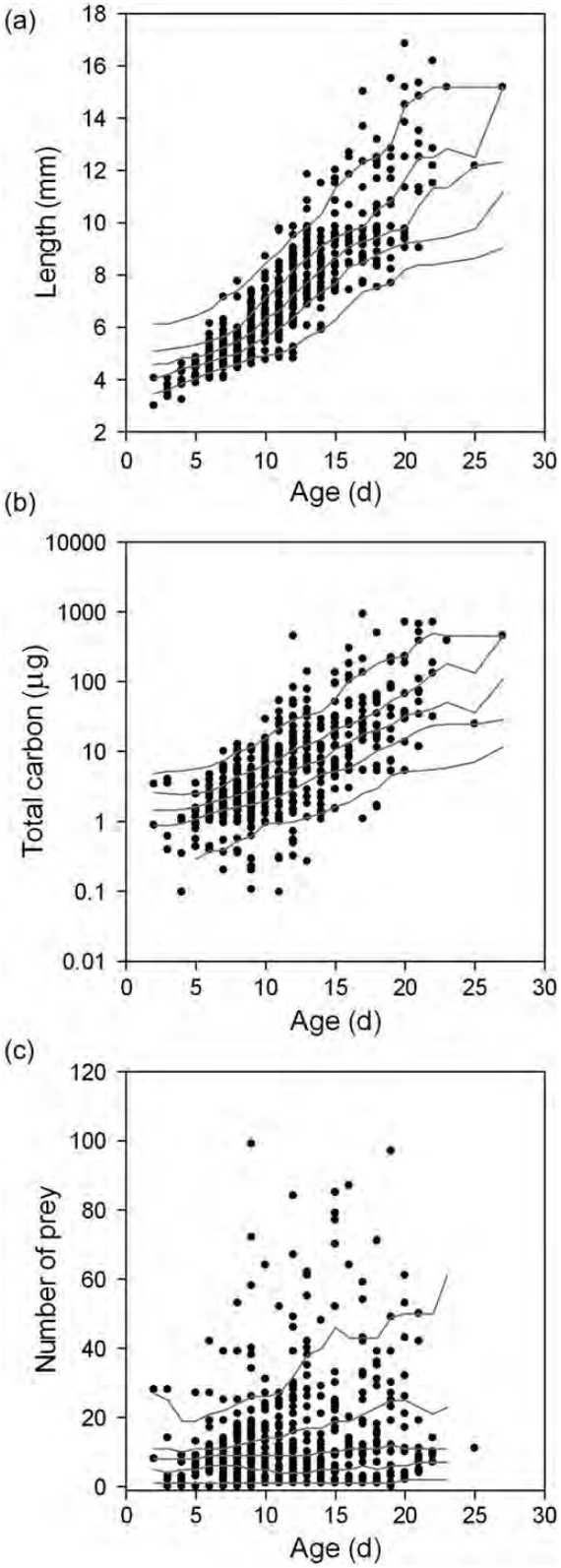

Figure 1. (a) Length (bandwidth = 0.75 d), (b) total carbon of prey per stomach (bandwidth = 1.45 d), and (c) number of prey per stomach (bandwidth = 1.95 d) in relation to otoliths estimated age of Atlantic mackerel larvae. Solid lines indicate the 10th, 30th, 50th, 70th, and 90th percentiles of the distribution of observations based on non-parametric local density estimation.

experienced early in life may drive future survival potential. Hence, the Markov chain of successful feeding events resulting in a fast growth trajectory would strongly depend on initial feeding success and the capacity of individuals to overcome the influence of environmental variability and stochasticity. Fast-growing individuals could in turn achieve large size-at-age, high swimming performance, and ultimately high feeding success through a positive feedback loop. Atlantic mackerel (*Scomber scombrus*) is an ideal candidate species for testing retroactive mechanisms linking feeding success to growth: the larval stage is characterized by fast yet variable growth, and intra-cohort cannibalism implies that the fastest-growing individuals rapidly acquire the ability to prey on their smaller siblings (Robert *et al.*, 2008). The latter characteristic likely explains the strong selection for fast growth usually occurring throughout the larval stage (Robert *et al.*, 2007).

A previous study by Robert *et al.* (2009) revealed relationships linking feeding success and growth performance to preferred prey availability in first-feeding Atlantic mackerel larvae. Both feeding success and growth increased exponentially at a decreasing rate until reaching satiation at a density of $\sim$1 µg C l^{-1} of their preferred *Pseudocalanus* sp. nauplii prey. The similarity of both relationships provided direct evidence for food limitation during the first-feeding stage and indirect evidence for the assumed link between larval growth and feeding success. In the present study, we provide a direct test to the expected relationship linking growth performance with feeding success. Non-parametric local density estimators (Pepin *et al.*, 1999; Dower *et al.*, 2009) are used to assess correlation among individual age-dependent percentile scores of larval states (body length, depth at anus, stomach content, growth). Furthermore, we contrast early life strategy of Atlantic mackerel to that of radiated shanny (*Ulvaria subbifurcata*) described by Dower *et al.* (2009).

Material and methods

Field methods

Mackerel larvae (standard length 3–18 mm) were sampled from July to mid-August in four consecutive years (1997–2000) during weekly one-day (16:00–24:00 h) surveys offshore of the Magdalen Islands, southern Gulf of St Lawrence (Robert *et al.*, 2009). Sampling methods for mackerel larvae and zooplankton are detailed in Robert *et al.* (2007, 2008). Briefly, the sampler consisted of a rectangular metal frame carrying four plankton nets deployed in a double-oblique tow pattern ($\sim$20 min duration at a ship speed of $\sim$1.3 m s^{-1}): two 750-µm mesh nets captured fish larvae, while two 64-µm mesh cylindrical nets sampled mesozooplankton. Temperature and depth profiles were obtained from a Vemco Minilog® probe set on the frame. Mackerel larvae were preserved in 95% ethanol for further otolith analyses, while mesozooplankton collected in the 64-µm mesh nets was fixed in a 4% formalin seawater solution. The standard lengths of preserved larvae were measured in the laboratory under the dissecting microscope and converted into fresh standard length using the regression equation provided by Migoya (1989). Stratified subsamples of mackerel larvae were then used for the assessment of growth and feeding success by randomly selecting individuals from predetermined length classes in each year. Over the 4 years of sampling, both feeding and growth patterns were evaluated in 516 larvae.

The analysis of larval stomach content is detailed in Robert *et al.* (2008). In summary, the digestive tract of each mackerel

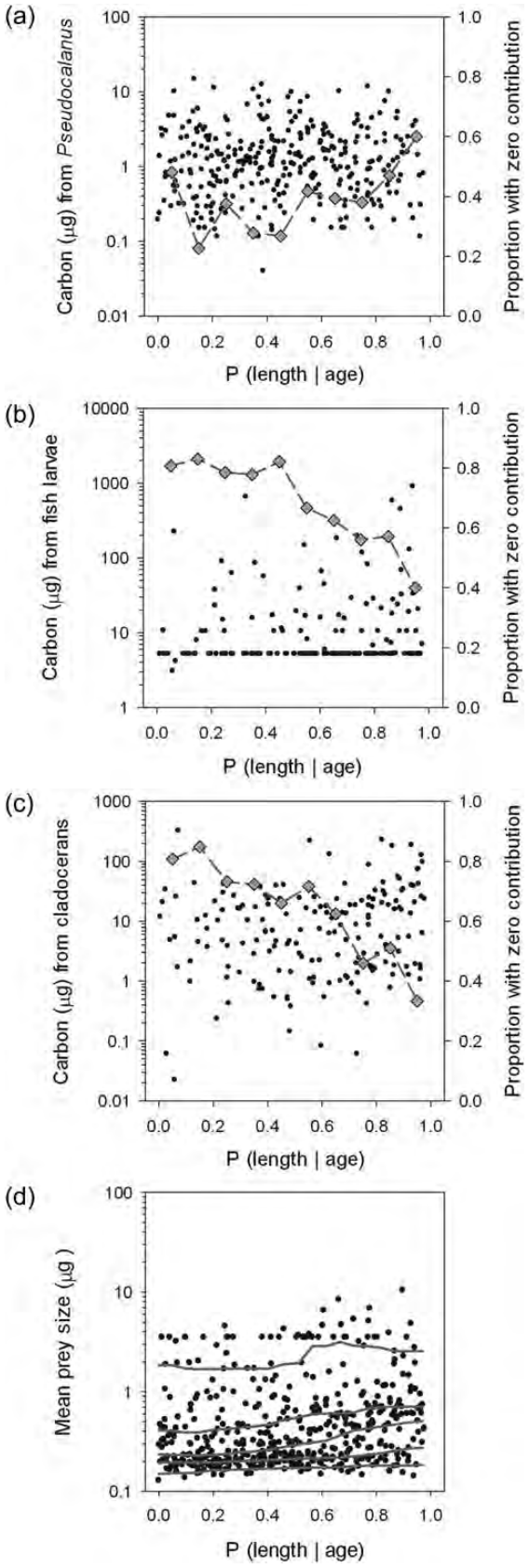

Figure 2. Carbon content of (a) *Pseudocalanus* sp., (b) fish larvae, (c) cladoceran prey in the larval diet, and (d) average prey size of individual larvae in relation to the percentile score of length-at-age of Atlantic mackerel larvae (black circles). In (a)–(c), the proportion of stomachs with zero contribution of each prey type for each 10th percentile score interval of length-at-age is represented by the grey diamonds and dashed line referenced to the right axis. In (d), solid lines indicate the 10th, 30th, 50th, 70th, and 90th percentiles of the distribution of observations based on non-parametric local density estimation.

larva was dissected under a stereoscopic microscope and each prey item was measured and identified to the lowest taxonomic level possible. Carbon content of each prey item was estimated using specific length-weight relationships (Robert *et al.*, 2008). For larval fish prey, tissue degradation due to rapid digestion often prevented the precise measurement of standard length. Because most identifiable larval fish prey were newly hatched Atlantic mackerel (Robert *et al.*, 2008), we adopted a conservative approach and considered the mean hatching size of mackerel (3.5 mm) to attribute a carbon value (5.168 µg C) to these digested prey.

Larval age and somatic growth trajectory were estimated from the number and width of otolith daily growth increments (Robert *et al.*, 2007). Sagittal otoliths were mounted on slides using Crystalbound® thermoplastic cement, and polished with 3M® 30 and 3 µm metallurgical lapping films when needed. Otolith microstructure was assessed using an optical microscope (×1000) connected to an Image-Pro Plus® image analysing system with a digital camera.

Data analysis

We used non-parametric local density estimators (Davison and Hinkley, 1997) to describe the change in variability in larval state (i.e. length, growth, feeding) with age. Details of the approach are outlined by Pepin *et al.* (1999). Briefly, the method provides a locally weighted estimate of the cumulative probability distribution (CDF) of observations as a function of a covariate x (such as length or age) and surrounding observations using kernel smoothing. In our analysis, the weighting function is $w(d) = e^{-d}$, where $d = |x_i - x|/b$, and b is a bandwidth parameter which describes how far "local" extends. We determined the value of b by cross–validation: we deleted each observation in turn, used the rest of the data to predict the deleted observation, computed the sum of squared differences of the residuals for all observations, then chose the value of b that minimized this sum. This was possible because of the large number of observations in our dataset, which produced a relatively smooth change in the CDF of variables in relation to age using cross-validation (i.e. the CDF was not over fit, which can happen when data are scarce or widely separated, as was encountered by Dower *et al.* (2009) who had to specify a bandwidth of 2.5 d). Relative to most generalized linear models, this approach has the advantage of making no assumptions about the underlying age- or length-dependence of the variance structure. Hence, the states [i.e. gut content, body length, body depth, and otolith growth (OG)] of each individual can be described in terms of age- or length-dependent percentile scores, providing relative indices of larval "performance" standardized over a uniform distribution ranging from 0 to 1.

Results

Length increased monotonically with age with some indication of an accelerating rate of increase in older larvae (Figure 1a). The scatter (i.e. the difference between the 10th and 90th percentiles

of the distribution) increased significantly from 1.34 mm in 2-d-old larvae to ~6 mm in 20-d-old larvae. Percentile scores of length-at-age [P(length|age)] were very weakly and negatively correlated with water temperature at capture ($r = -0.28$, $p < 0.001$).

Only 21 of the 516 mackerel larvae (4.1%) had empty stomachs. Total stomach carbon content followed a non-linear relationship with age (Figure 1b). The logarithm of scatter was relatively constant with age. Deviations of percentile scores from the median did not show evidence of a strong diurnal pattern in feeding success. Percentile scores of total stomach carbon content at age [P(carbon|age)] were weakly and negatively correlated with water temperature at capture ($r = -0.16$, $p < 0.001$). The maximum number of prey per stomach also increased with age (Figure 1c). While the median increased only slightly from 8 prey in 2-d-old larvae to 11 prey in 20-d-old larvae, the 90th percentile increased from ~20 to ~50 prey over the same age interval (Figure 1c).

The calanoid copepods *Pseudocalanus* sp. and *Temora* sp., cladocerans, and fish larvae were found in 62, 35, 34, and 30% of stomachs, respectively. Together, these four prey categories accounted for an average proportion of 0.68 of prey found in mackerel stomachs (median = 0.77, s.d. = 0.29; interquartile range: 0.5–0.91). The contribution of *Pseudocalanus* sp. to the total carbon was largely independent of the percentile score of length-at-age, although the relative frequency of individuals found without this prey item increased slightly in larger-at-age individuals (Figure 2a). In contrast, mackerel larvae that were small-at-age tended to have lower relative and absolute contributions of carbon from larval fish prey relative to individuals that were large-at-age (Figure 2b). Cladocerans were also more likely to be found in the stomachs of larger individuals at a given age, although no trend was observed between cladoceran carbon content and the percentile score of length-at-age when this prey taxon was found in the stomach (Figure 2c). The changes are reflected in the near doubling of the median average prey size of individuals that were large-at-age relative to the smallest individuals at age (Figure 2d).

Before growth analyses, we assessed the strength of the link between OG (distance from hatch mark to the edge) and standard length, as well as the potential decoupling between these two growth metrics with changes in environmental conditions (e.g. Folkvord *et al.*, 2000). To address this issue, the linear relationship of length-at-age was first estimated (L–A; $L = 1.67 + 0.49\,A$, $r = 0.87$, $p < 0.001$; Figure 1a). OG was then modelled in relation to standard length using non-linear least squares because of increasing variability in the former with increasing length (OG–L; $\mathrm{OG} = -1.9 + 0.98\,L^{1.55}$, $r = 0.96$, $p < 0.001$; Figure 3a). In the eventuality of decoupling between OG and standard length, the distribution of residuals of the OG–L relationship should differ between individuals with high and low growth rates (residuals from L–A). The residuals from the L–A relationship were not

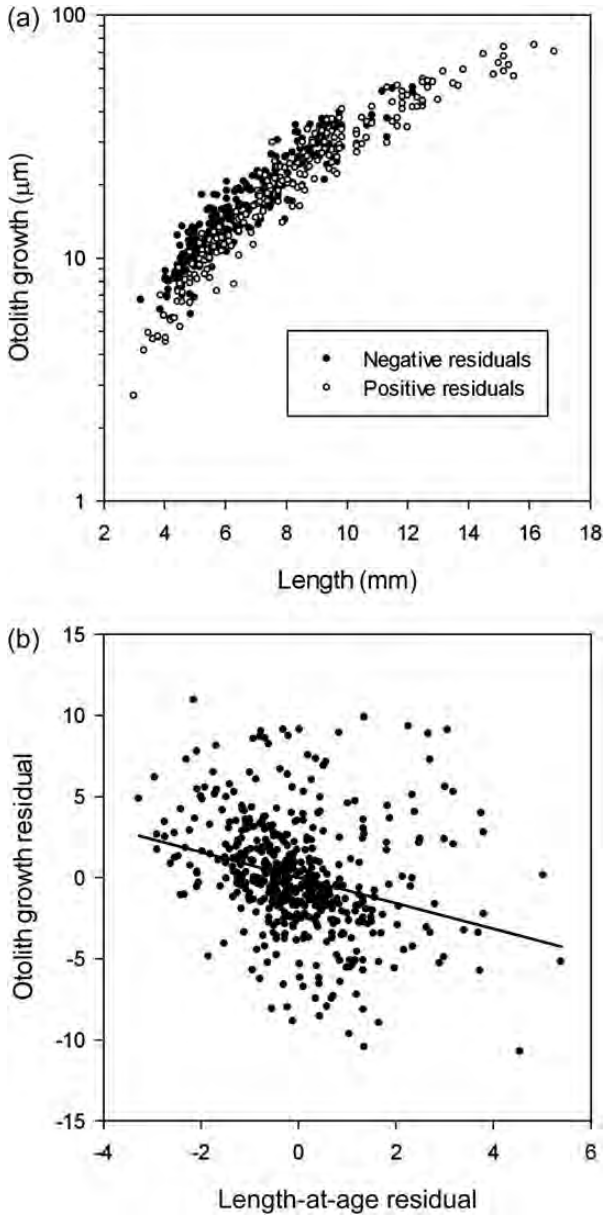

Figure 3. (a) OG in relation to standard length. Closed symbols represent individuals with negative residuals from the linear length-at-age relationship (smaller at age); open symbols represent individuals with positive residual from the length-at-age relationship (larger at age). (b) Residuals from the otolith–length relationship plotted against the residuals of the length-at-age relationship.

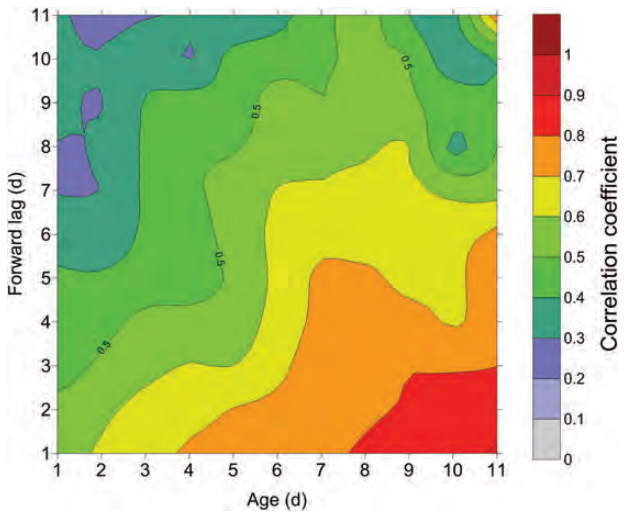

Figure 4. Age-dependent serial correlation coefficient (r, value represented by the colour scale) of otoliths increment widths of Atlantic mackerel larvae. Forward lag is the number of daily increments after a given otolith increment.

independent of those from the OG–L relationship ($r = -0.28$, $p < 0.001$, $n = 516$; Figure 3b), indicating a small degree of decoupling between otolith and somatic growth in Atlantic mackerel. Slow-growing individuals were characterized by greater cumulative OG at length relative to younger individuals at the same length, though based on a relatively weak trend that accounts for less than 8% of the variance in residuals of the OG–L relationship.

We found strong serial correlation in growth of Atlantic mackerel, which tended to increase with age (Figure 4). The *e*-folding scale (time-scale for r to decrease to the value of $1/e = 0.368$) was about 5 d in the youngest larvae and increased to 10 d or more when the larva reached ~1 week of age.

The percentile score of total carbon ingested by mackerel larvae [P(carbon|age)] was strongly correlated with length-at-age [P(length|age); $r = 0.48$, $p < 0.001$], whereas the relationship with the number of prey per stomach [P(number|age)] was much weaker ($r = 0.15$, $p < 0.001$; Figure 5). Overall, larger individuals at a given age were more likely to have a larger prey mass in their stomach; however, greater ingestion rate was achieved by feeding on larger organisms rather than on a greater number of smaller prey (Figure 2).

Except the youngest larval age class (1–5 d), the percentile score of total prey carbon at age was always positively correlated with increment width (Figure 6). The percentile score of the number of prey in the stomach at age was nearly uncorrelated with increment width, except the oldest larval age class (16–20 d) from the age of 10 d on (Figure 6b).

Body depth at anus, often used as an index of condition in larval fish, followed an allometric relationship with SL according to a power of 1.44, which was significantly greater than direct proportionality ($t = 60.3$, $p < 0.001$; Figure 7a). The age-dependent percentile score of body depth [P(body depth|age)] was strongly correlated with OG [P(OG|age); $r = 0.74$, $p < 0.001$] (Figure 7b). A weaker relationship between the age-dependent

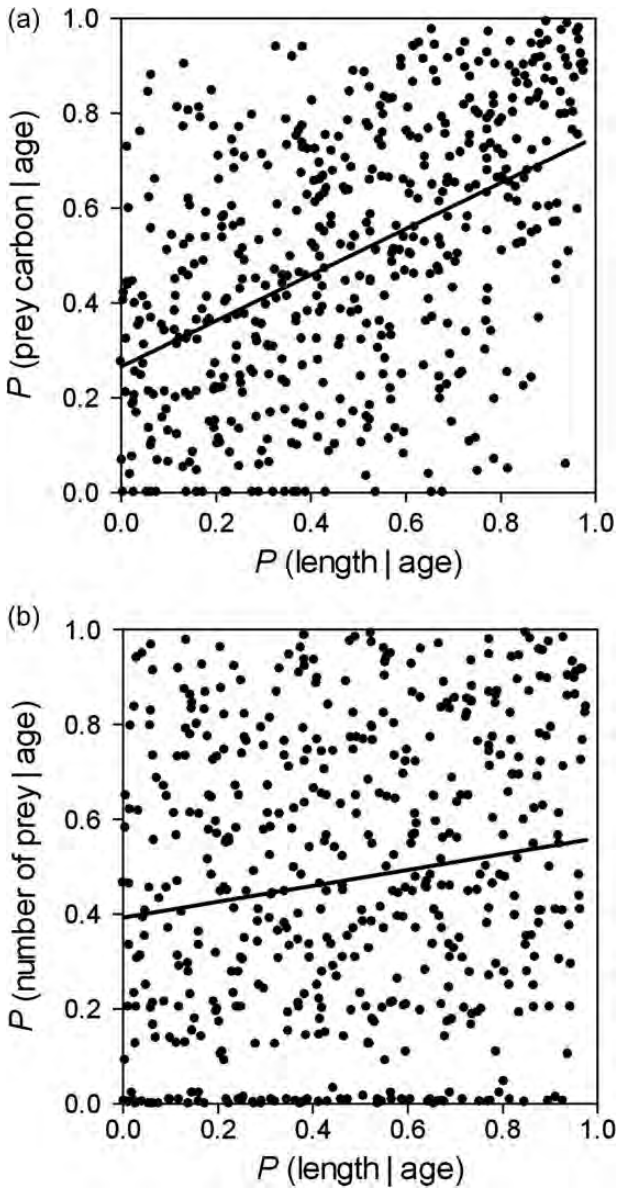

Figure 5. Percentile score of (top panel) total prey carbon and (bottom panel) number of prey in relation to percentile score of length-at-age.

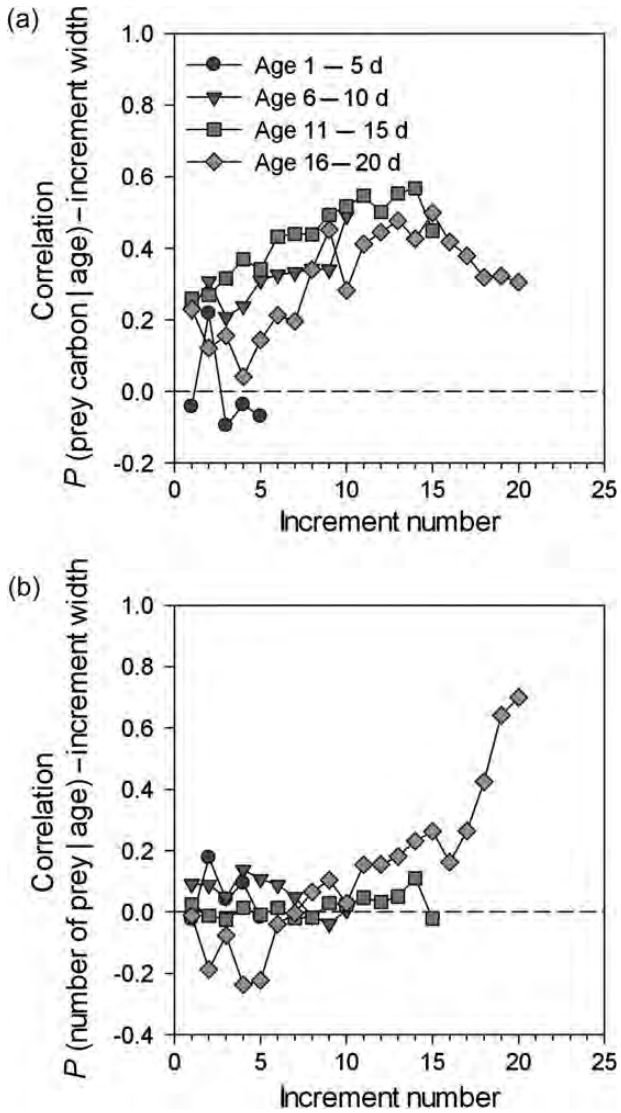

Figure 6. Age-specific correlation of otolith increment width with (a) percentile score of total prey carbon and (b) number of prey per stomach.

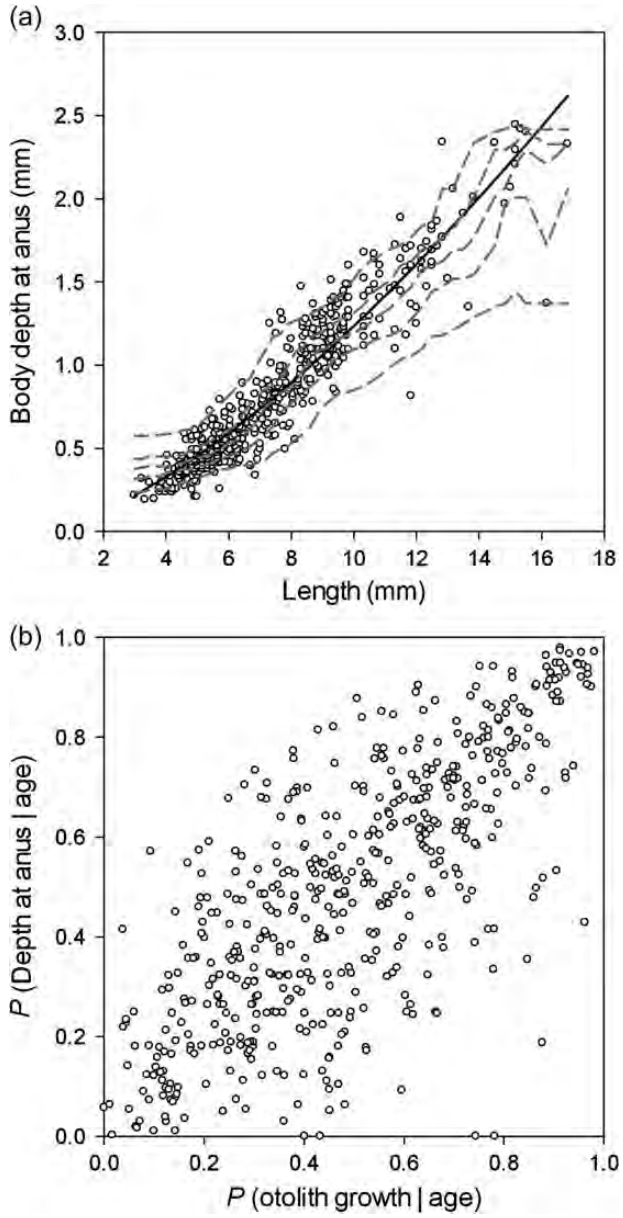

Figure 7. (a) Body depth at anus in relation to the standard length of mackerel larvae. The solid line represent least squares fit to the allometric relationship $Y = 0.045\ X^{1.44}$ [$r = 0.94$, $p < 0.001$; s.e.(multiplier) = 0.0024, s.e.(exponent) = 0.024)]. The short dashed lines represent the 10th, 30th, 50th, 70th, and 90th percentiles of the distribution of observations based on a bandwidth of 0.9 mm. (b) Percentile score of body depth at anus in relation to the percentile score of increment width.

percentile score of body depth and total prey carbon ($r = 0.51$, $p < 0.001$) (not shown) was found, similar to that between prey carbon and length-at-age (Figure 5a). The length-dependent percentile score of body depth at anus [P(body depth|length)], a common index of condition that does not require ageing (Ferron and Leggett, 1994), was correlated with both OG at age ($r = 0.37$, $p < 0.001$) and total prey carbon at age ($r = 0.27$, $p < 0.001$), but not to length-at-age [P(length|age); $r = -0.011$, $p > 0.2$].

Discussion

Although random events are likely to play some role in an individual's growth history, it is inevitable that fish larvae achieving good growth rely on some considerable degree of effective foraging rather than exclusively on good luck. A large body of literature supports the growth-survival paradigm that fast-growing individuals generally survive in a larger proportion relative to their slower-growing counterparts (e.g. Meekan and Fortier, 1996; Robert *et al.*, 2007; Takasuka *et al.*, 2007). A key assumption of the paradigm is that fast growth of these survivors is generally achieved through superior feeding (Anderson, 1988; Cushing, 1990). Variability in individual feeding success is mainly determined by the combination of individual differences in ability to capture prey and spatio-temporal variability in adequate prey availability. Our results clearly demonstrate that individuals achieving higher growth rate at a given age were generally those that foraged the most efficiently. Growth achieved on a given day was significantly correlated with indices of both short-term (stomach content) and long-term (depth at anus) feeding success. These findings are similar to those for radiated shanny (Dower *et al.*, 2009), but the relationship between carbon stomach content and length-at-age explained approximately three times more variance in mackerel than in shanny. The percentile score of total prey carbon at age was always positively correlated with increment width past the first-feeding stage (Figure 6a). Moreover, the correlation coefficient increased with age, suggesting that an individual's past growth history becomes increasingly reflected in its ability to capture prey. The absence of correlation between the percentile score of the number of prey and increment width (Figure 6b) before the age of 16 d indicates that this retroaction loop is achieved by increasing prey size rather than prey number (Figure 2; Robert *et al.*, 2008). In combination with the strong autocorrelation in OG (Figure 4), these results indicate that feeding success achieved by Atlantic mackerel at the onset of exogenous feeding can have long-lasting consequences to growth patterns, which may in turn determine the survival probability of an individual.

Feeding success is the outcome of the probabilities of encounter, attack, and capture, which is affected by both the environment (e.g. physical structure and dynamics, prey type) and individual ability related to morphological features and behaviour (Hunter, 1980; Buskey *et al.*, 1993). Larvae of both Atlantic mackerel and radiated shanny emerge during early summer, when prey are generally abundant and the water column is stratified. Morphologically, mackerel larvae have a larger mouth than radiated shanny of the same length (Ware and Lambert, 1985; Pepin and Penney, 1997), thereby providing them with opportunities to feed on larger prey and which they take the advantage of by feeding on fish larvae at an early stage of their ontogeny (Ware and Lambert, 1985; Fortier and Villeneuve, 1996; Robert *et al.*, 2008), whereas shanny feed almost exclusively on nauplii and copepodites of calanoid copepods (Dower *et al.*, 2009; Young *et al.*, 2010). These contrasting patterns of prey preference also suggest that mackerel may be considered an aggressive predator capable of pursuing and catching highly active prey. Dower *et al.* (2009) proposed that the feeding abilities of radiated shanny were probably limited, citing evidence from a decoupling of feeding patterns and reconstructed growth histories when shanny larvae were undergoing transitions from feeding on nauplii to copepodites. The results of the morphological and behavioural differences

between larvae of Atlantic mackerel and radiated shanny are apparent in the greater degree of autocorrelation of individual growth rates in the former relative to the latter (Figure 4; Dower *et al.*, 2009). Effective predators are more likely to be able to maintain optimal growth rates relative to predators that are less efficient. Although we do not have information on the maximum feeding rates of Atlantic mackerel larvae, we know that under most circumstances radiated shanny do not achieve maximal feeding rates, with the majority of individuals achieving less than 50% of their maximum daily weight-specific consumption rate (Young *et al.*, 2010). This would, in turn, affect their ability to maintain their growth rates and thereby lead to weaker autocorrelation as a result of day-to-day variations in feeding success relative to species that are more effective at achieving higher relative feeding rates, as may be the case for Atlantic mackerel. When the data from Young *et al.* (2010) are contrasted with this study, two features become apparent (Figure 8). First, there is less scatter (i.e. variance) in the data for Atlantic mackerel relative to radiated shanny; second, the amount of material found in stomachs of radiated shanny begins to level off at a length of ~7 mm, a size at which Atlantic mackerel increase the diversity of their prey and feed more extensively on cladocerans and fish larvae (Robert *et al.*, 2008). Obligated fast growth resulting from intracohort cannibalism is likely the main factor explaining the high food intake observed throughout the larval and early juvenile stages of Atlantic mackerel. Extending similar analyses to other species would provide insight into interspecific differences in feeding ability if patterns of autocorrelation are shown to exhibit corresponding changes with immediate measures of state (e.g. stomach content).

Previous studies have demonstrated considerable evidence of decoupling between otolith and somatic growth in larval fish exposed to suboptimal feeding conditions (Secor and Dean, 1989, 1992; Campana, 1990; Folkvord *et al.*, 2000). Under most circumstances, slow-growing individuals under poor feeding conditions have larger otoliths at length than do individuals with faster growth rates. Dower *et al.* (2009) were unable to find statistical significant evidence for this in radiated shanny, which seldom feeds at maximal rates (Young *et al.*, 2010). Contrastingly, we found uncoupling in Atlantic mackerel, which have fuller stomachs than shanny at a given length, particularly in large individuals. In all instances, the contrast in the residuals from the OG–L relationship of fast- vs. slow-growing individuals, defined as their position relative to a length-at-age relationship, is generally small relative to the overall OG–L function but does indicate that some level of error would be incurred by using otolith size alone as an index of condition. Departures from a direct functional response in both otolith and somatic growth may be of little importance when contrasting age-dependent growth histories to assess the significance of selective mortality (Meekan and Fortier, 1996; Baumann *et al.*, 2003) but the issue may be of particular consequence in attempting to reconstruct body size over time (Campana, 1990; Francis, 1990; Secor and Dean, 1992) as well as in the development of inferences between OG and feeding conditions. Such decoupling could result from a slower response in OG relative to somatic growth due to the deterioration in feeding conditions (Folkvord *et al.*, 2000) or from a minimum level of OG occurring independent of a larva's metabolic state (Secor and Dean, 1989, 1992). As a result, OG would be considered to have stronger serial correlation and thereby provide a reflection of the "average" conditions encountered by each larva, relative to somatic growth. The degree of decoupling will be the result of the sensitivity of growth rates to changes in ingestion rates as well as the magnitude of variations in feeding success among individuals. Given that we found less variation in stomach contents in Atlantic mackerel relative to radiated shanny but that we found greater evidence for decoupling between otolith and somatic growth rates, we can infer that differences in the sensitivity of these two physiological processes appear to be greater in mackerel. One must be cautious about this interpretation, however, because this may also depend on the extent to which individuals achieve maximal feeding rates, which we know for radiated shanny (Bochdansky *et al.*, 2008) but not for mackerel, and possibly as a result of differences in the functional relationship of otolith and somatic growth rates with ingestion rates, as suggested by Folkvord *et al.* (2000). If we assume that ingestion follows a Holling type II response relative to prey availability, the greatest rate of change in feeding rates occurs at low prey concentrations rather than at concentrations at which larvae can achieve maximal feeding rates. Thus, larvae in suboptimal feeding conditions would be more likely to exhibit variations in feeding success, and thereby greater decoupling between somatic and OG, than would individuals feeding near maximal ingestion rates. We have reason to believe, however, that the occurrence of suboptimal feeding conditions in our study is unlikely to influence our interpretation about the greater sensitivity of mackerel. Growth rates measured in this study are at the upper range of those measured by Ware and Lambert (1985) at average temperatures ~15°C, and greater than those measured under laboratory conditions by Mendiola *et al.* (2007). This suggests that mackerel larvae from our study were feeding close to their maximal ingestion rates, whereas most of shanny larvae examined by Dower *et al.* (2009) were feeding well below 50% of their maxima (Young *et al.*, 2010). Although previous studies have inferred that decoupling

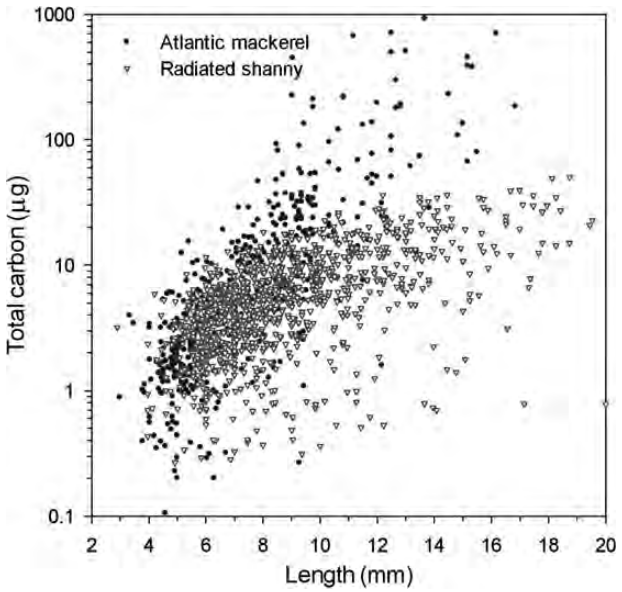

Figure 8. Comparison of total prey carbon per stomach in relation to length for Atlantic mackerel and radiated shanny. Data for radiated shanny are from Young *et al.* (2010) and represent the combined information from several years of sampling using protocols similar to those used in this study.

between otolith and somatic growth is the result of poor or rapid changes in feeding conditions, the contrast we note between radiated shanny, feeding at suboptimal rates, and Atlantic mackerel, likely feeding near their maximum rate, may indicate that taxonomic differences may also affect the link between these two indices of development.

Beyond approaches based on the analysis of otolith microstructure, the state or condition of larval fish has been evaluated using a variety of morphological, biochemical (e.g. nucleic acid ratios), and histochemical (e.g. liver, pancreatic or intestinal enzymes) indices (Ferron and Leggett, 1994; Gisbert *et al.*, 2008). The value of each index in detecting subtle changes in the state of larvae depends on how much of an individual's past is represented by changes in the metric(s). Although only otolith can provide an individual's daily growth history, multivariate approaches based on morphometric measurements have often proven useful in interpreting the state of an individual, e.g. with elements related to body depth and/or girth frequently demonstrating a high degree of sensitivity to changes in feeding conditions (e.g. Lochmann and Ludwig, 2003; Morton, 2012). Our comparison of the percentile scores of anal body depth revealed moderate to strong relationships with age-dependent scores for growth rates and stomach contents, confirming the value of this simple morphometric index as a measure of an individual's condition. More importantly, these relationships were ~3.5–4 times stronger than those based on length-dependent scores. This sharp contrast in the correspondence between the different metrics of state based on age- vs. size-dependent perspectives suggests that the history of individual larvae may play a significant role in determining the state of the animal at the time of capture. Developmental norms and ontogenetic events may largely follow weight- or length-dependent relationships (Ferron and Leggett, 1994) but variability around these norms can result in differential feeding abilities (Portt and Balon, 1984). Many processes in aquatic systems are well represented using size-dependent relationships, which has been exploited in attempts at generalizations (Houde, 1989; Pepin, 1991) as well as in modelling (e.g. Hufnagl and Peck, 2011), but these approaches have essentially overlooked how differences in the ontogenetic development of each individual might have varied and affected their capacity to cope with variations in feeding conditions. Studies of ontogenic events are generally qualitative (e.g. Baglole *et al.*, 1997; He *et al.*, 2012) but Morton (2012) suggested that differential energetic allocation during ontogeny explains some of the variations in growth among species based on a path model that aimed to predict larval body mass based on biochemical and histological variables. Although it is uncommon to consider variations in ontogenetic state in population studies of early life stages, it is important to bear in mind that such initiatives track organisms that are undergoing developmental events likely to have energetic consequences to an individual's capacity to feed and avoid predators and that will also reflect its history.

Acknowledgements

We thank L. Michaud, L. Létourneau, V. Perron, V. Gagné, M. Pilote, and H. Cloutier for their precious contribution to laboratory analyses. Suggestions from D. H. Secor and one anonymous reviewer helped improve an earlier version of the manuscript. Support from the Natural Science and Engineering Research Council of Canada (NSERC) and the NSERC Research Network GLOBEC-Canada to LF is acknowledged.

References

Anderson, J. T. 1988. A review of size dependent survival during pre-recruit stages of fishes in relation to recruitment. Journal of Northwest Atlantic Fisheries Science, 8: 55–66.

Baglole, C. J., Murray, H. M., Goff, G. P., and Wright, G. M. 1997. Ontogeny of the digestive tract during larval development of yellowtail flounder: a light microscopic and mucous histochemical study. Journal of Fish Biology, 51: 120–134.

Baumann, H., Pepin, P., Davidson, F. J., Mowbray, F., Schnack, D., and Dower, J. F. 2003. Reconstruction of environmental histories to investigate patterns of larval radiated shanny (*Ulvaria subbifurcata*) growth and selective survival in a large bay of Newfoundland. ICES Journal of Marine Science, 60: 243–258.

Bochdansky, A. B., Grønkjær, P., Pepin, P., and Leggett, W. C. 2008. Food limitation in larval fish: ontogenetic variation in feeding scope and its potential effect on survival. Marine Ecology Progress Series, 367: 239–248.

Buskey, E. J., Coulter, C., and Strom, S. 1993. Locomotory patterns of microzooplankton: potential effects on food selectivity of larval fish. Bulletin of Marine Science, 53: 29–43.

Campana, S. E. 1990. How reliable are growth back-calculations based on otoliths? Canadian Journal of Fisheries and Aquatic Sciences, 47: 2219–2227.

Chambers, R. C., and Leggett, W. C. 1987. Size and age at metamorphosis in marine fishes - an analysis of laboratory-reared winter flounder (*Pseudopleuronectes americanus*) with a review of variation in other species. Canadian Journal of Fisheries and Aquatic Sciences, 44: 1936–1947.

Cushing, D. H. 1990. Plankton production and year-class strength in fish populations: an update of the match/mismatch hypothesis. Advances in Marine Biology, 26: 249–294.

Davison, A. C., and Hinkley, D. V. 1997. Bootstrap Methods and Their Application. Cambridge University Press, New York.

Dower, J. F., Pepin, P., and Kim, G.-C. 2009. Covariation in feeding success, size-at-age and growth in larval radiated shanny (*Ulvaria subbifurcata*): insights based on individuals. Journal of Plankton Research, 31: 235–247.

Ferron, A., and Leggett, W. C. 1994. An appraisal of condition measures for marine fish larvae. Advances in Marine Biology, 30: 217–303.

Folkvord, A., Blom, G., Johannessen, A., and Moksness, E. 2000. Growth-dependent age estimation in herring (*Clupea harengus* L.) larvae. Fisheries Research, 46: 91–103.

Fortier, L., and Villeneuve, A. 1996. Cannibalism and predation on fish larvae by larvae of Atlantic mackerel, *Scomber scombrus*: trophodynamics and potential impact on recruitment. Fishery Bulletin, 94: 268–281.

Francis, R. I. C. C. 1990. Back-calculation of fish length: a critical review. Journal of Fish Biology, 36: 883–902.

Gisbert, E., Ortiz-Delgado, J. B., and Sarasquete, C. 2008. Nutritional cellular biomarkers in early life stages of fish. Histology and Histopathology, 23: 1525–1539.

He, T., Xiao, Z., Liu, Q., Ma, D., Xu, S., Xiao, Y., and Li, J. 2012. Ontogeny of the digestive tract and enzymes in rock bream *Oplegnathus fasciatus* (Temminck et Schlegel 1844) larvae. Fish Physiology and Biochemistry, 38: 297–308.

Hjort, J. 1914. Fluctuations in the great fisheries of northern Europe viewed in light of biological research. Rapports et Procès-Verbaux des Réunions du Conseil Permanent International pour l'Exploration de la Mer, 20: 1–228.

Houde, E. D. 1989. Comparative growth, mortality, and energetics of marine fish larvae: temperature and implied latitudinal effects. Fishery Bulletin, 87: 471–495.

Houde, E. D. 2008. Emerging from Hjort's shadow. Journal of Northwest Atlantic Fisheries Science, 41: 53–70.

Hufnagl, M., and Peck, M. A. 2011. Physiological individual-based modelling of larval Atlantic herring (*Clupea harengus*) foraging and growth: insights on climate-driven life-history scheduling. ICES Journal of Marine Science, 68: 1170–1188.

Hunter, J. R. 1980. The feeding behavior and ecology of marine fish larvae. *In* Fish Behavior and Its Use in the Capture and Culture of Fishes, pp. 287–330. Ed. by J. E. Bardach, J. J. Magnuson, R. C. May, and J. M. Reinhart. ICLARM Conference Proceedings 5, Manilla, Philippines.

Llopiz, J. K., and Cowen, R. K. 2008. Precocious, selective and successful feeding of larval billfishes in the oceanic Straits of Florida. Marine Ecology Progress Series, 358: 231–244.

Lochmann, S. E., and Ludwig, G. M. 2003. Relative triacylglycerol and morphometric measures of condition in sunshine bass fry. North American Journal of Aquaculture, 65: 191–202.

Meekan, M. G., and Fortier, L. 1996. Selection for fast growth during the larval life of Atlantic cod *Gadus morhua* on the Scotian Shelf. Marine Ecology Progress Series, 137: 25–37.

Mendiola, D., Ibaibarriaga, L., and Alvarez, P. 2007. Thermal effects on growth and time to starvation during the yolk-sac larval period of Atlantic mackerel *Scomber scombrus* L. Journal of Fish Biology, 70: 895–910.

Migoya, M. C. 1989. Étude de la croissance des larves de maquereau bleu (*Scomber scombrus*) dans le golfe du Saint-Laurent, à partir de l'examen de la microstructure des otolithes. MSc thesis, Université du Québec à Rimouski, Rimouski, QC. 83 pp.

Miller, T. J., Crowder, L. B., Rice, J. A., and Marschall, E. A. 1988. Larval size and recruitment mechanisms in fishes: toward a conceptual framework. Canadian Journal of Fisheries and Aquatic Sciences, 45: 1657–1670.

Morton, K. E. 2012. Development of larval fish: a multi-species perspective. PhD thesis, Memorial University of Newfoundland, St. John's, NL. xix + 247 pp.

Pepin, P. 1991. Effect of temperature and size on development, mortality, and survival rates of the pelagic early life history stages of marine fish. Canadian Journal of Fisheries and Aquatic Sciences, 48: 503–518.

Pepin, P., Dower, J. F., and Benoît, H. P. 2001. The role of measurement error on the interpretation of otolith increment width in the study of growth in larval fish. Canadian Journal of Fisheries and Aquatic Sciences, 58: 2204–2212.

Pepin, P., Evans, G. T., and Shears, T. H. 1999. Patterns of RNA/DNA ratios in larval fish and their relationship to survival in the field. ICES Journal of Marine Science, 56: 697–706.

Pepin, P., and Penney, R. W. 1997. Patterns of prey size and taxonomic composition in larval fish: are there general size-dependent models? Journal of Fish Biology, 51: 84–100.

Portt, C. B., and Balon, E. K. 1984. A potential source of error when estimating ecological production of fishes using back-calculations. Environmental Biology of Fishes, 10: 301–303.

Robert, D., Castonguay, M., and Fortier, L. 2007. Early growth and recruitment in Atlantic mackerel: discriminating the effects of fast growth and selection for fast growth. Marine Ecology Progress Series, 337: 209–219.

Robert, D., Castonguay, M., and Fortier, L. 2008. Effects of intra- and inter-annual variability in prey field on the feeding selectivity of larval Atlantic mackerel (*Scomber scombrus*). Journal of Plankton Research, 30: 673–688.

Robert, D., Castonguay, M., and Fortier, L. 2009. Effects of preferred prey density and temperature on feeding success and recent growth in larval mackerel of the southern Gulf of St. Lawrence. Marine Ecology Progress Series, 377: 227–237.

Secor, D. H., and Dean, J. M. 1989. Somatic growth effects on the otolith—fish size relationship in young pond-reared striped bass, *Morone saxatilis*. Canadian Journal of Fisheries and Aquatic Sciences, 46: 113–121.

Secor, D. H., and Dean, J. M. 1992. Comparison of otolith-based back-calculation methods to determine individual growth histories of larval striped bass, *Morone saxatilis*. Canadian Journal of Fisheries and Aquatic Sciences, 49: 1439–1454.

Takasuka, A., Aoki, I., and Mitani, I. 2003. Evidence of growth-selective predation on larval Japanese anchovy *Engraulis japonicus* in Sagami Bay. Marine Ecology Progress Series, 252: 223–238.

Takasuka, A., Aoki, I., and Oozeki, Y. 2007. Predator-specific growth-selective predation on larval Japanese anchovy *Engraulis japonicus*. Marine Ecology Progress Series, 350: 99–107.

Ware, D. M., and Lambert, T. C. 1985. Early life history of Atlantic mackerel (*Scomber scombrus*) in the southern Gulf of St. Lawrence. Canadian Journal of Fisheries and Aquatic Sciences, 42: 577–592.

Young, K. V., Pepin, P., and Dower, J. F. 2010. Interannual variability in feeding rate and niche breadth of radiated shanny (*Ulvaria subbifurcata*) larvae from coastal Newfoundland. Journal of Plankton Research, 32: 815–827.

Handling Editor: Howard Browman

ICES Journal of Marine Science

ICES Journal of Marine Science (2014), 71(4), 1010–1021. doi:10.1093/icesjms/fst041

Contribution to the Themed Section: 'Larval Fish Conference'

Original Article

The effect of variable winter severity on size-dependent overwinter mortality caused by acute thermal stress in juvenile red drum (*Sciaenops ocellatus*)

Deena A. Anderson* and Frederick S. Scharf

Department of Biology and Marine Biology, University of North Carolina Wilmington, 601 South College Road, Wilmington, NC 28403, USA

**Corresponding author: tel: +1 302 588 2604; fax: +1 910 962 4066; e-mail: daa2211@uncw.edu*

Anderson, D. A., and Scharf, F. S. 2014. The effect of variable winter severity on size-dependent overwinter mortality caused by acute thermal stress in juvenile red drum (*Sciaenops ocellatus*). – ICES Journal of Marine Science, 71: 1010–1021.

Received 31 October 2012; accepted 2 March 2013; advance access publication 11 April 2013.

Mortality during winter can impact the population dynamics of fish at temperate latitudes. The red drum (*Sciaenops ocellatus*) supports valuable coastal fisheries throughout its range in the southeastern United States. At the northern edge of its distribution, severe winters may cause considerable overwinter loss and size-selective mortality among juveniles. We conducted a series of laboratory experiments to quantify overwinter survivorship of age 0 fish. To determine thermal tolerance, fish were exposed to various minima (1, 3, or 5°C) for up to 14 d. The effect of winter severity on survivorship was then evaluated by exposing fish to simulated cold-front events of varying frequency and duration. Body size was incorporated as a factor into each set of experiments. Age 0 red drum were intolerant of even brief exposure to temperatures $\leq$3°C and experienced mortality after prolonged exposure to 5°C. Higher frequency of simulated cold-front events impacted survivorship more than longer-event duration, and recovery time between events improved survivorship. Size-dependent mortality was only evident for fish exposed to mild and moderate winter severity conditions, with larger fish surviving longer. For juvenile red drum, severe winters may cause high mortality independent of body size, whereas size-dependent year-class restructuring may occur during milder winters.

Keywords: acute cold stress, overwinter mortality, red drum, size-selectivity, winter severity.

Introduction

Overwinter mortality can represent an important process that shapes the population dynamics of fish at temperate latitudes, especially during early life. The association between autumn and spring abundance can often be disrupted during winter, an indication that year-class strength may not be established until after the first winter of life (Hurst and Conover, 1998; Michaletz, 2010). Many studies have noted decreased food availability in winter causing fish to exhaust energy reserves and starve (reviewed in Hurst, 2007). However, at extreme cold temperatures, the depletion of energy stores may no longer determine survival; rather, acute thermal stress can disrupt osmoregulatory function and be the primary cause of death (Hochachka, 1988; Belkovskiy *et al.*, 1991; Johnson and Evans, 1996; McCollum *et al.*, 2003). Exposure to extended periods of extreme cold and the associated acute thermal stress may, in fact, account for much of the observed overwinter mortality for several important US Mid-Atlantic fish stocks (Malloy and Targett, 1991; Hurst and Conover, 1998; Lankford and Targett, 2001).

Winter mortality has often been found to be size-dependent, with the potential for lasting influences on cohort demographics. Small fish are generally hypothesized to be more vulnerable to overwinter starvation due to their higher relative energetic demands coupled with a reduced capacity for lipid storage (Post and Evans, 1989). In addition, smaller individuals may also be more susceptible to osmotic failure caused by acute thermal stress due to a larger ratio of gill surface area to body mass (Hughes, 1984). Several field (Hunt, 1969; Post *et al.*, 1998;

Michaletz, 2010) and laboratory (Post and Evans, 1989; Johnson and Evans, 1991; Pangle *et al.*, 2004) studies have provided evidence for size-selective winter mortality that removes a greater fraction of small individuals. Alternatively, in some cases, small fish have been noted to experience greater relative survival when exposed to extreme cold temperatures, possibly related to improved acclimation as a result of faster protein turnover in small fish (Lankford and Targett, 2001; Slater *et al.*, 2007). Mortality during winter may also be size-independent (Cnaani *et al.*, 2000; McCollum *et al.*, 2003). Finally, even under identical winter conditions, size-selective mortality may be a dominant process for some species, but not for others (Toneys and Coble, 1979; Hales and Able, 2001).

Both the intensity of size selection and the overall magnitude of overwinter mortality can vary interannually. For size-selective mortality to occur, sufficient intracohort contrast in body size must exist and be coupled with high and non-random mortality (Sogard, 1997). If prewinter body sizes are relatively large on average, the disproportionate mortality of small fish may be unobservable or weak in given years due to fewer individuals being small enough to be susceptible to winter stress (Hurst and Conover, 1998). However, if juvenile growth rates during autumn are density-dependent, numerically large year classes may result in many small individuals that are more susceptible to cold-related sources of mortality at the onset of winter (Ludsin and DeVries, 1997). In contrast, during severe winters, high rates of mortality can negatively impact an entire cohort regardless of body size (McCollum *et al.*, 2003; Michaletz, 2010). Therefore, it is plausible that density-dependent processes will have a greater impact on overwinter survival during mild or moderate winters. The strength of size selectivity can also vary across a latitudinal gradient. Empirical evidence supports the notion that size-dependent overwinter mortality caused by acute cold stress should be less common at the extremes of a species' geographic range since threshold temperatures may affect all fish equally (Michaletz, 2010), whereas others have demonstrated strong size selection caused by starvation at the edges of a species' distribution, especially at northern range limits (Post *et al.*, 1998). Ultimately, the existence and strength of size-dependent mortality during winter may be influenced by various factors, including cohort demographics and winter severity (Shuter and Post, 1990).

The red drum (*Sciaenops ocellatus*) is a temperate marine fish that experiences variable winter conditions throughout its range in the US South Atlantic and Gulf of Mexico. The species is highly prized as a sportfish, and recent management efforts have promoted recovering stocks (SEDAR, 2009). Adults spawn in coastal waters during late summer and autumn (Ross *et al.*, 1995; Stewart and Scharf, 2008); offspring are then transported to estuarine habitats. Early juveniles are demersal and experience variable growth during autumn (Rooker *et al.*, 1999). Juvenile and subadult red drum generally occupy estuarine habitats for 3–4 years before joining the mature adult segment of the stock in mostly nearshore oceanic habitats (Ross *et al.*, 1995).

Evidence from both long-term surveys and focused studies indicates that overwinter mortality could have a considerable impact on red drum fishery recruitment. Scharf (2000) identified a clear lack of association between age 0 and 1 abundance indices collected over 20+ years along the Texas coast. Similarly, an abundance index for juvenile red drum estimated annually since 1991 in North Carolina waters showed only modest correlation with subsequent fishery landings data, with a substantial amount of unexplained variation (Bacheler *et al.*, 2008). Field-based estimates of age 0 red drum overwinter loss (mortality plus any potential emigration) from a North Carolina estuary have ranged between 35 and 90% (Stewart and Scharf, 2008; Martin, 2009). The spawning period for red drum is relatively protracted (Comyns *et al.*, 1989; Stewart and Scharf, 2008; Martin, 2009), which generates up to threefold variation in body sizes before winter (Martin, 2009). An examination of pre- and post-winter cohort demographics in North Carolina revealed evidence of selective overwinter mortality, with both early-hatched and fast-growing individuals realizing higher survivorship (Martin, 2009). Intracohort variability in survivorship was also observed for recently settled red drum in a Texas estuary (Rooker *et al.*, 1999).

Given the potential contribution of first-year processes in determining the year-class strength of red drum, a more comprehensive understanding of the patterns and mechanisms of overwinter mortality is warranted. Here, we report on the outcome of a series of controlled laboratory experiments devised to determine the size-dependent response of first-year juvenile red drum to variable winter conditions. The objectives of our experiments were to: (i) estimate the survival patterns of juvenile red drum exposed to different thermal minima; (ii) evaluate the influence of winter severity, indexed using the duration and frequency of cold-front events, on juvenile red drum survivorship; and (iii) test for size-selective mortality patterns across a range of winter conditions. Experiments were designed specifically to assess the potential effects of acute cold stress associated with exposure to extreme cold temperatures, rather than longer-term effects related to starvation.

Material and methods

Fish collection and experimental setup

Age 0 red drum were collected during autumn 2010 and 2011 in the New River estuary, NC, USA. Sites identified as juvenile red drum habitats during prior research (Stewart and Scharf, 2008) were accessed by boat and sampled using a 30.5 × 2.0-m beach-seine (6.0 and 3.0 mm stretched mesh in the wings and bag, respectively). At each site, dissolved oxygen (mg l^{-1}), salinity (psu), and temperature (°C) were recorded using an YSI Model 85 multiprobe. Juvenile red drum (~30–60 mm total length (*TL*)) were removed from the catch and transported to the laboratory in aerated containers (140 l). Fish were transferred to holding tanks (900 l) that were part of a recirculating system maintained at ambient autumn water temperatures (~15°C) and moderate salinities (~17 psu). Juvenile red drum were fed to satiation once daily with a combination of larval fish feed (Marubeni Nisshin Feed Co., Ltd, Tokyo, Japan) and thawed adult *Artemia*. Although laboratory conditions may have promoted faster growth relative to field conditions, we attempted to regulate growth during holding and acclimation by maintaining cool water temperatures and feeding fish only a maintenance ration (≤5% mass d^{-1}). Holding tanks were monitored daily for dissolved oxygen, salinity, and temperature and were maintained on a 10/14-h light/dark photoperiod to simulate natural light conditions in coastal waters of the US Mid-Atlantic during winter. Any dead individuals were removed daily and counted. Fish were acclimated to laboratory holding tanks for a minimum of 4 weeks before the start of an experiment.

Controlled experiments were conducted during two consecutive winters (2010/2011 and 2011/2012) using circular, polyethylene tanks (94 l), which were housed in an environmentally controlled chamber. Air temperature in the chamber was set

below the minimum water temperature of any of the experimental treatments, and water in individual tanks was heated to specific treatment temperatures using titanium heaters (1000 W; Process Technology, Mentor, OH, USA) and digital temperature controllers with $\pm 1.0^{\circ}$C accuracy. Water quality in each tank was maintained with a power filter (AquaClear 30, Hagen Corp., Montreal, Canada) that provided mechanical and biological filtration. A temperature data logger (HOBO Pro v2, Onset Computer Corporation, Boston, MA, USA) was tethered underwater in each tank and programmed to record hourly water temperature. Salinities were maintained at mid-estuary levels of 18–23 psu, and the chamber was programmed for a 10/14-h light/dark photoperiod. Between each replicate run, filters were cleaned, a new carbon pack installed, and an 80% water change was performed.

Past water temperature data collected during winter (1 December–1 March) by the US Geological Survey (USGS) National Water Information System was analysed to identify typical and extreme winter weather patterns along the North Carolina coast. Specifically, we examined data collected from 2007 to 2011 in the New River estuary at Jacksonville, NC (USGS site 0209303205), and from 1999 to 2009 in the Pamlico River estuary at Washington, NC (USGS site 02084472). These data were used to determine the average winter water temperatures and thermal minima occurring in North Carolina coastal waters occupied by juvenile red drum. Minimum daily temperatures during winter at the New River estuary site ranged from 1.6 to 6.7°C, whereas daily minima in the Pamlico River estuary ranged from 0.4 to 5.2°C. We also examined historical fluctuations in the minimum water temperature along the North Carolina coast during winter to define mild and severe winters based on the frequency and the duration of extreme cold events associated with the passage of fronts (hereafter referred to as cold-front events). These natural cold-front events can be described generally as a rapid decrease in temperature, followed by a brief period holding at a minimum temperature, then a gradual increase in temperature. Typical natural cold-front events exhibited a water temperature decrease of $\geq 2^{\circ}$C in 24 h or $\geq 3^{\circ}$C in 36 h. For each event, we calculated the rate of temperature decline and recovery, along with the time spent at the minimum temperature. Combining cold-front data from both of the estuaries with historical water temperature data, the average rate of decline over 24 h was 2.34°C, with a maximum temperature drop of 4.8°C in 24 h. The vast majority of these events included 1–4 consecutive days at a minimum temperature, with roughly between 0 and 10 separate events each winter. Therefore, the historical water temperature data provided a framework that was used to identify appropriate temperature treatments within each set of experiments.

Thermal-tolerance experiments

During winter 2010/2011, experiments were designed to determine the thermal tolerance of juvenile red drum exposed to different minimum water temperatures. Treatment levels included water temperatures of 1, 3, and 5°C, selected based on the observed minimum temperatures during winter in North Carolina estuaries. Although 1 and 3°C occur less frequently than 5°C in North Carolina estuaries, juvenile red drum overwintering in these estuarine habitats can be exposed to temperatures as low as 1°C during severe winters. A control treatment level of 10°C was selected to mimic the average winter estuarine temperatures. To test for the effect of body size, fish were separated into large (grand mean $\pm$ s.d. = 90.98 $\pm$ 12.51 mm *TL*, 7.05 $\pm$ 2.72 g wet weight) and small (72.58 $\pm$ 12.89 mm *TL*, 3.85 $\pm$ 1.93 g wet weight) groups, which differed significantly in body size, both overall (*TL*: $F = 187.5$, $p < 0.001$; weight: $F = 164.2$, $p < 0.001$) and within each trial (all $p < 0.001$ for both *TL* and weight comparisons). Each trial consisted of eight tanks (2 body size treatment levels $\times$ 4 temperature treatment levels), with each tank containing 15 individuals. The experimental response was proportional survival and was measured for each replicate tank. The use of 15 individuals within each tank provided an adequate level of precision to measure the response of each replicate. Each experimental trial lasted ~3 weeks, and three trials were completed between 11 January and 26 March 2011. Within small- and large-size groups, body sizes were not significantly different among treatments within each trial (small: all $p \geq 0.622$ for *TL* and ≥ 0.805 for weight; large: all $p \geq 0.833$ for *TL* and ≥ 0.775 for weight). While body sizes of both size groups were larger in subsequent trials due to fish growth in the holding tanks, significant levels of contrast (at least 15.20 mm *TL* and 2.66 g difference between small and large groups) were maintained between size groups during each replicate trial.

To initiate each experimental trial, fish were measured for *TL* (mm) and wet weight (g) as they were transferred from holding tanks to the experimental tanks in the environmental chamber. Fish were acclimated to 10°C water temperatures for at least 48 h before each trial. For non-control tanks, water temperature was then decreased by 1°C d^{-1} until the specified treatment level temperature was reached. For observational purposes, day 1 of each trial was defined as the day when all non-control tanks reached 5°C. Each trial then continued for 14 d. For 3 and 1°C treatment levels, water temperature was decreased by 1°C each day thereafter until the specified temperature was reached. Observations were completed three times a day at ~08:00, 12:00, and 16:00. During each observation, fish behaviour and any mortality were recorded, along with water temperature and salinity. Fish were fed to satiation with adult *Artemia* during the midday observation, and feeding behaviours were documented. Mortality was defined using two factors: no response to stimulus and no opercular movement (Lankford and Targett, 2001). Dead fish were removed with a dipnet, and the observation time was assigned as time of death. Weight and *TL* were recorded for each dead fish.

Cold-front-event simulations

During winter 2011/2012, experiments were designed to determine the effects of exposure to variable winter severity, characterized by the frequency and the duration of cold-front events, on juvenile red drum survivorship. Given the historical variability that we identified in both the number (0–10 events per winter) and the duration (1–4 d at minimum temperatures) of cold-front events, we elected to index winter severity based on these two traits.

First, we defined a simulated cold-front event as a decrease from 8 to 3°C over 36 h, exposure to a 3°C minimum for a specified duration (see below), followed by a temperature recovery to 8°C over 48 h. A 5°C drop over 36 h was slightly more rapid than the average decrease observed in the historical estuary temperature data, but it was conservative relative to the observed maximum declines of over 4°C in 24 h. Although minimum temperatures associated with cold-front events varied to some degree within the historical data, we chose 3°C as the minimum

temperature reached during each simulated event based on the results from our thermal-tolerance experiments. Juvenile red drum survived at 3°C, but acute cold stress was apparent, and fish began to experience mortality within a short time after exposure. We varied the frequency of cold-front events by exposing fish to either three consecutive events or two events separated by a recovery period at 8°C the same length as a cold-front event. Duration, or the total time spent at the minimum temperature, was set at either 24 or 48 h. Each frequency (high = 3, low = 2) was crossed with each duration (long = 48 h, short = 24 h) to create four distinct winter severity treatment levels (Figure 1). The most severe winter conditions consisted of three consecutive cold-front events, each including 48 h at the minimum temperature, whereas mild winter conditions were simulated by exposure to two cold-front events each including only 24 h at the minimum temperature, separated by a recovery period. The other two treatment levels were deemed to represent intermediate winter conditions. Each winter severity treatment level was tested for two body size groups, resulting in eight replicate tanks (4 winter severity treatment levels × 2 body size groups) for each of three trials, which were run consecutively from 25 January to 7 April 2012. Fish were assigned to either a large (73.97 ± 7.72 mm *TL*, 3.66 ± 1.33 g wet weight) or a small (52.29 ± 5.17 mm *TL*, 1.32 ± 0.38 g wet weight) body size group, which were statistically distinct both overall (*TL*: $F = 1046$, $p < 0.001$; weight: $F = 544.2$, $p < 0.001$) and within each trial (all $p < 0.001$ for both *TL* and weight). Individual tanks contained 16 juvenile red drum to achieve sufficient precision in survival estimates; however, any individuals that died during the acclimation period were removed from the experiment and not replaced.

Fish were weighed and measured before being randomly assigned to experimental tanks. All fish were then held at 8°C for a 48-h acclimation period. All tanks within each trial were exposed to the first cold-front event beginning on day 1. Since each short-duration, cold-front event lasted 5 d, trials consisting of short-duration events (either three cold-front events or two cold-front events, separated by a recovery period) lasted 15 d. Similarly, each long-duration, cold-front event lasted 6 d, so trials lasted 18 d to complete all events. Observations were made when treatments required temperature adjustments, which occurred every 9 h during temperature decrease and every 12 h during temperature recovery. While fish were held at the minimum temperature, observations were made every 12 h. Fish behaviour and any mortalities, as well as water temperature and salinity, were recorded. Fish were fed to satiation at the earliest observation time each day. Similar to the thermal-tolerance experiments, growth occurred in the holding tanks across trials, but significant levels of contrast in body size were maintained (at least 20.89 mm *TL* and 2.19 g weight difference between small and large groups). Similar to thermal-tolerance experiments, no significant differences existed within small or large body size groups in any of the trials (small: all $p \geq 0.416$ for *TL* and ≥ 0.654 for weight; large: all $p \geq 0.763$ for *TL* and ≥ 0.787 for weight).

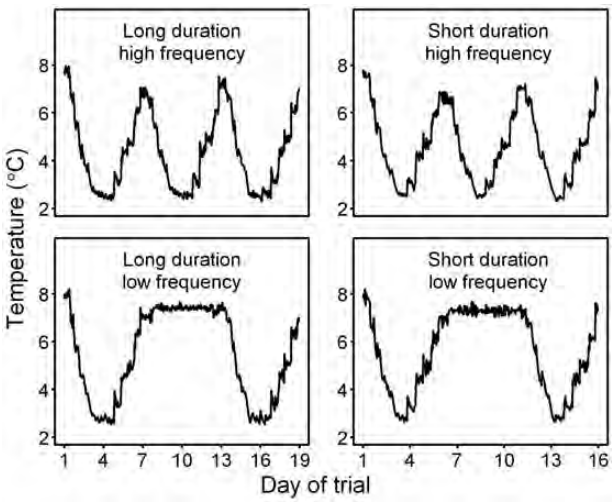

Figure 1. Experimental design for cold-front-event simulations. Four levels of winter severity were simulated by varying the duration held at the 3°C minimum water temperature (long = 48 h, short = 24 h) and the frequency of events (high = 3, low = 2). The total time for trials including long-duration events was slightly longer (by 3 d) and is represented in the scale of the *x*-axes.

Data analysis

To assess fish condition after exposure to experimental treatments, Fulton's condition factor ($K = \text{weight}/\text{length}^3 \times 10^5$) was calculated for each individual then averaged for each replicate tank. The condition factor was estimated for each fish both at the start and at the end of each trial, or upon death. For both sets of winter experiments, the initial condition did not differ among treatments (thermal tolerance: $F = 0.249$, $p = 0.862$; cold-front-event simulation: $F = 0.822$, $p = 0.482$). Fish in the small body size groups had higher initial condition than those in the large body size groups (thermal tolerance: $F = 20.129$, $p < 0.001$; cold-front-event simulations: $F = 14.337$, $p < 0.001$); this was expected based on growth allometries (Froese, 2006). No significant interaction between treatment and body size was detected in either winter. The final condition was assessed by comparing the relative change in the condition factor (ΔK = initial K − final K) among treatments and body sizes during each winter using a two-way analysis of variance (ANOVA).

The effects of our experimental treatments on juvenile red drum survivorship were also analysed using two-way ANOVA models in which we considered both body size and temperature treatment as fixed effects. Since some thermal minima treatments of the first winter resulted in no survivors, the analysis was conducted using median survival time (median lethal time = LT_{50}) per replicate tank as the response variable. For the cold-front-event simulation experiments, proportional survivorship per tank at the end of each trial was analysed as the response variable, after first applying a logit transformation (Warton and Hui, 2011). Any *post hoc* multiple comparisons were conducted using Tukey's honestly significant difference (HSD) test with an experiment-wise error rate of 0.05.

Survival analysis was used to examine the effects of our experimental treatments on patterns of mortality at a finer temporal scale. In this study, the response variable was time until death, our event of interest. We also incorporated right-censored data (i.e. individuals that did not experience death) into our survival analysis, since survivors remained in several trials. Additionally, a subset of fish was sacrificed for physiological analysis of tissue samples to assess potential osmoregulatory disruptions related to acute cold stress as part of a separate study. Fish that were sacrificed during thermal-tolerance experiments were not censored,

since they exhibited moribund behaviours indicating imminent mortality. However, during the cold-front-event simulations, apparently healthy fish were sacrificed at set times due to the complex nature of the temperature regimes. These fish did not display the obvious signs of death before being sacrificed, thus they were censored in our analysis.

For our survival analysis, the Kaplan–Meier survival curves were first generated to graphically illustrate general survival patterns (Kaplan and Meier, 1958). To further compare survival patterns among temperature treatments and body sizes, the semi-parametric Cox proportional hazards model was applied to the data (Cox, 1972). Since fish were grouped in tanks to which the treatment was applied, responses of individual fish may not have been independent. This could be due to behavioural interactions or unmeasured random effects within tanks. To test for clustering in responses due to lack of independence, a shared gamma frailty model was used (Rondeau *et al.*, 2003). The hazard function for the shared frailty model is expressed as:

$$\lambda_{ij}(t|\nu_i) = \nu_i\lambda_0(t)\exp(\beta_i X_{ij}) = \nu_i\lambda_{ij}(t), \quad (1)$$

with the baseline function $\lambda_0(t)$, the covariate X_{ij} associated with regression coefficient β, and the random effect ν_i for the ith group, which were individual tanks in our case (see Rondeau *et al.* (2012) for additional details on shared frailty models). Model parameters were estimated based on a maximization of the penalized likelihood using frailtypack in R (R Development Core Team, 2012; Rondeau *et al.*, 2012). The presence of heterogeneity among subjects located within a given tank was determined using a modified Wald test of the variance for the frailty term (Rondeau *et al.*, 2012). After initial testing, we concluded that there were no significant random effects within tanks. Therefore, the frailty term ν_i could be excluded from the model, which then simplified to a basic Cox proportional hazards model, where the hazard function is expressed as:

$$\lambda_j(t) = \lambda_0(t)\exp(\beta_j X_j), \quad (2)$$

which was also estimated using a penalized likelihood approach in R. Although we deemed that a frailty parameter was not necessary, tanks were still analysed as clustered groups to account for a potential lack of independence among individual fish. The Cox model was then applied to determine both treatment and body size effects. To distinguish the effects of winter severity conditions, body sizes were combined in the Cox model. The effect of body size on survival patterns was determined using pairwise comparisons of large- and small-size groups within each treatment level. A significance level of $\alpha = 0.05$ was used for all tests.

Results

Behavioural observations and fish condition

At water temperatures below 5°C, juvenile red drum exhibited reduced affinity for food, with limited observations of actual foraging when prey was offered. Fish activity, aside from lack of feeding, was also reduced by extreme cold temperatures. Generally, fish were stationary at water temperatures below 5°C and often rested at the bottom of the tank displaying very little movement. During simulated cold-front events in which fish were held for specified durations at 3°C, normal behaviour resumed once water temperature recovered to ~7°C.

The average change in fish condition (mean ΔK) for 10, 5, 3, and 1°C treatments during cold-tolerance experiments with body sizes combined was 0.070, 0.074, 0.062, and 0.057, respectively, with no significant effects of temperature treatment, body size, or their interaction (two-way ANOVA, all $p \geq 0.242$; Figure 2). During cold-front-event simulations, with body sizes combined, the mean ΔK was 0.095, 0.081, 0.063, and 0.035 for short/low, long/low, short/high, and long/high winter severity treatments, respectively. Similarly, no significant effect of winter severity treatment, body size, or their interaction was detected (two-way ANOVA, all $p \geq 0.141$; Figure 2).

Thermal-tolerance experiments

Thermal-minima treatment levels of 1 and 3°C resulted in 0% survivorship for age 0 red drum, whereas fish held at 5°C realized mean ± s.d. survivorship of 20.0 ± 4.2%, and we observed no mortality for control fish held at 10°C (Table 1). No significant interactive effect of temperature treatment and body size on median lethal time was detected ($F = 0.139$, $p = 0.872$; Table 3), which enabled clear interpretation of the main effects. For the 1, 3, and 5°C treatment levels, the median lethal times were 5.17, 6.25, and 11.33 d, respectively, which were significantly different (ANOVA; $F = 18.228$, $p < 0.001$; Table 3; Figure 3a). *Post hoc* comparisons revealed that the median survival time for fish held at 5°C was significantly greater than that held at 1°C ($p < 0.001$) and 3°C ($p = 0.002$), which were not different from each other. The time-specific patterns of mortality varied considerably among the thermal minima (Figure 4a). It is noteworthy that fish in the 1°C treatment did not reach the minimum temperature until day 5, with a mean ± s.d. survivorship of only 28.9 ± 4.8% at the point when 1°C was attained. Within 24 h of reaching 1°C, no survivors remained in any of the trials for this treatment level. Fish in the 3°C treatment experienced more gradual mortality, with survivorship declining to zero within 6 d after arriving at the minimum temperature on day 3. Survivorship in the 5°C treatments remained above 90% for ~6 d, after which mortality increased steadily for the remainder of each trial.

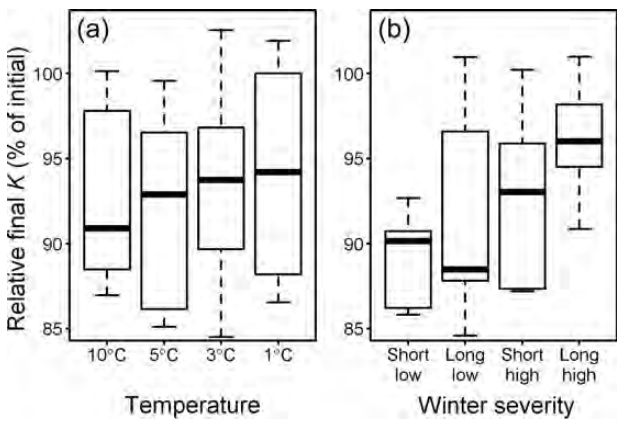

Figure 2. Box and whisker plots of relative final condition factor (final K/initial $K \times 100\%$) for (a) thermal-tolerance experiments and (b) cold-front-event simulations. For interpretation, a fish maintaining its initial condition ($\Delta K = 0$) would have a relative final condition factor of 100%. Thick line within each box = median. Whiskers extend to maximum and minimum values. Statistical differences do not exist among treatment groups within each winter, as determined by Tukey's HSD test ($\alpha = 0.05$).

Table 1. Numbers of fish and mean *TL* (mm) used in thermal-tolerance and cold-front-event simulation experiments, along with survivorship results

	Thermal-tolerance experiments				Cold-front-event simulations			
Treatment level	**1°C**	**3°C**	**5°C**	**10°C**	**Long/high**	**Short/high**	**Long/low**	**Short/low**
n	90	88	90	88	82	84	83	84
Small body size	72.1	72.6	73.0	72.6	51.9	52.1	52.3	52.9
Large body size	92.0	90.1	90.9	90.9	73.7	73.8	74.0	74.5
Small survival (%)	0	0	26.7	100	21.7	39.4	50.6	55
Large survival (%)	0	0	13.3	100	12.6	71.9	85	97.6
Overall survival (%)	0	0	20	100	17	55.8	68.3	76.4

During each set of experiments, replicate trials consisted of eight tanks (4 temperature treatments × 2 body sizes) with 13–16 juvenile red drum per tank. Survivorship results are means for three replicate trials.

Table 2. Parameter estimates generated from fitting Cox proportional hazards models.

Treatment level	β	exp(β)	s.e.(β)	***p*-value**
10°C	−12.159	$5.241e^{-6}$	9.154	0.184
3°C	2.403	11.054	0.244	<0.001
1°C	3.952	52.030	0.288	<0.001
Long/low	−0.014	0.986	0.293	0.962
Short/high	0.925	2.523	0.276	<0.001
Long/high	1.562	4.770	0.251	<0.001

The response of each of the thermal-tolerance treatment levels is relative to the 5°C treatment level response. Cold-front-event simulation effects are relative to the treatment level simulating the mildest winter severity (short duration/low frequency). Hazard ratios are expressed by exp(β).

Table 3. ANOVA results for thermal-tolerance and cold-front-event simulation experiments including body size as a factor.

Factor	**Sum of squares**	**d.f.**	**Mean square**	***F***	***p*-value**
Thermal-tolerance experiments					
Temperature	122.365	2	61.182	18.228	<0.001
Body size	0.038	1	0.0383	0.011	0.917
Temperature × size	0.932	2	0.466	0.139	0.872
Residual	40.279	12	3.357		
Cold-front-event simulations					
Winter severity	30.312	3	10.104	5.240	0.010
Body size	10.446	1	10.446	5.417	0.033
Severity × size	7.030	3	2.343	1.215	0.336
Residual	30.854	16	1.928		

The response for thermal-tolerance experiments was median survival time (LT_{50}). For cold-front-event simulations, the response was logit-transformed final survivorship.

The Cox analysis predicted the effects of different minimum temperatures relative to the model for the mildest treatment level (thermal minimum = 5°C). Temperatures of 1 and 3°C both had a highly significant effect on survival ($p < 0.001$ for both; Table 2) relative to the 5°C group. The hazard ratio indicated that individuals held at 3°C were more than 11-fold likely to experience mortality than those held at 5°C. Likewise, fish held at 1°C were more than 52-fold likely to die than those held at 5°C. The relative risk was non-existent (the hazard ratio was not significant) for control fish held at 10°C.

Size-dependent mortality was not evident during thermal-tolerance experiments (Table 3; Figure 3a). Although the temperature treatment significantly affected LT_{50}, the effect of body size was not significant ($F = 0.011$, $p = 0.917$). Similarly, hazard ratios did not differ significantly between large- and small-size groups within any of the temperature treatment levels (Table 4).

Cold-front-event simulations

Fish subjected to the mildest winter conditions, indexed by short-duration, cold-front events occurring at low frequency, experienced the highest mean survivorship (Table 1). Both the long-duration/low-frequency and the short-duration/high-frequency treatment levels produced intermediate survivorship, whereas the treatment level simulating the most severe winter conditions, long-duration/high-frequency, resulted in the lowest survivorship. Similar to thermal-tolerance experiments, no significant interactive effects of winter severity treatment and body size were detected ($F = 1.215$, $p = 0.336$; Table 3), which enabled a clear interpretation of the main effects. Final survivorship was significantly different ($F = 5.240$, $p = 0.010$; Table 3; Figure 3b) among winter severity treatment levels. The survivorship of fish exposed to the most severe winter conditions (long-duration/high-frequency) was significantly lower than for fish exposed to the low-frequency treatments, both short- ($p = 0.009$) and long-duration events ($p = 0.035$), but was not statistically different from the survivorship of fish exposed to the high-frequency/short-duration treatment. Although the overall timing of mortality varied across winter conditions, temporal patterns were similar (Figure 4b). In each case, fish generally survived the first cold-front event well, with >90% survivorship for all treatment levels at the end of the first cold-front event. Fish subjected to either of the low-frequency treatment levels maintained survival above 90% through the non-front-recovery period, then experienced greater mortality during the second cold-front event. Mortality increased successively for fish subjected to each of the high-frequency treatment levels during the second and third cold-front events. Survivorship decreased by ∼10% during the 24-h event duration when fish were held at 3°C, while longer-duration (48 h) events resulted in ∼20% lower survivorship during the frontal period. Fish subjected to each level of winter severity experienced some delayed mortality following the passage of a simulated cold front, with greater delayed mortality for fish exposed to the most severe winter conditions.

Survivorship, when exposed to the mildest winter conditions (short-duration/low-frequency), was used to determine relative risk when we estimated the Cox proportional hazards model. Exposure to the long-duration/low-frequency treatment level did not significantly affect the relative survival of fish ($p = 0.962$,

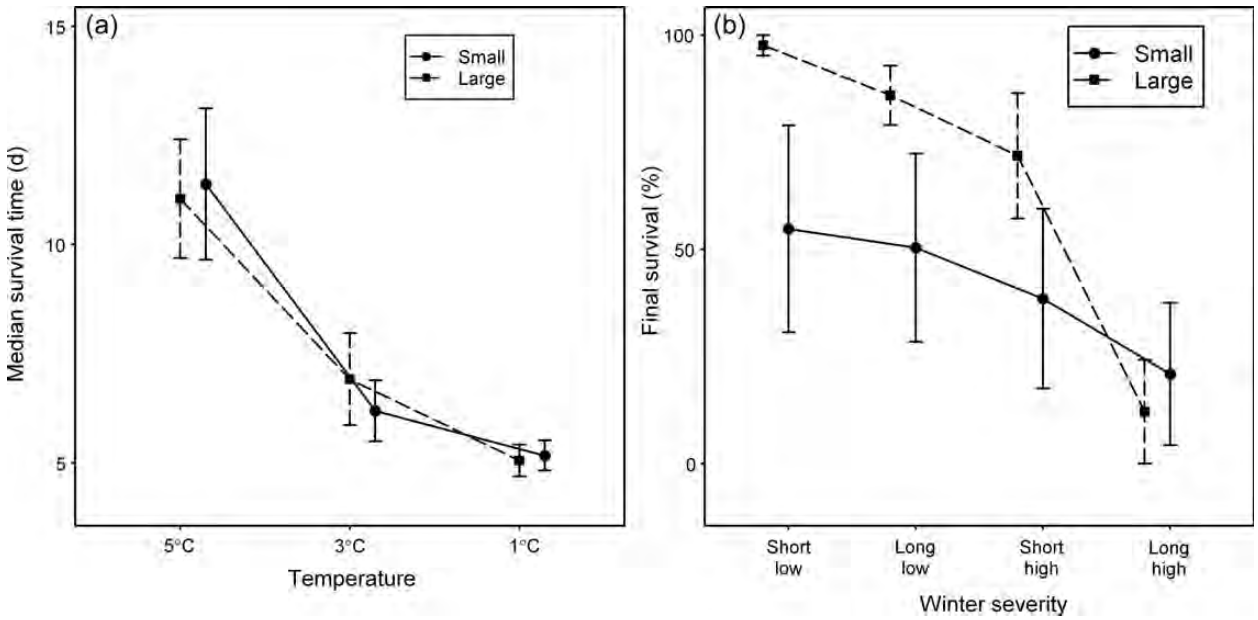

Figure 3. Survivorship results for thermal-tolerance experiments (a) and cold-front-event simulations (b). (a) The median survival time (LT_{50}) by the body size group for 1, 3, and 5°C treatment levels. (b) The final survivorship (%) by the body size group in each of the four winter severity simulations. Responses (median survival time or final survivorship) were averaged across replicate trials. Body size is distinguished as small (black circle) or large (black square). Error bars = 1 s.e., calculated by dividing s.d. by $\sqrt{3}$, where 3 = number of replicate tanks. In each panel, symbols are offset slightly for clarity.

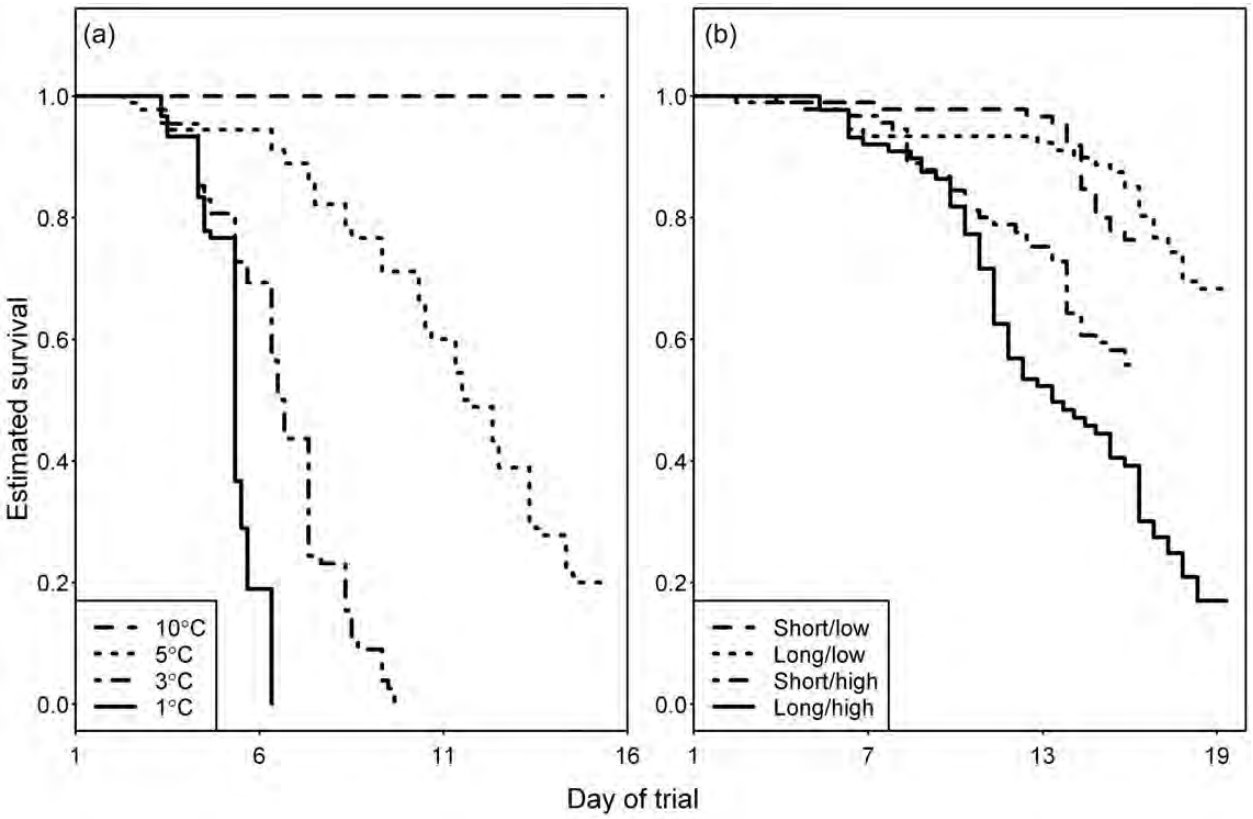

Figure 4. The Kaplan–Meier survival curves for (a) thermal-tolerance experiments and (b) cold-front-event simulations. Treatment levels that ended with survivors were right-censored in the analysis.

Table 4. Cox proportional hazard ratios expressed as exp(β) for small fish relative to large fish during thermal-tolerance experiments and cold-front-event simulations.

Temperature/winter severity	exp(β)	*p*-value
1°C	0.934	0.752
3°C	1.437	0.109
5°C	0.736	0.198
Short/low	27.200	<0.001
Long/low	3.938	0.003
Short/high	3.353	<0.001
Long/high	1.036	0.883

Table 2). However, fish subjected to both high-frequency treatment levels experienced greater mortality risk relative to simulated winters with a low frequency of cold-front events. The relative risk of mortality was 2.52-fold ($p < 0.001$) and 4.77-fold ($p < 0.001$) greater for fish subjected to the short-duration/high-frequency and long-duration/high-frequency treatment levels, respectively.

Mortality was dependent on body size when fish were exposed to varying levels of winter severity indexed by the duration and the frequency of cold-front events (Table 3; Figure 3b). The final survivorship was significantly ($F = 5.417$, $p = 0.033$) affected by body size. Hazard ratios also differed between large and small body sizes in three of the four winter severity treatment levels (Table 4). When subjected to the mildest winter conditions, small fish had a risk of mortality 27.2-fold greater than large fish. Smaller fish also experienced greater relative mortality risk (~three–fourfold greater risk, depending on the treatment level) than large fish when exposed to moderate winter conditions. In contrast, no difference in the hazard ratio between small and large fish was observed for fish exposed to the most severe winter conditions.

Discussion

Impact of variable winter severity on survival

Juvenile red drum exposed to water temperatures ≤5°C experienced mortality caused by acute cold stress. Specifically, exposure to thermal extremes ≤3°C resulted in rapid death. As water temperatures were reduced (at a rate of 1°C d^{-1}), we noted considerable declines in survivorship (e.g. ~40% mortality at 2°C) before reaching temperature minima, which resulted in only a small portion (~30%) of individuals remaining alive to experience our most extreme thermal challenge (1°C minimum temperature). Furthermore, within 4 h of exposure to 1°C water temperatures, an additional 10% of the fish expired, and no survivors remained after 16 h. Our findings are similar to previous studies reporting on the limits to low-temperature tolerance for red drum. Procarione and King (1993) found that 50% mortality was reached at water temperatures between 2.6 and 3.5°C for both Texas and South Carolina juvenile red drum acclimated to 14 or 16°C conditions. Their findings also provided evidence that acclimation temperature before exposure to extreme cold affected survivorship, with fish acclimated to cold conditions performing better. Miranda and Sonski (1985) reported a similar susceptibility of juvenile red drum to cold temperatures and also observed a modest effect of acclimation temperature on survivorship. Minimum water temperatures causing 50% mortality in their study were 1.9 and 2.4°C for fish acclimated to 15 and 25°C, respectively. Our findings related to fish condition after exposure to the experimental treatments support acute cold stress, rather than nutritional deficiency, as the proximate cause of death. Exposure to winter conditions, both mild and severe, resulted in a decrease in final K relative to initial K, most likely attributable to decreased feeding rates at cold temperatures. However, the average change in the condition factor (ΔK) did not differ among temperature treatments or body sizes. In fact, we noted a trend for larger decreases in K for fish exposed to milder temperature treatments, which we attributed simply to those fish being exposed to winter conditions, and thus reduced feeding rates, for a longer period. Alternatively, mortality occurred much earlier for fish exposed to more extreme temperature treatments, with less time for reduced feeding rates to impact fish condition.

Our results confirm the likely importance of episodic cold events in causing mortality of red drum during juvenile life stages. Indeed, mass mortality events for coastal fish, including red drum, have occurred with some regularity along the Texas coast (Gunter, 1941; McEachron *et al.*, 1994). Previous laboratory results (Miranda and Sonski, 1985; Procarione and King, 1993) indicate that acclimation to colder conditions can buffer the impacts of episodic cold events, implying that red drum acclimated to winter conditions in North Carolina may be more resistant to extreme and rapid declines in water temperature. Winter fish kills have historically been rare in North Carolina coastal waters (see annual reports compiled by the NC Department of Natural Resources; http://portal.ncdenr.org/web/wq/ess/fishkillsmain), with reports of red drum mortality during these events being infrequent. However, cold temperatures that have been found to be lethal to red drum occur much more regularly in North Carolina coastal systems than along the northern Gulf of Mexico coast. Prolonged exposure to extreme cold temperatures is likely to result in the mortality of red drum, regardless of acclimatization, as has been observed for other species (Hurst and Conover, 1998; McCollum *et al.*, 2003; Fetzer *et al.*, 2011). We observed higher survivorship for juvenile red drum held at 5°C, relative to 1–3°C temperatures, but total survival after 14 d exposure was still only 20%, and half of the fish had died by ~11 d. Therefore, even exposure to less extreme winter water temperatures may result in high levels of mortality for juvenile red drum if the exposure is prolonged.

Juvenile red drum were able to tolerate exposure to water temperatures as low as 3°C for brief periods, as evidenced by the results from experiments simulating the occurrence of cold-front events. Initial survivorship was relatively higher when fish were faced with abrupt, but short, exposure to stressful temperatures compared with continuous, prolonged exposure during thermal-tolerance experiments. Mortality reached 18 and 29% after exposure to 3°C for 24 and 48 h, respectively, during thermal-tolerance experiments. In contrast, all four winter severity treatment levels in our cold-front simulation experiments maintained >90% survivorship through the completion of the first cold-front event, which included a 24- or 48-h exposure to 3°C. Higher survivorship occurred despite exposure to simulated cold-front events that were characterized by 1°C temperature decreases every 9 h compared with more gradual (1°C d^{-1}) reductions in water temperature during thermal-tolerance experiments. Despite the more rapid rate of temperature decline, the brevity of the exposure yielded a survival advantage for fish during the cold-front simulations. Similar to our findings during the thermal-tolerance experiments, Ma *et al.* (2007) observed that the mortality of juvenile red drum had reached 50% within 24 h of exposure to 3°C. The temperatures in their study had been decreased gradually from 12 to 3°C over 18 d (1°C 2 d^{-1}), resulting in prolonged exposure to cold

temperatures before reaching 3°C. These findings support the notion that cumulative exposure to stressful water temperatures is the primary driver of increased mortality. The importance of cumulative exposure to temperatures near the lower lethal limit has also been suspected to be a major factor determining mortality rates for other temperate fish (Hurst and Conover, 1998; McCollum *et al.*, 2003; Fetzer *et al.*, 2011). For red drum, perhaps minimizing exposure to any temperatures <5°C may be more beneficial to survival than sufficient acclimation to cold conditions.

Another potentially important aspect of winter severity that may impact survivorship is the temporal spacing of cold-front events. During our thermal-tolerance experiments, all fish expired within 6 d of reaching 3°C. Fish exposed to a high frequency of long-duration, cold-front events experienced thermal minima for 48 h during each of three events, resulting in six cumulative days held at 3°C. Despite equivalent durations held at 3°C, fish in the simulated cold-front experiment realized a survival rate of 17% compared with 0% in the thermal-tolerance experiment. The amount of time between each cold-front event, when fish were exposed to rising and falling temperatures, though brief, appeared to provide fish with some relief from the effects of cold stress. It is unclear whether this represented a recovery period or if experiencing rapidly changing temperatures each day acclimatized fish to the cold-front events. Perez-Dominguez *et al.* (2006) exposed recently settled red drum to either diel fluctuations or constant temperatures, followed by a simulated cold-front event (10°C decrease in 24 h). Fish that had experienced daily thermal rhythms maintained higher survivorship during the subsequent rapid-cooling event. Thus, exposure to low and fluctuating temperatures during the diel cycle may provide thermal acclimation, meaning that previous exposure to mild cold-front events could enhance survivorship during more extreme events. Alternatively, repeated exposure to extreme temperatures with only relatively short refuge periods may still result in high rates of mortality. Juvenile red drum exposed to a high frequency of simulated cold-front events in this study experienced an increased risk of mortality with each successive event (Figure 5). This may mean that time spent at temperatures above lower lethal limits needs to be of sufficient duration to enable the recovery of physiological function and promote survival. When comparing our cold-front-event treatment levels, those that included a longer period between successive cold-front events generated the higher survivorship of juvenile red drum, suggesting that fish are able to survive multiple cold-front events, provided that they are short in duration and with ample recovery time between them.

Size-dependent response to acute cold stress

When subjected to prolonged exposure to extreme cold temperatures or severe winter conditions, red drum showed no size-dependence in survivorship. However, when exposed to moderate or mild winter conditions, larger red drum juveniles experienced higher survivorship. Size-dependent patterns of overwinter mortality have been detected for a large number of freshwater and estuarine fish, with the vast majority of studies documenting higher survivorship for larger individuals (e.g. Post and Evans, 1989; Pangle *et al.*, 2004; Michaletz, 2010). Most evidence points to starvation as the primary mechanism of size-dependent overwinter mortality, due to the combination of higher weight-specific metabolic rates and lower lipid reserves in smaller individuals (Hurst, 2007). In cases where acute cold stress is the suspected cause of death, the evidence for size-dependence is equivocal. Hurst and Conover (2002) detected no effects of body size on juvenile striped bass survivorship when exposed to ambient winter conditions as well as simulated cold-front events. Similarly, McCollum *et al.* (2003) found no difference in survival between large and small age 0 white crappies (*Pomoxis annularis*) that were suspected to have died as a result of osmoregulatory failure during winter. In contrast, and similar to our findings, both Fetzer *et al.* (2011) and Johnson and Evans (1996) observed greater susceptibility to acute cold stress for smaller individuals. Some evidence also exists for larger individuals suffering higher rates of mortality when faced with acute cold stress (Lankford and Targett, 2001).

Whether the suspected cause of death is starvation (Michaletz, 2010) or acute cold stress (McCollum *et al.*, 2003), the size-dependence of overwinter mortality is more pronounced during milder winters. Our findings for juvenile red drum support this idea. When fish were subjected to prolonged exposure to extreme cold temperatures, both large and small individuals

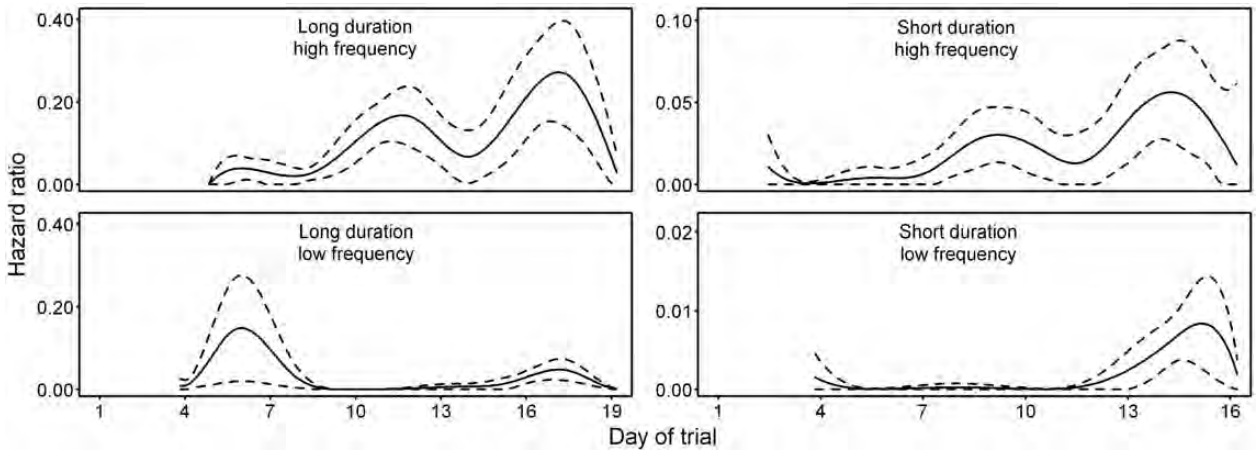

Figure 5. Cox proportional hazard ratios relative to time of trial for each cold-front-event simulation. Note the differences in the scale of the *y*-axes which reflects differences in the overall magnitude of the hazard ratios among winter severity simulations.

experienced low survivorship. Similarly, during exposure to the most severe winter conditions based on the frequency and the duration of cold-front events, mortality of juvenile red drum was not dependent on body size. Only during exposure to moderate and mild winter conditions did we see evidence of size-dependent mortality, with larger fish realizing higher survivorship. When conditions are most extreme, the combined effects of minimum water temperature and exposure time can exceed survival thresholds of all individuals, regardless of body size, resulting in size-independent overwinter mortality (Fetzer *et al.*, 2011). Hurst and Conover (1998) observed clear size-dependence in overwinter mortality of juvenile striped bass only during the mildest winter that they analysed and suggested that the strength of size-selective mortality should be expected to vary with winter severity for most temperate fish. We suspect that the importance of body size in shaping overwinter mortality patterns of juvenile red drum is likely to vary considerably from year to year based on climatic fluctuations.

For first-year fish, cohort demographic traits such as age and growth rate can also often contribute to variation in overwinter mortality because of their role in determining body size distributions at the onset of winter. In the US Mid-Atlantic, red drum spawning may begin as early as mid-July and extend until late October (Ross *et al.*, 1995; Stewart and Scharf, 2008). Later hatching times coupled with reduced growth potential at colder autumn water temperatures (Lanier and Scharf, 2007) can lead to small body sizes for some individuals before winter. When combined with variable autumn growth among individuals, the moderately protracted spawning season of red drum can typically generate prewinter size distributions with up to threefold variation (Martin, 2009). While hatch timing may primarily be driven by abiotic processes, individual growth rates are often also influenced by multiple biotic processes. Dense cohorts can compete for limited food and experience reduced growth during the first year of life, providing a template for size-selective overwinter mortality (e.g. Martino and Houde, 2012). Early hatch timing increases the length of the growing season before the first winter and usually provides access to optimal growth conditions for the longest duration, which has been found to produce higher overwinter survival for several fish species (Henderson *et al.*, 1988; Ludsin and DeVries, 1997; Post *et al.*, 1998). For species like red drum that spawn during late summer and early autumn, hatch timing and autumn growth conditions may be especially critical for determining not only the strength of size-dependence, but also the overall magnitude of overwinter mortality in a given year.

Recruitment implications

The influence of environmental variability on the population dynamics of marine fish is often strongest near the edges of a species' distribution. In a review, Myers (1998) found that environment–recruitment correlations were most robust near the limits of a species' geographical range. Fish living near their range limits are expected to respond more directly to abiotic processes and thus display greater variability in recruitment and population density. Although the range of red drum has extended up to Massachusetts in waters along the US Atlantic coast (Hildebrand and Schroeder, 1927), currently they are only rarely encountered north of Virginia. Moreover, the consistent presence of first-year juveniles has only been documented as far north as North Carolina. Therefore, winter conditions typical of the North Carolina coast are likely the most severe experienced by prerecruit red drum throughout their range, with the potential for greater environmental forcing on red drum population dynamics relative to fish overwintering farther south along the Atlantic coast or in the Gulf of Mexico. Several recent examples highlight the impact of winter conditions during juvenile life stages in shaping year-class success of marine fish (Hare and Able, 2007; Ojaveer *et al.*, 2011; Martino and Houde, 2012). Each of these cases involved either strong environmental forcing during cold winters or prewinter compensatory processes that facilitated the function of winter as a recruitment bottleneck. We conclude that the greatest likelihood for significant modification of red drum year classes caused by environmental variability exists at the northernmost edge of their distribution along the US Atlantic coast.

The use of fishery-independent sampling of age 0 fish to develop an index of recruitment is widely practiced within fishery resource management. However, for many marine fish species, the abundance of early larval stages can often be poorly correlated with eventual fishery recruitment; rather, late larval and early juvenile stages may provide a more reliable index of year-class success (Bradford, 1992). Because of its longer duration, processes occurring during the juvenile stage have been implicated to dampen and, in some cases, regulate the recruitment of marine fish (van der Veer *et al.*, 2000; Houde, 2008). Therefore, many recruitment indices are based on juvenile abundance surveys; however, only rarely has the performance of these indices been validated (e.g. Wilhite *et al.*, 2003). The North Carolina Division of Marine Fisheries has estimated relative abundance for juvenile red drum during autumn of each year since 1991. Bacheler *et al.* (2008) recently evaluated the performance of the index and concluded that temporal and spatial coverage was sufficient to quantify relative year-class size and that the calculation of the index was computationally sound. A positive association was noted between autumn juvenile abundance and fishery landings 2 years later, but the relationship left a considerable amount of variation unexplained. Winter mortality after the estimation of the index could contribute substantially to this variation and modify the red drum year-class size. Our experimental results indicate that juvenile red drum are most vulnerable to mortality when water temperatures remain $<5^{\circ}C$ for extended periods or when exposed to frequent cold-front events. Size-selective mortality, and resulting restructuring of cohort demographics, is not likely to occur during the most severe winters. However, mild and moderate winter conditions may remove a greater fraction of small fish, meaning that delayed spawning or poor autumn growing conditions could exacerbate any effects of winter. Therefore, the accurate assessment of the effects of overwinter mortality on red drum year-class success will likely require both an understanding of the factors that determine prewinter size distribution and the size-dependent response to winter severity.

Acknowledgements

We thank several individuals for providing assistance throughout the course of this study, especially J. Vanderfleet, C. Rumbarger, and J. White. UNCW facilities personnel ensured consistent operation of the environmental chamber, and the UNCW Center for Marine Science provided small boats for our use. We also thank two anonymous reviewers for providing comments that improved the manuscript. The study was funded by North Carolina Sea Grant. Additional support was provided to D. Anderson by the

UNCW Department of Biology and Marine Biology, the UNCW Graduate School, and the Got-Em-On Live Bait Club.

References

Bacheler, N. M., Paramore, L. M., Buckel, J. A., and Scharf, F. S. 2008. Recruitment of juvenile red drum in North Carolina: spatio-temporal patterns of year-class strength and validation of a seine survey. North American Journal of Fisheries Management, 28: 1086–1098.

Belkovskiy, N. M., Lega, Y. V., and Chernitskiy, A. G. 1991. Disruption of water-salt metabolism in rainbow trout, *Salmo gairdneri*, in seawater at low temperatures. Journal of Ichthyology, 31: 134–141.

Bradford, M. J. 1992. Precision of recruitment predictions from early life stages of marine fishes. Fishery Bulletin US, 90: 439–453.

Cnaani, A., Gall, G. A. E., and Hulata, G. 2000. Cold tolerance of tilapia species and hybrids. Aquaculture International, 8: 289–298.

Comyns, B. H., Lyczkowski-Shultz, J., Rakocinski, C. F., and Steen, J. P., Jr. 1989. Age and growth of red drum larvae in the north-central Gulf of Mexico. Transactions of the American Fisheries Society, 118: 159–167.

Cox, D. R. 1972. Regression models and life-tables. Journal of the Royal Statistical Society: Series B, Methodological, 34: 187–220.

Fetzer, W. W., Brooking, T. E., Jackson, J. R., and Rudstam, L. G. 2011. Overwinter mortality of gizzard shad: evaluation of starvation and cold temperature stress. Transactions of the American Fisheries Society, 140: 1460–1471.

Froese, R. 2006. Cube law, condition factor and weight-length relationships: history, meta-analysis and recommendations. Journal of Applied Ichthyology, 22: 241–253.

Gunter, G. 1941. Death of fishes due to cold on the Texas coast, January 1940. Ecology, 22: 203–208.

Hales, L. S., Jr, and Able, K. W. 2001. Winter mortality, growth, and behavior of young-of-the-year of four coastal fishes in New Jersey (USA) waters. Marine Biology, 139: 45–54.

Hare, J. A., and Able, K. W. 2007. Mechanistic links between climate and fisheries along the east coast of the United States: explaining population outbursts of Atlantic croaker (*Micropogonias undulatus*). Fisheries Oceanography, 16: 31–45.

Henderson, P. A., Holmes, R. H. A., and Bamber, R. N. 1988. Size-selective overwintering mortality in the sand smelt, *Atherina boyeri* Risso, and its role in population regulation. Journal of Fish Biology, 33: 221–233.

Hildebrand, S. F., and Schroeder, W. C. 1927. Fishes of Chesapeake Bay. Bulletin of the US Bureau of Fisheries, 43: 1–366.

Hochachka, P. W. 1988. Channels and pumps—determinants of metabolic cold adaptation strategies. Comparative Biochemistry and Physiology, 90B: 515–519.

Houde, E. D. 2008. Emerging from Hjort's shadow. Journal of Northwest Atlantic Fishery Science, 41: 53–70.

Hughes, G. M. 1984. General anatomy of the gills. *In* Fish Physiology, 10A, 1st edn, pp. 1–72. Ed. by W. S. Hoar, and D. J. Randall. Academic Press, New York. 456 pp.

Hunt, R. L. 1969. Overwinter survival of wild fingerling brook trout in Lawrence Creek, Wisconsin. Journal of the Fisheries Research Board of Canada, 26: 1473–1483.

Hurst, T. P. 2007. Causes and consequences of winter mortality in fishes. Journal of Fish Biology, 71: 315–345.

Hurst, T. P., and Conover, D. O. 1998. Winter mortality of young-of-the-year Hudson River striped bass (*Morone saxatilis*): size-dependent patterns and effects on recruitment. Canadian Journal of Fisheries and Aquatic Sciences, 55: 1122–1130.

Hurst, T. P., and Conover, D. O. 2002. Effects of temperature and salinity on survival of young-of-the-year Hudson River striped bass (*Morone saxatilis*): implications for optimal overwintering habitats. Canadian Journal of Fisheries and Aquatic Sciences, 59: 787–795.

Johnson, T. B., and Evans, D. O. 1991. Behavior, energetics, and associated mortality of young-of-the-year white perch (*Morone americana*) and yellow perch (*Perca flavescens*) under simulated winter conditions. Canadian Journal of Fisheries and Aquatic Sciences, 48: 672–680.

Johnson, T. B., and Evans, D. O. 1996. Temperature constraints on overwinter survival of age-0 white perch. Transactions of the American Fisheries Society, 125: 466–471.

Kaplan, E. L., and Meier, P. 1958. Nonparametric-estimation from incomplete observations. Journal of the American Statistical Association, 53: 457–481.

Lanier, J. M., and Scharf, F. S. 2007. Experimental investigation of spatial and temporal variation in estuarine growth of age-0 juvenile red drum (*Sciaenops ocellatus*). Journal of Experimental Marine Biology and Ecology, 349: 131–141.

Lankford, T. E., and Targett, T. E. 2001. Low-temperature tolerance of age-0 Atlantic croakers: recruitment implications for US Mid-Atlantic estuaries. Transactions of the American Fisheries Society, 130: 236–249.

Ludsin, S. A., and DeVries, D. R. 1997. First-year recruitment of large-mouth bass: the interdependency of early life stages. Ecological Applications, 7: 1024–1038.

Ma, L., Saillant, E., Gatlin, D., III, Neill, W., Vega, R., and Gold, J. 2007. Heritability of cold tolerance in red drum. North American Journal of Aquaculture, 69: 381–387.

Malloy, K. D., and Targett, T. E. 1991. Feeding, growth, and survival of juvenile summer flounder *Paralichthys dentatus*: experimental analysis of the effects of temperature and salinity. Marine Ecology Progress Series, 72: 213–223.

Martin, C. R. 2009. Intracohort variation in vital rates of age-0 red drum (*Sciaenops ocellatus*): testing for demographic restructuring during winter. Masters thesis, Department of Biology and Marine Biology. University of North Carolina Wilmington, Wilmington, NC, USA. 67 pp.

Martino, E. J., and Houde, E. D. 2012. Density-dependent regulation of year-class strength in age-0 juvenile striped bass (*Morone saxatilis*). Canadian Journal of Fisheries and Aquatic Sciences, 69: 430–446.

McCollum, A. B., Bunnell, D. B., and Stein, R. A. 2003. Cold, northern winters: the importance of temperature to overwinter mortality of age-0 white crappies. Transactions of the American Fisheries Society, 132: 977–987.

McEachron, L. W., Matlock, G. C., Bryan, C. E., Unger, P., Cody, T. J., and Martin, J. H. 1994. Winter mass mortality of animals in Texas bays. Northeast Gulf Science, 13: 121–138.

Michaletz, P. H. 2010. Overwinter survival of age-0 gizzard shad in Missouri reservoirs spanning a productivity gradient: roles of body size and winter severity. Transactions of the American Fisheries Society, 139: 241–256.

Miranda, L., and Sonski, A. 1985. Survival of red drum fingerlings in fresh water: dissolved solids and thermal minima. Proceedings of the Annual Conference of SEAFWA, 39: 228–237.

Myers, R. A. 1998. When do environment–recruitment correlations work? Reviews in Fish Biology and Fisheries, 8: 285–305.

Ojaveer, E., Arula, T., Lankov, A., and Shpilev, H. 2011. Impact of environmental deviations on the larval and year-class abundances in the spring spawning herring (*Clupea harengus membras* L.) of the Gulf of Riga (Baltic Sea) in 1947–2004. Fisheries Research, 107: 159–168.

Pangle, K. L., Sutton, T. M., Kinnunen, R. E., and Hoff, M. H. 2004. Overwinter survival of juvenile lake herring in relation to body size, physiological condition, energy stores, and food ration. Transactions of the American Fisheries Society, 133: 1235–1246.

Perez-Dominguez, R., Holt, S. A., and Holt, G. J. 2006. Environmental variability in seagrass meadows: effects of nursery environment cycles on growth and survival in larval red drum *Sciaenops ocellatus*. Marine Ecology Progress Series, 321: 41–53.

Post, D. M., Kitchell, J. F., and Hodgson, J. R. 1998. Interactions among adult demography, spawning date, growth rate, predation,

overwinter mortality, and the recruitment of largemouth bass in a northern lake. Canadian Journal of Fisheries and Aquatic Sciences, 55: 2588–2600.

Post, J. R., and Evans, D. O. 1989. Size-dependent overwinter mortality of young-of-the-year yellow perch (*Perca flavescens*): laboratory, *in situ* enclosure, and field experiments. Canadian Journal of Fisheries and Aquatic Sciences, 46: 1958–1968.

Procarione, L. S., and King, T. L. 1993. Upper and lower temperature tolerance limits for juvenile red drums from Texas and South Carolina. Journal of Aquatic Animal Health, 5: 208–212.

R Development Core Team. 2012. R: a Language and Environment for Statistical Computing. R Foundation for Statistical Computing, Vienna, Austria. ISBN 3-900051-07-0, http://www.R-project.org/.

Rondeau, V., Commenges, D., and Joly, P. 2003. Maximum penalized likelihood estimation in a gamma-frailty model. Lifetime Data Analysis, 9: 139–153.

Rondeau, V., Mazroui, Y., and Gonzalez, J. R. 2012. frailtypack: an R package for the analysis of correlated survival data with frailty models using penalized likelihood estimation or parametrical estimation. Journal of Statistical Software, 47: 1–28.

Rooker, J. R., Holt, S. A., Holt, G. J., and Fuiman, L. A. 1999. Spatial and temporal variability in growth, mortality, and recruitment potential of postsettlement red drum, *Sciaenops ocellatus*, in a subtropical estuary. Fishery Bulletin US, 97: 581–590.

Ross, J. L., Stevens, T. M., and Vaughan, D. S. 1995. Age, growth, mortality, and reproductive biology of red drums in North Carolina waters. Transactions of the American Fisheries Society, 124: 37–54.

Scharf, F. S. 2000. Patterns in abundance, growth, and mortality of juvenile red drum across estuaries on the Texas Coast with implications for recruitment and stock enhancement. Transactions of the American Fisheries Society, 129: 1207–1222.

SEDAR. 2009. Stock assessment report: Atlantic red drum. Southeast Data, Assessment, and Review, North Charleston, South Carolina, United States. 18. 56 pp.

Shuter, B. J., and Post, J. R. 1990. Climate, population viability, and the zoogeography of temperate fishes. Transactions of the American Fisheries Society, 119: 314–336.

Slater, J. J., Lankford, T. E., and Buckel, J. A. 2007. Overwintering ability of young-of-the-year bluefish *Pomatomus saltatrix*: effect of ration and cohort of origin on survival. Marine Ecology Progress Series, 339: 259–269.

Sogard, S. M. 1997. Size-selective mortality in the juvenile stage of teleost fishes: a review. Bulletin of Marine Science, 60: 1129–1157.

Stewart, C. B., and Scharf, F. S. 2008. Estuarine recruitment, growth, and first-year survival of juvenile red drum in North Carolina. Transactions of the American Fisheries Society, 137: 1089–1103.

Toneys, M. L., and Coble, D. W. 1979. Size-related, first winter mortality of freshwater fishes. Transactions of the American Fisheries Society, 108: 415–419.

van der Veer, H. W., Geffen, A. J., and Witte, J. I. J. 2000. Exceptionally strong year classes in plaice *Pleuronectes platessa*: are they generated during the pelagic stage only, or also in the juvenile stage? Marine Ecology Progress Series, 199: 255–262.

Warton, D. I., and Hui, F. K. C. 2011. The arcsine is asinine: the analysis of proportions in ecology. Ecology, 92: 3–10.

Wilhite, M. L., Maki, K. L., Hoenig, J. M., and Olney, J. E. 2003. Toward validation of a juvenile index of abundance for American shad in the York River, Virginia. American Fisheries Society Symposium, 35: 285–294.

Handling editor: Emory Anderson

ICES Journal of Marine Science

ICES Journal of Marine Science (2014), 71(4), 1022–1029. doi:10.1093/icesjms/fst033

Contribution to the Themed Section: 'Larval Fish Conference'

Original Article

Night-time predation on post-settlement Japanese black rockfish *Sebastes cheni* in a macroalgal bed: effect of body length on the predation rate

Hikari Kinoshita, Yasuhiro Kamimura, Ken-Ichiro Mizuno, and Jun Shoji*

Takehara Fisheries Research Laboratory, Hiroshima University, 5-8-1 Minato-machi, Takehara, Hiroshima 725-0024, Japan

**Corresponding author: tel: +81 846 22 2362; fax: +81 846 23 0038; e-mail: jshoji@hiroshima-u.ac.jp*

Kinoshita, H., Kamimura, Y., Mizuno, K-I., and Shoji, J. 2014. Night-time predation on post-settlement Japanese black rockfish *Sebastes cheni* in a macroalgal bed: effect of body length on the predation rate. – ICES Journal of Marine Science, 71: 1022–1029.

Received 27 September 2012; accepted 14 February 2013; advance access publication 19 July 2013.

Recent field studies have pointed out that the vulnerability of juvenile fish to predation is higher than anticipated during night-time in vegetated habitats. Effects of abundance, body length, and growth rate on predation were examined in juvenile Japanese black rockfish in 2009–2011 in a macroalgal bed. Juvenile rockfish abundance ranged between 2.5 and 49.0 ind. 100 m^{-2} and the biomass of potential predators (piscivorous fish >82.5 mm) between 140.0 and 601.3 g 100 m^{-2}. *Sebastes inermis* was the most dominant predator, compromising more than 50% by wet weight on all sampling days. Comparison of the total length of juveniles surviving (as original population, OP) and that of juveniles ingested (IG) by predators provided the evidence of the size-selective predation on juvenile rockfish on three of seven sampling days. The juvenile predation rate estimated as abundance of IG (N 100 m^{-2})/(abundance of IG + OP (N 100 m^{-2})) × 100100 varied between 0.4 and 12.5%. Neither juvenile rockfish abundance nor predator biomass had a significant effect on the juvenile predation rate, whereas the juvenile body length had a significant effect, smaller individuals being more vulnerable to predation. The growth-selective predation was not detected. Macroalgal habitats, although functioning as nurseries during the day, may contribute as feeding grounds for piscivorous fish predators at night leading to enhanced nocturnal predation rates.

Keywords: juvenile, macroalgal bed, night-time, predation, rockfish.

Introduction

Even a small change in the mortality rate can significantly alter the accumulative survival ratio during the early life stages of fish (Houde, 1987). There is only limited information on the growth rate of larvae and juveniles before being predated compared with that of live (surviving) individuals, since the larval and juvenile individuals that are prone to mortality via predation are difficult to differentiate for samples collected in the field. Consequently, tracking the decrease in the number of surviving individuals provides us with mortality and survival rates that each fish cohort or population undergoes in nature (Secor and Houde, 1995; Rooker *et al.*, 1999; Shoji and Tanaka, 2007). However, it is still difficult to identify the source of mortality, since dead fish are rapidly removed from the population that can be sampled by conventional methods.

Generally, physical processes (e.g. temperature, transportation, etc.), starvation, and predation are the major sources of mortality in fish early life stages (Houde, 1989). Predation is considered as the most important among the sources of mortality as it prevails in all of egg, yolk-sac, larval, and juvenile stages. Relative contribution of predation tends to increase during the later stages when other sources of mortality (physical processes, starvation, disease, etc.) become less significant with fish growth. It is easier to obtain evidence of mortality due to predation [determining which individual has been ingested (IG) by predators and extracted from its original cohort or population] under laboratory conditions than in the field. Abundance, size, and growth rate of fish have been reported to be significant determinants for selection by their predators in both laboratory

experiments and nature (Cowan and Houde, 1992; Scharf *et al.*, 1998; Buckel *et al.*, 1999).

Previous studies have provided the morphological information of dead fish by the analysis of stomach contents of predators, which were sampled together with the surviving larvae (Takasuka *et al.*, 2004). Furthermore, comparison of back-calculated growth rates using otolith microstructures between IG and surviving fish revealed effects of fish vital rates on within-cohort selection by predators. The direction of selection (positive, negative, or no selection) on prey growth rates has been suggested to vary under different biotic conditions in nature such as species and size of predators (Takasuka *et al.*, 2007). However, there is still only limited information on growth-selective predation due to difficulties in concurrently collecting prey and predator samples.

Recently, vulnerability to the predation of juvenile fish has been suggested to vary over a diel cycle even in single marine ecosystems in shallow waters. Nocturnal migration and an increase in the biomass of piscivorous fish predators were observed in seagrass beds of coastal waters of Australia and Japan (Hindell *et al.*, 2000; Guest *et al.*, 2003; Kinoshita *et al.*, 2012). Seagrass beds have been considered to serve as important fish nurseries due to high prey availability and low vulnerability to predation based on studies most of which were conducted during the daytime (Heck *et al.*, 2003). Over annual cycles on the average night-time composes half of diel cycle. The daily amount of predation needs to be estimated by summing predation losses during the daytime and the night-time especially if the predation rate significantly differs between these periods. Therefore, vegetated habitats may contribute as good feeding grounds where nocturnal piscivorous fish can efficiently forage prey due to the high abundance of juvenile fish and the possible decrease in swimming performance of the juvenile fish during the night-time (Blaxter, 1986; Masuda, 2009).

The genus *Sebastes* is widely distributed in temperate and Subarctic coastal waters of the world and is important fisheries resources (Love *et al.*, 2002; Kai and Nakabo, 2008). Some *Sebastes* species are highly dependent on substrata such as vegetation and rocks during some period of their lives (Love *et al.*, 1991, 2002). The abundance of juveniles recruits to coastal habitats is considered as one of the important determinants for their year-class strength (Love *et al.*, 1991; Laidig *et al.*, 2007). Japanese black rockfish *S. cheni* dominates seagrass and macroalgal beds in temperate coastal water of the western North Pacific (Nakabo, 2002; Kai and Nakabo, 2008). Juveniles migrate from offshore to the vegetated habitats in early spring at ~20 mm in total length (TL) and dominate the fish community through summer (Kamimura and Shoji, 2009; Shoji *et al.*, 2011). Juvenile black rockfish at 20–60 mm exclusively feed on copepods in the Seto Inland Sea, Japan (Kamimura *et al.*, 2011). Since stomachs of the juveniles are mostly filled with copepods throughout the vegetation-dependent period (20–60 mm), mortality due to starvation is considered as minimal during this period (Kamimura *et al.*, 2011). Analysis of stomach contents of piscivorous fish and tethering experiments using juvenile rockfish revealed that significant increases in the predator biomass and the predation rate of juvenile rockfish occur during night-time (Kinoshita *et al.*, 2012). However, how the possible effects of biotic conditions (such as prey abundance, predator size, and biomass) affect the juvenile predation rates have not been clarified.

In the present study, juvenile rockfish were collected with their predators during night-time in a macroalgal bed in the central Seto Inland Sea to (i) estimate the juvenile predation rate during night-time and (ii) examine if size- and growth-selective predation prevails in night-time.

Material and methods

Field survey

Fish sampling and environmental surveys were conducted on a vegetated area (~50 m in width and 500 m in length) off the southwest coast of Aba Island, central Seto Inland Sea, Japan (Figure 1). Aba Island is an uninhabited island with a coast of ~2 km on its southwestern side. The vegetation is dominated by patches of macroalgae (mostly *Sargassum filicinum*, *S. fusiformis*, and *Chorda filum*) during winter to spring (Kamimura *et al.*, 2011). The mean biomass (wet weight) of the macroalgae fluctuates between 100 and 3500 g m^{-2} within a year (Kamimura and Shoji, 2009). The seabed of the macroalgal bed is comprised primarily of sand with occasional small stones (<100 mm in diameter), on which the macroalgae grow.

Biological and physical surveys were conducted during night-time (21:00–03:00 h) on 9 April 2009, 6 April 2010, and 16 March, 1 and 18 April, and 2 and 25 May 2011 (Table 1), a period when macroalgal growth is notable and rockfish juveniles are abundant (Kamimura and Shoji, 2009). A round seine net (2 m in height,

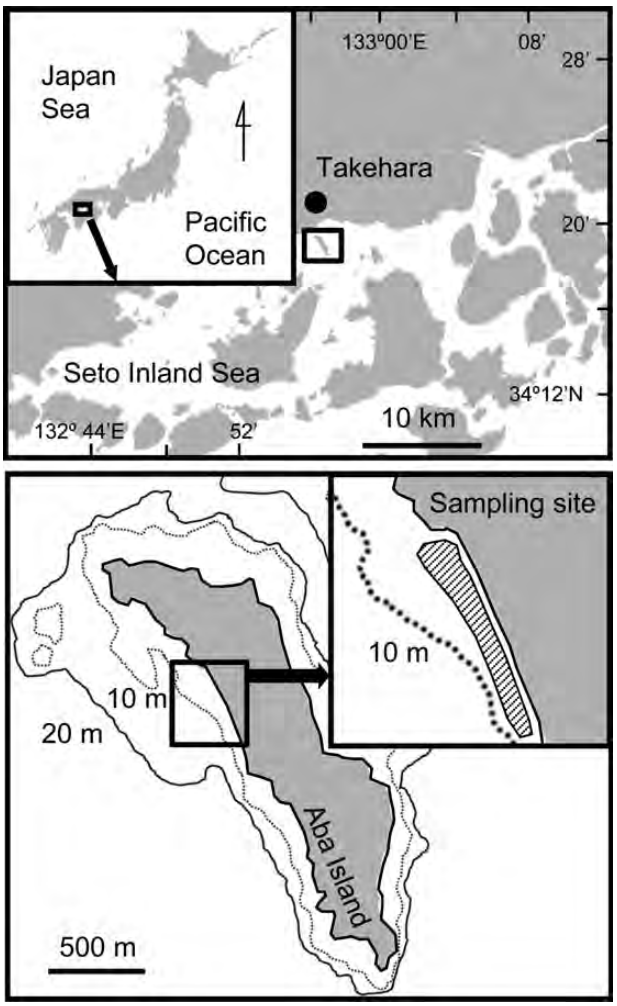

Figure 1. Map showing the sampling site off Aba Island, central waters of the Seto Inland Sea. Depth contours are indicated in the bottom panels.

30 m in length, and 5 mm in mesh aperture: Kamimura *et al*., 2011) was used to sample fish during a tidal level between 50 and 150 cm, when the edge of the vegetated area was close to the shore. Three sides of a square (10 m in side length) were surrounded using the seine net, with the other side facing to the shore, and this was carried out at four separate locations randomly selected within the vegetated area. Each fish collection covered an area of 100 m^2. Fish samples were preserved in 10% seawater formalin solution. Since swimming and schooling behaviour of juvenile rockfish at 20–60 mm TL did not significantly differ under light intensity <100 lux (covering the natural light intensity during night-time at the sampling site under new to full moons; H. Nakano and J. Shoji, unpublished data), all fish samples collected under different moon phases (Table 1) were combined for the analysis of effect of the juvenile body length on their predation rate. Water temperature and salinity were measured at each sampling.

Table 1. Summary of sampling dates, mean abundances of juvenile rockfish *S. cheni* as OP, and those IG by piscivorous fish predators and predation rates.

Year	Month	Date	Moon phase	Mean (s.d.) abundance (N 100 m^{-2}) of OP	IG	Mean (s.d.) predation rate (%)
2009	April	9	Full	49.0 (19.8)	5.0 (2.9)	9.9 (6.1)
2010	April	6	Half	43.0 (24.0)	1.0 (0.8)	2.0 (1.6)
2011	March	16	Full	8.3 (8.8)	0.8 (1.0)	5.3 (6.3)
2011	April	1	New	2.5 (3.1)	0.3 (0.5)	12.5 (25.0)
2011	April	18	Full	45.0 (29.3)	2.0 (1.8)	3.2 (2.8)
2011	May	2	New	31.5 (30.8)	0.8 (0.5)	4.5 (6.6)
2011	May	25	Half	31.8 (26.2)	0.3 (0.5)	0.4 (0.8)

Each mean value is shown with standard deviation (s.d.).

Laboratory procedure

Fish were identified and TL (mm) and wet weight were measured in the laboratory. Piscivorous fish of >82.5 mm TL were categorized as potential predators of juvenile rockfish *S. cheni* according to the stomach content analysis on fish community in the habitat of juvenile rockfish (Kinoshita *et al*., 2012). The biomass of the potential predators was considered as a proxy of vulnerability of juveniles to predation. Stomach contents of the potential predators were identified, enumerated, and weighed. TLs of the juvenile rockfish found in the stomachs of the predators (IG fish) were compared with those of the surviving juvenile rockfish (original population collected by the seine net with the predators, OP) on the same sampling day to detect the size-selective predation of juvenile rockfish. TLs of IG and OP were compared by the Wilcoxon test within the same sampling day to exclude the possible effects of temporal variability in the juvenile body size on the size-selective predation. Among the predatory fish that IG juvenile rockfish, *Sebastes inermis* (adult stage) was the most dominant, accounting for 96% in number followed by conger eel *Conger myriaster* (young stage, 4%; Table 2). TLs of IG and OP were compared by predatory fish species on 9 April 2009 when the juvenile rockfish were IG by two predatory species (*S. inermis* and *C. myriaster*).

The predation rate (R_p, %) of the juvenile rockfish was estimated for each sampling trial by the following equation: R_p = abundance of IG (N 100 m^{-2})/(abundance of IG + OP (N 100 m^{-2})) × 100. To detect the possible effects of density and body size of juvenile rockfish and predator biomass on the predation rate, exploratory analysis was conducted with the abundance and the mean TL of juvenile rockfish and predator biomass as explanatory variables and

Table 2. TL of juvenile rockfish *S. cheni* IG by sampling date and predator.

Year	Date	Predator Species	Predator TL (mm)	TL (mm) of juvenile rockfish IG
2009	April 9	*S. inermis*	158	18.0, 19.0
		S. inermis	128	20.6
		S. inermis	180	22.3, 25.5
		S. inermis	150	16.6, 18.0, 22.6
		S. inermis	154	19.6, 23.2
		S. inermis	164	14.4
		S. inermis	126	15.0
		S. inermis	154	23.1, 24.1
		S. inermis	128	17.4
		C. myriaster	260	22.3, 22.3, 23.2, 23.2 25.7
2010	April 6	*S. inermis*	138	28.4
		S. inermis	252	23.6
		S. inermis	132	24.9
		S. inermis	179	27.0
2011	March 16	*S. inermis*	132	17.2
		S. inermis	127	19.3
		S. inermis	145	19.3
	April 1	*S. inermis*	217	16.9
	April 18	*S. inermis*	175	15.6
		S. inermis	135	21.9, 20.3, 19.1, 18.8
		S. inermis	194	18.0, 18.5, 20.6
	May 2	*S. inermis*	163	26.9
		S. inermis	103	24.1
		S. inermis	216	19.5
	May 25	*S. inermis*	180	26.0

the predation rate as a dependent variable. The analysis was performed for data pooled from the 3 years and for a single year (2011) to exclude the year effect of juvenile abundance, body size, and predator biomass.

Analysis on growth-selective predation

Growth trajectory was established and compared between OP and IG to examine the effect of the growth rate on predation. Juveniles *S. cheni* collected by two additional tows on 6 April 2011 were processed for otolith analysis. Stomach contents of the potential predators were removed and preserved in 99% ethanol during the field sampling. Surviving juvenile rockfish collected by the seine were also preserved in 99% ethanol for otolith analysis (as OP for comparison with IG). In the laboratory, stomach contents of the potential predators were identified. Juvenile rockfish found in a stomach of the dominant predator, *S. inermis* (TL = 137.0 mm, $n = 1$), were processed for otolith analysis. Juvenile rockfish obtained from the stomachs of other predatory fish were not processed for the comparison of growth trajectory between OP and IG due to small sample size (the number of IG per stomach was <3 in other predatory fish). To minimize the possible effects of ingestion and digestion by the predators and ethanol preservation on the TL of juvenile rockfish, the regression equation between the TL and the otolith radius of juvenile rockfish (Kamimura *et al.*, 2012) was applied to estimate their live TL. Right lapilli otoliths were dissected from the juvenile rockfish (OP, $n = 23$; IG, $n = 14$) under a dissecting microscope and mounted on a glass slide with an epoxy resin. The daily rings of the otoliths (Kamimura *et al.*, 2012) were counted and the radius of each ring from the nucleus was measured using a light microscope connected to an otolith analysing system (Ratoc System Engineering). A measurement transect was set from the nucleus along the maximum radius. All intersections of the daily rings along the transect to the otolith margin were recorded.

Growth trajectory of OP and IG was back-calculated using the biological intercept method (Campana, 1990; Watanabe and Kuroki, 1997). Otolith daily rings start to be deposited at age 0 (the extrusion) in Japanese black rockfish (Kamimura *et al.*, 2012). Based on the linear relationship between otolith radii and TL (Guido *et al.*, 2004; Kamimura *et al.*, 2012), the TL at age was estimated for OP and IG following the equation: $L_a = L_c + (R_a - R_c)(L_c - L_e)(R_c - R_e)^{-1}$, where L_a and L_c are the fish size at age a and capture, R_a, R_c, and R_e the otolith radius at age a, capture, and extrusion, and L_e the mean fish size at age 0 (extrusion, 6.2 mm TL; Kamimura *et al.*, 2012). The recent 5-d mean growth rate (G_5, mm d^{-1}) was estimated for each age and that for the 5 d before the capture was compared between OP and IG.

Results

Juvenile rockfish and predators

In all, 187 (19.3–43.1 mm), 172 (20.8–37.6 mm), and 476 (18.9–33.3 mm) juvenile rockfish were collected in 2009, 2010, and 2011, respectively (Figure 2). The mean ($\pm$ s.d.) abundance of the juveniles ranged between 2.5 ± 3.15 100 m^{-2} (1 April 2011) and 49.0 ± 19.8 100 m^{-2} (9 April 2009; Table 1).

The mean biomass of the potential predators ranged between 140.0 ± 115.4 g 100 m^{-2} (18 April 2011) and 601.3 ± 90.4 g 100 m^{-2} (9 April 2009; Figure 3). In all, 42, 87, and 220 potential predators were collected in 2009, 2010, and 2011, respectively. *Sebastes inermis* was the most dominant among eight piscivorous fish species collected (*Sebastes cheni*, *S. ventricosus*, *S. inermis*, *S. hubbsi*, conger eel *C. myriaster*, spotbelly greenling *Hexagrammos agrammus*, fat greenling *Hexagrammos otakii*, and *Pseudoblennius cottoides*) and contributed more than 85% in number and 50% in biomass of the predatory fish on each sampling day. Sampling date had a significant effect on predator biomass (Kruskal–Wallis test, $p = 0.027$). The predator biomass on 18 March 2011 was significantly lower than those on 9 April 2009 and 6 April 2010 (Tukey's *post hoc* test, $p < 0.05$).

Plots of the body length of juvenile rockfish to those of predators showed that most of the predators IG juvenile rockfish at 10–20% of their body length (Figure 4). There was no significant effect of the body length of predators on that of IG juveniles within the size range examined in the present study ($p > 0.05$).

Size-selective predation

In all, 20 (14.4–25.7 mm), 4 (23.6–28.4 mm), and 16 (15.6–26.9 mm) juvenile rockfish (as IG) were found in the stomachs of predators in 2009, 2010, and 2011, respectively (Figure 2, Table 2). The mean ($\pm$ s.d.) abundance of IG ranged between 0.3 ± 0.5 100 m^{-2} (1 April and 25 May 2011) and 5.0 ± 2.95 100 m^{-2} (9 April 2009; Table 1). The TL of IG was significantly smaller than that of OP on 9 April 2009 (Wilcoxon test, $p < 0.0001$), 16 March 2011 ($p = 0.006$), and 18 April 2011 ($p < 0.0001$), whereas no difference was detected between OP and IG on the other four sampling days (6 April 2010 and 1 April, 2 May, and 25 May 2011; $p > 0.05$). Comparison of the TL between IG and OP by predatory fish species (*S. inermis* and conger eel) on 9 April 2009 when juvenile rockfish was IG by two predatory fish showed a significant difference in the TL between OP and IG for *S. inermis* ($p < 0.001$) but for conger eel ($p = 0.128$).

Predation rate

The mean ($\pm$ s.d.) predation rate varied between 0.4 ± 0.8 (25 May 2011) and 12.5 ± 25.0 (1 April 2011; Table 1). The mean TL of juvenile rockfish had a significant effect on variability in the juvenile predation rate (for all years: $y = 3487.4\ e^{-0.264\ x}$, $n = 7$, $r^2 = 0.794$, $p = 0.007$), whereas neither juvenile abundance nor predator biomass did (Figure 5). The mean predation rate decreased with the increase in the mean juvenile TL. The same level of significance was observed when data from only 2011 were used for the regression ($y = 2876.6\ e^{-0.261\ x}$, $n = 5$, $r^2 = 0.936$, $p = 0.007$). The effect of the mean TL on the predation rate was not significant when the data on 25 May 2011 were excluded.

Growth-selective predation

The mean ($\pm$ s.d.) and the range of TL of OP were 26.7 ± 1.4 and 24.6–29.9 mm and those of IG were 28.1 ± 1.2 and 26.6–30.7 mm, respectively (Table 3). The mean ($\pm$ s.d.) and the range of age estimated from the otolith microstructures of OP were 80.9 ± 5.3 and 66–112 d and those of IG were 79.2 ± 4.6 and 72–88 d, respectively. The mean G_5 showed high variability before day −70 (70 d before capture) and increased from ca. 0.2 to 0.4 mm d^{-1} during the period from day −60 to −30, then decreased from 0.4 to 0.3 during the period from day −30 to capture (Figure 6). There was no significant difference detected in G_5 between OP and IG, although the mean G_5 of IG was higher than that of OP at most ages.

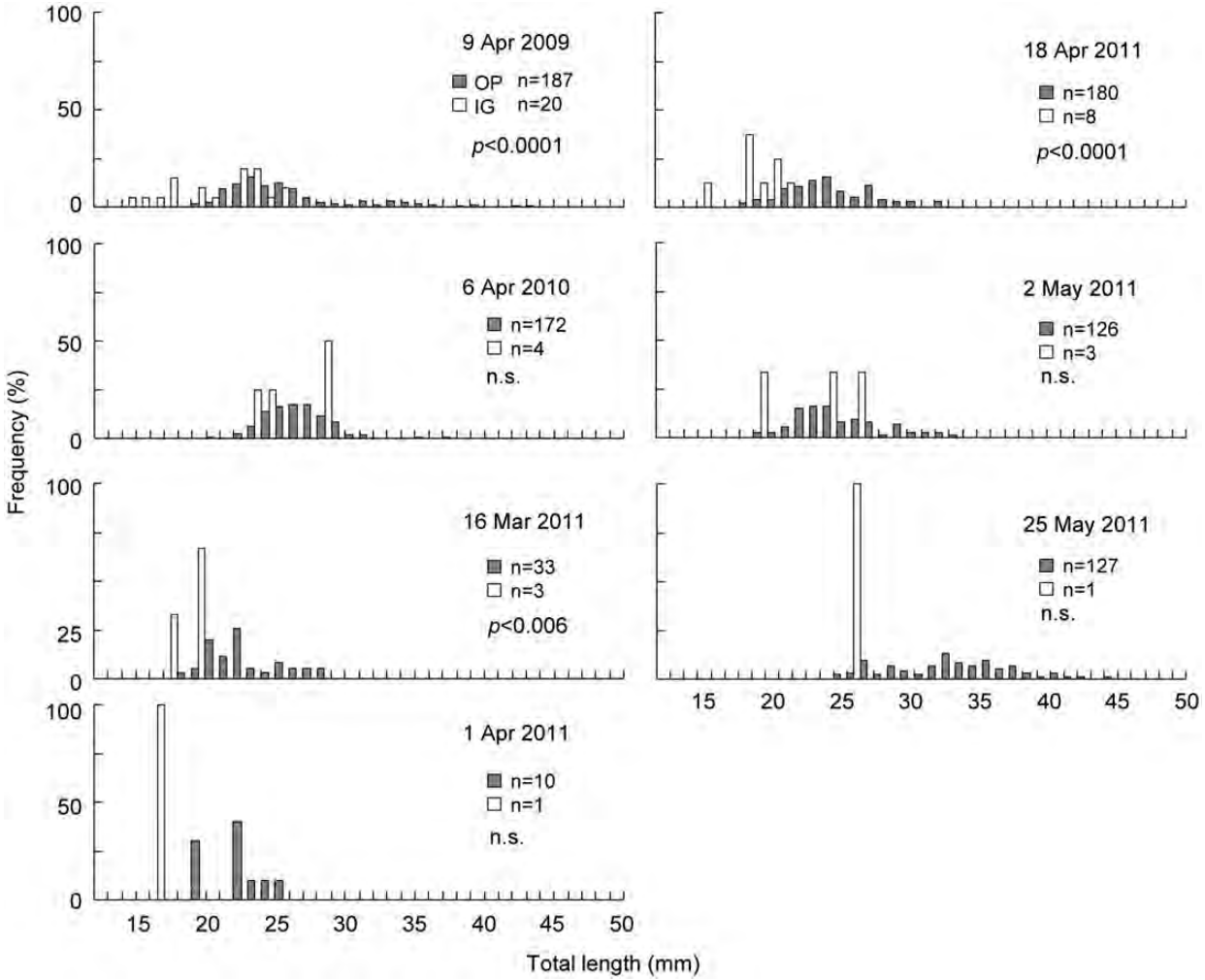

Figure 2. Length frequency distribution of juvenile rockfish *S. cheni* as OP and those IG by piscivorous fish predators by sampling day.

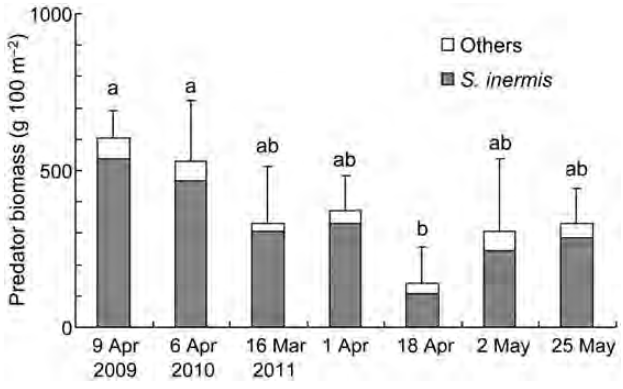

Figure 3. Mean predator biomass on each sampling day. Different alphabetical characters indicate the significant difference among sampling date (Kruskal–Wallis test followed by Tukey, $p < 0.05$) and vertical bars show the standard deviation. The biomass data were divided into *S. inermis*, the most dominant predatory species, and others.

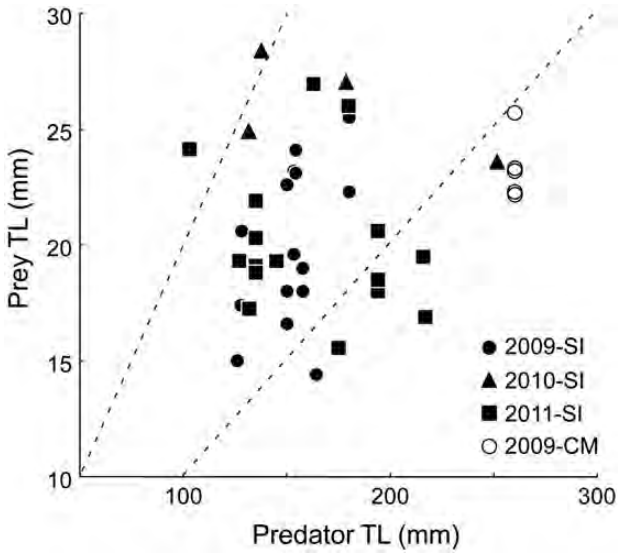

Figure 4. Plots of the TL of juvenile rockfish *S. cheni* IG on the TL of their predators. Sampling years (2009–2011) and predator species (SI, *S. inermis*; CM, conger eel *C. myriaster*) are indicated. Broken lines, prey–predator size relationship = 0.1 and 0.2.

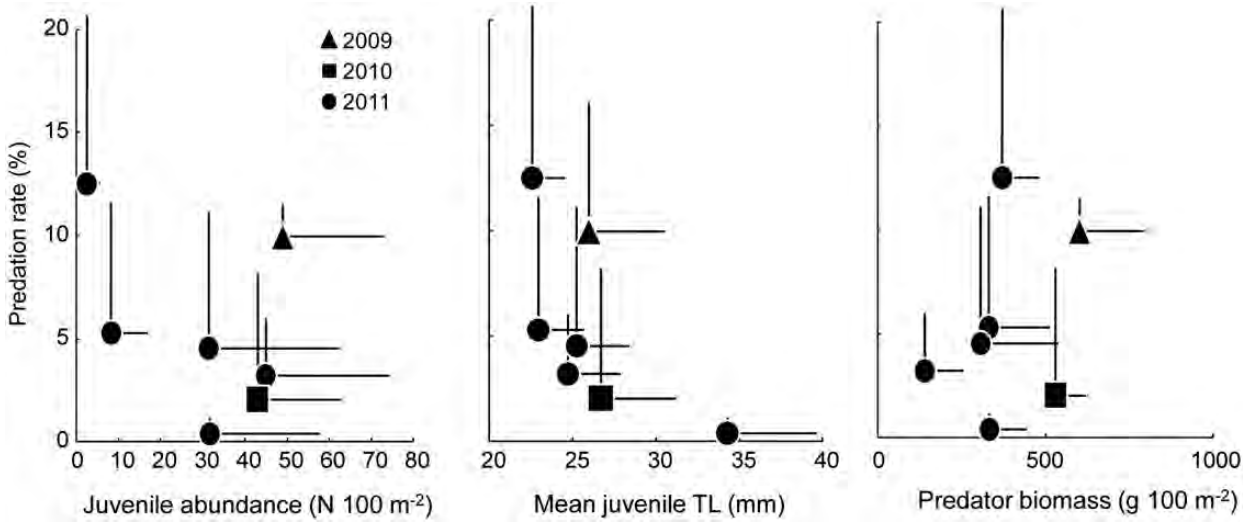

Figure 5. Plots of the juvenile rockfish *S. cheni* predation rate on juvenile abundance (left), mean juvenile TL (middle), and predator biomass (right). There was a significant effect of the mean juvenile TL on the predation rate. Vertical and horizontal bars indicate the standard deviation.

Discussion

Predation as the significant source of mortality for the post-immigration juveniles

In the present study, the instantaneous predation rate of juvenile rockfish was estimated to be 0.4–12.5% based on the abundance of OP and IG in the macroalgal bed off Aba Island in the central Seto Inland Sea. These values approximate to the predation rate (5.0%; Kinoshita *et al.*, 2012) estimated for juvenile rockfish in a seagrass bed off another island (Ikuno Island) in adjacent waters (~5 km from Aba Island). Based on the time to 90% gastric evacuation of piscivorous fish (5–10 h to 90% evacuation; Nashida and Tominaga, 1987; Buckel and Conover, 1996), the predators could ingest and digest juvenile fish within half of the duration of one night period in summer (10 h). Therefore, the overnight predation rate of juvenile rockfish in the macroalgal bed would be estimated as 0.8–25.0% d^{-1}, which approximates daily mortality coefficients (Z) of 0.008–0.288. These estimates are lower than the mean Z during larval stages of estuarine species (0.266; Houde and Zastrow, 1993) and larval to early juvenile stages of estuarine species (0.045–0.719 in striped bass *Morone saxatilis*, Secor and Houde, 1995; 0.129–0.193 in red drum *Sciaenops ocellatus*, Rooker *et al.*, 1999; 0.031–0.095 in Japanese temperate bass *Lateolabrax japonicus*, Shoji and Tanaka, 2007).

Juvenile Japanese black rockfish exclusively feed on copepods, which are abundant in the macroalgal bed (Kamimura *et al.*, 2011). Juveniles seem to have a high prey availability during the period of post-immigration to macroalgal beds since the feeding incidence (% of guts with prey organisms) of juveniles at 20–60 mm TL approximates 100% (Kamimura *et al.*, 2011). Therefore, we found no reason for the positive emigration of juvenile rockfish out of the macroalgal beds where their prey organisms are abundant. In addition, it is plausible that predation contributes to the majority of the total mortality of juvenile rockfish during the post-immigration period because of the high feeding incidence. Comparison of the fish community structure between daytime and night-time revealed a significant increase in piscivorous fish biomass during night-time in Ikuno Island (Kinoshita *et al.*, 2012). No juvenile rockfish were found in stomachs of the piscivorous fish during the daytime, whereas they were IG by the predators during night-time in seagrass and macroalgal beds (Kinoshita *et al.*, 2012; present study). Tethering

Table 3. Sample size, range, and mean of TL range and age of juvenile rockfish *S. cheni* as OP and those IG by piscivorous fish predators.

	OP	IG
Number of fish	23	14
TL (mm)		
Range	24.6–29.9	26.6–30.7
Mean (s.d.)	26.7 (1.4)	28.1 (1.2)
Age (d)		
Range	66–112	72–88
Mean (s.d.)	80.9 (5.3)	79.2 (4.6)

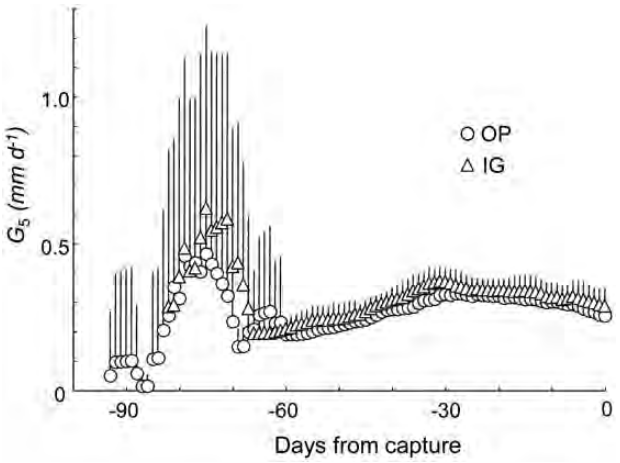

Figure 6. Comparison of the mean growth rate (G_5; mm d^{-1}) during recent 5 d period on each age between the OP and IG juvenile rockfish *S. cheni*. There was no significant difference in G_5 between OP and IG (Wilcoxon test, $p = 0.085$).

experiment showed that the vulnerability of juvenile rockfish to predation during night-time (90% per one night) was significantly higher than that during daytime (0%; Kinoshita *et al.*, 2012). We conclude that the majority of predation on juvenile rockfish occurred during night-time.

Factors affecting the predation rate

Predation on juvenile rockfish (*S. cheni*) by *S. inermis* was considered to be the most important interspecific interaction in the spring–summer fish community in the macroalgal bed off Aba Island. The percentage biomass of *S. inermis* was higher than 50% of the total biomass of potential predators on all sampling days. In addition, 83.3% (in number) of IG juvenile rockfish were found in stomachs of *S. inermis*. Juvenile rockfish dominate the macroalgal bed from spring through summer, composing 60–80% in number of all fish (Kamimura and Shoji, 2009). In the present study, stomach content analysis for the predators showed that the contribution of other juvenile fish as a prey source for piscivorous fish predators was minimal (<5% of all fish IG). Based on the data available, the juvenile abundance of other fish species and their fluctuations seem not to have a large effect on the interaction between juvenile rockfish and their predators.

Neither juvenile rockfish abundance nor predator biomass had a significant effect on the juvenile predation rate. Generally, density-dependent processes have been reported as an important source of mortality in fish early life stages of a variety of species and ecosystems (Jenkins *et al.*, 1991; Kimmerer *et al.*, 2000; Imre *et al.*, 2005; Martino and Houde, 2010). A shift in habitat from a broad area (pelagic zone) to a more spatially restricted nursery is suggested to correspond to the timing when density-dependent regulation starts to operate in juvenile fish in coastal habitats (Shoji and Tanaka, 2007). The abundance of striped bass *M. saxatilis* juveniles has been shown to alter selectivity by piscivorous fish predator (bluefish *Pomatomus saltatrix*) on themselves in Hudson River estuary (Buckel *et al.*, 1999). Although the abundance of post-immigration juvenile rockfish did not significantly affect the juvenile predation rate, selectivity, ration, or biomass of the predators are possibly altered by the juvenile rockfish abundance if the juvenile abundance showed a higher fluctuation than that observed during the survey period (2009–2011). An extremely high abundance of immigrating juveniles would affect the behaviour and structure of the predatory fish community through making the vegetated habitats as a good feeding ground for the piscivorous fish predators, although these habitats usually serve as nurseries for juvenile fish (Heck *et al.*, 2003).

The TL of juvenile rockfish, rather than their abundance or predator biomass, had a significant effect on the juvenile predation rate. Recent laboratory experiments observed a significant increase in burst and cruise swimming speeds and a decrease in the nearest neighbour distance of juvenile rockfish from 20 to 40 mm TL under a variety of light conditions (10^{-1}–10^{5} lux), indicating the development of antipredator behaviour during the post-immigration period (H. Nakano and J. Shoji, unpublished data). Since adult *S. inermis* feed on various trophic prey items (Nakabo, 2002), they would shift their feeding target from piscine prey to invertebrate organisms such as amphipods when the size or abundance of their piscine prey is not optimal enough for their successful feeding. However, further analysis on data with larger variability in juvenile body size and abundance, and predator species and biomass would be needed as the data from one sampling day (25 May 2011) seemed to have a large affect on the relationship between the juvenile body length and the predation rate in the present study.

Size- and growth-selective predation

Comparison of the TL of OP and IG revealed that the growth-selective predation prevailed in juvenile rockfish population on three sampling days, although statistical analysis was not conducted due to the small sample size on the other sampling days. Juvenile rockfish form schools with individuals of different body lengths between 20 and 60 mm (Kamimura *et al.*, 2011). Generally, larger fish with higher antipredator performance have a higher probability to survive predation (Bailey and Houde, 1989; Masuda, 2009). It is plausible that larger juvenile rockfish have a greater chance to survive predation by piscivorous fish predators than smaller ones due to the development of antipredator behaviour even during night-time when nocturnal pisicivorous predators (including *S. inermis*) tend to be more capable of catching juvenile fish. We conclude that positive size selection (higher probability of survival of larger individuals) operated in the juvenile rockfish.

Significant selection for fast-growing individual was not detected in the present study. The G_5 as a proxy of physiological condition (Takasuka *et al.*, 2003) of juvenile rockfish was not significantly different between OP and IG. Generally, fast-growing fish have a higher probability to avoid predators due to their better physiological condition so that more chance to survive when compared with slower growing fish within a school or population. Recent studies have reported that growth selective processes do not always prevail towards a fixed direction (positive, negative, or no selection) and can vary with the variability in environmental conditions, even under a predator–prey interaction by the same species (Munch and Conover, 2003; Takasuka *et al.*, 2007). In the present survey field, variability in juvenile rockfish growth might be small so that growth-selective mechanisms were not detected, since plenty of copepod prey was supplied to juvenile rockfish in the macroalgal bed (Kamimura *et al.*, 2011). Future analysis under different levels of juvenile immigration abundance and prey availability may provide further information on variability in direction and strength of growth-selective processes of juvenile rockfish.

In conclusion, vegetated habitats such as macroalgal and seagrass beds have been considered as important nurseries for young fish, since these habitats serve as a predation refuge. Present results provided evidence of the night-time predation on juvenile rockfish in their predation refuge. There seems to be a paradox: these habitats do contribute as a feeding ground for piscivorous fish predators especially during night-time, while they have been considered as important nursery for young fish.

Acknowledgements

We express our thanks to Sadaharu Iwasaki and staff of Takehara Fisheries Research Laboratory and Geinan Fisherman's Associations for their assistance with the field survey. This research was supported by the Environment Research and Technology Development Fund of the Ministry of the Environment (E-1102) and Grant-in-Aid for Scientific Research (B-24380107) to JS.

References

Bailey, K. M., and Houde, E. D. 1989. Predation on eggs and larvae of marine fishes and the recruitment problem. Advances in Marine Biology, 25: 1–83.

Blaxter, J. H. S. 1986. Development of sense organs and behaviour of teleost larvae with special reference to feeding and predator avoidance. Transactions of the American Fisheries Society, 115: 98–114.

Buckel, J. A., and Conover, D. O. 1996. Gastric evacuation rates of piscivorous young-of-the-year bluefish. Transactions of the American Fisheries Society, 125: 591–599.

Buckel, J. A., Conover, D. O., Steinberg, N. D., and McKown, K. A. 1999. Impact of age-0 bluefish (*Pomatomus saltatrix*) predation on age-0 fishes in the Hudson River estuary: evidence for density-dependent loss of juvenile striped bass (*Morone saxatilis*)? Canadian Journal of Fisheries and Aquatic Sciences, 56: 275–287.

Campana, S. E. 1990. How reliable are growth back-calculations based on otolith? Canadian Journal of Fisheries and Aquatic Sciences, 47: 2219–2227.

Cowan, J. H., Jr, and Houde, E. D. 1992. Size-dependent predation on marine fish larvae by Ctenophores, Scyphomedusae, and Planktivorous fish. Fisheries Oceanography, 1: 113–126.

Guest, M. A., Connolly, R. M., and Loneragan, N. R. 2003. Seine nets and beam trawls compared by day and night for sampling fish and crustaceans in shallow seagrass habitat. Fisheries Research, 64: 185–196.

Guido, P., Katayama, S., and Omori, M. 2004. Classification of juvenile rockfish, *Sebastes inermis*, to *Zostera* and *Sargassum* beds, using the macrostructure and chemistry of otoliths. Marine Biology, 145: 1243–1255.

Heck, K. L., Jr., Hays, G., and Orth, R. J. 2003. Critical evaluation of the nursery role hypothesis for seagrass meadows. Marine Ecology Progress Series, 253: 123–136.

Hindell, J. S., Jenkins, G. P., and Keough, M. J. 2000. Variability in abundances of fishes associated with seagrass habitats in relation to diets of predatory fishes. Marine Biology, 136: 725–737.

Houde, E. D. 1987. Fish early life dynamics and recruitment variability. American Fisheries Society Symposium, 2: 17–29.

Houde, E. D. 1989. Subtitles and episodes in the early life of fishes. Journal of Fish Biology, 35 (Suppl. A): 29–38.

Houde, E. D., and Zastrow, C. E. 1993. Ecosystem- and taxon-specific dynamic and energetics properties of larval fish assemblages. Bulletin of Marine Science, 53: 290–335.

Imre, I., Grant, J. W. A., and Cunjak, R. A. 2005. Density-dependent growth of young-of-the-year Atlantic salmon *Salmo salar* in Catamaran Brook, New Brunswick. Journal of Animal Ecology, 74: 508–516.

Jenkins, G. P., Young, J. W., and Davis, T. L. O. 1991. Density dependence of larval growth of a marine fish, the southern bluefin tuna, *Thunnus maccoyii*. Canadian Journal of Fisheries and Aquatic Sciences, 48: 1358–1363.

Kai, Y., and Nakabo, T. 2008. Taxonomic review of the *Sebastes inermis* species complex (Scorpaeniformes: Scorpaenidae). Ichthyological Research, 55: 238–259.

Kamimura, Y., Kasai, A., and Shoji, J. 2011. Production and prey source of juvenile black rockfish *Sebastes cheni* in a mixed vegetation area of seagrass and macroalgae off Aba Island, central Seto Inland Sea, Japan: an estimation of the economic value of a fish nursery. Aquatic Ecology, 45: 367–376.

Kamimura, Y., Mizuno, K., Toshito, S., Noda, T., Hirakawa, K., Tamaki, H., and Shoji, J. 2012. Validation of daily periodicity of otolith increment formation and application for growth analysis of wild juvenile black rockfish *Sebastes cheni*. Aquaculture Science, 60: 413–416.

Kamimura, Y., and Shoji, J. 2009. Seasonal changes in the fish assemblages in a mixed vegetation area of seagrass and macroalgae in the central Seto Inland Sea. Aquaculture Science, 57: 233–241.

Kimmerer, W. J., Cowan, J. H., Miller, L. W., and Rose, K. A. 2000. Analysis of an estuarine striped bass (*Morone saxatilis*) population: influence of density-dependent mortality between metamorphosis and recruitment. Canadian Journal of Fisheries and Aquatic Sciences, 57: 478–486.

Kinoshita, H., Kamimura, Y., Hirai, K., Mizno, K., Iwamoto, Y., and Shoji, J. 2012. Vulnerability of juvenile fish to piscivorous fish predators increases during nighttime in a seagrass bed in the central Seto Inland Sea, Japan. Bulletin of the Japanese Society of Fisheries Oceanography, 76: 24–30.

Laidig, T. E., Chess, J. R., and Howard, D. F. 2007. Relationship between abundance of juvenile rockfishes (*Sebastes* spp.) and environmental variables documented off northern California and potential mechanisms for the covariation. Fishery Bulletin US, 105: 39–48.

Love, M. S., Carr, M. H., and Haldorson, L. J. 1991. The ecology of substrate-associated juveniles of the genus *Sebastes*. Environmental Biology of Fishes, 30: 225–243.

Love, M. S., Yoklavich, M., and Thorsteinson, L. 2002. The Rockfishes of the Northeast Pacific. University of California Press, Berkeley, CA. 404 pp.

Martino, E. J., and Houde, E. D. 2010. Recruitment of striped bass in Chesapeake Bay: spatial and temporal environmental variability and availability of zooplankton prey. Marine Ecology Progress Series, 409: 213–228.

Masuda, R. 2009. Behavioral ontogeny of marine pelagic fishes with the implications for the sustainable management of fisheries resources. Aqua Bioscience Monograph, 2: 1–56.

Munch, S. B., and Conover, D. O. 2003. Rapid growth results in increased susceptibility to predation in *Menidia menidia*. Evolution, 57: 2119–2127.

Nakabo, T. 2002. Fishes of Japan with Pictorial Keys to the Species, English edn. Tokai University Press, Tokyo. 1749 pp.

Nashida, K., and Tominaga, O. 1987. Studies on groundfish communities in the coastal waters of northern Niigata Prefecture. Seasonal changes of feeding habits and daily rations of young flounder, *Paralichthys olivaceus*. Bulletin of Japan Sea Regional Fisheries Research Laboratory, 37: 39–56.

Rooker, J. R., Holt, S. A., Holt, G. J., and Fuiman, L. A. 1999. Spatial and temporal variability in growth, mortality, and recruitment potential of postsettlement red drum, *Sciaenops ocellatus*, in a subtropical estuary. Fishery Bulletin US, 97: 581–590.

Scharf, F. S., Buckel, J. A., Juanes, F., and Conover, D. O. 1998. Predation by juvenile piscivorous bluefish (*Pomatomus saltatrix*): the influence of prey to predator size ratio and prey type on predator capture success and prey profitability. Canadian Journal of Fisheries and Aquatic Sciences, 55: 1695–1703.

Secor, D. H., and Houde, E. D. 1995. Temperature effects on the timing of striped bass egg production, larval viability, and recruitment potential in the Patuxent River (Chesapeake Bay). Estuaries, 18: 527–544.

Shoji, J., and Tanaka, M. 2007. Density-dependence in post-recruit Japanese seaperch *Lateolabrax japonicus* in the Chikugo River, Japan. Marine Ecology Progress Series, 334: 255–262.

Shoji, J., Toshito, S., Mizuno, K., Kamimrua, Y., Hori, M., and Hirakawa, K. 2011. Possible effects of global warming on fish recruitment: shifts in spawning season and latitudinal distribution can alter growth of fish early life stages through the changes in daytime. ICES Journal of Marine Science, 68: 1165–1169.

Takasuka, A., Aoki, I., and Mitani, I. 2003. Evidence of growth-selective predation on larval Japanese anchovy *Engraulis japonicus* in Sagami Bay. Marine Ecology Progress Series, 252: 223–238.

Takasuka, A., Aoki, I., and Mitani, I. 2004. Three synergistic growth-related mechanisms in the short-term survival of larval Japanese anchovy *Engraulis japonicus* in Sagami Bay. Marine Ecology Progress Series, 270: 217–228.

Takasuka, A., Aoki, I., and Oozeki, Y. 2007. Predator-specific growth-selective predation on larval Japanese anchovy *Engraulis japonicus*. Marine Ecology Progress Series, 350: 99–107.

Watanabe, Y., and Kuroki, T. 1997. Asymptotic growth trajectories of larval sardine (*Sardinops melanostictus*) in the coastal waters off central Japan. Marine Biology, 127: 369–378.

Handling editor: Francis Juanes